Investigation on the pyruvate uptake, release and metabolism of cultured rat brain astrocytes

Dissertation

Zur Erlangung des Grades eines

Doktors der Naturwissenschaften (Dr. rer. nat.)

des Fachbereiches 2 (Biologie/Chemie)

an der Universität Bremen

Nadine Denker

2024

Dekan des Fachbereichs:	Prof. Dr. Christian Wild
Erste Gutachterin:	Prof. Dr. Blanca Aldana
Zweite Gutachterin:	Prof. Dr. Kirsten Hattermann-Koch
Verteidigungsdatum:	06.09.2024

Versicherung an Eides Statt

Ich, Nadine Denker,

versichere an Eides Statt durch meine Unterschrift, dass ich die vorstehende Arbeit selbständig und ohne fremde Hilfe angefertigt und alle Stellen, die ich wörtlich dem Sinne nach aus Veröffentlichungen entnommen habe, als solche kenntlich gemacht habe, mich auch keiner anderen als der angegebenen Literatur oder sonstiger Hilfsmittel bedient habe.

Ich versichere an Eides Statt, dass ich die vorgenannten Angaben nach bestem Wissen und Gewissen gemacht habe und dass die Angaben der Wahrheit entsprechen und ich nichts verschwiegen habe.

Die Strafbarkeit einer falschen eidesstattlichen Versicherung ist mir bekannt, namentlich die Strafandrohung gemäß § 156 StGB bis zu drei Jahren Freiheitsstrafe oder Geldstrafe bei vorsätzlicher Begehung der Tat bzw. gemäß § 161 Abs. 1 StGB bis zu einem Jahr Freiheitsstrafe oder Geldstrafe bei fahrlässiger Begehung.

Bremen, Juli 2024

X

Nadine Denker

Table of Contents

I. Danksagung

Zuallererst möchte ich mich bei Prof. Dr. Ralf Dringen bedanken. Ralf, vielen Dank für die Chance, in deiner Arbeitsgruppe zu promovieren, und für die ausgiebige Unterstützung über die letzten Jahre! Ich schätze es sehr, dass deine Tür immer offen stand und man mit jeder Frage zu dir kommen konnte. Deine Begeisterung für wissenschaftliche Themen ist äußerst ansteckend und hat mich stets motiviert.

Mein besonderer Dank gilt auch Prof. Dr. Blanca Aldana und Prof. Dr. Kirsten Hattermann-Koch für die Bereitschaft, die Gutachten zu meiner vorliegenden Dissertation zu erstellen. Danke für die Unterstützung!

Ein herzliches Dankeschön an Antonia, Carmen, Chris, Gabi, Nico, Patrick, Yvonne und alle weiteren Mitglieder der AG Dringen. Die vielen spaßigen Stunden im Labor, begleitet von objektiv betrachtet mal mehr, mal weniger guter Musik, werde ich nicht vergessen. In dieser intensiven Zeit konnte ich jederzeit auf eure Unterstützung zählen, sei es durch Gespräche, Diskussionen oder praktische Hilfe, und dafür bin ich euch sehr dankbar.

Zum Abschluss möchte ich mich bei meiner Familie und meinen Freunden bedanken, allen voran bei meinen Eltern Rosi und Detlev. Vielen Dank für eure immense Unterstützung. Ich habe die gemeinsamen Abende und die Gespräche mit euch sehr genossen und bin froh, euch zu haben. Auch wenn es ein bisschen ungewöhnlich sein mag, möchte ich mich ebenso bei Diego, unserem Pferd, bedanken. Jeden Moment, den ich mit ihm verbringen durfte, war ein Augenblick Entspannung.

Danke an meinen Freund Carlino, der es in Kauf genommen hat, mich während meiner Zeit in Bremen nur am Wochenende zu sehen. Vielen Dank für deine Unterstützung und das manchmal benötigte gute Zureden. Mit dir habe ich immer Spaß und ich freue mich auf alles, was jetzt kommt.

II. Summary

Astrocytes play a pivotal role in brain metabolism and in neuroprotection. These cells are considered as very glycolytic, consuming large amounts of glucose that is mainly converted into lactate. The α-keto acid pyruvate is a key player of cellular metabolism that links cytosolic and mitochondrial metabolism as the end product of glycolysis. Pyruvate can also be exported from astrocytes and is in brain believed to have neuroprotective functions. In order to elucidate the pathways involved in astrocytic pyruvate metabolism, primary rat astrocyte cultures were used as model systems to investigate pyruvate consumption and release.

Of the different substrates tested (pyruvate, lactate, β-hydroxybutyrate, alanine and acetate) that are known to be metabolized in mitochondria, pyruvate was consumed most efficiently by cultured astrocytes incubated in the absence of glucose. Astrocytes exhibited a nearly time-proportional, concentration-dependent consumption of extracellular pyruvate with apparent Michaelis-Menten kinetic [$K_M = 0.6 \pm 0.1$ mM, $V_{max} = 5.1 \pm 0.8$ nmol/(min x mg protein)]. Lactate and alanine generated and released in pyruvate-fed astrocytes accounted for approximately 60 % and 10 %, respectively, of the pyruvate consumed within 3 h. The presence of AR-C155858, a monocarboxylate transporter 1 (MCT1)-inhibitor, or the application of 10-fold excess of the MCT1 substrates lactate and β-hydroxybutyrate strongly impaired the astrocytic consumption of extracellular pyruvate. Inhibition of the mitochondrial pyruvate carrier (MPC) by UK5099, as well as inhibition of the respiratory chain by the complex III inhibitor Antimycin A also prevented pyruvate consumption. In contrast, BAM15, a mitochondrial uncoupler, strongly accelerated pyruvate consumption in glucose-deprived astrocytes.

In the presence of glucose, astrocytes established a transient extracellular steady-state concentration of pyruvate between 150 µM and 300 µM, while lactate in contrast was continuously released and accumulated to millimolar concentrations. In DMEM culture medium, the extracellular pyruvate concentration remained almost constant for days. In amino acid-free incubation buffer, this almost constant extracellular pyruvate level was established within 5 h, with an initial pyruvate release rate of around 60 nmol/(h x mg), and was maintained for several hours. By consumption of excess extracellular pyruvate in the presence of glucose, astrocytes established similar extracellular pyruvate concentrations. Furthermore, pyruvate release was observed in glucose-free incubation buffer after

application of mannose, lactate, fructose, sorbitol or alanine. MCT1 inhibition by AR-C155858 decreased the extracellular pyruvate concentration, while MPC inhibition by UK5099 strongly increased the release of glycolytically derived pyruvate. Both antimycin A and BAM15 application resulted in a complete loss of extracellular pyruvate accumulation.

The data presented demonstrate that MCT1 is the main transporter involved in pyruvate consumption and release. Modulation of mitochondrial processes revealed a strong involvement of the mitochondrial metabolism in pyruvate utilization. Overall, alterations of pyruvate metabolism presumably modify the intracellular pyruvate concentration, thereby influencing pyruvate consumption and release, as astrocytes seem to establish an equilibrium between their extracellular and intracellular pyruvate concentration.

III. Zusammenfassung

Astrozyten spielen eine zentrale Rolle im Hirnstoffwechsel und in der Neuroprotektion. Diese Zellen gelten als sehr glykolytisch und verbrauchen große Mengen an Glukose, welche hauptsächlich in Laktat umgewandelt wird. Die α-Ketosäure Pyruvat ist ein Schlüsselmolekül des zellulären Stoffwechsels, welches den cytosolischen und mitochondrialen Stoffwechsel als Endprodukt der Glykolyse verbindet. Pyruvat kann auch aus Astrozyten exportiert werden und es wird angenommen, dass es im Gehirn neuroprotektive Funktionen hat. Um die am astrozytären Pyruvat-Stoffwechsel beteiligten Wege aufzuklären, wurden primäre Ratten-Astrozytenkulturen als Modellsysteme verwendet, um Pyruvat-Verbrauch und Freisetzung zu untersuchen.

Von den verschiedenen getesteten Substraten (Pyruvat, Laktat, β-Hydroxybutyrat, Alanin und Acetat), die bekannterweise in Mitochondrien verstoffwechselt werden können, wurde Pyruvat am effizientesten von den in Abwesenheit von Glukose inkubierten kultivierten Astrozyten konsumiert. Astrozyten zeigten einen nahezu zeitproportionalen, konzentrationsabhängigen Verbrauch von extrazellulärem Pyruvat mit scheinbarer Michaelis-Menten-Kinetik [K_M = 0,6 ± 0,1 mM, V_{max} = 5,1 ± 0,8 nmol/(min x mg Protein)]. Laktat und Alanin, welche von mit Pyruvat gefütterten Astrozyten erzeugt und freigesetzt wurden, machten etwa 60 % bzw. 10 % des innerhalb von 3 Stunden verbrauchten Pyruvats aus. Die Anwesenheit von AR-C155858, einem Monocarboxylat-Transporter 1 (MCT1)-Inhibitor, oder die Applikation eines 10-fachen Überschusses der MCT1-Substrate Laktat und β-Hydroxybutyrat verringerten den astrozytären Verbrauch von extrazellulärem Pyruvat stark. Die Hemmung des mitochondrialen Pyruvatcarriers (MPC) durch UK5099 sowie die Hemmung der Atmungskette durch den Komplex-III-Inhibitor Antimycin A inhibierten ebenfalls den Pyruvatverbrauch. Im Gegensatz dazu beschleunigte BAM15, ein mitochondrialer Entkoppler, den Pyruvatverbrauch in glukose-deprivierten Astrozyten stark.

In Gegenwart von Glukose stellten Astrozyten eine vorübergehende extrazelluläre Steady-State-Konzentration von Pyruvat zwischen 150 µM und 300 µM ein, während Laktat im Gegensatz dazu kontinuierlich freigesetzt wurde und sich zu millimolaren Konzentrationen anreicherte. In DMEM-Kulturmedium blieb die extrazelluläre Pyruvatkonzentration über Tage hinweg nahezu konstant. In aminosäurefreiem Inkubationspuffer wurde dieses nahezu

konstante extrazelluläre Pyruvatlevel innerhalb von 5 Stunden mit einer anfänglichen Pyruvatfreisetzungsrate von etwa 60 nmol/(h x mg) erreicht und über mehrere Stunden aufrechterhalten. Durch den Verbrauch von überschüssigem extrazellulärem Pyruvat in Gegenwart von Glukose stellten Astrozyten ähnliche extrazelluläre Pyruvatkonzentrationen ein. Ebenso wurde die Pyruvatfreisetzung in glukosefreiem Inkubationspuffer nach Gabe von Mannose, Laktat, Fruktose, Sorbit oder Alanin beobachtet. Die Inhibition von MCT1 durch AR-C155858 verringerte die extrazelluläre Pyruvatkonzentration, während eine MPC-Inhibition durch UK5099 die Freisetzung von glykolytisch gewonnenem Pyruvat stark erhöhte. Sowohl die Applikation von Antimycin A als auch von BAM15 führte zu einem vollständigen Verschwinden der extrazellulären Pyruvatakkumulation.

Die vorgelegten Daten zeigen, dass MCT1 der wichtigste Transporter des Pyruvatverbrauches als auch der Pyruvatfreisetzung ist. Die Modulation mitochondrialer Prozesse zeigte eine starke Beteiligung des mitochondrialen Stoffwechsels an der Pyruvatverwertung. Insgesamt modifiziert eine Veränderung des Pyruvat-Stoffwechsels vermutlich die intrazelluläre Pyruvat-Konzentration und beeinflusst damit den Pyruvat-Verbrauch sowie die Freisetzung, da Astrozyten offenbar ein Gleichgewicht zwischen ihrer extrazellulären und intrazellulären Pyruvat-Konzentration herstellen.

IV. Abbreviations

ADP	Adenosine diphosphate
ALAT	Alanine aminotransferase
AMP	Adenosine monophosphate
AMPK	AMP-activated protein kinase
AQP	Aquaporin
AST	Aspartate aminotransferase
ATP	Adenosine triphosphate
BBB	Blood brain barrier
CNS	Central nervous system
CoA	Coenzyme A
CPT	Carnitine palmitoyltransferase
CSF	Cerebrospinal fluid
DHAP	Dihydroxyacetonephosphate
DMEM	Dulbecco's modified Eagle's medium
DNA	Deoxyribonucleic acid
EAAT	Excitatory amino acid transporters
e.g.	*exempli gratia,* for example
FAD	Flavin adenine dinucleotide (oxidized)
$FADH_2$	Flavin adenine dinucleotide (reduced)
Fig.	Figure
g	Gram
GABA	γ-Aminobutyric acid
GAP	Glyceraldehyde 3-phosphate
GAT	GABA transporter
GC	Gas chromatography
GDH	Glutamate dehydrogenase
GFAP	Glial fibrillary acidic protein
GLAST	Glutamate/aspartate transporter
GLT	Glutamate transporter
GLUT	Glucose transporter
GPT	Glutamate pyruvate transaminase
GR	Glutathione reductase
GSH	Glutathione
GSSG	Glutathione disulfate
GST	Glutathione-S-transferase
GTP	Guanosine triphosphate
h	Hour(s)
HEPES	2-[4-(2-Hydroxyethyl)piperazin-1-yl]ethane-1-sulfonic acid
IB	Incubation buffer

IC_{50}	Half maximal inhibitory concentration
i.e.	*id est*, that is
IMM	Inner mitochondrial membrane
K_i	Inhibitory constant
K_M	Michaelis-Menten constant
LDH	Lactate dehydrogenase
MAS	Malate-aspartate-shuttle
MCT	Monocarboxylate transporter
ME	Malic enzyme
mg	Milligram
min	Minute
mL	Milliliter
mM	Millimolar
MPC	Mitochondrial pyruvate carrier
MRI	Magnetic resonance imaging
mRNA	Messenger ribonucleic acid
MS	Mass spectrometry
NAD^+	Nicotinamide adenine dinucleotide (oxidized)
NADH	Nicotinamide adenine dinucleotide (reduced)
$NADP^+$	Nicotinamide adenine dinucleotide phosphate (oxidized)
NADPH	Nicotinamide adenine dinucleotide phosphate (reduced)
NBCe	Electrogenic Na^+/HCO_3^- cotransporter
NMR	Nuclear magnetic resonance
PC	Pyruvate carboxylase
PDH	Pyruvate dehydrogenase complex
PDK	Pyruvate dehydrogenase kinase
PDP	Pyruvate dehydrogenase phosphatase
PEP	Phosphoenolpyruvate
PEPCK	Phosphoenolpyruvate carboxykinase
PFK	6-Phosphofructokinase
PFKFB	6-phosphofructo-2-kinase/fructose-2,6-bisphosphatase
3PG	3-Phosphoglycerate
PKM	Pyruvate kinase muscle isoform
PPP	Pentose phosphate pathway
SOD	Superoxide dismutase
ROS	Reactive oxygen species
TCA	Tricarboxylic acid
TNF	Tumor necrosis factor

1 Introduction

1.1 The cells of the brain

1.1.1 Neurons and glial cells

As our brain determines who we are as humans, it is probably the most fascinating but also complex organ. Even though it only accounts for approximately 2 % of our whole-body mass, the brain metabolizes around 20 % of the total glucose consumed at rest (5.6 ± 1.26 mg glucose per 100 g human brain tissue per minute, or 4.7 ± 1.0 g glucose per hour for the whole brain), and is thereby one of our top energy consumers (Wang *et al.* 2012).

The brain is part of the central nervous system (CNS), which also includes the spinal cord (Rua and McGavern 2018). The CNS is surrounded by three layers of connective tissues, the meninges (from out to inside: dura mater, arachnoid mater, pia mater), and a watery liquid that fills the subarachnoid space, the cerebrospinal fluid (CSF) (Rua and McGavern 2018). Since the CNS develops from a neural tube during embryonic development, the brain is a cavity-containing organ, with hollow spaces known as ventricles, also filled with CSF (Greene and Copp 2009, Sweetman and Linninger 2011).

No development of a cell system is as complicated as that of the nervous system. The brain consists of various highly specialized cell types (**Fig. 1-1**). Adjacent cells in the brain can substantially differ in shape, function, and metabolism, resulting in a beneficial but required cooperation between cells (Bonvento and Bolanos 2021, Borst *et al.* 2021, Roumes *et al.* 2023). The most prominent cells in the CNS are neurons, the crucial cells for information processing and signal transduction (Herculano-Houzel 2012, Arendt 2020, Ma *et al.* 2023). With roughly 86 billion neurons in a human brain, they account for around half of the total number of brain cells and are highly specialized and heterogenous (Herculano-Houzel 2012), although fairly vulnerable to changes in their extracellular environment (Verma *et al.* 2022). Neurons differ in their neurotransmitters, morphology, receptor expression, myelination, and many other features, depending on their location, surrounding, and function (Armand *et al.* 2021, Rizo 2022). Neurons are postmitotic. After they have differentiated from proliferating precursor cells into still immature neuroblasts, they no longer divide (Urbach and Witte 2019). Furthermore, the maturing of neurons from immature neuroblasts is

susceptible to disruption, as correct tissue migration, synapse formation, and an ideal environment are crucial for their development, and there is a generation of an excess of immature neuroblasts to compensate for potential cell loss (Lüllmann-Rauch and Asan 2015). Nonetheless, impaired or dying neurons cannot be easily replaced by cell division. Studies have shown the existence of adult neuronal stem cells and neurogenesis, that partially contributes to replacement of damaged neurons (Eriksson *et al.* 1998, Chareyron *et al.* 2021, Guo *et al.* 2022, Petrelli *et al.* 2023). However, this replacement is limited to the hippocampus and the lateral ventricles, and it is insufficient to replace large quantities of neurons (Arzate and Covarrubias 2020). Thus, a stable and suitable environment for healthy neurons is crucial to maintain brain function and to prevent neurodegenerative disease.

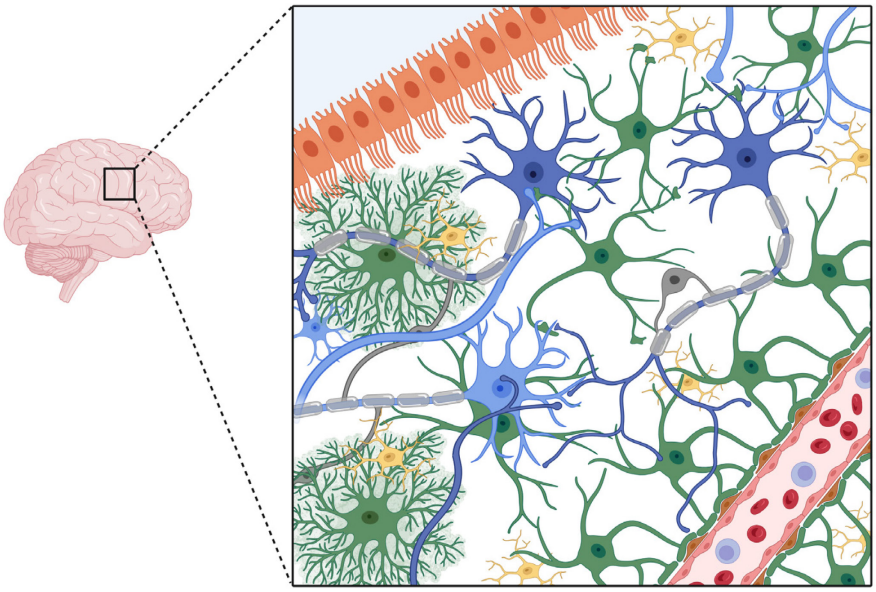

Figure 1-1: Schematic illustration of cell types in the brain. The different cell types of the brain and their connections are shown with no intention to depict real proportions. Blue = neurons, green = astrocytes, grey = oligodendrocytes, ependymal cells = orange, microglia = yellow. Created with Biorender.

This local environment in the brain is provided by glial cells. In general, glial cells can be divided into two groups, microglia and macroglia (Rowitch and Kriegstein 2010). Microglia are the innate immune system of the CNS, and widely spread and evenly distributed (Borst *et al.* 2021). In contrast to neurons and macroglial cells, they are not derived from the neuroepithelium, but immigrated to the CNS during embryonic development (Hattori 2022). Additionally to their immune functions, microglia also mediate synapse remodeling, oligodendrocyte maturing and myelin formation, and contribute to glial scar formation (Borst *et al.* 2021, Zhang *et al.* 2022a). Under homeostatic conditions, microglia have long lifetimes and low proliferation rates that increase upon activation by pro-inflammatory cytokines (Füger *et al.* 2017, Qin *et al.* 2023). Extensive pro-inflammatory activation has

been associated with neurodegenerative disease (Cherry *et al.* 2014, Aldana 2019, Perea *et al.* 2022, Qin *et al.* 2023).

Macroglia are subdivided into three different cell types: Ependymal cells, oligodendrocytes, and astrocytes (Wolburg *et al.* 2009, Rowitch and Kriegstein 2010). Ependymal cells, columnar macroglial cells that create thin epithelia-like boundary structures, line the ventricular surface and the central canal of the spinal cord (Wolburg *et al.* 2009). They are connected solely by gap junctions or leaky tight junctions, thereby enabling exchange between brain tissue and CSF (Wolburg *et al.* 2009). Specialized ependymal cells form the blood-CSF barrier by connections via strong tight junctions in the choroid plexus, circumventricular organs and in the hypothalamus-hypophyseal system. This barrier is essential as the blood vessels in these areas are permeable, e.g., to facilitate the production of CSF in the choroid plexus or to exchange signals from blood to brain and *vice versa* (Wolburg *et al.* 2009). Ependymal cells bear microvilli and kinocilia to sustain CSF movement and thus CSF homeostasis (Wolburg *et al.* 2009, Liu *et al.* 2014, Nelles and Hazrati 2022). Impairment of ependymal cells is associated with a variety of neurodegenerative disease (Nelles and Hazrati 2022).

Oligodendrocytes, the myelinating cells of the CNS, are crucial for the fast forwarding of neuronal signals (Kuhn *et al.* 2019). They are mainly found in the axon-rich white matter, their side of action (Kuhn *et al.* 2019). With protrusions of their plasma membrane, oligodendrocytes connect to neurons and form multiple compact layers around the neuronal axon, myelin (Chen *et al.* 2022), which is highly enriched in lipids in an unusual cholesterol-rich composition (Nave and Werner 2014). Furthermore, oligodendrocytes may also contribute to the nutrition of axons (Nave and Werner 2014). The rapid signal transduction along myelinated axons (saltatory conduction) is facilitated by the nodes of Ranvier, narrow unmyelinated areas in between myelin sheaths that are enriched in voltage-controlled Na^+ and K^+ channels (Eshed-Eisenbach *et al.* 2023).

The last large group of non-neuronal cells in the brain are astrocytes. They play crucial roles in many important processes including brain development (De Majo *et al.* 2020, Lopez-Ortiz and Eyo 2023), (ion) homeostasis (Theparambil *et al.* 2020, Van Putten *et al.* 2021, Lopez-Ortiz and Eyo 2023), protection against oxidative stress and toxins (Dringen *et al.* 2015, Chen *et al.* 2020, Matoba *et al.* 2022), signal transduction (Oliveira and Araque 2022, Andersen and Schousboe 2023b), or brain energy metabolism (Rose *et al.* 2020, Beard *et al.*

2021, Bonvento and Bolanos 2021, Dienel *et al.* 2023, Roumes *et al.* 2023, Rae *et al.* 2024). Their many functions will be described below in more detail.

1.1.2 Astrocytes

Astrocytes were first described in 1891 (von Lenhossék 1891) and named for their star-like shape. Already two years later, the diverse morphology of astrocytes was highlighted (Andriezen 1893). Like neurons and oligodendrocytes, astrocytes develop from neuroepithelial stem cells (Kessaris *et al.* 2008). Astrogenesis starts towards the end of neurogenesis, where different immature progenitors are distributed throughout the brain and develop into distinct mature astrocytes. It is interesting to note that this predominantly happens after previous infiltration by microglia (Reemst *et al.* 2016). Even though astrocytes appear quite late during brain development, they play crucial roles in distribution and stabilization of blood vessels, blood-brain barrier formation, neuronal stem cell migration and proliferation, guidance of axons, synaptogenesis, synapse elimination, and overall neuronal survival (**Fig. 1-2**) (Reemst *et al.* 2016, De Majo *et al.* 2020, Lopez-Ortiz and Eyo 2023). Later in life, astrocytes also participate in memory formation by, e.g., modulating signal transmission and synaptic plasticity (**Fig. 1-2**) (Bohmbach *et al.* 2023, Marty-Lombardi *et al.* 2024). Superficially, astrocytes can be divided into two groups (Zhang and Barres 2010). Fibrous astrocytes, which possess a few long and rather straight processes, and are mainly found in the white matter. Secondly, protoplasmic astrocytes, which are bushy with many branched processes, and are more frequently found in the grey matter, the area enriched with neuronal cell bodies (Zhang and Barres 2010).

1.1.2.1 Role in distribution and clearance processes

Astrocytes play an important role in the distribution of peripheral substrates into the brain as they cover blood vessels with their end feet (Daneman and Prat 2015, Cheslow and Alvarez 2016). Astrocytic processes or end feet connect astrocytes among themselves, other glial cells, neurons, synapses or capillary endothelial cells. By gap junctions, intercellular channels that consist of two connected hemichannels with six oligomerized connexins each, astrocytes are connected with adjacent astrocytes or oligodendrocytes (Orthmann-Murphy *et al.* 2008). This tight network of glia cells allows an easy, fast, and widespread distribution of signals and metabolic substrates (**Fig. 1-2**), forming an extensive functional network (Rose *et al.* 2020). Astrocytes play a pivotal role particularly for the provision of energy substrates

to neurons, as neurons have only limited storage capacities and limited access to energy-providing compounds (Weber and Barros 2015, Bonvento and Bolanos 2021, Roumes *et al.* 2023). As cells with high energy demand, neurons need a fast, sufficient and continuous energy supply, which is among others facilitated by astrocytes (Vergara *et al.* 2019, Roumes *et al.* 2023). Overall, astrocytes and their metabolism play a central role in the brain energy metabolism (Bonvento and Bolanos 2021, Dienel *et al.* 2023, Rae *et al.* 2024).

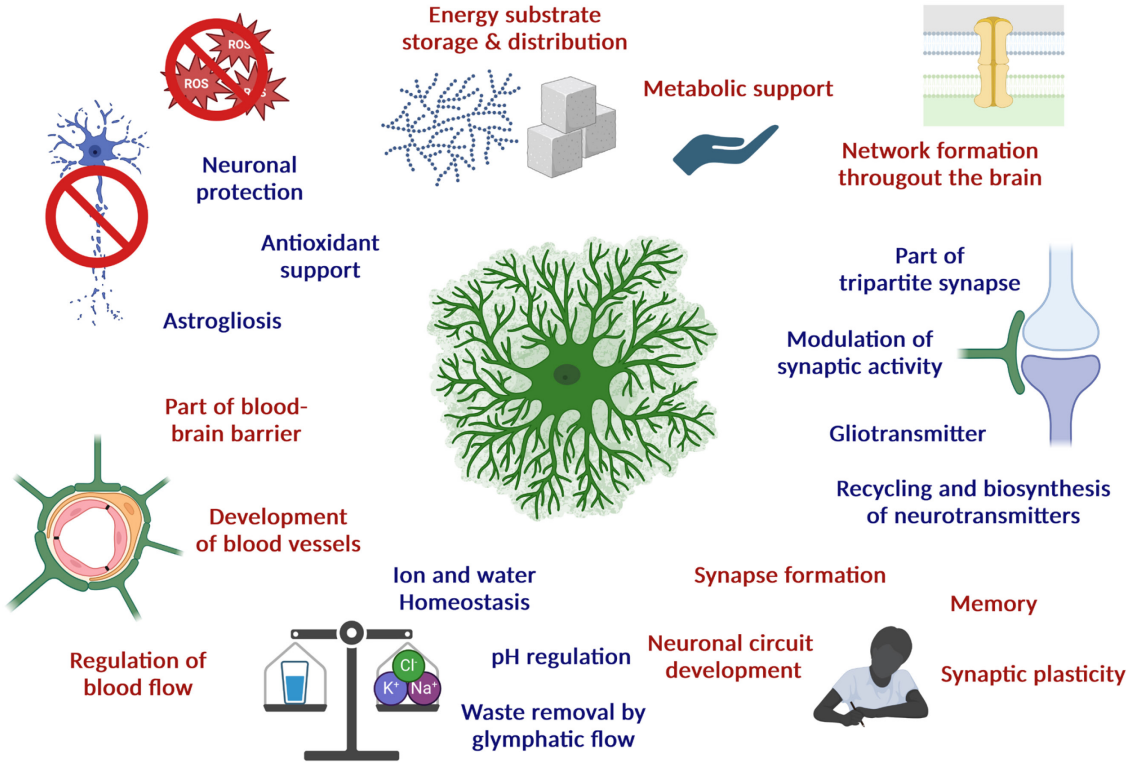

Figure 1-2: Visualization of crucial functions and processes involving astrocytes in the brain. Created with Biorender.

Astrocytes play an important role in the establishing and maintenance of the blood-brain barrier (BBB; **Fig. 1-2**) (Kadry *et al.* 2020, Pociute *et al.* 2024). Their end feet form the outer barrier (glia limitans), and outline a tunnel-shaped perivascular space in which blood vessels are located (Daneman and Prat 2015). These blood vessels consist of endothelial cells connected by tight junctions, and are surrounded by a thin basal lamina consisting of extracellular matrix components such as laminin, collagen IV, fibronectin, and heparan sulphate proteoglycan (Liebner *et al.* 2000, Halder *et al.* 2022). Pericytes, cells that are necessary for correct BBB formation and function, are embedded in this basal lamina (Bell *et al.* 2010, Daneman *et al.* 2010). Astrocytes do not only provide structure, but also regulate the size of blood vessels, the number of junctional proteins between endothelial cells, and the permeability and function of the BBB in general (Cheslow and Alvarez 2016).

In addition to their contribution to the BBB (Kadry *et al.* 2020), astrocytes play a vital role in the brain's waste clearance system for macromolecules (**Fig. 1-2**) (Jessen *et al.* 2015, Rasmussen *et al.* 2022). This system, known as the glymphatic system, is crucial due to the absence of the traditional lymphatic system in the brain (Jessen *et al.* 2015). CSF, penetrating into the brain parenchyma alongside the blood vessels in the relatively loose basal lamina driven by arterial wall pulsatility, can pass the astrocytes and enter the parenchyma via aquaporin-4 (AQP4), a water channel known to be involved in water and ion homeostasis (Hubbard *et al.* 2015, Jessen *et al.* 2015, Rasmussen *et al.* 2022). The surplus of interstitial fluid created by the CSF inflow into parenchyma is drained via paravenous routes established by astrocyte end feet covering veins, thereby creating a flow which passively clears the brain of macromolecules (Iliff *et al.* 2012, Rasmussen *et al.* 2022). Consequently, AQP4 is highly expressed in astrocytes adjacent to arteries, veins, ventricle, and the subarachnoid space (Hubbard *et al.* 2015). Furthermore, the flux and clearance of solutes was severely impaired in mice lacking AQP4 (Iliff *et al.* 2012). During sleep or anesthesia, clearance by the glymphatic flow is enhanced due to an increased extracellular space in consequence of reduced noradrenergic signaling (Xie *et al.* 2013). In contrast, astrocytic swelling upon inflammatory stimuli (Goshi *et al.* 2020) or AQP4 increase after, e.g., traumatic brain injury (Kapoor *et al.* 2013) leads to impaired CSF and interstitial fluid flow (Plog and Nedergaard 2018). This could lead to a reduced clearance of released cytokines, enhancing inflammation and pathophysiological changes (Rasmussen *et al.* 2022). In addition to waste clearance, the glymphatic system contributes to paracrine signaling and distribution of nutrients or therapeutic agents throughout the brain (Plog and Nedergaard 2018).

1.1.2.2 Involvement in neurotransmission

With its fine processes, a single astrocyte was estimated to interact with an impressive number of up to 600 dendrites and around 140,000 synapses (Bushong *et al.* 2002, Halassa *et al.* 2007). Particularly at glutaminergic synapses, astrocytes perform protective and regulatory tasks, actively contribute to information processing of the brain, which consolidated the concept of a "tripartite synapse" (**Fig. 1-2**) (Lalo *et al.* 2021). Glutamate, the most abundant excitatory neurotransmitter in the brain, can overstimulate neurons if not scavenged properly from the synaptic cleft, leading to excitotoxicity and cell death (Zhou and Danbolt 2014, Andersen *et al.* 2021). Compared to astrocytes, neurons express relatively little glutamate transporters (Todd and Hardingham 2020). They rely on

astrocytes to take up excessive glutamate via excitatory amino acid transporters (EAAT) and maintain a non-toxic, homeostatic environment (Brown 1999, Mahmoud *et al.* 2019, Todd and Hardingham 2020). Those high affinity transporters facilitate the unfavourable glutamate import by simultaneous import of one H^+, three Na^+, and antiport of one K^+ (Todd and Hardingham 2020). According to their need, EAATs are enriched in astrocytic processes connected to glutaminergic synapses (Zhou and Sutherland 2004, Todd and Hardingham 2020). By glutamate uptake, astrocytes not only protect neurons, but also actively regulate and modulate the signal transmission (**Fig. 1-2**) (Lalo *et al.* 2021). Furthermore, astrocytes express different ionotropic and metabotropic glutamatergic receptors (Lalo *et al.* 2021). The activation of these receptors has been shown to modulate EAAT activities (Lalo *et al.* 2021), and to result in a Ca^{2+}-mediated rapid increase in EAATs in the extracellular membrane that are integrated from intracellular EAAT clusters (Al Awabdh *et al.* 2016). To a smaller extent, astrocytes also contribute to γ-aminobutyric acid (GABA) homeostasis, the brain's most abundant inhibitory neurotransmitter, via specific GABA transporters (GATs) (Schousboe *et al.* 2013, Andersen *et al.* 2020). Furthermore, astrocytes play an important role in the recycling and maintenance of both, the neuronal glutamate and GABA pools (Hertz and Rothman 2016, Andersen *et al.* 2020, Andersen *et al.* 2021, Andersen and Schousboe 2023b).

In the recent past, astrocytes were revealed to release so-called "gliotransmitters" upon neuronal activation through a variety of neurotransmitters (Oliveira and Araque 2022). In contrast to neurons, astrocytes lack electrical excitability, but waves of Ca^{2+} can be observed propagating from one astrocyte to another upon neuronal activation (Schipke and Kettenmann 2004). As a consequence, gliotransmitters are released (Lalo *et al.* 2021, Wang *et al.* 2023). Additionally, Ca^{2+}-independent mechanism have also been described (Wang *et al.* 2023). Those small neuroactive molecules such as adenosine, ATP, D-serine, or even GABA or glutamate can enable bidirectional communication, shape synaptic activity, and were shown to stimulate axonal regeneration (Goenaga *et al.* 2023, Wang *et al.* 2023). For instance, the release of purinergic gliotransmitters by astrocytes increased the excitation of sleep-promoting neurons via a stimulation of synaptic adenosine A1 receptors (Choi *et al.* 2022).

To ensure ongoing neuronal firing, regulation of extracellular ion concentrations is crucial. Astrocytes play a central role in maintaining brain K^+ homeostasis, which is released by neurons to reestablish the resting membrane potential (Larsen *et al.* 2016, Bataveljic *et al.*

2024). Astrocytes express a multitude of transporters through which the K^+ influx against the concentration gradient is mediated (Olsen *et al.* 2015, Bataveljic *et al.* 2024). Two main contributors for the K^+ uptake are discussed: The ATP-dependent Na^+/K^+-ATPase, one of the cell's most energy-consuming structures (Harris *et al.* 2012), facilitates K^+ influx and Na^+ efflux against their concentration gradients to maintain the transmembrane ion gradient (Larsen *et al.* 2016). Furthermore, at high extracellular K^+ concentrations, the glia-specific K^+-channel Kir4.1 contributes to K^+ influx, and is thought to use the hyperpolarized resting membrane potential for K^+ import since it does not rely on ATP for transport (Larsen *et al.* 2014, Olsen *et al.* 2015). Impairment of both, astrocytic Na^+/K^+-ATPase and Kir4.1, was connected to elevated extracellular K^+ concentrations, impaired glutamate uptake, neuronal hyperactivity, and ultimately to pathologies such as epilepsy, neurodegenerative disease, or neurodevelopmental disorders (Albrecht and Zielińska 2017, Kahanovitch *et al.* 2018, Sun *et al.* 2022).

1.1.2.3 Defense in oxidative stress and inflammation

Astrocytes contribute to the flux-mediated clearance of potential toxic waste (Rasmussen *et al.* 2022). Further, they locally protect the surrounding tissue against toxins and oxidative stress caused by reactive oxygen species (ROS) (**Fig. 1-2**) (Chen *et al.* 2020). ROS, which include the superoxide anion radical ($O_2^{\cdot-}$), hydrogen peroxide (H_2O_2), peroxides in general (R-O-O-H (or R)), and the highly active hydroxyl radical ($\cdot OH$) (Fridovich 1999), are continuously produced in the brain at high rate due to brains high energy demand and resulting high metabolic activity (Lee *et al.* 2021). Particularly during oxidative phosphorylation, ROS is formed, as single electrons are transported in several steps of the respiratory chain, which increases the likelihood of superoxide formation (Fridovich 1999). High ROS levels can damage macromolecules such as DNA, lipids, and proteins, thereby impairing cellular functions (Lee *et al.* 2021), and an imbalance between oxidative stress and defense mechanisms has been shown to play a crucial role in many neurodegenerative disorders (Kim *et al.* 2015). Astrocytes, that are less vulnerable to oxidative stress than neurons (Schmuck *et al.* 2002), were shown to effectively scavenge H_2O_2, and to protect neurons from ROS induced cell toxicity (Dringen and Hamprecht 1997, Wang and Cynader 2001, Watts *et al.* 2005, Bell *et al.* 2011). As a primary defense mechanism, astrocytes express high levels of superoxide dismutase (SOD) and catalase (Copin *et al.* 1992, Dringen and Hamprecht 1997). These enzymes detoxify $O_2^{\cdot-}$ to H_2O_2 and oxygen, and H_2O_2 to water and oxygen, respectively (Hodgson and Fridovich 1975, Glorieux and Calderon 2017).

Furthermore, astrocytes have been shown to express glutathione peroxidase (GPx) and glutathione reductase (GR), as well as glutathione-S-transferase (GST) for the defense against oxidative stress and xenobiotics (Copin *et al.* 1992, Dringen and Hamprecht 1997, Matoba *et al.* 2022). Glutathione (GSH), a tripeptide consisting of glycine, cysteine and glutamate, is present in astrocytes in millimolar concentrations (Dringen *et al.* 2015), and acts as a strong nucleophile (Mayer and Ofial 2019). It can either covalently conjugate to electrophiles, e.g. reactive aldehydes, donate electrons to radicals, or serve as a cofactor or substrate for enzymatic detoxification (Dringen *et al.* 2015, Mayer and Ofial 2019). GPx and GR take part in the GSH-GSSG redox cycle, were GPx mediates the GSH-dependent peroxide reduction generating glutathione disulfide (GSSG), and GR reduces GSSG back to GSH in a NADPH-dependent reaction (Dringen *et al.* 2015). The phase-II enzyme GST mediates the covalent coupling of GSH to endogenous substrates or xenobiotics, that are usually detoxified as a result, and transported out of the cells by multidrug resistance proteins (Mrp's) (Dringen *et al.* 2015, Arend *et al.* 2024), which are ATP-binding cassette (ABC) transporters (Cole 2014). Not only GSH-conjugates, but also GSSG and GSH itself are released by astrocytes, mainly mediated by Mrp1 (Hirrlinger and Dringen 2005, Arend *et al.* 2024), but also by hemichannels under pathophysiological conditions (Rana and Dringen 2007). In the extracellular space, GSH can be broken down into its components, which can be taken up by neurons, fueling their neuronal GSH synthesis and thereby enhancing their resilience against oxidative stress (Dringen *et al.* 2001, Ruedig and Dringen 2004, Pérez-Sala and Pajares 2023).

Nonetheless, it is important to emphasize that reactive species, especially H_2O_2, are not only toxic by-products of metabolism, but also important signaling molecules (Rampon *et al.* 2018, Tauffenberger and Magistretti 2021, Vicente-Gutierrez *et al.* 2021). Signaling H_2O_2 is believed to be mainly produced by membrane-bound NADPH oxidase complexes (NOX), of which several isoforms are expressed in astrocytes (Reinehr *et al.* 2007, Rampon *et al.* 2018). Furthermore, astrocytic derived mitochondrial ROS was shown to modulate astrocytic metabolism, and even overall behavior and cognitive functions in mice (Vicente-Gutierrez *et al.* 2019).

Astrocytes do not only play an essential role in the healthy brain. Upon tissue damage or inflammation, nearby astrocytes can undergo a complex process called "astrogliosis" (**Fig. 1-2**), that is characterized by diverse changes in gene expression, morphology, and function (Sofroniew 2015, Liddelow *et al.* 2024). Those "reactive astrocytes" can be regulated by a

variety of extracellular effector molecules like cytokines, transmitters, or serum proteins released from damaged blood vessels, whereby they themselves respond by releasing effectors (Sofroniew 2015, Liddelow *et al.* 2024). It depends on the context whether the changes are advantageous or disadvantageous (Liddelow *et al.* 2024). In mouse models of spinal cord injury, an impaired astrogliosis lead to increased inflammation and neuronal malfunction (Okada *et al.* 2006). In contrast, cytokines released by astrocytes can induce damage to the surrounding tissue. Cultured astrocytes were shown to release TNFα, a pro-inflammatory cytokine, upon stimulation by the microglial pro-inflammatory cytokines (Schlotterose *et al.* 2023). Furthermore, severe injury has been shown to lead to a strong astrogliosis with astrocytic proliferation and formation of densely packed cell layers and, under contribution of microglia, non-neuronal cells, and extracellular matrix components, even to the formation of a glial scar (Sofroniew and Vinters 2010, Perez *et al.* 2021). Although this glial scar shields the CNS from potential danger such as an escalating immune response or toxins, its compact form also prevents axon regrowth and impacts functional recovery (He *et al.* 2020).

1.1.3 Astrocyte cultures as model systems to study the brain

To investigate the properties of a specific brain cell type, complex systems like whole brains or cell organoids may prove unsuitable due to challenges in distinguishing individual cells. Cell culture systems offer a solution by providing cell type enriched (Tulpule *et al.* 2014), or even single cell type (Yeh and Hsu 2019) cultures, thereby reducing system complexity and highlighting the characteristics of a given cell type. This focused approach offers the opportunity to analyze differences in metabolic pathways and to make initial assessments of their implications in cell networks (Andersen *et al.* 2021, Qi *et al.* 2021, Morant-Ferrando *et al.* 2023). In the presented thesis, rat primary astrocyte cultures, derived from neonatal Wistar rats, were used to study the pyruvate metabolism of astrocytes. Briefly, the cells were harvested within a maximum of 24 h postnatal, and were plated with a density of approximately 300,000 viable cells per mL and well of a 24-well plate (Tulpule *et al.* 2014). The cell culture medium (DMEM containing 25 mM glucose and 10 % fetal calf serum) was changed every seventh day and one day prior to experiments to guarantee standardized conditions. These cultures contain mainly glial fibrillary acidic protein (GFAP)-positive astrocytes (**Fig. 1-3**), but also minor contaminations of oligodendrocytes, microglia and ependymal cells (Hamprecht and Löffler 1985, Petters and Dringen 2014, Tulpule *et al.*

2014). If not stated otherwise, cells were maintained for at least 14 days to ensure confluence (**Fig. 1-3**), but were not used for more than 28 days after seeding. Aspects of the pyruvate metabolism of primary rat astrocytes were shown to vary with culture age (see **Chapter 2.2**),. Efforts were made to minimize variations in the culture age within an experiment in order to prevent inaccuracies.

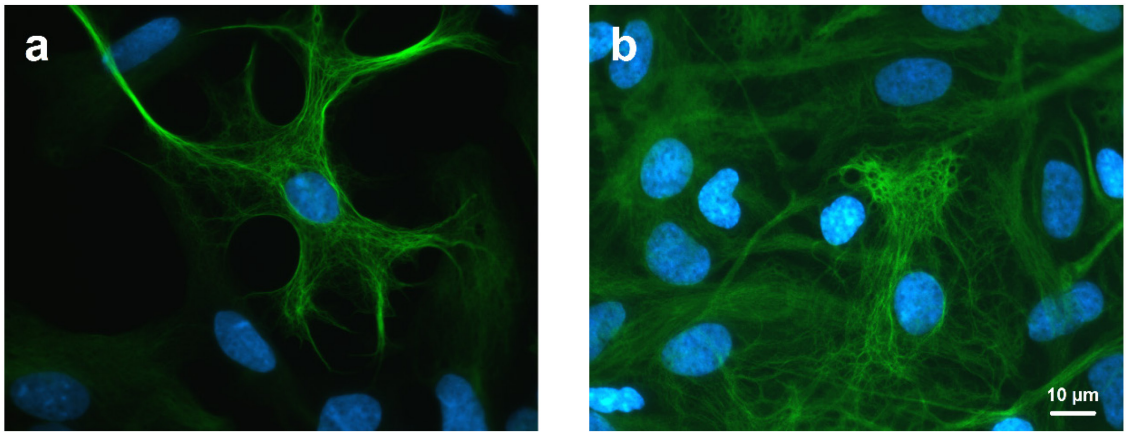

Figure 1-3: GFAP staining of maturing or confluent rat astrocyte cultures. Cultured astrocytes were fixes and stained for glial fibrillary acidic protein (GFAP; green) after 7 d (**a**) and 14 d (**b**) of seeding with a GFAP antibody (diluted 1:500) and a Cy2 conjugated secondary antibody (diluted 1:200). Cell nuclei (blue) were stained with DAPI (1 µg/ml). The primary antibody was purchased from Agilent (Santa Clara, USA), the secondary antibody from BIOZOL (Eching, Germany), and DAPI was purchased from Sigma-Aldrich (Darmstadt, Germany).

Various types of astrocyte cultures are frequently used as astrocyte models, e.g., primary cultures, immortalized astrocytes from a primary origin, or C6 cells from rat glioma (Galland *et al.* 2019). In direct comparison with immortalized cell cultures, primary astrocytes have been demonstrated to be the favorable model system, as their features correlated more closely to *in vivo* findings (Galland *et al.* 2019). In general, primary cultures are enriched in the respective cell type of interest. There are different protocols to produce primary astrocyte cultures, but all seem to result in a purity of around 95 % (Tulpule *et al.* 2014, Galland *et al.* 2019). Impurities, primarily consisting of small quantities of glial cells like oligodendrocytes, microglia, and ependymal cells (Hamprecht and Löffler 1985, Tulpule *et al.* 2014), must be considered. These impurities can render these cell cultures unsuitable for certain experimental approaches. Furthermore, the origin of the cell culture must be taken into consideration, since, e.g., human astrocytes from neocortex are 2.6-fold larger in diameter and more complex compared to their rodent analogue, suggesting that human astrocytes are able to envelop more synapses (Oberheim *et al.* 2009).

Since astrocytes develop and mature rather late (Reemst *et al.* 2016), their maturation is not fully complete when harvested from newborn rats (Lange *et al.* 2012). The artificial maturation via addition of fetal calf serum ensures the expression of important astrocytic enzymes, but cannot fully compensate the diverse signals caused by different extracellular milieus *in vivo* (Lange *et al.* 2012). Moreover, as different astrocytes might originate from different progenitors prior to harvesting (Reemst *et al.* 2016), there could already be a mixture of differently primed astrocytes with different gene expression. Nonetheless, several observations made for astrocytes on cell cultures could be transferred *in vivo* (Hertz *et al.* 2017, Schousboe *et al.* 2019, Theparambil *et al.* 2020). Especially with regard to metabolic questions, primary astrocytes seem to be a good model, since their gene expression of metabolic enzymes closely resemble that of freshly isolated astrocytes (Hertz *et al.* 2007, Lovatt *et al.* 2007, Lange *et al.* 2012). Moreover, primary cultures have proven to be important for studying the mechanisms of astrocytic involvement in various pathologies (Lange *et al.* 2012).

Astrocytic proliferation in astrocyte mono-cultures, or in co-cultures with oligodendrocytes was shown to be contact-inhibited when cell density increased (Nakatsuji and Miller 1998). Regulatory membrane proteins, as well as a changed composition of cell-cycle proteins were proposed to be involved in this contact inhibition in astrocytes (Nakatsuji and Miller 2001, Lanosa and Colombo 2008). Non-proliferating astrocyte cultures seem to be good models to investigate the metabolism of adult brain cells rather than proliferating cell cultures, as mature astrocytes do not proliferate if not triggered (Nakatsuji and Miller 2001, Sofroniew and Vinters 2010). Furthermore, non-proliferating cultures are more homogeneous in their protein composition (Nakatsuji and Miller 2001), hence the results obtained are less disturbed by inter-individual differences in the proliferation stage.

Even though astrocyte cultures are great to study individual aspects and underlying mechanism, it is an isolated system and the obtained findings have to be verified in the broader context. Co-cultures might partially help to overcome that obstacle (Goshi *et al.* 2020), but are still far from *in vivo*. Nevertheless, if these limitations are considered, cell cultures are powerful and relatively easy-to-use tools for investigations of special features of cell types.

1.2 Pyruvate: Chemistry and metabolism

Pyruvate, the deprotonated form of pyruvic acid (German: "Brenztraubensäure", 2-Oxopropanoic acid; **Fig. 1-4a**), was first isolated 1834 by the French chemist Théophile-Jules Pelouze, and a year later discovered by the Swedish chemist Jöns Jacob Berzelius (Berzelius 1835). Berzelius named it after his first method of isolation: Dry distillation of tartaric acid or its racemate (German: "Wein-" or "Traubensäure"(racemate); **Fig. 1-4b**), where *pyr* is derived from ancient Greek for *fire* (German: "Feuer", maybe "Brennen"), and *uva* from Latin for *grape* (German: Traube) (Berzelius 1835). In this method, dry tartaric acid was distilled at around 200°C. The resulting product was then distilled a second time in a water bath, fractioning into two parts, leaving the pyruvic acid in the second yellowish, viscous fraction (**Fig. 1-4c**) (Berzelius 1835).

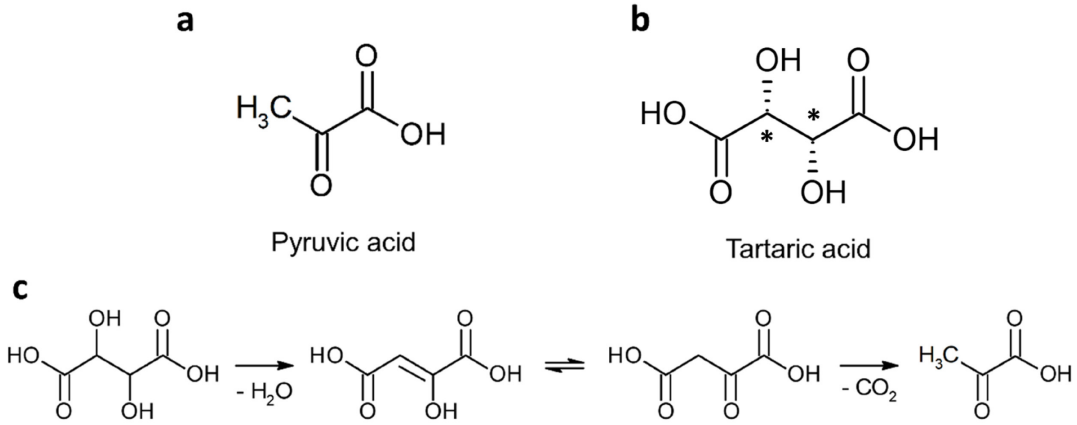

Figure 1-4: Pyruvic acid was first isolated and discovered from tartaric acid. While pyruvic acid (**a**) with its α-keto function has no chiral center, tartaric acid (**b**) has two. The chiral centers are marked with *. During dry distillation, tartaric acid pyrolyzes under heat and forms a compound that can exhibit keto-enol tautomerism (**c**). This β-ketoacid decarboxylates to pyruvic acid (**c**) Reaction mechanism after Moldoveanu (Moldoveanu 2010). Created with ChemSketch.

In its pure form, pyruvic acid (Molecular weight: 88.06) is a transparent liquid with an acetic acid-like smell that is miscible with water, alcohol, and ether (O'Neil *et al.* 2006). With a pK_S (25°C) value of 2.49 (O'Neil *et al.* 2006), over 99.99 % of pyruvic acid at neutral pH is present in its deprotonated form, pyruvate.

For a greater yield of pyruvic acid, tartaric acid can be distilled at 220°C in the presence of potassium hydrogen sulphates as dehydrating agents, followed by separation under vacuum (Li *et al.* 2001). But as this is quite costly, pyruvic acid today is produced mostly biotechnologically, typically by yeast or *Escherichia coli* (Li *et al.* 2001, Yuan *et al.* 2022). As pyruvate has a carboxyl as well as a keto group, it can be used as a precursor molecule for

the synthesis of a variety of compounds by industry, e.g. the drug L-DOPA (Park *et al.* 1998) or the essential amino acid L-tryptophan (Li *et al.* 2001).

In many living organisms, pyruvate is as the end product of glycolysis a key metabolic intermediate that links cytosolic and mitochondrial metabolism (**Fig. 1-5**), with several unique beneficial biological properties including antioxidative and anti-inflammatory effects. One glucose that enters glycolysis yields two pyruvates, and a net profit of 2 ATP (Dienel 2019a). After uptake into mitochondria, pyruvate can be completely oxidized to CO_2. In a first pyruvate dehydrogenase complex (PDH)-mediated step, pyruvate is decarboxylated, and acetyl-CoA is formed (Stacpoole 2017). Subsequently, acetyl-CoA enters the tricarboxylic acid (TCA) cycle, where the two remaining carbons are oxidized to CO_2 (Borkum 2023). The reducing agents (NADH, $FADH_2$) formed in the TCA cycle enable proton transport over the inner mitochondrial membrane via the respiratory chain, and the established proton gradient is used for ATP formation via ATP synthase (Rich and Marechal 2010). Aerobic mitochondrial energy production is more efficient than glycolysis, producing around 15 times more ATP (Dienel 2019a).

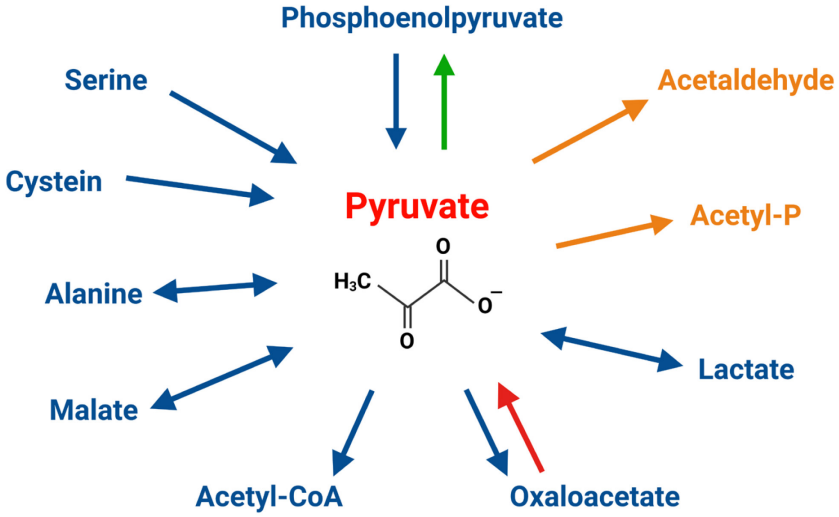

Figure 1-5: Enzymatic and spontaneous formation and conversion of pyruvate. Unidirectional arrows indicate irreversible reactions, while bidirectional arrows indicate reversible reactions. The blue, green, and orange arrows represent enzymatically catalyzed reactions. The green arrow denotes a reaction present only in plants and microorganisms. The orange arrows and texts represent reactions present only in microorganisms. The red arrow indicates the spontaneous decarboxylation of the β-keto acid oxaloacetate to pyruvate. P = phosphate. Created with Biorender.

Under anaerobic conditions, pyruvate undergoes reduction to lactate by lactate dehydrogenase (LDH) with simultaneous oxidation of NADH to NAD^+ to ensure the continuation of glycolysis (Pineda *et al.* 2007). In highly active and proliferating cells, e.g., cancer cells, metabolism is shifted to a more glycolytic state, and the pyruvate reduction

also takes place to a greater extent in an oxygen-rich environment (aerobic glycolysis) (Barros *et al.* 2021).

However, pyruvate is not just a metabolic intermediate that enables energy production. In mitochondria, pyruvate can also be carboxylated to oxaloacetate via pyruvate carboxylase (PC), and oxaloacetate can enter the TCA cycle to replenish intermediates that have been used elsewhere for biosynthesis (Utter and Keech 1963, Schousboe *et al.* 2019). Furthermore, pyruvate is the starting point of gluconeogenesis, a process that mainly takes place in the liver and kidneys (Sahoo *et al.* 2023), but also in astrocytes (Dringen *et al.* 1993b, Yip *et al.* 2016). Depending on the tissue, gluconeogenesis serves to locally refill glycogen levels (Dringen *et al.* 1993b), or to maintain stable blood glucose concentrations in situations of deficiency (Yip *et al.* 2016).

Pyruvate can not only be derived from glucose, but also from alternative energy substrates, such as mannose or fructose, which can be converted into intermediates of glycolysis (Dringen *et al.* 1994, Bergbauer *et al.* 1996). In the liver, pyruvate can even be produced from glycerol that was derived from lipolysis and channeled into glycolysis (Jin *et al.* 2023). Upon protein degradation or utilization of amino acids from food, some glucogenic amino acids can be transformed into pyruvate. In a reversible transamination mediated by the alanine amino transferase (ALAT), also named glutamate pyruvate transaminase (GPT), alanine is transaminated to pyruvate while α-ketoglutarate is converted to glutamate (Bröer *et al.* 2007). Conversely, alanine is also formed from pyruvate, a reaction that is used by muscle cells, e.g., to remove excess ammonium produced by a breakdown of amino acids during increased activity (Sarabhai and Roden 2019). Ammonium is continuously fixed by amidation of α-ketoglutarate to glutamate, and the alanine formed from subsequent glutamate transamination by ALAT is transported to the liver for further processing (Sarabhai and Roden 2019). Serine in turn can be converted to pyruvate by ammonium release in a reaction catalyzed by serine dehydratase (Foltyn *et al.* 2005). Other amino acids that were reported to provide pyruvate include cysteine, and glycine (Yu *et al.* 2019, McBride *et al.* 2024). Via oxaloacetate production, pyruvate contributes to aspartate generation, and downstream of the TCA cycle also to glutamate production via α-ketoglutarate (Schousboe *et al.* 2013, Schousboe *et al.* 2019). By gluconeogenesis, pyruvate is even linked to the synthesis of serine, glycine, and cysteine via 3-phosphoglycerate (Maugard *et al.* 2021).

Additionally, pyruvate provides carbon for cytosolic fatty acid synthesis. Acetyl-CoA derived from pyruvate in mitochondria leaves mitochondria as citrate, which was derived from

acetyl-CoA and oxaloacetate in the TCA cycle. In the cytosol, acetyl-CoA is again formed, and can enter fatty acid synthesis (Szutowicz and Lysiak 1980, Rose *et al.* 2020). The simultaneously released oxaloacetate can be reduced to malate, and this malate could facilitate efflux of another citrate from mitochondria via the citrate/malate-exchanger (Rose *et al.* 2020). Furthermore, pyruvate can be derived from malate by reversible oxidative decarboxylation catalyzed by cytosolic or mitochondrial NAD^+- or $NADP^+$-dependent malic enzyme (ME), yielding NADH or NADPH, of which the latter could be used for fatty acid synthesis (Chang and Tong 2003).

In general, metabolic pathways like glycolysis and energy producing processes that utilize pyruvate are highly conserved between species (Peregrín-Alvarez *et al.* 2009). Nevertheless, some individuals have additional metabolic pathways that use pyruvate. For example, the yeast *Saccharomyces cerevisiae* produces acetaldehyde and subsequently ethanol from pyruvate during alcoholic fermentation (Rieger *et al.* 1983), or produces cytosolic acetyl-CoA via a pathway involving a cytosolic pyruvate decarboxylase (Pronk *et al.* 1994). Interestingly, the pathway of alcoholic fermentation can even be present in obligate aerobe species (Lockington *et al.* 1997). In different microorganisms, pyruvate is oxidized to acetyl-phosphate to facilitate a subsequent ATP production by an acetate kinase (Hertzberger *et al.* 2013, Lian *et al.* 2014). In plants adapted to hot, sunny, and/or dry weather, pyruvate is part of the C_4-pathway that allows increased CO_2 fixation and accumulation near active chloroplasts by upstream binding and local release of CO_2 (Gowik and Westhoff 2011). In this context, pyruvate can be directly phosphorylated to phosphoenolpyruvate (Gowik and Westhoff 2011).

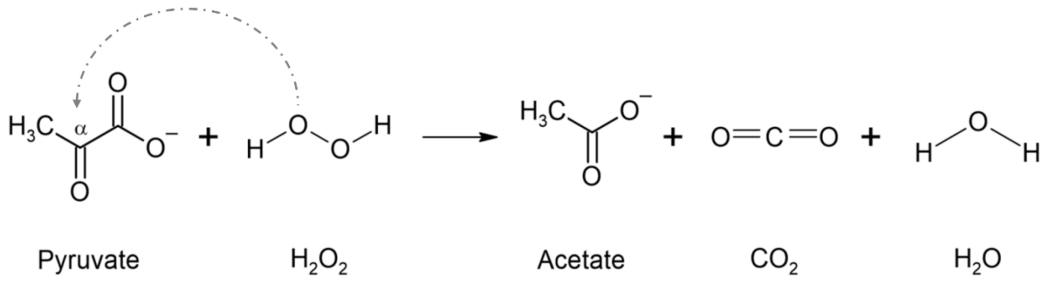

Figure 1-6: Chemical decarboxylation of pyruvate by hydrogen peroxide (H_2O_2). Pyruvate and H_2O_2 react under physiological conditions to acetate, CO_2 and H_2O. The α-carbonyl group is labeled with α and the nucleophilic attack by H_2O_2 is indicated by the gray dashed arrow. Created with ChemSketch.

Pyruvate as an α-keto acid is able to detoxify hydrogen peroxide by chemical decarboxylation (**Fig. 1-6**) (Guarino *et al.* 2019). The nucleophilic attack of an oxygen of hydrogen peroxide at the α-carbonyl group of pyruvate forms an unstable intermediate,

which decomposes to acetate, CO_2, and water (**Fig. 1-6**) (Guarino *et al.* 2019). This H_2O_2-scavanging effect is not specific to pyruvate, but was also shown for other α-keto acids (Nath *et al.* 1995). Pyruvate is also able to reduce the strong oxidizing agent peroxynitrite, the reaction product of nitric oxide and superoxide anion. Here, two acetate and CO_2 are formed, and nitrite is formed instead of water (Vásquez-Vivar *et al.* 1997). In cell culture medium, pyruvate is often added as a protective antioxidant, which seems to be especially important for cells plated in low density (O'Donnell-Tormey *et al.* 1987, Giandomenico *et al.* 1997). Additionally, application of pyruvate has been shown to have various positive effects on cell cultures or *in vivo* (**Table 1-1**), demonstrating its beneficial properties, in addition to its clear crucial functions in cellular metabolism.

Table 1-1: Exemplary list of pathological conditions, disease or other circumstances that are positively improved by externally supplied pyruvate.

Biological system	Conditions improved by externally supplied pyruvate	Reference
Central nervous system	Ischemia	(Lee *et al.* 2001, Ryou *et al.* 2012)
	Leigh syndrome	(Koga *et al.* 2012)
	Neuronal survival	(Selak *et al.* 1985)
	Oxidative stress	(Desagher *et al.* 1997, Wang and Cynader 2001)
Cardio vascular system	Dilated cardiomyopathy	(Hermann *et al.* 1999)
	Failing myocardium	(Hasenfuss *et al.* 2002)
	Haemorrhagic shock	(Mongan *et al.* 1999, Mongan *et al.* 2001, Koustova *et al.* 2003, Hu *et al.* 2013)
	Hypoxic cardiac event	(Zabielska *et al.* 2018)
	Ischemia	(Petrat *et al.* 2011, Mallet *et al.* 2018)
	Oxidative stress	(Plotnikov *et al.* 2019)
Renal system	Diabetic nephropathy	(Zhang *et al.* 2020)
Overall system	Athletic endurance	(Jäger *et al.* 2008)
	Systemic inflammation	(Effenberger-Neidnicht *et al.* 2019)
Non-mammal systems	Lifespan in fly	(Xu *et al.* 2024)
	Oxidative stress in fungi	(Zhang *et al.* 2018)
	Resistance against water deficiency in sugarcane	(Dias *et al.* 2024)

1.3 Pyruvate metabolism in astrocytes

1.3.1 Cytosolic pyruvate formation and metabolism

In astrocytes as a rather glycolytic cell type, pyruvate is primarily derived via glycolysis from glucose, the brain's main energy substrate (Dienel 2019a, Beard *et al.* 2021, Bonvento and Bolanos 2021, Rae *et al.* 2024). Per mol glucose consumed, glycolysis yields 2 mol pyruvate, 2 mol ATP and 2 mol NADH (**Fig. 1-7**) (Dienel 2019a). In astrocytes, glycolysis is described to be highly active due to the high expression of phosphofructo-2-kinase/fructose-2,6-bisphosphatase 3 (PFKFB3) (**Fig. 1-7**), an isoform of PFKFB with high kinase activity (Bonvento and Bolanos 2021). This enzyme facilitates the phosphorylation of fructose-6-phosphate to fructose-2,6-bisphosphate. Fructose-2,6-bisphosphate increases the activity of 6-phosphofructokinase-1 (PFK1), a pivotal regulatory enzyme of glycolysis, being its most potent allosteric activator (Bonvento and Bolanos 2021). Glycolytic pyruvate production by astrocytes was shown to be upregulated by extracellular ATP application in a Ca^{2+}-dependent manner, and by glutamate application in a Na^{+}-dependent manner (Juaristi *et al.* 2019). The extracellular application of both, ATP and glutamate, caused a drop of the cellular ATP/ADP ratio, and resulted in a rapid increase in cytosolic pyruvate levels as well as in increased respiration (Juaristi *et al.* 2019). Furthermore, cultured astrocytes were shown to increase their intracellular pyruvate concentration upon inhibition of oxidative phosphorylation (Sotelo-Hitschfeld *et al.* 2015), and in response to extracellular K^{+} stimulation (Fernández-Moncada *et al.* 2018). In the context of the presented thesis, astrocyte cultures were shown to release pyruvate (Selak *et al.* 1985, Wang and Cynader 2001, Kala and Hertz 2005), and pyruvate was shown to have neuroprotective functions (see **Table 1-1**).

Moreover, astrocytes are capable of metabolizing glucose-6-phosphate via the pentose-phosphate pathway (PPP), although this pathway is less active than glycolysis under physiological conditions (Bonvento and Bolanos 2021, TeSlaa *et al.* 2023, Watermann *et al.* 2023). The PPP's main function is the provision of 5-carbon sugar phosphates for biosynthesis, and of NADPH for oxidative defence and biosynthesis (TeSlaa *et al.* 2023). But, unused carbons can re-enter glycolysis via fructose-6-phosphate and glycerinealdehyde-3-phosphate, which are generated in the non-oxidative branch of PPP (Bolaños 2016, TeSlaa *et al.* 2023), thus yielding pyruvate.

In addition to consuming externally supplied glucose, astrocytes have been shown to contain glucose stores in the form of glycogen (Markussen *et al.* 2023), which undergo constant degradation and regeneration even in the presence of glucose (Petit *et al.* 2021, Markussen *et al.* 2023). Thus, pyruvate can also be derived from glycogen mobilized in the presence or absence of glucose (Dienel 2019b, Markussen *et al.* 2023). Indeed, astrocyte cultures were proven to release lactate from glycogen under glucose deprivation (Dringen *et al.* 1993a), which is an indicator for pyruvate production.

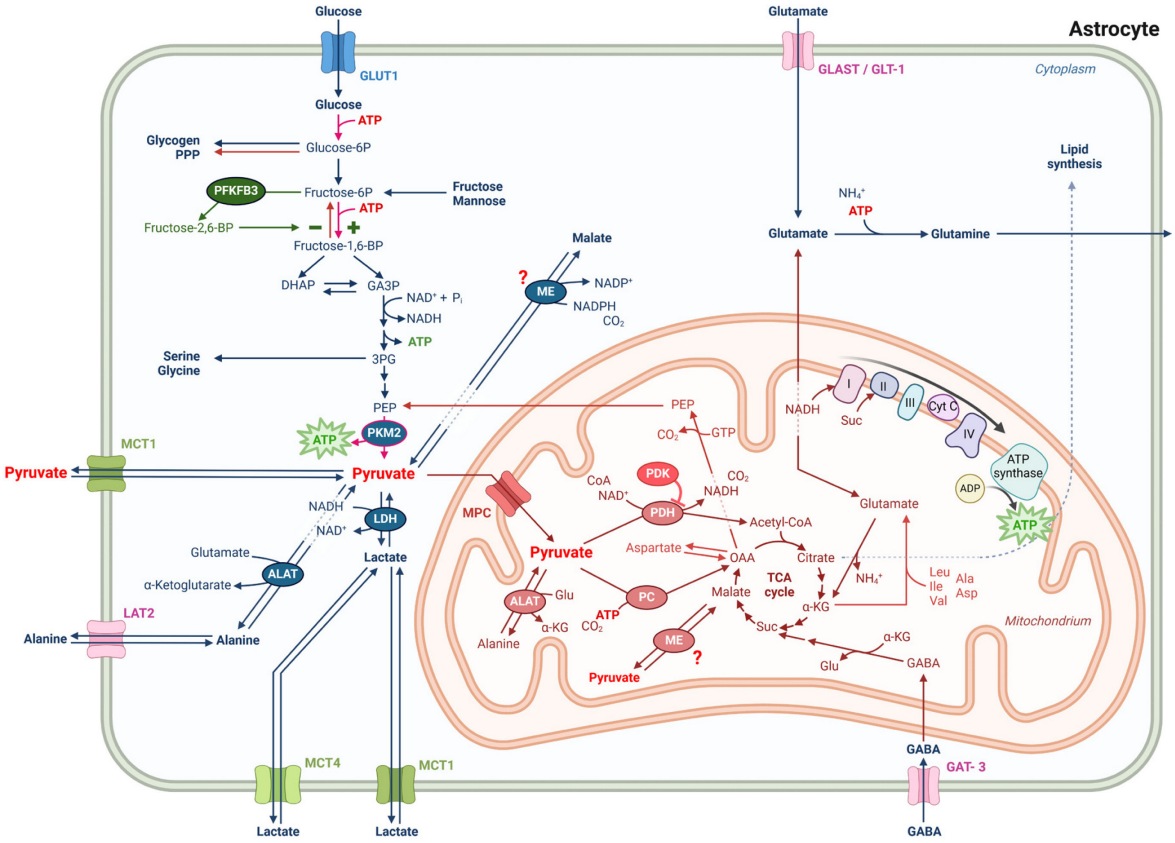

Figure 1-7: Important aspects of cytosolic and mitochondrial pyruvate metabolism in astrocytes. Acetyl-CoA = acetyl coenzyme A; Ala = alanine; ALAT = alanine amino transaminase; Asp = aspartate; CoA = coenzyme A; DHAP = dihydroxyacetone phosphate; Fructose-6P = fructose-6-phosphate; Fructose-1,6-BP = fructose 1,6-bisphosphate; Fructose-2,6-BP = fructose-2,6-bisphosphate; GABA = γ-aminobutyric acid; GAT-1/3 = GABA transporter 1/3; GA3P = glyceraldehyde 3-phosphate; GLAST = glutamate/aspartate transporter; Glu = glutamate; GLT-1 = glutamate-transporter 1; Glucose-6P = glucose-6-phosphate; GLUT1 = glucose transporter 1; Ile = isoleucine; α-KG = α-ketoglutarate; LAT2 = L-type amino acid transport 2; LDH = lactate dehydrogenase; Leu = leucine; ME = malic enzyme; MCT1 = monocarboxylate transporter 1; MCT4 = monocarboxylate transporter 4; MPC = mitochondrial pyruvate carrier; OAA = oxaloacetate; PC = pyruvate carboxylase; PDH = pyruvate dehydrogenase complex; PEP = phosphoenolpyruvate; PFKFB3 = 6-phosphofructo-2-kinase/fructose-2,6-bisphosphatase 3; 3PG = 3-phosphoglycerate; P_i = inorganic phosphate; PKM2 = pyruvate kinase M2; PPP = pentose phosphate pathway; Suc = succinate; Val = valine. To simplify the illustration, protons as well as ions involved in transport processes were not shown. The pink arrows mark the irreversible steps of glycolysis. The red question marks highlight the currently unclear cellular distribution of ME. Created with Biorender.

The production of lactate by astrocytes can be considered a sign of pyruvate production, given that the two compounds are in a direct equilibrium with one another via the oxidoreductase LDH (**Fig. 1-7**) (Dienel 2019a). Pyruvate can be generated through the oxidation of lactate catalyzed by LDH using NAD^+ as cofactor (Dienel 2019a). Lactate can also serve as an alternative energy substrate (Arend *et al.* 2019, Harders *et al.* 2024). However, the thermodynamic equilibrium of the LDH reaction strongly favors lactate production (Bak and Schousboe 2017), facilitating the simultaneous re-oxidation of NADH to NAD^+ important for enabling an ongoing glycolysis. Accordingly, a high lactate/pyruvate ratio has been described for cultured mouse astrocytes, that was demonstrated to increase by application of NH_4^+ (Kala and Hertz 2005). In general, LDH is present in high activity in astrocytes (Tulpule *et al.* 2014), and total LDH purified from primary astrocyte cultures revealed a K_M value for pyruvate of 84 µM (O'Brien *et al.* 2007). Both subunits of LDH, M and H, have been reported to be expressed and all isoforms (tetramers, LDH-1 - LDH-5) are present in astrocytes (Bittar *et al.* 1996, O'Brien *et al.* 2007). Cultured astrocytes (Pellerin and Magistretti 1994, Kala and Hertz 2005, Arend *et al.* 2019), as well as astrocytes *in vivo* (Sotelo-Hitschfeld *et al.* 2015) were shown to release large amounts of lactate from glucose. Furthermore, astrocyte cultures were shown to be able to directly produce, and release lactate from consumed extracellular pyruvate (Hamprecht and Dringen 1994). Astrocytic lactate production has been extensively studied (Rae *et al.* 2024). It has been proposed that astrocytic lactate may serve as an alternative neuronal energy substrate, which production by astrocytes can be enhanced locally in brain by neuron-astrocyte interactions (Pellerin and Magistretti 1994, Bonvento and Bolanos 2021, Roumes *et al.* 2023). The results obtained for astrocytic lactate production offer insights into the astrocytic pyruvate production, given the exclusive lactate production by pyruvate reduction.

Alanine may serve as another source for pyruvate formation in astrocytes (Waagepetersen *et al.* 2002b). Astrocytes have been described to express alanine aminotransferase (ALAT), also known as glutamate pyruvate transaminase (GPT), which catalyzes the reversible transamination of alanine to pyruvate, whereby α-ketoglutarate serves as an amino group acceptor, and glutamate is derived (**Fig. 1-7**) (Rose *et al.* 2020, Rae *et al.* 2024). Astrocytes were shown to express both the cytosolic GPT1 and mitochondrial GPT2 isoforms (Baytas *et al.* 2022). Consequently, astrocyte cultures have been demonstrated to consume ^{13}C-labeled alanine, and subsequently release labeled lactate (Zwingmann *et al.* 2001), which has to be produced via pyruvate. Under those experimental conditions, the activity of mitochondrial glutamate dehydrogenase (GDH) was enhanced, presumable to provide sufficient α-

ketoglutarate as the amino acceptor for transamination (Zwingmann *et al.* 2001). Due to its ability to supply pyruvate for mitochondrial energy production, extracellularly applied alanine was shown be able to maintain high ATP levels in glucose-deprived astrocytes (Harders *et al.* 2024). The reversible nature of the transamination was demonstrated by the production and release of alanine from metabolized pyruvate by astrocyte cultures (Hamprecht and Dringen 1994).

Pyruvate could also be derived from malate catalyzed by malic enzyme (ME), either from extracellularly applied malate (McKenna *et al.* 1990) or in a process termed "pyruvate recycling" (Cerdan 2017). The latter is described in detail later. ME facilitates the reversible oxidative decarboxylation of malate to pyruvate (Cerdan 2017), whereby $NADP^+$ is predominantly used as a cofactor rather than NAD^+ (Bukato *et al.* 1995). But, whether functional ME is expressed in the cytosol and in mitochondria of astrocytes, or in just one compartment is a topic of controversial debate (McKenna *et al.* 1995, Vogel *et al.* 1998a, Vogel *et al.* 1998b, Alves *et al.* 2000, Cerdan 2017). Even though the decarboxylation of malate to pyruvate is reversible (Cerdan 2017), to my knowledge no astrocytic ME-mediated malate production from pyruvate has been reported so far in the literature.

1.3.2 Mitochondrial pyruvate metabolism

Pyruvate as the end product of glycolysis links cytosolic and mitochondrial metabolism (**Fig. 1-7**). Therefore, it must be transported into mitochondria. In contrast to the outer mitochondrial membrane, pyruvate cannot freely pass the inner mitochondrial membrane (Tavoulari *et al.* 2023). Here, the proton-coupled import is mediated by the mitochondrial pyruvate carrier (MPC; **Fig. 1-7**), a heterodimer composed of MPC1 and MPC2 (McCommis and Finck 2015, Xu *et al.* 2021, Tavoulari *et al.* 2023). MPC has been shown to be functionally expressed in astrocytes (Arce-Molina *et al.* 2020). Pyruvate import into astrocytic mitochondria was demonstrated to be lowered by acidification of the mitochondrial matrix by extracellular application of high concentrations of NH_4^+, thus abolishing the proton gradient, which resulted in increased lactate production (Lerchundi *et al.* 2015). Moreover, NO was shown to decrease the rate of mitochondrial pyruvate consumption by impairment of mitochondrial respiration (San Martín *et al.* 2017). Interestingly, even though ATP-induced Ca^{2+} signalling increased the intracellular pyruvate concentration in astrocytes (Juaristi *et al.* 2019), it did not increase the mitochondrial pyruvate import (San Martín *et al.*

2014). Using genetically-encoded pyruvate sensors, cytosolic and mitochondrial steady-state concentrations in astrocytes were found to be in the low micromolar range; however, the values varied considerable between individual cells (Arce-Molina *et al.* 2020). The median mitochondrial pyruvate concentration (21 µM) was thereby found to be lower than the median cytosolic concentration (33 µM) (Arce-Molina *et al.* 2020).

In mitochondria, pyruvate can be oxidatively decarboxylated and connected to CoA, yielding acetyl-CoA and NADH (**Fig. 1-7**) (Rose *et al.* 2020). This acetyl-CoA formation is mediated by the pyruvate dehydrogenase complex (PDH) (Rose *et al.* 2020), a multienzyme complex comprised of three enzymes involved in pyruvate oxidation and acetyl-CoA formation plus regulatory enzymes (Stacpoole 2017). Among the regulatory enzymes, the expression of all four pyruvate dehydrogenase kinase (PDK) isoforms, and both pyruvate dehydrogenase phosphatase (PDP) isoforms known has been demonstrated in astrocytes (Halim *et al.* 2010). However, inactivation of the PDH by phosphorylation was shown to be relatively high in astrocytes (Halim *et al.* 2010). Single cell analysis revealed high expression levels of PDK4 mRNA, a regulatory kinase associated with high PDH phosphorylation (Zhang *et al.* 2014). Thus, PDH activity is believed to be relatively low in astrocytes (Halim *et al.* 2010, Rose *et al.* 2020). Nonetheless, 15 to 20 % of the total pyruvate metabolism in astrocytes was estimated to be pyruvate dehydrogenase-mediated (Schousboe *et al.* 2019).

Acetyl-CoA derived from pyruvate can enter the TCA cycle, where acetyl-CoA combines with oxaloacetate to form citrate (**Fig. 1-7**) (Rose *et al.* 2020, Rae *et al.* 2024). The pyruvate-derived acetyl-CoA can be fully oxidized to CO_2, or serves, when transported as citrate into the cytosol, as a major precursor for fatty acid synthesis (Rose *et al.* 2020, Rae *et al.* 2024). Additionally, mitochondrial pyruvate utilization seems to be connected to mitochondrial fatty acid β-oxidation, even in conditions of adequate nutrition. Astrocytes lacking carnitine palmitoyltransferase 1a (CPT1a), a transferase facilitating the transport of long-chain fatty acids into mitochondria (Rose *et al.* 2020, Rae *et al.* 2024), demonstrated increased mitochondrial pyruvate utilization and respiration even in the presence of glucose (Morant-Ferrando *et al.* 2023).

Per mol pyruvate oxidized in mitochondria via PDH and TCA cycle, 3 moles of CO_2, 4 moles of NADH and 1 mol of GTP are formed (Dienel 2019a, Rose *et al.* 2020). Additionally, when succinate is oxidized to fumarate in the TCA cycle by the mitochondrial membrane-anchored succinate dehydrogenase, its covalently bound prosthetic group FAD is reduced to $FADH_2$ (Rose *et al.* 2020). Those energy-rich electrons carried by NADH and $FADH_2$ can be

utilized by the respiratory chain to form the proton-gradient over the inner mitochondrial membrane (IMM), which is subsequently used for ATP production (**Fig. 1-7**). Glucose-deprived astrocytes have been demonstrated to sufficiently utilize pyruvate for energy production (Harders *et al.* 2023, Harders *et al.* 2024). Around 15 moles of ATP are formed per mol pyruvate oxidized in the mitochondrion (Dienel 2019a). In addition, electrons from cytosolic NADH derived in glycolysis might be transported into mitochondria by shuttle systems such as the malate-aspartate shuttle (McKenna *et al.* 2006) or glycerol-3-phosphate shuttle (Juaristi *et al.* 2017). Their activity in astrocytes remains a controversial topic (McKenna *et al.* 2006, Berkich *et al.* 2007, Li *et al.* 2012, Juaristi *et al.* 2017, Liu *et al.* 2021). But, for astrocytes to metabolize pyruvate in mitochondria, cytosolic NAD^+ regeneration from NADH for an ongoing glycolysis has to be facilitated by other means than pyruvate reduction to lactate (Rose *et al.* 2020). In summary, with the addition of 2 moles of ATP formed during glycolysis and taking into account a proton-leaking IMM, it was estimated that approximately 32 moles of ATP are formed per mole of glucose consumed (Dienel 2019a).

Furthermore, pyruvate can be carboxylated to oxaloacetate in mitochondria through an ATP-dependent reaction facilitated by pyruvate carboxylase (PC; **Fig. 1-7**), a key anaplerotic enzyme that is in brain almost exclusively expressed in astrocytes (Shank *et al.* 1985, Cesar and Hamprecht 1995, Sonnewald and Rae 2010). It has been observed that elevated extracellular K^+ levels, but not glutamate levels, induce increased carbon fixation via enhanced PC activity (Kaufman and Driscoll 1992). Moreover, AMP-activated protein kinase (AMPK) activation in astrocytes has been found to augment glycolysis and pyruvate carboxylation by PC, thus increasing the capacity of the TCA cycle (Voss *et al.* 2020). Approximately 10 to 20 % of the brain's total pyruvate metabolism is estimated to be accounted for by astrocytic pyruvate carboxylation (Hertz and Hertz 2003, Schousboe *et al.* 2019). This oxaloacetate produced via PC is crucial for the maintenance of TCA cycle function, as oxaloacetate derived from pyruvate replenishes carbons lost in biosynthesis pathways utilizing TCA cycle intermediates (Rose *et al.* 2020).

In addition to entering the TCA cycle, pyruvate-derived oxaloacetate can in astrocytes be decarboxylated to phosphoenolpyruvate (PEP) by mitochondrial phosphoenolpyruvate carboxykinase (PEPCK), using GTP as phosphate donor (**Fig. 1-7**) (Schmoll *et al.* 1995, Yip *et al.* 2016). PEP in turn can be transported out of mitochondria into the cytosol, where it can be utilized to maintain or replenish cellular glycogen stores by *de novo* glucose synthesis

(Rose *et al.* 2020). In the brain, this process known as gluconeogenesis, is specific to astrocytes (Rose *et al.* 2020). Correspondingly, astrocyte cultures were demonstrated to incorporate labeled lactate into their glycogen stores (Dringen *et al.* 1993b), which must first be oxidized to pyruvate. Furthermore, brain tissue was shown to produce glucose from pyruvate precursors, which could even be enhanced by application of the gluconeogenic hormone glucagon (Bhattacharya and Datta 1993).

1.3.3 Pyruvate in glutamate, glutamine and GABA metabolism

One example of the importance of anaplerotic pyruvate metabolism by PC is the *de novo* glutamate/glutamine synthesis, that in brain contributes to the maintenance of glutamate and GABA neurotransmitter pools (Andersen and Schousboe 2023b). For this purpose, α-ketoglutarate exits the TCA cycle for glutamate and subsequent glutamine synthesis (**Fig. 1-7**) (Andersen and Schousboe 2023b). It has been demonstrated that α-ketoglutarate derived from oxaloacetate, produced from pyruvate via PC, directly contributes to the synthesis of glutamate and glutamine (Voss *et al.* 2020, Andersen and Schousboe 2023b). In the final step converting α-ketoglutarate to glutamate, pyruvate is in turn produced, as α-ketoglutarate is in part transaminated to glutamate by ALAT utilizing alanine (Westergaard *et al.* 1996). Other amino group donors are branched chain amino acids (Cole *et al.* 2012) and aspartate (Westergaard *et al.* 1996).

Conversely to *de novo* glutamate synthesis, glutamate taken up by astrocytes by high-affinity electrogenic transporters can undergo transamination to form α-ketoglutarate, which can enter the TCA cycle (Todd and Hardingham 2020, Andersen and Schousboe 2023b). This reaction can be mediated by ALAT, simultaneously converting pyruvate to alanine, thus lowering cellular pyruvate levels (Westergaard *et al.* 1996). However, this transamination only plays a minor role under physiological conditions, where glutamate is predominately deaminated to α-ketoglutarate and NH_4^+ by glutamate dehydrogenase (GDH) (Westergaard *et al.* 1996). For glutamate to be fully oxidized and utilized as an energy substrate, its carbon backbone must leave the TCA cycle and it has to be converted to pyruvate (Andersen and Schousboe 2023b). This reverse production of pyruvate from glutamate or other TCA cycle intermediates and precursors was demonstrated for the mammalian brain, and termed “pyruvate recycling” (Cerdan *et al.* 1990). Facilitated by the combined action of PEPCK and pyruvate kinase (PK), or malic enzyme (ME), pyruvate can be derived from oxaloacetate or malate, respectively (Cerdan *et al.* 1990, Hertz and Hertz 2003,

Cerdan 2017, Andersen and Schousboe 2023b). The presence of glutamate in a label pattern that can only be derived by pyruvate recycling was shown for cultured astrocytes (Waagepetersen *et al.* 2002a). It was argued that, due to higher ME activity compared to PEPCK activity, pyruvate is mainly recycled from malate, and not from oxaloacetate (Waagepetersen *et al.* 2002a). However, the methods applied to date do not allow for the distinction of the extent to which pyruvate originates from either of these pathways (Waagepetersen *et al.* 2002a, Cerdan 2017, Andersen and Schousboe 2023b).

In addition to the full oxidation of pyruvate derived from glutamate, parts of pyruvate were also shown to be converted to lactate upon application of glutamate (Sonnewald *et al.* 1996, Westergaard *et al.* 1996). In this case the pyruvate generation from TCA cycle intermediates or precursors is referred to as partial pyruvate recycling (Andersen and Schousboe 2023b). Given that glutamate deamination to α-ketoglutarate is primarily facilitated by GDH, it has been observed that lactate production through pyruvate recycling from glutamate is reduced in astrocytes with decreased GDH activity (Nissen *et al.* 2015). Furthermore, in those astrocytes lacking GDH activity to degrade glutamate, transamination of glutamate and oxaloacetate to α-ketoglutarate and aspartate via aspartate aminotransferase (AST) was increased, and pyruvate carboxylation was augmented to compensate for the increased oxaloacetate withdrawal from this reaction (Nissen *et al.* 2015).

In addition to glutamate, astrocytes also take up GABA (Andersen and Schousboe 2023a). To be metabolized in the TCA cycle, GABA is converted to succinate in two steps (**Fig. 1-7**) catalysed by GABA transaminase and succinate semialdehyde dehydrogenase (Andersen *et al.* 2020, Andersen and Schousboe 2023b). The reaction mediated by GABA transaminase yields succinate semialdehyde with α-ketoglutarate as the amino group acceptor (Andersen *et al.* 2020). ALAT can facilitate a subsequent transamination of derived glutamate, using pyruvate as the amino group acceptor, regenerating α-ketoglutarate. Labelled nitrogen of [^{15}N]GABA was detected in alanine in brain slices, in which oxidative metabolism of GABA was shown to be mainly facilitated by astrocytes. However, most GABA nitrogen was utilized for glutamine synthesis (Andersen *et al.* 2020).

1.3.4 Pyruvate transport over the plasma membrane

Short-chain monocarboxylates such as pyruvate, but also lactate and ketone bodies, are mainly imported and exported over the outer cell membrane by passive transport facilitated

by proton-coupled monocarboxylate transporters (MCTs) (Nguyen *et al.* 2022). Astrocytes express two isoforms of those transporters, MCT1 (*SLC16A1*) (Bröer *et al.* 1997) and MCT4 (*SLC16A3*) (Dimmer *et al.* 2000). Astrocytic pyruvate is believed to be transported mainly by the ubiquitous MCT1 (**Fig. 1-7**), which exhibits a K_M of around 1 mM for pyruvate (Nguyen *et al.* 2022). In contrast to its relatively high affinity for pyruvate, MCT1 shows lower affinity for lactate (K_M= 3.5 mM) and ketone bodies (K_M β-hydroxybutyrate= 12.5 mM, K_M acetoacetate = 5.5 mM) (Carpenter and Halestrap 1994, Bröer *et al.* 1998). Indeed, astrocytes derived from MCT1 knockout mice showed a strong decrease in pyruvate uptake (Philips *et al.* 2022). Moreover, cultures astrocytes demonstrated a K_M value of around 1 mM and an apparent V_{max} of around 7.5 nmol / (min * mg protein) for pyruvate uptake (Hamprecht and Dringen 1994). Interestingly, MCTs have been reported to undergo cross-stimulation, triggered by an increased activation of the transporter in response to the presence of another ligand on the opposing side (Dimmer *et al.* 2000, Mächler *et al.* 2016). Accordingly, astrocytes were shown to accelerate their lactate release upon pyruvate application, likely due to this trans-acceleration (Mächler *et al.* 2016). Given that substantially lower K_M values have been documented for MCT4 for lactate transport than for pyruvate transport (Contreras-Baeza *et al.* 2019, Felmlee *et al.* 2020), this transporter is not considered in the context of pyruvate transport (Nguyen *et al.* 2022).

1.4 Pharmacological modulation of astrocytic metabolism

As astrocytes and astrocytic metabolism play an important role in brain functions, homeostasis, or in diseases, it is highly important to get a better insight into the involved pathways. One method to elucidate the role of a certain pathway is to study the resulting consequences of either inhibition or enhancement of this pathway. Since genetical knockout approaches can be costly and inadequate due to, e.g., insufficient transfection of all target cells or strong off-target effects (Zhang *et al.* 2022b), pharmacological modulation can be the appropriate course of action to study metabolic questions. In cell culture approaches, pharmacological modulators can be easily applied at any time for various time frames and in various concentrations. This brings the opportunity to even study potentially fatal situations for at least a short period of time (Steinmeier *et al.* 2020, Harders *et al.* 2023). However, solubility (Thapa *et al.* 2017), stability (Yang *et al.* 2008), the transport to the side of action (Ovens *et al.* 2010), and mechanism of action of the compounds (Ovens *et al.* 2010) have to be taken into consideration to ensure functionality, and to prevent false-negative

results. For example, pure chemical reactions of the pharmacological modulator and a cellular component could severely lower the concentration available (Yang *et al.* 2008). Moreover, potential side effects due to additional targets have to be considered (Gottfried *et al.* 2013), as they might lead to the generation of inaccurate results. The latter can often be easily prevented by application of a different inhibitor concentration that correlates with only the specific effect rather than the side effect (Carpenter and Halestrap 1994, Yang *et al.* 2014).

1.4.1 Modulation of transport processes

In astrocytes, transport of pyruvate, lactate, and ketone bodies is mainly facilitated by proton-coupled MCTs. Astrocytes express the isoforms MCT1 and MCT4, which exhibit different kinetic properties (Bröer *et al.* 1998, Dimmer *et al.* 2000, Contreras-Baeza *et al.* 2019). To elucidate the role of the individual transporters for pyruvate consumption and release, MCT1 and MCT4 can be inhibited by AR-C155858 (Ovens *et al.* 2010) and AZD0095 (Goldberg *et al.* 2023), respectively.

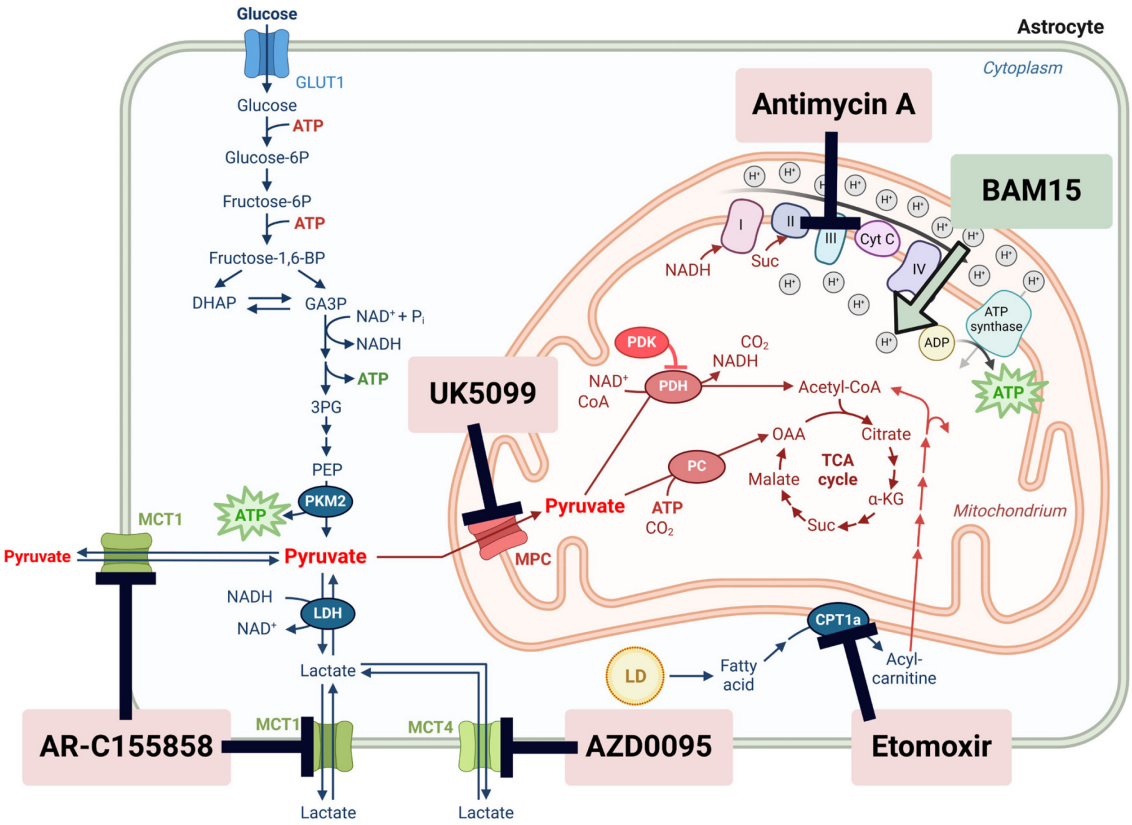

Figure 1-8: Pharmacological inhibitors of astrocytic metabolism. This illustration shows the target points of the inhibitors (highlighted in red) AR-C155858 (MCT1 inhibitor), AZD0095 (MCT4 inhibitor), UK5099 (MPC inhibitor), etomoxir (CPT1a inhibitor), and antimycin A (complex III inhibitor). The green arrow indicates the action of BAM15, a mitochondrial uncoupler (highlighted in green). Created with Biorender.

The specific MCT1 (and MCT2) inhibitor AR-C155858 (**Fig. 1-8**), a pyrrolopyrimidinedione derivate (**Fig. 1-9a**), was first developed as an immunomodulator targeting hyperactive T-cells by suppressing cell proliferation due to feedback inhibition of accelerated glycolysis by intracellular lactate accumulation (Guile *et al.* 2006). The kinetic properties of AR-C155858 inhibition were characterized in inhibition studies performed on erythrocytes (Ovens *et al.* 2010), a glycolytic cell type without mitochondria that relies on MCT1 for lactate export (Poole and Halestrap 1994, Siems *et al.* 2000). MCT1-mediated lactate transport was shown to be inhibited by AR-C155858 with a low K_i of 2.3 nM (Ovens *et al.* 2010). But, the inhibition of lactate transport by AR-C15585 in *Xenopus* oocytes expressing MCT1 was shown to be delayed, and MCT1 was also blocked after microinjection of AR-C155858 into the oocytes, suggesting that AR-C155858 has to enter the cell to reach its intracellular site of action (Ovens *et al.* 2010). Later, it was shown that AR-C155858 itself serves as a substrate for MCT1 (Guan *et al.* 2019). Thus, care must be taken not to inhibit the uptake of AR-C155858. The inhibitor binds to the transmembrane helices 7 – 10, and its specificity seems to be explained by amino acids that are conserved in-between MCT1 and MCT2 (Nancolas *et al.* 2015). The use of AR-C155858 administration as an anticancer therapeutic is still under active investigation (Choi *et al.* 2023, Lopez *et al.* 2023).

For astrocytes, inhibition of MCT1 by AR-C155858 was shown to be as efficient as a MCT1 knockout (Philips *et al.* 2022). Acetoacetate, β-hydroxybutyrate as well as lactate uptake into cortical astrocytes derived from mice fed with an either carbohydrate-rich, or ketogenic diet was almost completely inhibited by 1 µM AR-C155858, even though the ketogenic diet was shown to increase MCT1 expression levels (Forero-Quintero *et al.* 2017). Interestingly, AR-C155858 was also applied to astrocytes expressing an intracellular pyruvate sensor to determine the rate of mitochondrial pyruvate consumption. Therefore, following the establishment of a constant intracellular pyruvate concentration by application of extracellular pyruvate in a glucose-free environment, AR-C155858 was applied to inhibit MCT1-mediated pyruvate uptake into astrocytes, and thus the mitochondrial pyruvate consumption rate was measured based on the reduction of intracellular pyruvate (San Martín *et al.* 2014, Lerchundi *et al.* 2015, San Martín *et al.* 2017). A similar approach was used to access differences in rates of intracellular lactate accumulation upon MCT1-inhibition by AR-C155858 in a glucose-rich milieu (Lerchundi *et al.* 2015).

Specific MCT4 inhibitors have just recently been described. Formerly, diclofenac or phloretin, that inhibit MCT4 but also lots of other targets (Gottfried *et al.* 2013, Elmetwalli

et al. 2023), were used due to a lack of appropriate specific alternatives (Dimmer *et al.* 2000, Sasaki *et al.* 2016). MCT4 is upregulated in highly glycolytic cells under hypoxic conditions (Ullah *et al.* 2006), e.g. in cancer cells, that adapt to such an environment by increased glycolytic flux with a higher production rate of lactate (Warburg effect) (Vaupel and Multhoff 2021). AZD0095 (**Fig. 1-9b**) was developed under the premise of exploiting this circumstance, and originates from a high throughput screening in which around 200,000 substances were tested for their usability as clinical candidates for cancer therapy (Goldberg *et al.* 2023). It exhibited the most favorable pharmacokinetic properties and low *in vitro*-tested side effects (Goldberg *et al.* 2023). With an IC_{50} of 1.3 nM and a demonstrated more than 1000 times selectivity for MCT4 over MCT1, AZD0095 was shown to be a high affinity inhibitor for MCT4 (**Fig. 1-8**) (Goldberg *et al.* 2023). To my knowledge, AZD0095 application on astrocytes has not been described in the literature thus far.

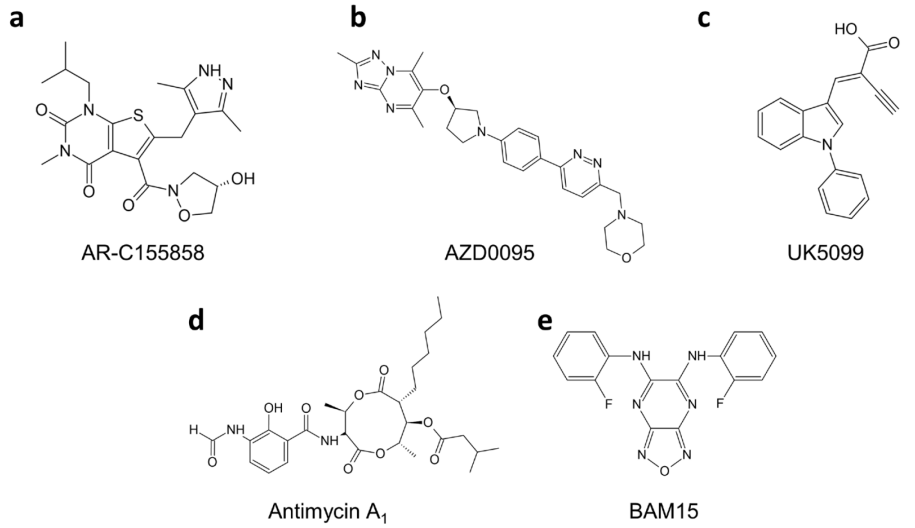

Figure 1-9: Structural formulas of inhibitors applied. Pictured are the chemical structural formulas of the MCT1 inhibitor AR-C155858 (**a**), the MCT4 inhibitor AZD0095 (**b**), the MPC inhibitor UK5099 (**c**), the complex III-inhibitor antimycin A_1 (**d**), and of the mitochondrial uncoupler BAM15 (**e**). Created with ChemSketch.

Pyruvate is taken up into mitochondria via the proton-coupled MPC, a heterodimer protein complex located in the inner mitochondrial membrane (Papa *et al.* 1971, Tavoulari *et al.* 2023). UK5099 (2-Cyano-3-(1-phenyl-1H-indol-3-yl)-2-propenoic acid; **Fig. 1-9c**), a well-established inhibitor of the MPC (**Fig. 1-8**), was already in use before the mechanism of pyruvate transport into mitochondria was elucidated (Halestrap 1975). It inhibits the MPC in a non-competitive, but reversible way with a half maximal inhibition concentration of 5 to 50 nM (Halestrap 1975, Shearman and Halestrap 1984). It is important to note that at high concentrations, UK5099 has been reported to exhibit some inhibitory potential on MCTs (Yang *et al.* 2014). Nevertheless, the K_i value of UK5099-mediated MCT inhibition is two to

three orders of magnitude higher than that for MPC (Carpenter and Halestrap 1994). The α-cyanopropionate group of UK5099 as well as the attached aromatic structure appear crucial for inhibition, as such analogs of UK5099 similarly prevented pyruvate uptake (Halestrap 1975). However, UK5099 exhibited the highest potency among the derivates used (Halestrap 1975). The crystal structure of the MPC has not yet been resolved, but computational simulations revealed that UK5099 was trapped in the center of the transporter and stably occupied some of the amino acids that are crucial for pyruvate transport (Xu *et al.* 2021). Thereby, the long-held theory of reversible covalent binding to a cysteine residue of the carrier could be disproved (Tavoulari *et al.* 2023).

UK5099 was shown to efficiently inhibit mitochondrial pyruvate transport in astrocytes (Arce-Molina *et al.* 2020). In glucose-deprived astrocytes, inhibition of the MPC by UK5099 and simultaneous inhibition of the carnitine palmitoyltransferase 1A (CPT1a) by etomoxir (**Fig. 1-8**) resulted in depletion of cellular ATP stores within 5 h, whereas inhibition by UK5099 alone did not affect the cellular ATP levels for 8 h (Harders *et al.* 2023). In contrast, acetyl-CoA and TCA cycle intermediate levels were lowered when mitochondrial pyruvate uptake was blocked in astrocytes by UK5099 (Chow *et al.* 2021). Besides elucidating the role of MPC-mediated pyruvate transport for specific compounds, UK5099 was used to access the dependency of astrocytes on mitochondrial oxidation of glycolytically-derived pyruvate, as well as the flexibility of this pathway (Qi *et al.* 2021). By measuring the oxygen consumption rate in the absence of inhibitors or in the presence of UK5099 without or with the addition of glutaminase and CPT1a inhibitors, this study revealed that astrocytes do not depend on mitochondrial oxidation of glucose-derived pyruvate in the presence of other metabolic pathways. However, this glucose oxidation pathway via pyruvate holds a high reserve capacity for when other pathways are impaired (Qi *et al.* 2021).

1.4.2 Modulation of mitochondrial metabolism

Once pyruvate has entered the astrocytic mitochondrion, it can be further metabolized. For example, pyruvate can be decarboxylated to acetyl-CoA and fuel the TCA cycle, which in turn produces reduction equivalents for ATP production via the respiratory chain. There are two potential ways to prevent mitochondrial oxidative ATP production. On one hand, it could be indirectly inhibited by a depletion of the proton gradient over the inner mitochondrial membrane by a mitochondrial uncoupler. On the other hand, the electron transport chain and thereby the electron flow could be directly inhibited.

BAM15, a mitochondrial uncoupler (**Fig. 1-8**) first described in 2013, is a good candidate to study the influence of depletion of the mitochondrial proton gradient, as it has no off-target effects on plasma membranes, a common problem of most other uncouplers (Kenwood *et al.* 2013). In general, the term "mitochondrial uncoupler" addresses compounds that enable oxidative phosphorylation-independent re-entry of protons into the mitochondrial matrix and thus separate the oxidation of the reduction equivalents from ATP production (Kenwood *et al.* 2013). There are physiologically occurring uncouplers, mitochondrial uncoupling proteins (UCPs), that are capable of returning protons to the mitochondrial matrix and seem to play a role in controlling oxidative stress by the decrease in mitochondrial membrane potential that is accompanied by an improved electron transport (Cadenas 2018). Pharmacological uncouplers are weak lipophilic bases like BAM15 (**Fig. 1-9e**), and act as protonophores (Kenwood *et al.* 2013). Those compounds are protonated on the outer side of the inner mitochondrial membrane and are, due to their chemical properties, able to diffuse through the inner mitochondrial membrane in their protonated and unprotonated form (Nagumune *et al.* 1993). Uncoupling by BAM15 strongly increases electron transport chain-dependent oxygen consumption (Kenwood *et al.* 2013). This is accompanied by increased energy expenditure, which exhibited beneficial effects like improved glucose utilization or a decreased body weight in mouse models of general or sarcopenic obesity (Axelrod *et al.* 2020, Dantas *et al.* 2022).

In glucose-deprived astrocytes, application of BAM15 led to a complete depletion of the total cellular ATP content within 2 h (Harders *et al.* 2023). Interestingly, glucose-fed astrocytes were able to maintain in the presence of BAM15 their cellular ATP stores at around 60 % of the initial ATP content (Harders *et al.* 2023). Furthermore, BAM15 was demonstrated to lower the glucose-dependent reduction of water-soluble tetrazolium salt 1 by 40 % (Watermann and Dringen 2023). Since this reduction is facilitated by cytosolic reduction equivalents, BAM15 is discussed to lower the availability of those reduction equivalents by increased utilization of cytosolic NADH in mitochondria (Watermann and Dringen 2023).

To study the effects of direct inhibition of the electron transport chain, the complex III inhibitor antimycin A (**Fig. 1-8**) is frequently used. Antimycin A was first discovered by Leben and Keitt in 1948 from an unidentified species of *Streptomyces*, when they obtained isolates that showed fungicidal properties (Leben and Keitt 1948). A year later, it was further analyzed and a name that reflected it's antimycotic and -biotic effect was assigned,

antimycin A (Dunshee *et al.* 1949). Antimycin A describes not one substance but rather a mixture of compounds with the same backbone but different side chains (Labs *et al.* 2016). Main components are antimycin A_1 (**Fig. 1-9e**), A_2, A_3, and A_4, but many more have been described (Xu *et al.* 2011, Liu *et al.* 2016). Antimycin A acts as a high-affinity inhibitor of complex III (ubiquinol-cytochrome c oxidoreductase) in a one to one stoichiometry in the cytochrome b-c_1 region (Slater 1973). Specifically, it inhibits the re-oxidation of cytochrome b_H and thereby the regeneration of QH_2 via the Q_i site (Gabellini *et al.* 1989).

A possible advantage of the inhibition of complex III compared to the inhibition of complex I by rotenone is the inhibition of the transfer of electrons not only from NADH but also from succinate via $FADH_2$ by complex II and thus a more pronounced blockade of the electron flow (Ragan and Heron 1978). Antimycin A was shown to increase ROS production and deplete GSH levels in different cell types (Park and You 2016, Guan *et al.* 2017), and the oxidative stress was shown to induce apoptosis (Yu *et al.* 2020). There have been attempts to utilize the antimycin A-mediated respiratory inhibition and ROS production for anticancer studies, and some interesting results have been obtained regarding the specificity of antimycin A or its derivates as anti-cancer drugs (Chevalier *et al.* 2016, Yu *et al.* 2020, Liu *et al.* 2023). But, implementation might be problematic as antimycin A still is a mitochondrial poison with high affinity for complex III.

The application of antimycin A to astrocytes results in a strong increase of lactate production by 3 to 3.5-fold (Pauwels *et al.* 1985, Arend *et al.* 2019), accompanied by increased glucose consumption (Arend *et al.* 2019). This increaseed glycolytic flux was able to maintain ATP levels for 5 h in antimycin A-treated astrocytes at approximately 40 % of the initial levels (Harders *et al.* 2023). Such a decrease of ATP levels was demonstrated to be accompanied by a reversible inhibition of gap junction permeability (Vera *et al.* 1996). Interestingly, creatine phosphate was lowered by antimycin A by 80 % within 30 min even in the presence of glucose (Karger *et al.* 2024). In the absence of glucose, antimycin A treated astrocytes were depleted of their creatine phosphate and ATP (Karger *et al.* 2024) within 5 min and 30 min, respectively. Furthermore, inhibition of the respiratory chain by antimycin A was shown to decreased astrocytic glutamate uptake by approximately 30 % (Swanson 1992). The metabolic attenuation of astrocytes by antimycin A was shown to be accompanied by a reversible depolarization of the cell membrane potential (Harold and Walz 1992).

1.5 Aim of this thesis

While the astrocytic metabolism has gathered increasing interest in research over the past 40 years, there is relatively little work published specifically focusing on the metabolite pyruvate. This thesis aims to gain a deeper insight into the processes involved in the consumption and release of pyruvate by astrocytes using primary rat astrocyte cultures as a model system.

First, this study will focus on characterizing astrocytic pyruvate consumption. Hence, the kinetic properties underlying pyruvate consumption, as well as the transport processes involved, will be investigated. Furthermore, pyruvate derived products will be identified, and mitochondrial involvement in pyruvate consumption will be studied.

Subsequently, pyruvate release by cultured rat astrocytes will be examined. Therefore, the capacity of astrocytes to produce pyruvate from glucose and other potential precursors and to export pyruvate will be investigated. The transporters and transport processes involved, as well as the influence of mitochondrial metabolism, will also be elucidated in relation to glucose-mediated pyruvate release. Finally, a potential influence of ROS on the extracellular pyruvate accumulation will be assessed.

1.6 References

Al Awabdh S, Gupta-Agarwal S, Sheehan DF, Muir J, Norkett R, Twelvetrees AE, Griffin LD and Kittler JT (2016). Neuronal activity mediated regulation of glutamate transporter GLT-1 surface diffusion in rat astrocytes in dissociated and slice cultures. *Glia*, **64**: 1252-1264

Albrecht J and Zielińska M (2017). Mechanisms of excessive extracellular glutamate accumulation in temporal lobe epilepsy. *Neurochem Res*, **42**: 1724-1734

Aldana BI (2019). Microglia-specific metabolic changes in neurodegeneration. *J Mol Biol*, **431**: 1830-1842

Alves PM, Nunes R, Zhang C, Maycock CD, Sonnewald U, Carrondo MJT and Santos H (2000). Metabolism of 3-^{13}C-malate in primary cultures of mouse astrocytes. *Dev Neurosci*, **22**: 456-462

Andersen JV, Jakobsen E, Westi EW, Lie MEK, Voss CM, Aldana BI, Schousboe A, Wellendorph P, Bak LK, Pinborg LH and Waagepetersen HS (2020). Extensive astrocyte metabolism of γ-aminobutyric acid (GABA) sustains glutamine synthesis in the mammalian cerebral cortex. *Glia*, **68**: 2601-2612

Andersen JV, Markussen KH, Jakobsen E, Schousboe A, Waagepetersen HS, Rosenberg PA and Aldana BI (2021). Glutamate metabolism and recycling at the excitatory synapse in health and neurodegeneration. *Neuropharmacology*, **196**: 108719

Andersen JV and Schousboe A (2023a). Glial glutamine homeostasis in health and disease. *Neurochem Res*, **48**: 1100-1128

Andersen JV and Schousboe A (2023b). Milestone review: Metabolic dynamics of glutamate and GABA mediated neurotransmission — The essential roles of astrocytes. *J Neurochem*, **166**: 109-137

Andriezen WL (1893). The neuroglia elements in the human brain. *BMJ*, **2**: 227-230

Arce-Molina R, Cortés-Molina F, Sandoval PY, Galaz A, Alegría K, Schirmeier S, Barros LF and San Martín A (2020). A highly responsive pyruvate sensor reveals pathway-regulatory role of the mitochondrial pyruvate carrier MPC. *eLife*, **9**: e53917

Arend C, Ehrke E and Dringen R (2019). Consequences of a metabolic glucose-depletion on the survival and the metabolism of cultured rat astrocytes. *Neurochem Res*, **44**: 2288-2300

Arend C, Grothaus IL, Waespy M, Ciacchi LC and Dringen R (2024). Modulation of multidrug resistance protein 1-mediated transport processes by the antiviral drug ritonavir in cultured primary astrocytes. *Neurochem Res*, **49**: 66-84

Arendt D (2020). The evolutionary assembly of neuronal machinery. *Curr Biol*, **30**: R603-R616

Armand EJ, Li J, Xie F, Luo C and Mukamel EA (2021). Single-cell sequencing of brain cell transcriptomes and epigenomes. *Neuron*, **109**: 11-26

Arzate DM and Covarrubias L (2020). Adult neurogenesis in the context of brain repair and functional relevance. *Stem Cells Dev*, **29**: 544-554

Axelrod CL, King WT, Davuluri G, Noland RC, Hall J, Hull M, Dantas WS, Zunica ER, Alexopoulos SJ, Hoehn KL, Langohr I, Stadler K, Doyle H, Schmidt E, Nieuwoudt S, Fitzgerald K, Pergola K, Fujioka H, Mey JT, Fealy C, Mulya A, Beyl R, Hoppel CL and Kirwan JP (2020). BAM15-mediated mitochondrial uncoupling protects against obesity and improves glycemic control. *EMBO Mol Med*, **12**: e12088

Bak LK and Schousboe A (2017). Misconceptions regarding basic thermodynamics and enzyme kinetics have led to erroneous conclusions regarding the metabolic importance of lactate dehydrogenase isoenzyme expression. *J Neurosci Res*, **95**: 2098-2102

Barros LF, Ruminot I, San Martin A, Lerchundi R, Fernandez-Moncada I and Baeza-Lehnert F (2021). Aerobic glycolysis in the brain: warburg and crabtree contra pasteur. *Neurochem Res*, **46**: 15-22

Bataveljic D, Pivonkova H, De Concini V, Hébert B, Ezan P, Briault S, Bemelmans A-P, Pichon J, Menuet A and Rouach N (2024). Astroglial Kir4.1 potassium channel deficit drives neuronal hyperexcitability and behavioral defects in Fragile X syndrome mouse model. *Nat Commun*, **15**: 3583

Baytas O, Davidson SM, Deberardinis RJ and Morrow EM (2022). Mitochondrial enzyme GPT2 regulates metabolic mechanisms required for neuron growth and motor function *in vivo*. *Hum Mol Genet*, **31**: 587-603

Beard E, Lengacher S, Dias S, Magistretti PJ and Finsterwald C (2021). Astrocytes as key regulators of brain energy metabolism: new therapeutic perspectives. *Front Physiol*, **12**: 825816

Bell KF, Al-Mubarak B, Fowler JH, Baxter PS, Gupta K, Tsujita T, Chowdhry S, Patani R, Chandran S, Horsburgh K, Hayes JD and Hardingham GE (2011). Mild oxidative stress activates Nrf2 in astrocytes, which contributes to neuroprotective ischemic preconditioning. *Proc Natl Acad Sci USA*, **108**: E1-E2

Bell RD, Winkler EA, Sagare AP, Singh I, LaRue B, Deane R and Zlokovic BV (2010). Pericytes control key neurovascular functions and neuronal phenotype in the adult brain and during brain aging. *Neuron*, **68**: 409-427

Bergbauer K, Dringen R, Verleysdonk S, Gebhardt R, Hamprecht B and Wiesinger H (1996). Studies on fructose metabolism in cultured astroglial cells and control hepatocytes: Lack of fructokinase activity and immunoreactivity in astrocytes. *Dev Neurosci*, **18**: 371 - 379

Berkich DA, Ola MS, Cole J, Sweatt AJ, Hutson SM and Lanoue KF (2007). Mitochondrial transport proteins of the brain. *J Neurosci Res*, **85**: 3367-3377

Berzelius J (1835). Ueber eine neue, durch Destillation von Wein-und Traubensäure erhaltene Säure. *Annalen der Pharmacie*, **13**: 61-63

Bhattacharya S and Datta A (1993). Is brain a gluconeogenic organ? *Mol Cell Biochem*, **125**: 51-57

Bittar P, Charnay Y, Pellerin L, Bouras C and Magistretti PJ (1996). Selective distribution of lactate dehydrogenase isoenzymes in neurons & astrocytes of human brain. *J Cereb Blood Flow Metab*, **16**: 1079-1089

Bohmbach K, Henneberger C and Hirrlinger J (2023). Astrocytes in memory formation and maintenance. *Essays Biochem*, **67**: 107-117

Bolaños JP (2016). Bioenergetics and redox adaptations of astrocytes to neuronal activity. *J Neurochem*, **139**: 115-125

Bonvento G and Bolanos JP (2021). Astrocyte-neuron metabolic cooperation shapes brain activity. *Cell Metab*, **33**: 1546-1564

Borkum JM (2023). The tricarboxylic acid cycle as a central regulator of the rate of aging: Implications for metabolic interventions. *Adv Biol*, **7**: 2300095

Borst K, Dumas AA and Prinz M (2021). Microglia: Immune and non-immune functions. *Immunity*, **54**: 2194-2208

Bröer S, Rahman B, Pellegri G, Pellerin L, Martin J-L, Verleysdonk S, Hamprecht B and Magistretti PJ (1997). Comparison of lactate transport in astroglial cells and monocarboxylate transporter 1 (MCT 1) expressing *Xenopus laevis* oocytes. *J Biol Chem*, **272**: 30096 - 30102

Bröer S, Schneider H-P, Bröer A, Rahman B, Hamprecht B and Deitmer JW (1998). Characterization of the monocarboxylate transporter 1 expressed in *Xenopus laevis* oocytes by changes in cytosolic pH. *Biochem J*, **333**: 167 - 174

Bröer S, Bröer A, Hansen JT, Bubb WA, Balcar VJ, Nasrallah FA, Garner B and Rae C (2007). Alanine metabolism, transport, and cycling in the brain. *J Neurochem*, **102**: 1758-1770

Brown D (1999). Neurons depend on astrocytes in a coculture system for protection from glutamate toxicity. *Mol Cell Neurosci*, **13**: 379 - 389

Bukato G, Kochan Z and Swierczynski J (1995). Purification and properties of cytosolic and mitochondrial malic enzyme isolated from human brain. *Int J Biochem Cell Biol*, **27**: 47-54

Bushong EA, Martone ME, Jones YZ and Ellisman MH (2002). Protoplasmic astrocytes in CA1 atratum radiatum occupy separate anatomical domains. *J Neurosci*, **22**: 183-192

Cadenas S (2018). Mitochondrial uncoupling, ROS generation and cardioprotection. *Biochim Biophys Acta Bioenerg*, **1859**: 940-950

Carpenter L and Halestrap AP (1994). The kinetics, substrate and inhibitor specificity of the lactate transporter of Ehrlich-Lettre tumour cells studied with the intracellular pH indicator BCECF. *Biochem J*, **304**: 751-760

Cerdan S, Künnecke B and Seelig J (1990). Cerebral metabolism of [1,2-$^{13}C_2$]acetate as detected by in vivo and in vitro ^{13}C NMR. *J Biol Chem*, **265**: 12916-12926

Cerdan S (2017). Twenty-seven years of cerebral pyruvate recycling. *Neurochem Res*, **42**: 1621-1628

Cesar M and Hamprecht B (1995). Immunocytochemical examination of neural rat and mouse primary cultures using monoclonal antibodies raised against pyruvate carboxylase. *J Neurochem*, **64**: 2312-2318

Chang G-G and Tong L (2003). Structure and function of malic enzymes, a new class of oxidative decarboxylases. *Biochemistry*, **42**: 12721–12733

Chareyron LJ, Banta Lavenex P, Amaral DG and Lavenex P (2021). Life and death of immature neurons in the juvenile and adult primate amygdala. *Int J Mol Sci*, **22**: 6691

Chen JF, Wang F, Huang NX, Xiao L and Mei F (2022). Oligodendrocytes and myelin: Active players in neurodegenerative brains? *Dev Neurobiol*, **82**: 160-174

Chen Y, Qin C, Huang J, Tang X, Liu C, Huang K, Xu J, Guo G, Tong A and Zhou L (2020). The role of astrocytes in oxidative stress of central nervous system: A mixed blessing. *Cell Proliferation*, **53**: e12781

Cherry JD, Olschowka JA and O'Banion MK (2014). Neuroinflammation and M2 microglia: The good, the bad, and the inflamed. *J Neuroinflammation*, **11**: 98

Cheslow L and Alvarez JI (2016). Glial-endothelial crosstalk regulates blood-brain barrier function. *Curr Opin Pharmacol*, **26**: 39-46

Chevalier A, Zhang Y, Khdour OM and Hecht SM (2016). Selective functionalization of antimycin A through an *N*-transacylation reaction. *Org Lett*, **18**: 2395-2398

Choi IS, Kim JH, Jeong JY, Lee MG, Suk K and Jang IS (2022). Astrocyte-derived adenosine excites sleep-promoting neurons in the ventrolateral preoptic nucleus: Astrocyte-neuron interactions in the regulation of sleep. *Glia*, **70**: 1864-1885

Choi MC, Kim SK, Choi YJ, Choi YJ, Kim S, Jegal KH, Lim SC and Kang KW (2023). Role of monocarboxylate transporter I/lactate dehydrogenase B-mediated lactate recycling in tamoxifen-resistant breast cancer cells. *Arch Pharmacal Res*, **46**: 907-923

Chow HM, Sun JKL, Hart RP, Cheng KKY, Hung CHL, Lau TM and Kwan KM (2021). Low-density lipoprotein receptor-related protein 6 cell surface availability regulates fuel metabolism in astrocytes. *Adv Sci*, **8**: 2004993

Cole JT, Sweatt AJ and Hutson SM (2012). Expression of mitochondrial branched-chain aminotransferase and alpha-keto-acid dehydrogenase in rat brain: implications for neurotransmitter metabolism. *Front Neuroanat*, **6**: 18

Cole SPC (2014). Multidrug resistance protein 1 (MRP1, ABCC1), a "multitasking" ATP-binding cassette (ABC) transporter. *J Biol Chem*, **289**: 30880-30888

Contreras-Baeza Y, Sandoval PY, Alarcón R, Galaz A, Cortés-Molina F, Alegría K, Baeza-Lehnert F, Arce-Molina R, Guequén A, Flores CA, San Martín A and Barros LF (2019). Monocarboxylate transporter 4 (MCT4) is a high affinity transporter capable of exporting lactate in high-lactate microenvironments. *J Biol Chem*, **294**: 20135-20147

Copin JC, Ledig M and Tholey G (1992). Free radical scavenging systems of rat astroglial cells in primary culture: Effects of anoxia and drug treatment. *Neurochem Res*, **17**: 677-682

Daneman R, Zhou L, Kebede AA and Barres BA (2010). Pericytes are required for blood-brain barrier integrity during embryogenesis. *Nature*, **468**: 562-566

Daneman R and Prat A (2015). The blood-brain barrier. *Cold Spring Harb Perspect Biol*, **7**: a020412

Dantas WS, Zunica ERM, Heintz EC, Vandanmagsar B, Floyd ZE, Yu Y, Fujioka H, Hoppel CL, Belmont KP, Axelrod CL and Kirwan JP (2022). Mitochondrial uncoupling attenuates sarcopenic obesity by enhancing skeletal muscle mitophagy and quality control. *J Cachexia Sarcopenia Muscle*, **13**: 1821-1836

De Majo M, Koontz M, Rowitch D and Ullian EM (2020). An update on human astrocytes and their role in development and disease. *Glia*, **68**: 685-704

Desagher S, Glowinski J and Prémont J (1997). Pyruvate protects neurons against hydrogen peroxide-induced toxicity. *J Neurosci*, **17**: 9060-9067

Dias MDS, Da Silva FDA, Fernandes PD, Farias CHDA, De Lima RF, Da Silva MDFC, Lima VRDN, De Lima AM, De Lacerda CN, Reis LS, Souza WBBD, Silva AARD and Arruda TFDL (2024). Beneficial effect of exogenously applied calcium pyruvate in alleviating water deficit in sugarcane as assessed by chlorophyll a fluorescence technique. *Plants*, **13**: 434

Dienel GA (2019a). Brain glucose metabolism: Integration of energetics with function. *Physiol Rev*, **99**: 949-1045

Dienel GA (2019b). Does shuttling of glycogen-derived lactate from astrocytes to neurons take place during neurotransmission and memory consolidation? *J Neurosci Res*, **97**: 863-882

Dienel GA, Schousboe A, McKenna MC and Rothman DL (2023). A tribute to Leif Hertz: The historical context of his pioneering studies of the roles of astrocytes in brain energy metabolism, neurotransmission, cognitive functions, and pharmacology identifies important, unresolved topics for future studies. *J Neurochem*, **168**: 461-495

Dimmer K-S, Friedrich B, Lang F, Deitmer JW and Bröer S (2000). The low-affinity monocarboxylate transporter MCT4 is adapted to the export of lactate in highly glycolytic cells. *Biochem J*, **350**: 219-227

Dringen R, Gebhardt R and Hamprecht B (1993a). Glycogen in astrocytes: possible function as lactate supply for neighboring cells. *Brain Res*, **623**: 208 - 214

Dringen R, Schmoll D, Cesar M and Hamprecht B (1993b). Incorporation of radioactivity from [^{14}C]lactate into the glycogen of cultured mouse astroglial cells. Evidence for gluconeogenesis in brain cells. *Biol Chem Hoppe Seyler*, **374**: 343 - 347

Dringen R, Bergbauer K, Wiesinger H and Hamprecht B (1994). Utilization of mannose by astroglial cells. *Neurochem Res*, **19**: 23-30

Dringen R and Hamprecht B (1997). Involvment of glutathione peroxidase and catalase in the disposal of exogenous hydrogen peroxide by cultured astroglial cells. *Brain Res*, **759**: 67-75

Dringen R, Gutterer JM, Gros C and Hirrlinger J (2001). Aminopeptidase N mediates the utilization of the GSH precursor CysGly by cultured neurons. *J Neurosci Res*, **66**: 1003-1008

Dringen R, Brandmann M, Hohnholt MC and Blumrich EM (2015). Glutathione-dependent detoxification processes in astrocytes. *Neurochem Res*, **40**: 2570-2582

Dunshee BR, Leben C, Keitt GW and Strong FM (1949). The isolation and properties of antimycin A. *J Am Chem Soc*, **71**: 2436-2437

Effenberger-Neidnicht K, Brauckmann S, Jägers J, Patyk V, Waack IN and Kirsch M (2019). Protective effects of sodium pyruvate during systemic inflammation limited to the correction of metabolic acidosis. *Inflammation*, **42**: 598-605

Elmetwalli A, Kamosh NH, El Safty R, Youssef AI, Salama MM, Abd El-Razek KM and El-Sewedy T (2023). Novel phloretin-based combinations targeting glucose metabolism in hepatocellular carcinoma through GLUT2/PEPCK axis of action: In silico molecular modelling and in vivo studies. *Med Oncol*, **41**: 12

Eriksson PS, Perfilieva E, Björk-Eriksson T, Alborn A-M, Nordborg C, Peterson DA and Gage FH (1998). Neurogenesis in the adult human hippocampus. *Nat Med*, **4**: 1313-1317

Eshed-Eisenbach Y, Brophy PJ and Peles E (2023). Nodes of Ranvier in health and disease. *J Peripher Nerv Syst*, **28**: S3-S11

Felmlee MA, Jones RS, Rodriguez-Cruz V, Follman KE and Morris ME (2020). Monocarboxylate transporters (SLC16): Function, regulation, and role in health and disease. *Pharmacol Rev*, **72**: 466-485

Fernández-Moncada I, Ruminot I, Robles-Maldonado D, Alegría K, Deitmer JW and Barros LF (2018). Neuronal control of astrocytic respiration through a variant of the Crabtree effect. *Proc Natl Acad Sci USA*, **115**: 1623-1628

Foltyn VN, Bendikov I, De Miranda J, Panizzutti R, Dumin E, Shleper M, Li P, Toney MD, Kartvelishvily E and Wolosker H (2005). Serine racemase modulates intracellular D-serine levels through an α,β-elimination activity. *J Biol Chem*, **280**: 1754-1763

Forero-Quintero LS, Deitmer JW and Becker HM (2017). Reduction of epileptiform activity in ketogenic mice: The role of monocarboxylate transporters. *Sci Rep*, **7**: 4900

Fridovich I (1999). Fundamental aspects of reactive oxygen species, or what's the matter with oxygen? *Ann N Y Acad Sci*, **893**: 13-18

Füger P, Hefendehl JK, Veeraraghavalu K, Wendeln A-C, Schlosser C, Obermüller U, Wegenast-Braun BM, Neher JJ, Martus P, Kohsaka S, Thunemann M, Feil R, Sisodia SS, Skodras A and Jucker M (2017). Microglia turnover with aging and in an Alzheimer's model via long-term *in vivo* single-cell imaging. *Nat Neurosci*, **20**: 1371-1376

Gabellini N, Gao Z, Oesterhelt D, Venturoli G and Melandri B (1989). Reconstruction of cyclic transport and photophosphorylation by incorporation of reaction center, cytochrom bc_1 complex and ATP synthase from *Rhodobacter capsulatus* into ubiquinone-10 / phospholipid vesicles. *Biochim Biophys Acta*, **974**: 202-210

Galland F, Seady M, Taday J, Smaili SS, Goncalves CA and Leite MC (2019). Astrocyte culture models: Molecular and function characterization of primary culture, immortalized astrocytes and C6 glioma cells. *Neurochem Int*, **131**: 104538

Giandomenico A, Cerniglia G, Biaglow J, Stevens C and Koch C (1997). The importance of sodium pyruvate in assessing damage produced by hydrogen peroxide. *Free Radic Biol Med*, **23**: 426 - 434

Glorieux C and Calderon PB (2017). Catalase, a remarkable enzyme: Targeting the oldest antioxidant enzyme to find a new cancer treatment approach. *Biol Chem*, **398**: 1095-1108

Goenaga J, Araque A, Kofuji P and Herrera Moro Chao D (2023). Calcium signaling in astrocytes and gliotransmitter release. *Front Synaptic Neurosci*, **15**: 1138577

Goldberg FW, Kettle JG, Lamont GM, Buttar D, Ting AKT, McGuire TM, Cook CR, Beattie D, Morentin Gutierrez P, Kavanagh SL, Komen JC, Kawatkar A, Clark R, Hopcroft L, Hughes G and Critchlow SE (2023). Discovery of clinical candidate AZD0095, a selective inhibitor of monocarboxylate transporter 4 (MCT4) for oncology. *J Med Chem*, **66**: 384-397

Goshi N, Morgan RK, Lein PJ and Seker E (2020). A primary neural cell culture model to study neuron, astrocyte, and microglia interactions in neuroinflammation. *J Neuroinflammation*, **17**: 155

Gottfried E, Lang SA, Renner K, Bosserhoff A, Gronwald W, Rehli M, Einhell S, Gedig I, Singer K, Seilbeck A, Mackensen A, Grauer O, Hau P, Dettmer K, Andreesen R, Oefner PJ and Kreutz M (2013). New aspects of an old drug – diclofenac targets MYC and glucose metabolism in tumor cells. *PLoS ONE*, **8**: e66987

Gowik U and Westhoff P (2011). The path from C3 to C4 photosynthesis. *Plant Physiol*, **155**: 56-63

Greene NDE and Copp AJ (2009). Development of the vertebrate central nervous system: Formation of the neural tube. *Prenat Diagn*, **29**: 303-311

Guan X-L, Wu P-F, Wang S, Zhang J-J, Shen Z-C, Luo H, Chen H, Long L-H, Chen J-G and Wang F (2017). Dimethyl sulfide protects against oxidative stress and extends lifespan via a methionine sulfoxide reductase A-dependent catalytic mechanism. *Aging Cell*, **16**: 226-236

Guan X, Rodriguez-Cruz V and Morris ME (2019). Cellular uptake of MCT1 inhibitors AR-C155858 and AZD3965 and their effects on MCT-mediated transport of L-lactate in murine 4T1 breast tumor cancer cells. *AAPS J*, **21**: 13

Guarino VA, Oldham WM, Loscalzo J and Zhang Y-Y (2019). Reaction rate of pyruvate and hydrogen peroxide: Assessing antioxidant capacity of pyruvate under biological conditions. *Sci Rep*, **9**: 19568

Guile SD, Bantick JR, Cheshire DR, Cooper ME, Davis AM, Donald DK, Evans R, Eyssade C, Ferguson DD, Hill S, Hutchinson R, Ingall AH, Kingston LP, Martin I, Martin BP, Mohammed RT, Murray C, Perry MWD, Reynolds RH, Thorne PV, Wilkinson DJ and Withnall J (2006). Potent blockers of the monocarboxylate transporter MCT1: Novel immunomodulatory compounds. *Bioorg Med Chem Lett*, **16**: 2260-2265

Guo N, McDermott KD, Shih YT, Zanga H, Ghosh D, Herber C, Meara WR, Coleman J, Zagouras A, Wong LP, Sadreyev R, Goncalves JT and Sahay A (2022). Transcriptional regulation of neural stem cell expansion in the adult hippocampus. *eLife*, **11**: e72195

Halassa MM, Fellin T, Takano H, Dong JH and Haydon PG (2007). Synaptic islands defined by the territory of a single astrocyte. *J Neurosci*, **27**: 6473-6477

Halder SK, Sapkota A and Milner R (2022). The impact of genetic manipulation of laminin and integrins at the blood-brain barrier. *Fluids Barriers CNS*, **19**: 50

Halestrap AP (1975). The mitochondrial pyruvate carrier. Kinetics and specificity for substrates and inhibitors. *Biochem J*, **148**: 85-96

Halim ND, McFate T, Mohyeldin A, Okagaki P, Korotchkina LG, Patel MS, Jeoung NH, Harris RA, Schell MJ and Verma A (2010). Phosphorylation status of pyruvate dehydrogenase distinguishes metabolic phenotypes of cultured rat brain astrocytes and neurons. *Glia*, **58**: 1168-1176

Hamprecht B and Löffler F (1985). Primary glial cultures as a model for studying hormone action. *Meth Enzymol*, **109**: 341-345

Hamprecht B and Dringen R (1994). On the role of glycogen and pyruvate uptake in astroglial-neuronal interaction. In: Pharmacology of Cerebral Ischemia: 191 - 202. Krieglstein J, Oberpichler-Schwenk H (eds), Pharmacology of Cerebral Ischemia, WVG, Stuttgart, Germany.

Harders AR, Arend C, Denieffe SC, Berger J and Dringen R (2023). Endogenous energy stores maintain a high ATP concentration for hours in glucose-depleted cultured primary rat astrocytes. *Neurochem Res*, **48**: 2241-2252

Harders AR, Spellerberg P and Dringen R (2024). Exogenous substrates prevent the decline in the cellular ATP content of primary rat astrocytes during glucose deprivation. *Neurochem Res*: 1188-1199

Harold D and Walz W (1992). Metabolic inhibition and electrical properties of type-1-like cortical astrocytes. *Neuroscience*, **47**: 203 - 211

Harris J, Jolivet R and Attwell D (2012). Synaptic energy use and supply. *Neuron*, **75**: 762-777

Hasenfuss G, Maier LS, Hermann H-P, LuErs C, HuNlich M, Zeitz O, Janssen PML and Pieske B (2002). Influence of pyruvate on contractile performance and Ca2+ cycling in isolated failing human myocardium. *Circulation*, **105**: 194-199

Hattori Y (2022). The behavior and functions of embryonic microglia. *Anat Sci Int*, **97**: 1-14

He Y, Liu X and Chen Z (2020). Glial scar—a promising target for improving outcomes after CNS injury. *J Mol Neurosci*, **70**: 340-352

Herculano-Houzel S (2012). The remarkable, yet not extraordinary, human brain as a scaled-up primate brain and its associated cost. *Proc Natl Acad Sci USA*, **109**: 10661-10668

Hermann HP, Pieske B, Schwarzmuller E, Keul J, Just H and Hasenfuss G (1999). Haemodynamic effects of intracoronary pyruvate in patients with congestive heart failure: an open study. *Lancet*, **353**: 1321-1323

Hertz L and Hertz E (2003). Cataplerotic TCA cycle flux determined as glutamate-sustained oxygen consumption in primary cultures of astrocytes. *Neurochem Int*, **43**: 355-361

Hertz L, Peng L and Dienel GA (2007). Energy metabolism in astrocytes: High rate of oxidative metabolism and spatiotemporal dependence on glycolysis/glycogenolysis. *J Cereb Blood Flow Metab*, **27**: 219-249

Hertz L and Rothman DL (2016). Glucose, lactate, β-hydroxybutyrate, acetate, GABA, and succinate as substrates for synthesis of glutamate and GABA in the glutamine-glutamate/GABA cycle. *Adv Neurobiol*, **13**: 9-42

Hertz L, Chen Y and Song D (2017). Astrocyte cultures mimicking brain astrocytes in gene expression, signaling, metabolism and K^+ uptake and showing astrocytic gene expression overlooked by immunohistochemistry and in situ hybridization. *Neurochem Res*, **42**: 254-271

Hertzberger RY, Pridmore RD, Gysler C, Kleerebezem M and Teixeira De Mattos MJ (2013). Oxygen relieves the CO_2 and acetate dependency of *Lactobacillus johnsonii* NCC 533. *PLoS ONE*, **8**: e57235

Hirrlinger J and Dringen R (2005). Multidrug resistance protein 1-mediated export of glutathione and glutathione disulfide from brain astrocytes. *Methods Enzymol*, **400**: 395-409

Hodgson EK and Fridovich I (1975). Interaction of bovine erythrocyte superoxide dismutase with hydrogen peroxide. Inactivation of the enzyme. *Biochemistry*, **14**: 5294-5299

Hu S, Bai XD, Liu XQ, Wang HB, Zhong YX, Fang T and Zhou FQ (2013). Pyruvate Ringer's solution corrects lactic acidosis and prolongs survival during hemorrhagic shock in rats. *J Emerg Med*, **45**: 885-893

Hubbard JA, Hsu MS, Seldin MM and Binder DK (2015). Expression of the astrocyte water channel aquaporin-4 in the mouse brain. *ASN Neuro*, **7**: 1759091415605486

Iliff JJ, Wang M, Liao Y, Plogg BA, Peng W, Gundersen GA, Benveniste H, Vates GE, Deane R, Goldman SA, Nagelhus EA and Nedergaard M (2012). A paravascular pathway facilitates CSF flow through the brain parenchyma and the clearance of interstitial solutes, including amyloid beta. *Sci Transl Med*, **4**: 147ra111

Jäger R, Metzger J, Lautmann K, Shushakov V, Purpura M, Geiss K-R and Maassen N (2008). The effects of creatine pyruvate and creatine citrate on performance during high intensity exercise. *J Int Soc Sport Nutr*, **5**: 4

Jessen NA, Munk AS, Lundgaard I and Nedergaard M (2015). The glymphatic system: A beginner's guide. *Neurochem Res*, **40**: 2583-2599

Jin ES, Malloy CR, Sharma G, Finn E, Fuller KNZ, Reyes YG, Lovell MA, Derderian SC, Schoen JA, Inge TH and Cree MG (2023). Glycerol as a precursor for hepatic de novo glutathione synthesis in human liver. *Redox Biol*, **63**: 102749

Juaristi I, García-Martín ML, Rodrigues TB, Satrústegui J, Llorente-Folch I and Pardo B (2017). ARALAR/AGC1 deficiency, a neurodevelopmental disorder with severe impairment of neuronal mitochondrial respiration, does not produce a primary increase in brain lactate. *J Neurochem*, **142**: 132-139

Juaristi I, Llorente-Folch I, Satrústegui J and Del Arco A (2019). Extracellular ATP and glutamate drive pyruvate production and energy demand to regulate mitochondrial respiration in astrocytes. *Glia*, **67**: 759-774

Kadry H, Noorani B and Cucullo L (2020). A blood–brain barrier overview on structure, function, impairment, and biomarkers of integrity. *Fluids Barriers CNS*, **17**: 69

Kahanovitch U, Cuddapah VA, Pacheco NL, Holt LM, Mulkey DK, Percy AK and Olsen ML (2018). MeCP2 deficiency leads to loss of glial Kir4.1. *eneuro*, **5**: e0194-0117.2018

Kala G and Hertz L (2005). Ammonia effects on pyruvate/lactate production in astrocytes-interaction with glutamate. *Neurochem Int*, **47**: 4-12

Kapoor S, Kim SM, Farook JM, Mir S, Saha R and Sen N (2013). Foxo3a transcriptionally upregulates AQP4 and induces cerebral edema following traumatic brain injury. *J Neurosci*, **33**: 17398-17403

Karger G, Berger J and Dringen R (2024). Modulation of cellular levels of adenosine phosphates and creatine phosphate in cultured primary astrocytes. *Neurochem Res*, **49**: 402-414

Kaufman EE and Driscoll BF (1992). Carbon dioxide fixation in neuronal and astroglial cells in culture. *J Neurochem*, **58**: 258-262

Kenwood BM, Weaver JL, Bajwa A, Poon IK, Byrne FL, Murrow BA, Calderone JA, Huang L, Divakaruni AS, Tomsig JL, Okabe K, Lo RH, Cameron Coleman G, Columbus L, Yan Z, Saucerman JJ, Smith JS, Holmes JW, Lynch KR, Ravichandran KS, Uchiyama S, Santos WL, Rogers GW, Okusa MD, Bayliss DA and Hoehn KL (2013). Identification of a novel mitochondrial uncoupler that does not depolarize the plasma membrane. *Mol Metab*, **3**: 114-123

Kessaris N, Pringle N and Richardson WD (2008). Specification of CNS glia from neural stem cells in the embryonic neuroepithelium. *Philos Trans R Soc Lond B Biol Sci* **363**: 71-85

Kim GH, Kim JE, Rhie SJ and Yoon S (2015). The role of oxidative stress in neurodegenerative diseases. *Exp Neurobiol*, **24**: 325-340

Koga Y, Povalko N, Katayama K, Kakimoto N, Matsuishi T, Naito E and Tanaka M (2012). Beneficial effect of pyruvate therapy on Leigh syndrome due to a novel mutation in PDH E1α gene. *Brain Dev*, **34**: 87-91

Koustova E, Rhee P, Hancock T, Chen H, Inocencio R, Jaskille A, Hanes W, Valeri CR and Alam HB (2003). Ketone and pyruvate Ringer's solutions decrease pulmonary apoptosis in a rat model of severe hemorrhagic shock and resuscitation. *Surgery*, **134**: 267-274

Kuhn S, Gritti L, Crooks D and Dombrowski Y (2019). Oligodendrocytes in development, myelin generation and beyond. *Cells*, **8**: 1424

Labs M, Rühle T and Leister D (2016). The antimycin A-sensitive pathway of cyclic electron flow: From 1963 to 2015. *Photosynth Res*, **129**: 231-238

Lalo U, Koh W, Lee CJ and Pankratov Y (2021). The tripartite glutamatergic synapse. *Neuropharmacology*, **199**: 108758

Lange SC, Bak LK, Waagepetersen HS, Schousboe A and Norenberg MD (2012). Primary cultures of astrocytes: Their value in understanding astrocytes in health and disease. *Neurochem Res*, **37**: 2569-2588

Lanosa XA and Colombo JA (2008). Cell contact-inhibition signaling as part of wound-healing processes in brain. *Neuron Glia Biol*, **4**: 27-34

Larsen BR, Assentoft M, Cotrina ML, Hua SZ, Nedergaard M, Kaila K, Voipio J and Macaulay N (2014). Contributions of the Na^+/K^+-ATPase, NKCC1, and Kir4.1 to hippocampal K^+ clearance and volume responses. *Glia*, **62**: 608-622

Larsen BR, Stoica A and MacAulay N (2016). Managing brain extracellular K^+ during neuronal activity: The physiological role of the Na^+/K^+-ATPase subunit isoforms. *Front Physiol*, **7**: 141

Leben C and Keitt GW (1948). An antibiotic substance active against certain phytopathogens. *Phytopathology*, **38**: 899-906

Lee J-Y, Kim Y-H and Koh J-Y (2001). Protection by pyruvate against transient forebrain ischemia in rats. *J Neurosci*, **21**: RC171-RC171

Lee KH, Cha M and Lee BH (2021). Crosstalk between neuron and glial cells in oxidative injury and neuroprotection. *Int J Mol Sci*, **22**: 13315

Lerchundi R, Fernández-Moncada I, Contreras-Baeza Y, Sotelo-Hitschfeld T, Mächler P, Wyss MT, Stobart J, Baeza-Lehnert F, Alegría K, Weber B and Barros LF (2015). NH_4^+ triggers the release of astrocytic lactate via mitochondrial pyruvate shunting. *Proc Natl Acad Sci USA*, **112**: 11090-11095

Li B, Hertz L and Peng L (2012). Aralar mRNA and protein levels in neurons and astrocytes freshly isolated from young and adult mouse brain and in maturing cultured astrocytes. *Neurochem Int*, **61**: 1325-1332

Li Y, Chen J and Lun S (2001). Biotechnological production of pyruvic acid. *Appl Microbiol Biotechnol*, **57**: 451-459

Lian Q, Cao H and Wang F (2014). The cost-efficiency realization in the *Escherichia coli*-based cell-free protein synthesis systems. *Appl Biochem Biotech*, **174**: 2351-2367

Liddelow SA, Olsen ML and Sofroniew MV (2024). Reactive astrocytes and emerging roles in central nervous system (CNS) disorders. *Cold Spring Harb Perspect Biol*, **5**: a041356

Liebner S, Kniesel U, Kalbacher H and Wolburg H (2000). Correlation of tight junction morphology with the expression of tight junction proteins in blood-brain barrier endothelial cells. *Eur J Cell Biol*, **79**: 707-717

Liu J, Zhu X, Kim SJ and Zhang W (2016). Antimycin-type depsipeptides: Discovery, biosynthesis, chemical synthesis, and bioactivities. *Nat Prod Rep*, **33**: 1146-1165

Liu S, Fu S, Wang G, Cao Y, Li L, Li X, Yang J, Li N, Shan Y, Cao Y, Ma Y, Dong M, Liu Q and Jiang H (2021). Glycerol-3-phosphate biosynthesis regenerates cytosolic NAD^+ to alleviate mitochondrial disease. *Cell Metab*, **33**: 1974-1987

Liu T, Jin X, Prasad RM, Sari Y and Nauli SM (2014). Three types of ependymal cells with intracellular calcium oscillation are characterized by distinct cilia beating properties. *J Neurosci Res*, **92**: 1199-1204

Liu Z, Ishikawa K, Sanada E, Semba K, Li J, Li X, Osada H and Watanabe N (2023). Identification of antimycin A as a c-Myc degradation accelerator via high-throughput screening. *J Biol Chem*, **299**: 105083

Lockington R, Borlace G and Kelly J (1997). Pyruvate decarboxylase and anaerobic survival in *Aspergillus nidulans*. *Gene*, **191**: 61 - 67

Lopez-Ortiz AO and Eyo UB (2023). Astrocytes and microglia in the coordination of CNS development and homeostasis. *J Neurochem*: in press, doi:10.1111/jnc.16006

Lopez E, Karattil R, Nannini F, Weng-Kit Cheung G, Denzler L, Galvez-Cancino F, Quezada S and Pule MA (2023). Inhibition of lactate transport by MCT-1 blockade improves chimeric antigen receptor T-cell therapy against B-cell malignancies. *J Immunother Cancer*, **11**: e006287

Lovatt D, Sonnewald U, Waagepetersen HS, Schousboe A, He W, Lin JHC, Han X, Takano T, Wang S, Sim FJ, Goldman SA and Nedergaard M (2007). The transcriptome and metabolic gene signature of protoplasmic astrocytes in the adult murine cortex. *J Neurosci*, **27**: 12255-12266

Lüllmann-Rauch R and Asan E (2015). Taschenlehrbuch Histologie. Georg Thieme Verlag, Stuttgart, New York

Ma H, Khaled HG, Wang X, Mandelberg NJ, Cohen SM, He X and Tsien RW (2023). Excitation–transcription coupling, neuronal gene expression and synaptic plasticity. *Nat Rev Neurosci*, **24**: 672-692

Mächler P, Wyss MT, Elsayed M, Stobart J, Gutierrez R, Alexandra, Kaelin V, Zuend M, Alejandro, Romero-Gómez I, Baeza-Lehnert F, Lengacher S, Bernard, Aebischer P, Pierre, L and Weber B (2016). In vivo evidence for a lactate gradient from astrocytes to neurons. *Cell Metab*, **23**: 94-102

Mahmoud S, Gharagozloo M, Simard C and Gris D (2019). Astrocytes maintain glutamate homeostasis in the CNS by controlling the balance between glutamate uptake and release. *Cells*, **8**: 184

Mallet RT, Olivencia-Yurvati AH and Bünger R (2018). Pyruvate enhancement of cardiac performance: Cellular mechanisms and clinical application. *Exp Biol Med*, **243**: 198-210

Markussen KH, Corti M, Byrne BJ, Craig W, Sun RC and Gentry MS (2023). The multifaceted roles of the brain glycogen. *J Neurochem*, **168**: 728-743

Marty-Lombardi S, Lu S, Ambroziak W, Schrenk-Siemens K, Wang J, Depaoli-Roach AA, Hagenston AM, Wende H, Tappe-Theodor A, Simonetti M, Bading H, Okun JG, Kuner R, Fleming T and Siemens J (2024). Neuron–astrocyte metabolic coupling facilitates spinal plasticity and maintenance of inflammatory pain. *Nat Metab*, **6**: 494-513

Matoba K, Dohi E, Choi EY and Kano SI (2022). Glutathione S-transferases control astrocyte activation and neuronal health during neuroinflammation. *Front Mol Biosci*, **9**: 1080140

Maugard M, Vigneron PA, Bolanos JP and Bonvento G (2021). l-Serine links metabolism with neurotransmission. *Prog Neurobiol*, **197**: 101896

Mayer RJ and Ofial AR (2019). Nucleophilicity of glutathione: A link to michael acceptor reactivities. *Angew Chem Int Ed*, **58**: 17704-17708

McBride MJ, Hunter CJ, Zhang Z, TeSlaa T, Xu X, Ducker GS and Rabinowitz JD (2024). Glycine homeostasis requires reverse SHMT flux. *Cell Metab*, **36**: 103-115

McCommis KS and Finck BN (2015). Mitochondrial pyruvate transport: a historical perspective and future research directions. *Biochem J*, **466**: 443-454

McKenna MC, Tildon JT, Couto R, Stevenson JH and Caprio FJ (1990). The metabolism of malate by cultured rat brain astrocytes. *Neurochem Res*, **15**: 1211-1220

McKenna MC, Tildon JT, Stevenson JH, Huang X and Kingwell KG (1995). Regulation of mitochondrial and cytosolic malic enzymes from cultured rat brain astrocytes. *Neurochemical Research*, **20**: 1491-1501

McKenna MC, Waagepetersen HS, Schousboe A and Sonnewald U (2006). Neuronal and astrocytic shuttle mechanisms for cytosolic-mitochondrial transfer of reducing equivalents: Current evidence and pharmacological tools. *Biochem Pharmacol*, **71**: 399-407

Moldoveanu S (2010). Chapter 17 Pyrolysis of carboxylic acids. In: Moldoveanu S (ed) Techniques and Instrumentation in Analytical Chemistry, **28**: 471-526. Elsevier.

Mongan P, Fontana J, Chen R and Bünger R (1999). Intravenous pyruvate prolongs survial during hemorrhagic shock in swine. *Am J Physiol Heart Circ Physiol*, **277**: H2253-H2263

Mongan PD, Capacchione J, Fontana J, West S and Bünger R (2001). Pyruvate improves cerebral metabolism during hemorrhagic shock. *Am J Physiol Heart Circ Physiol*, **281**: H854 - H864

Morant-Ferrando B, Jimenez-Blasco D, Alonso-Batan P, Agulla J, Lapresa R, Garcia-Rodriguez D, Yunta-Sanchez S, Lopez-Fabuel I, Fernandez E, Carmeliet P, Almeida A, Garcia-Macia M and Bolaños JP (2023). Fatty acid oxidation organizes mitochondrial supercomplexes to sustain astrocytic ROS and cognition. *Nat Metab*, **5**: 1290–1302

Nagumune H, Fukushima Y, Takada J, Yoshida K, Unami A, Shimooka T and Terada H (1993). The lipophilic weak base [Z]-5-methyl-2-[2-(1-naphthyl)ethenyl]--4-piperidinopyridine (AU-1421) is a potent protonophore type cationic uncoupler of oxidative phosphorylation in mitochondria. *Biochim Biophys Acta*, **1141**: 231-237

Nakatsuji Y and Miller RH (1998). Homotypic cell contact-dependent inhibition of astrocyte proliferation. *Glia*, **22**: 379-389

Nakatsuji Y and Miller RH (2001). Density dependent modulation of cell cycle protein expression in astrocytes. *J Neurosci Res*, **66**: 487-496

Nancolas B, Richard and Andrew (2015). Identification of key binding site residues of MCT1 for AR-C155858 reveals the molecular basis of its isoform selectivity. *Biochem J*, **466**: 177-188

Nath K, Ngo E, Hebbel R, Croatt A, Zhou B and Nutter L (1995). α-Ketoacids scavange H_2O_2 in vitro and in vivo and reduce menadione-induced DNA injury and cytotoxicity. *Am J Physiol*, **268**: C227-C236

Nave K-A and Werner HB (2014). Myelination of the nervous system: Mechanisms and functions. *Annu Rev Cell Dev Biol*, **30**: 503-533

Nelles DG and Hazrati LN (2022). Ependymal cells and neurodegenerative disease: Outcomes of compromised ependymal barrier function. *Brain Commun*, **4**: fcac288

Nguyen YTK, Ha HTT, Nguyen TH and Nguyen LN (2022). The role of SLC transporters for brain health and disease. *Cell Mol Life Sci*, **79**: 20

Nissen JD, Pajęcka K, Stridh MH, Skytt DM and Waagepetersen HS (2015). Dysfunctional TCA-cycle metabolism in glutamate dehydrogenase deficient astrocytes. *Glia*, **63**: 2313-2326

O'Donnell-Tormey J, Nathan CF, Lanks K, Deboer CJ and De La Harpe J (1987). Secretion of pyruvate. An antioxidant defense of mammalian cells. *J Exp Med*, **165**: 500-514

O'Neil M, Heckelman P and Koch C (2006). The Merck Index. An encyclopaedia of chemicals, drugs and biologicals. Merck & Co, Whitehouse Station NJ 2006

O'Brien J, Kla KM, Hopkins IB, Malecki EA and McKenna MC (2007). Kinetic parameters and lactate dehydrogenase isozyme activities support possible lactate utilization by neurons. *Neurochem Res*, **32**: 597-607

Oberheim NA, Takano T, Han X, He W, Lin JHC, Wang F, Xu Q, Wyatt JD, Pilcher W, Ojemann JG, Ransom BR, Goldman SA and Nedergaard M (2009). Uniquely hominid features of adult human astrocytes. *J Neurosci*, **29**: 3276-3287

Okada S, Nakamura M, Katoh H, Miyao T, Shimazaki T, Ishii K, Yamane J, Yoshimura A, Iwamoto Y, Toyama Y and Okano H (2006). Conditional ablation of Stat3 or Socs3 discloses a dual role for reactive astrocytes after spinal cord injury. *Nat Med*, **12**: 829-834

Oliveira JF and Araque A (2022). Astrocyte regulation of neural circuit activity and network states. *Glia*, **70**: 1455-1466

Olsen ML, Khakh BS, Skatchkov SN, Zhou M, Lee CJ and Rouach N (2015). New insights on astrocyte ion channels: critical for homeostasis and neuron-glia signaling. *J Neurosci*, **35**: 13827-13835

Orthmann-Murphy JL, Abrams CK and Scherer SS (2008). Gap junctions couple astrocytes and oligodendrocytes. *J Mol Neurosci*, **35**: 101-116

Ovens MJ, Davies AJ, Wilson MC, Murray CM and Halestrap AP (2010). AR-C155858 is a potent inhibitor of monocarboxylate transporters MCT1 and MCT2 that binds to an intracellular site involving transmembrane helices 7-10. *Biochem J*, **425**: 523-530

Papa S, Francavilla A, Paradies G and Meduri B (1971). The transport of pyruvate in rat liver mitochondria. *FEBS Letters*, **12**: 285-288

Park H, Lee J and Kim H (1998). Production of L-DOPA(3,4-dihydroxyphenyl-L-alanine) from benzene by using a hybrid pathway. *Biotechnol Bioeng*, **58**: 339 - 343

Park WH and You BR (2016). Antimycin A induces death of the human pulmonary fibroblast cells via ROS increase and GSH depletion. *Int J Oncol*, **48**: 813-820

Pauwels PJ, Opperdoes FR and Trouet A (1985). Effects of antimycin, glucose deprivation, and serum on cultures of neurons, astrocytes, and neuroblastoma cells. *J Neurochem*, **44**: 143-148

Pellerin L and Magistretti PJ (1994). Glutamate uptake into astrocytes stimulates aerobic glycolysis: a mechanism coupling neuronal activity to glucose utilization. *Proc Natl Acad Sci USA*, **91**: 10625-10629

Perea JR, Bolós M, Cuadros R, García E, García-Escudero V, Hernández F, McManus RM, Heneka MT and Avila J (2022). p38 inhibition decreases tau toxicity in microglia and improves their phagocytic function. *Mol Neurobiol*, **59**: 1632-1648

Peregrín-Alvarez JM, Sanford C and Parkinson J (2009). The conservation and evolutionary modularity of metabolism. *Genome Biol*, **10**: R63

Pérez-Sala D and Pajares MA (2023). Appraising the role of astrocytes as suppliers of neuronal glutathione precursors. *Int J Mol Sci*, **24**: 8059

Perez JC, Gerber YN and Perrin FE (2021). Dynamic diversity of glial response among species in spinal cord injury. *Front Aging Neurosci*, **13**: 769548

Petit JM, Eren-Kocak E, Karatas H, Magistretti P and Dalkara T (2021). Brain glycogen metabolism: A possible link between sleep disturbances, headache and depression. *Sleep Med Rev*, **59**: 101449

Petrat F, Ronn T and de Groot H (2011). Protection by pyruvate infusion in a rat model of severe intestinal ischemia-reperfusion injury. *J Surg Res*, **167**: e93-e101

Petrelli F, Scandella V, Montessuit S, Zamboni N, Martinou J and Knobloch M (2023). Mitochondrial pyruvate metabolism regulates the activation of quiescent adult neural stem cells. *Sci Adv*, **9**: eadd5220

Petters C and Dringen R (2014). Comparison of primary and secondary rat astrocyte cultures regarding glucose and glutathione metabolism and the accumulation of iron oxide nanoparticles. *Neurochem Res*, **39**: 46-58

Philips T, Thompson EG, Vijayakumar BG, Kent ER, Miller SJ, Vidensky S, Farah MH and Rothstein JD (2022). Astrocyte MCT1 expression does not contribute to the axonal degenerative phenotype observed with ubiquitous MCT1 depletion. *bioRxiv*: 2022.2011.2027.518094

Pineda JR, Callender R and Schwartz SD (2007). Ligand binding and protein dynamics in lactate dehydrogenase. *Biophys J*, **93**: 1474-1483

Plog BA and Nedergaard M (2018). The glymphatic system in central nervous system health and disease: Past, present, and future. *Annu Rev Pathol*, **13**: 379-394

Plotnikov E, Losenkov I, Epimakhova E and Bohan N (2019). Protective effects of pyruvic acid salt against lithium toxicity and oxidative damage in human blood mononuclear cells. *Adv Pharm Bull*, **9**: 302-306

Pociute A, Pivoriunas A and Verkhratsky A (2024). Astrocytes dynamically regulate the blood-brain barrier in the healthy brain. *Neural Regen Res*, **19**: 709-710

Poole RC and Halestrap AP (1994). N-terminal protein sequence analysis of the rabbit erythrocyte lactate transporter suggests identity with the cloned monocarboxylate transport protein MCT1. *Biochem J*, **303**: 755-759

Pronk JT, Wenzel TJ, Luttik MAH, Klaassen CCM, Scheffers WA, Steensma HY and Van Dijken JP (1994). Energetic aspects of glucose metabolism in a pyruvate-dehydrogenase-negative mutant of *Saccharomyces cerevisiae*. *Microbiology*, **140**: 601-610

Qi G, Mi Y, Shi X, Gu H, Brinton RD and Yin F (2021). ApoE4 impairs neuron-astrocyte coupling of fatty acid metabolism. *Cell Reports*, **34**: 108572

Qin J, Ma Z, Chen X and Shu S (2023). Microglia activation in central nervous system disorders: A review of recent mechanistic investigations and development efforts. *Front Neurol*, **14**: 1103416

Rae CD, Baur JA, Borges K, Dienel G, Carlos, Douglass SR, Drew K, João, Duran J, Kann O, Kristian T, Lee-Liu D, Lindquist BE, McNay EC, Robinson MB, Rothman DL, Rowlands BD, Ryan TA, Scafidi J, Scafidi S, Shuttleworth CW, Swanson RA, Uruk G, Vardjan N, Zorec R and McKenna MC (2024). Brain energy metabolism: A roadmap for future research. *J Neurochem*, **168**: 910-954

Ragan CI and Heron C (1978). The interaction between mitochondrial NADH-ubiquinone oxidoreductase and ubiquinol-cytochrome *c* oxidoreductase. Evidence for stoicheiometric association. *Biochem J*, **174**: 783-790

Rampon C, Volovitch M, Joliot A and Vriz S (2018). Hydrogen peroxide and redox regulation of developments. *Antioxidants*, **7**: 159

Rana S and Dringen R (2007). Gap junction hemichannel-mediated release of glutathione from cultured rat astrocytes. *Neurosci Lett*, **415**: 45-48

Rasmussen MK, Mestre H and Nedergaard M (2022). Fluid transport in the brain. *Physiol Rev*, **102**: 1025-1151

Reemst K, Noctor SC, Lucassen PJ and Hol EM (2016). The indispensable roles of microglia and astrocytes during brain development. *Front Hum Neurosci*, **10**: 566

Reinehr R, Görg B, Becker S, Qvartskhava N, Bidmon HJ, Selbach O, Haas HL, Schliess F and Häussinger D (2007). Hypoosmotic swelling and ammonia increase oxidative stress by NADPH oxidase in cultured astrocytes and vital brain slices. *Glia*, **55**: 758-771

Rich PR and Marechal A (2010). The mitochondrial respiratory chain. *Essays Biochem*, **47**: 1-23

Rieger M, Kappeli O and Fiechter A (1983). The role of limited respiration in the incomplete oxidation of glucose by *Saccharomyces Cerevisiae*. *Microbiology*, **129**: 653-661

Rizo J (2022). Molecular mechanisms underlying neurotransmitter release. *Annu Rev Biophys*, **51**: 377-408

Rose J, Brian C, Pappa A, Panayiotidis MI and Franco R (2020). Mitochondrial metabolism in astrocytes regulates brain bioenergetics, neurotransmission and redox balance. *Front Neurosci*, **14**: 536682

Roumes H, Pellerin L and Bouzier-Sore AK (2023). Astrocytes as metabolic suppliers to support neuronal activity and brain functions. *Essays Biochem*, **67**: 27-37

Rowitch DH and Kriegstein AR (2010). Developmental genetics of vertebrate glial–cell specification. *Nature*, **468**: 214-222

Rua R and McGavern DB (2018). Advances in meningeal immunity. *Trends Mol Med*, **24**: 542-559

Ruedig C and Dringen R (2004). TNFα increases activity of γ-glutamyl transpeptidase in cultured rat astroglial cells. *J Neurosci Res*, **75**: 536-543

Ryou M-G, Liu R, Ren M, Sun J, Mallet RT and Yang S-H (2012). Pyruvate protects the brain against ischemia–reperfusion injury by activating the erythropoietin signaling pathway. *Stroke*, **43**: 1101-1107

Sahoo B, Srivastava M, Katiyar A, Ecelbarger C and Tiwari S (2023). Liver or kidney: Who has the oar in the gluconeogenesis boat and when? *World J Diabetes*, **14**: 1049-1056

San Martín A, Ceballo S, Baeza-Lehnert F, Lerchundi R, Valdebenito R, Contreras-Baeza Y, Alegría K and Barros LF (2014). Imaging mitochondrial flux in single cells with a FRET sensor for pyruvate. *PLoS ONE*, **9**: e85780

San Martín A, Arce-Molina R, Galaz A, Pérez-Guerra G and Barros LF (2017). Nanomolar nitric oxide concentrations quickly and reversibly modulate astrocytic energy metabolism. *J Biol Chem*, **292**: 9432-9438

Sarabhai T and Roden M (2019). Hungry for your alanine: when liver depends on muscle proteolysis. *J Clin Invest*, **129**: 4563-4566

Sasaki S, Futagi Y, Ideno M, Kobayashi M, Narumi K, Furugen A and Iseki K (2016). Effect of diclofenac on SLC16A3/MCT4 by the Caco-2 cell line. *Drug Metab Pharmacokinet*, **31**: 218-223

Schipke CG and Kettenmann H (2004). Astrocyte responses to neuronal activity. *Glia*, **47**: 226-232

Schlotterose L, Cossais F, Lucius R and Hattermann K (2023). Breaking the circulus vitiosus of neuroinflammation: Resveratrol attenuates the human glial cell response to cytokines. *Biomed Pharmacother*, **163**: 114814

Schmoll D, Fuhrmann E, Gebhardt R and Hamprecht B (1995). Significant amounts of glycogen are synthesized from 3-carbon compounds in astroglial primary cultures from mice with participation of the mitochondrial phosphoenolpyruvate carboxykinase isoenzyme. *Eur J Biochem*, **227**: 308-315

Schmuck G, Rohrdanz E, Tran-Thi QH, Kahl R and Schluter G (2002). Oxidative stress in rat cortical neurons and astrocytes induced by paraquat *in vitro*. *Neurotox Res*, **4**: 1-13

Schousboe A, Bak LK and Waagepetersen HS (2013). Astrocytic control of biosynthesis and turnover of the neurotransmitters glutamate and GABA. *Front Endocrinol*, **4**: 102

Schousboe A, Waagepetersen HS and Sonnewald U (2019). Astrocytic pyruvate carboxylation: Status after 35 years. *J Neurosci Res*, **97**: 890-896

Selak I, Skaper S and Varon S (1985). Pyruvate participation in the low molecular weight trophic activity for central nervous system neurons in glia-conditioned media. *J Neurosci*, **5**: 23-28

Shank RP, Bennett GS, Freytag SO and Campbell GL (1985). Pyruvate carboxylase: an astrocyte-specific enzyme implicated in the replenishment of amino acid neurotransmitter pools. *Brain Res*, **329**: 364-367

Shearman MS and Halestrap AP (1984). The concentration of the mitochondrial pyruvate carrier in rat liver and heart mitochondria determined with α-cyano-β-(1-phenylindol-3-yl)acrylate. *Biochem J*, **223**: 673-676

Siems WG, Sommerburg O and Grune T (2000). Erythrocyte free radical and energy metabolism. *Clinical nephrology*, **53**: S9-17

Slater E (1973). The mechanism of action of the respiratory inhibitor, antimycin. *Biochim Biophys Acta*, **301**: 129-154

Sofroniew MV and Vinters HV (2010). Astrocytes: Biology and pathology. *Acta Neuropathol*, **119**: 7-35

Sofroniew MV (2015). Astrogliosis. *Cold Spring Harb Perspect Biol*, **7**: a020420

Sonnewald U, Westergaard N, Jones P, Taylor A, Bachelard HS and Schousboe A (1996). Metabolism of [U-$^{13}C_5$]glutamine in cultured astrocytes studied by NMR spectroscopy: First evidence of astrocytic pyruvate recycling. *J Neurochem*, **67**: 2566-2572

Sonnewald U and Rae C (2010). Pyruvate carboxylation in different model systems studied by ^{13}C MRS. *Neurochem Res*, **35**: 1916-1921

Sotelo-Hitschfeld T, Niemeyer MI, Mächler P, Ruminot I, Lerchundi R, Wyss MT, Stobart J, Fernández-Moncada I, Valdebenito R, Garrido-Gerter P, Contreras-Baeza Y, Schneider BL, Aebischer P, Lengacher S, San Martín A, Le Douce J, Bonvento G, Magistretti PJ, Sepúlveda FV, Weber B and Barros LF (2015). Channel-mediated lactate release by K^+-stimulated astrocytes. *J Neurosci*, **35**: 4168-4178

Stacpoole PW (2017). Therapeutic targeting of the pyruvate dehydrogenase complex/pyruvate dehydrogenase kinase (PDC/PDK) axis in cancer. *J Natl Cancer Inst*, **109**: djx071

Steinmeier J, Kube S, Karger G, Ehrke E and Dringen R (2020). β-Lapachone induces acute oxidative stress in rat primary astrocyte cultures that is terminated by the NQO1-inhibitor dicoumarol. *Neurochem Res*, **45**: 2442-2455

Sun J, Zheng Y, Chen Z and Wang Y (2022). The role of Na^+-K^+-ATPase in the epileptic brain. *CNS Neurosci Ther*, **28**: 1294-1302

Swanson RA (1992). Astrocyte glutamate uptake during chemical hypoxia in vitro. *Neurosci Lett*, **147**: 143-146

Sweetman B and Linninger AA (2011). Cerebrospinal fluid flow dynamics in the central nervous system. *Ann Biomed Eng*, **39**: 484-496

Szutowicz A and Lysiak WZ (1980). Regional and subcellular distribution of ATP-citrate lyase and other enzymes of acetyl-CoA metabolism in rat brain. *J Neurochem*, **35**: 775-785

Tauffenberger A and Magistretti PJ (2021). Reactive oxygen species: Beyond their reactive behavior. *Neurochem Res*, **46**: 77-87

Tavoulari S, Sichrovsky M and Kunji ERS (2023). Fifty years of the mitochondrial pyruvate carrier: New insights into its structure, function, and inhibition. *Acta Physiol*, **238**: e14016

TeSlaa T, Ralser M, Fan J and Rabinowitz JD (2023). The pentose phosphate pathway in health and disease. *Nat Metab*, **5**: 1275-1289

Thapa RK, Choi H-G, Kim JO and Yong CS (2017). Analysis and optimization of drug solubility to improve pharmacokinetics. *J Pharm Investig*, **47**: 95-110

Theparambil SM, Hosford PS, Ruminot I, Kopach O, Reynolds JR, Sandoval PY, Rusakov DA, Barros LF and Gourine AV (2020). Astrocytes regulate brain extracellular pH via a neuronal activity-dependent bicarbonate shuttle. *Nat Commun*, **11**: 5073

Todd AC and Hardingham GE (2020). The regulation of astrocytic glutamate transporters in health and neurodegenerative diseases. *Int J Mol Sci*, **21**: 9607

Tulpule K, Hohnholt MC, Hirrlinger J and Dringen R (2014). Primary cultures of astrocytes and neurons as model systems to study the metabolism and metabolite export from brain cells. In: Hirrlinger J and Waagepetersen HS (eds) Neuromethods: Brain Energy Metabolism, **90**: 45-72. Humana Press, New York.

Ullah MS, Davies AJ and Halestrap AP (2006). The plasma membrane lactate transporter MCT4, but not MCT1, is up-regulated by hypoxia through a HIF-1α-dependent mechanism. *J Biol Chem*, **281**: 9030-9037

Urbach A and Witte OW (2019). Divide or commit – revisiting the role of cell cycle regulators in adult hippocampal neurogenesis. *Front Cell Dev Biol*, **7**: 55

Utter MF and Keech DB (1963). Pyruvate carboxylase. *J Biol Chem*, **238**: 2603-2608

Van Putten MJAM, Fahlke C, Kafitz KW, Hofmeijer J and Rose CR (2021). Dysregulation of astrocyte ion homeostasis and its relevance for stroke-induced brain damage. *Int J Mol Sci*, **22**: 5679

Vásquez-Vivar J, Denicola A, Radi R and Augusto O (1997). Peroxynitrite-mediated decarboxylation of pyruvate to both carbon dioxide and carbon dioxide radical anion. *Chem Res Tox*, **10**: 786-794

Vaupel P and Multhoff G (2021). Revisiting the Warburg effect: historical dogma *versus* current understanding. *J Physiol*, **599**: 1745-1757

Vera B, Sánchez-Abarca LI, Bolaños JP and Medina JM (1996). Inhibition of astrocyte gap junctional communication by ATP depletion is reversed by calcium sequestration. *FEBS Letters*, **392**: 225-228

Vergara RC, Jaramillo-Riveri S, Luarte A, Moenne-Loccoz C, Fuentes R, Couve A and Maldonado PE (2019). The energy homeostasis principle: Neuronal energy regulation drives local network dynamics generating behavior. *Front Comput Neurosci*, **13**: 49

Verma M, Lizama BN and Chu CT (2022). Excitotoxicity, calcium and mitochondria: A triad in synaptic neurodegeneration. *Transl Neurodegener*, **11**: 3

Vicente-Gutierrez C, Bonora N, Bobo-Jimenez V, Jimenez-Blasco D, Lopez-Fabuel I, Fernandez E, Josephine C, Bonvento G, Enriquez JA, Almeida A and Bolaños JP (2019). Astrocytic mitochondrial ROS modulate brain metabolism and mouse behaviour. *Nat Metab*, **1**: 201-211

Vicente-Gutierrez C, Jimenez-Blasco D and Quintana-Cabrera R (2021). Intertwined ROS and metabolic signaling at the neuron-astrocyte interface. *Neurochem Res*, **46**: 23-33

Vogel R, Hamprecht B and Wiesinger H (1998a). Malic enzyme isoforms in astrocytes: comparative study on activities in rat brain tissue and astroglia-rich primary cultures. *Neurosci Lett*, **247**: 123-126

Vogel R, Jennemann G, Seitz J, Wiesinger H and Hamprecht B (1998b). Mitochondrial malic enzyme: Purification from bovine brain, generation of an antiserum, and immunocytochemical localization in neurons of rat brain. *J Neurochem*, **71**: 844-852

von Lenhossék M (1891). Zur Kenntnis der Neuroglia des menschlichen Rückenmarks. *Verh Anat Ges*, **5**: 193 - 221

Voss CM, Andersen JV, Jakobsen E, Siamka O, Karaca M, Maechler P and Waagepetersen HS (2020). AMP-activated protein kinase (AMPK) regulates astrocyte oxidative metabolism by balancing TCA cycle dynamics. *Glia*, **68**: 1824-1839

Waagepetersen HS, Qu H, Hertz L, Sonnewald U and Schousboe A (2002a). Demonstration of pyruvate recycling in primary cultures of neocortical astrocytes but not in neurons. *Neurochem Res*, **27**: 1431-1437

Waagepetersen HS, Sonnewald U, Larsson OM and Schousboe A (2002b). A Possible Role of Alanine for Ammonia Transfer Between Astrocytes and Glutamatergic Neurons. *J Neurochem*, **75**: 471-479

Wang F, Ruppell KT, Zhou S, Qu Y, Gong J, Shang Y, Wu J, Liu X, Diao W, Li Y and Xiang Y (2023). Gliotransmission and adenosine signaling promote axon regeneration. *Dev Cell*, **58**: 660-676

Wang XF and Cynader MS (2001). Pyruvate released by astrocytes protects neurons from copper-catalyzed cysteine neurotoxicity. *J Neurosci*, **21**: 3322 - 3331

Wang Z, Ying Z, Bosy-Westphal A, Zhang J, Heller M, Later W, Heymsfield SB and Muller MJ (2012). Evaluation of specific metabolic rates of major organs and tissues: Comparison between nonobese and obese women. *Obesity*, **20**: 95-100

Watermann P, Arend C and Dringen R (2023). G6PDi-1 is a potent inhibitor of G6PDH and of pentose phosphate pathway-dependent metabolic processes in cultured primary astrocytes. *Neurochem Res*, **48**: 3177-3189

Watermann P and Dringen R (2023). β-lapachone-mediated WST1 reduction as indicator for the cytosolic redox metabolism of cultured primary astrocytes. *Neurochem Res*, **48**: 2148-2160

Watts LT, Rathinam ML, Schenker S and Henderson GI (2005). Astrocytes protect neurons from ethanol-induced oxidative stress and apoptotic death. *J Neurosci Res*, **80**: 655-666

Weber B and Barros LF (2015). The astrocyte: Powerhouse and recycling center. *Cold Spring Harb Perspect Biol*, **7**: a020396

Westergaard N, Drejer J, Schousboe A and Sonnewald U (1996). Evaluation of the importance of transamination versus deamination in astrocytic metabolism of [U-^{13}C] glutamate. *Glia*, **17**: 160-168

Wolburg H, Wolburg-Buchholz K, Mack A and Reichenbach A (2009). Ependymal cells. In: Squire L (ed) Encyclopedia of Neuroscience: 1133-1140. Academic Press.

Xie L, Kang H, Xu Q, Chen MJ, Liao Y, Thiyagarajan M, O'Donnell J, Christensen DJ, Nicholson C, Iliff JJ, Takano T, Deane R and Nedergaard M (2013). Sleep drives metabolite clearance from the adult brain. *Science*, **342**: 373-377

Xu L-Y, Quan X-S, Wang C, Sheng H-F, Zhou G-X, Lin B-R, Jiang R-W and Yao X-S (2011). Antimycins A19 and A20, two new antimycins produced by marine actinomycete Streptomyces antibioticus H74-18. *J Antibiot*, **64**: 661-665

Xu L, Phelix CF and Chen LY (2021). Structural insights into the human mitochondrial pyruvate carrier complexes. *J Chem Inf Model*, **61**: 5614-5625

Xu Y, Liu X, Jin H, Li X and Shen J (2024). Diet supplementation with sodium pyruvate increases sleep time and lifespan in *Drosophila* model. *Arch Insect Biochem*, **115**: e22069

Yang J, Ruchti E, Petit J-M, Jourdain P, Grenningloh G, Allaman I and Magistretti PJ (2014). Lactate promotes plasticity gene expression by potentiating NMDA signaling in neurons. *Proc Natl Acad Sci USA*, **111**: 12228-12233

Yang L, Kombu RS, Kasumov T, Zhu S-H, Cendrowski AV, David F, Anderson VE, Kelleher JK and Brunengraber H (2008). Metabolomic and mass isotopomer analysis of liver gluconeogenesis and citric acid cycle I. Interrelation between gluconeogenesis and cataplerosis; formation of methoxamates from aminooxyacetate and ketoacids. *J Biol Chem*, **283**: 21978-21987

Yeh C-F and Hsu C-H (2019). Chapter 7 - Microfluidic techniques for single-cell culture. In: Barh D and Azevedo V (eds) Single-Cell Omics, **1**: 137-151. Elsevier.

Yip J, Geng X, Shen J and Ding Y (2016). Cerebral gluconeogenesis and diseases. *Front Pharmacol*, **7**: 521

Yu L, Teoh ST, Ensink E, Ogrodzinski MP, Yang C, Vazquez AI and Lunt SY (2019). Cysteine catabolism and the serine biosynthesis pathway support pyruvate production during pyruvate kinase knockdown in pancreatic cancer cells. *Cancer Metab*, **7**: 13

Yu TJ, Hsieh CY, Tang JY, Lin LC, Huang HW, Wang HR, Yeh YC, Chuang YT, Ou-Yang F and Chang HW (2020). Antimycin A shows selective antiproliferation to oral cancer cells by oxidative stress-mediated apoptosis and DNA damage. *Environ Toxicol*, **35**: 1212-1224

Yuan W, Du Y, Yu K, Xu S, Liu M, Wang S, Yang Y, Zhang Y and Sun J (2022). The production of pyruvate in biological technology: A critical review. *Microorganisms*, **10**: 2454

Zabielska MA, Adamus J, Kowalski R, Gebicki J, Slominska EM, Khalpey Z and Smolenski RT (2018). Cardioprotective effect of N-methylnicotinamide salt of pyruvate in experimental model of cardiac hypoxia. *Pharmacol Rep*, **70**: 378-384

Zhang C, Kang J, Zhang X, Zhang Y, Huang N and Ning B (2022a). Spatiotemporal dynamics of the cellular components involved in glial scar formation following spinal cord injury. *Biomed Pharmacother*, **153**: 113500

Zhang X, St. Leger RJ and Fang W (2018). Stress-induced pyruvate accumulation contributes to cross protection in a fungus. *Environ Microbiol*, **20**: 1158-1169

Zhang X, Jin X, Sun R, Zhang M, Lu W and Zhao M (2022b). Gene knockout in cellular immunotherapy: Application and limitations. *Cancer Lett*, **540**: 215736

Zhang XM, Deng H, Tong JD, Wang YZ, Ning XC, Yang XH, Zhou FQ and Jin HM (2020). Pyruvate-enriched oral rehydration solution improves glucometabolic disorders in the kidneys of diabetic *db/db* mice. *J Diab Res*, **2020**: 1-13

Zhang Y and Barres BA (2010). Astrocyte heterogeneity: An underappreciated topic in neurobiology. *Curr Opin Neurobiol*, **20**: 588-594

Zhang Y, Chen K, Sloan SA, Bennett ML, Scholze AR, O'Keeffe S, Phatnani HP, Guarnieri P, Caneda C, Ruderisch N, Deng S, Liddelow SA, Zhang C, Daneman R, Maniatis T, Barres BA and Wu JQ (2014). An RNA-sequencing transcriptome and splicing database of glia, neurons, and vascular cells of the cerebral cortex. *J Neurosci*, **34**: 11929-11947

Zhou J and Sutherland ML (2004). Glutamate transporter cluster formation in astrocytic processes regulates glutamate uptake activity. *J Neurosci*, **24**: 6301-6306

Zhou Y and Danbolt NC (2014). Glutamate as a neurotransmitter in the healthy brain. *J Neural Transm*, **121**: 799-817

Zwingmann C, Richter-Landsberg C and Leibfritz D (2001). ^{13}C isotopomer analysis of glucose and alanine metabolism reveals cytosolic pyruvate compartmentation as part of energy metabolism in astrocytes. *Glia*, **34**: 200-212

2 Results

2.1 Publication 1

Consumption and Metabolism of Extracellular Pyruvate by Cultured Rat Brain Astrocytes

Denker N., Harders A.R., Arend C., Dringen R. (2023)

Neurochemical Research 48: 1438 – 1454
DOI: 10.1007/s11064-022-03831-6

Contribution of Nadine Denker:

- 100 % of the experimental work to obtain the data shown in Figures 2, 3, 4, 5, 7, 8 and in Table 1
- 80 % of the experimental work to obtain the data shown in Figure 1
- Experimental preparation for collection of data for Figure 6
- Preparation of all figures and tables
- 50 % of preparation of the first draft of the manuscript

(20 % of data shown in Figure 1 were acquired by Antonia Harders and the data shown in Figure 6 were acquired by Dr. Christian Arend)

Neurochemical Research (2023) 48:1438–1454
https://doi.org/10.1007/s11064-022-03831-6

ORIGINAL PAPER

Neurochemical Research (2023) 48:1438–1454

For mitochondrial metabolism of pyruvate, cytosolic pyruvate has to be imported into mitochondria. This transport is mediated by the mitochondrial pyruvate carrier (MPC), a hetero-oligomeric complex formed by the two proteins MPC1 and MPC2 [22, 23]. MPC is functionally expressed in astrocytes [23]. Within the mitochondrial matrix of astrocytes, the pyruvate dehydrogenase complex (PDC) oxidatively decarboxylates pyruvate to acetyl coenzyme A (acetyl-CoA) [7, 20]. The activity of this enzyme has been reported to limit the oxidative metabolism of pyruvate and of substances which are metabolized via pyruvate [24]. Astrocytes in culture have been reported to maintain a rather low activity of PDC under unstressed conditions [24]. Acetyl-CoA can enter the TCA cycle in astrocytes [8] or can be used for the synthesis of the ketone bodies acetoacetate and beta-hydroxybutyrate (bHB) [25, 26]. The oxaloacetate needed for citrate synthesis with acetyl CoA can be generated by the anaplerotic pyruvate carboxylase which is considered as an astrocyte specific enzyme in brain [27, 28].

Astrocytes have been reported to release pyruvate and such astrocyte-derived extracellular pyruvate has been shown to be antioxidative and neuroprotective [29, 30]. Extracellular pyruvate can also be taken up by astrocytes in a saturable and pH-dependent process [31], mainly mediated by the monocarboxylate transporter (MCT) 1 which is expressed in astrocytes [32–34] and has a K_m value of around 1 mM for its substrate pyruvate [35]. Studies using radioactively labelled pyruvate revealed that pyruvate is efficiently taken up and rapidly converted to lactate and alanine in cultured astrocytes [31].

Despite the importance of pyruvate as central cellular metabolic intermediate, surprisingly little information is available on the processes which are involved in the consumption of extracellular pyruvate by astrocytes. To address such questions, we have investigated the transport processes involved in astrocytic pyruvate consumption as well as mitochondrial processes which may modulate astrocytic pyruvate consumption. The results presented here demonstrate that, compared to other substrates of mitochondrial metabolism, astrocytes consume pyruvate more efficiently in the absence of glucose and that MCT1 as well as the mitochondrial pyruvate carrier are involved in the consumption of extracellular pyruvate. Furthermore, pyruvate consumption by astrocytes depends strongly on the activity of mitochondrial respiration. Finally, the main products of pyruvate consumption by glucose-starved astrocytes are lactate and alanine, which are found to be released from these cells.

Materials and Methods

Materials

Dulbecco's modified Eagles medium (DMEM) and penicillin G/streptomycin sulfate solution (Pen/Strep) were obtained from Thermo Fisher Scientific (Schwerte, Germany). Fetal calf serum (FCS), antimycin A, BAM15 and UK5099 were purchased from Sigma-Aldrich (Darmstadt, Germany). AR-C155858 was purchased at Tocris (Bristol, UK). All enzymes used were purchased from Roche Diagnostics (Mannheim, Germany). The Acetic Acid Assay kit (ACS Manual Format) was from Megazyme (Bray, Ireland). The Cell Titer Glo® 2.0 Assay Kit for ATP quantification was from Promega (Walldorf, Germany). Other chemicals of the highest purity available were obtained from Merck (Darmstadt, Germany), Sigma-Aldrich (Darmstadt, Germany), Roth (Karlsruhe, Germany), AppliChem (Darmstadt, Germany) or Thermo Fisher Scientific (Schwerte, Germany). Sterile cell culture materials and unsterile 96-well plates and black microtiter plates were purchased from Sarstedt (Nümbrecht, Germany).

Astrocyte Cultures

Astrocyte-rich primary cultures were prepared as previously described in detail from the brains of newborn Wistar rats [36]. Cells were seeded in a density of 300,000 cells per well in 1 mL culture medium (90% DMEM containing 25 mM glucose, 44.6 mM sodium bicarbonate, 1 mM pyruvate, 20 U/mL penicillin G, 20 µg/mL streptomycin sulfate, supplemented with 10% FCS) into wells of 24-well dishes. The cultures were maintained in a humidified atmosphere with 10% CO_2 in a Sanyo CO_2 incubator (Osaka, Japan). The culture medium was renewed every 7th day and 1 day prior to an experiment. Confluent astrocytes cultures of an age between 14 and 28 days in culture were used for the experiments. Astrocyte-rich primary cultures are strongly enriched in astrocytes and contain only low amounts of contaminating microglial cells and oligodendrocytes [36, 37].

Experimental Incubation of the Cells

For cell incubations, the medium was completely aspirated from the cultures, the cells were washed twice with 1 mL pre-warmed (37 °C) glucose-free incubation buffer (IB; 145 mM NaCl, 20 mM HEPES, 5.4 mM KCl, 1.8 mM $CaCl_2$, 1 mM $MgCl_2$, 0.8 mM Na_2HPO_4, pH adjusted with NaOH to 7.4 at 37 °C) and subsequently incubated for up to 5 h at 37 °C in the humidified atmosphere of a CO_2-free incubator with 250 µL of IB that had been supplemented with

pyruvate, other energy substrates, inhibitors of transporters and/or modulators of metabolic pathways. Appropriate solvent controls were performed for incubations with compounds that had been dissolved as concentrated stock solutions in DMSO. The final DMSO concentration in such media did not exceed 1.1% and the presence of DMSO in the concentrations used did not have any effect on the parameters investigated (data not shown). After the given incubation periods the incubation medium was harvested for determination of metabolite concentrations and cell viability. Cells were washed twice with 1 mL ice-cold (4 °C) phosphate-buffered saline (PBS; 10 mM potassium phosphate buffer pH 7.4 containing 150 mM NaCl) and either lysed as described below for ATP quantification or stored frozen until the protein determination was performed.

Determination of Cell Viability and Initial Protein Content

To test for potential cell toxicity of a given treatment the extracellular activity of the cytosolic enzyme LDH was determined after the treatment for 10 µL media samples and compared with the initial cellular LDH activity of untreated cells, as previously described in detail [36]. Cellular protein content per well was determined by the Lowry method [38] using bovine serum albumin as standard protein.

Determination of Extracellular Substrates and Metabolites

Pyruvate was quantified in a microtiter plate assay by the LDH and NADH-dependent reduction to lactate by a method adapted from Clarke and Payton [39]. Media volumes between 25 and 180 µL were diluted with 80 mM Tris-HCl buffer pH 7.2, containing 200 mM NaCl, to a total volume of 180 µL in wells of a microtiter plate before 180 µL reaction mixture (0.4 mM NADH and 4 U LDH in 80 mM Tris-HCl buffer pH 7.2, containing 200 mM NaCl) per well was added to reach a final initial NADH concentration of 0.2 mM. The decline observed in NADH absorbance determined at 340 nm after completion of the reaction (around 3 min) was measured in a microtiter plate spectrophotometer (Multiskan Sky microtiter spectrophotometer, Thermo Fisher Scientific, Schwerte, Germany) and used to calculate the pyruvate concentration in the sample.

Extracellular alanine was determined by a coupled enzymatic reaction in microtiter plates. In this assay, alanine is first transaminated by glutamate-pyruvate transaminase to pyruvate which is subsequently reduced by LDH to lactate and analyzed by the decrease in NADH absorbance at 340 nm. As the later reaction will also quantify pyruvate that may as well be present in the media samples analyzed, the concentration of alanine was calculated by the difference of signals obtained for reactions containing the complete reaction components and those containing only the pyruvate assay components. Media samples of 90 µL were mixed with 90 µL of the pyruvate reaction mixture (containing 0.8 mM NADH and 8 U LDH in 80 mM Tris-HCl buffer pH 7.2, containing 200 mM NaCl) in a microtiter plate well. After 3 min of incubation at room temperature (RT), the pyruvate-dependent decline in absorbance at 340 nm was completed and the concentration of pyruvate was calculated (pathlength of 0.5 cm for 180 µL per well). Thereafter, 180 µL of the second reaction mixture for alanine quantification (containing 0.7 U GPT and 10 mM α-ketoglutarate in 80 mM Tris-HCl buffer pH 7.2 containing 200 mM NaCl) was added. The decline in absorbance at 340 nm was measured after 90 min incubation at 37 °C in a humidified atmosphere. The concentration of pyruvate plus alanine was calculated (pathlength of 1 cm for 360 µL per well) from the decline in absorbance. The alanine concentration in the samples was calculated by subtracting the concentration of pyruvate determined (after addition of the first reaction mixture) from the sum of the concentrations of alanine plus pyruvate determined (after the addition of the second reaction mixture).

The concentration of extracellular glucose or lactate in the incubation medium was determined by coupled enzymatic assays as previously described in detail [36] for media sample volumes between 10 and 90 µL.

Extracellular acetate was quantified by using an acetate kit (Megazyme© Acetic Acid Assay Kit, ACS Manual Format) according to the information provided by the supplier in a modification adapted to microtiter plates. The acetyl-coenzyme A synthetase (ACS) provided in the kit activates acetate to Acetyl-CoA which is subsequently combined with oxaloacetate to citrate (citrate synthase, CS). The oxaloacetate needed for this reaction is generated from malate by malate dehydrogenase (MDH) and this supply is quantified by the NADH-dependent increase in absorbance at 340 nm caused by the MDH reaction. For acetate quantification, 90 µL fresh media samples or acetate standards in incubation buffer (concentrations between 0 and 600 µM) were mixed with 90 µL of a first reaction mixture (containing CS and MDH) containing appropriate volumes of the kit solutions adapted to the microtiter plate format to determine acetate-independent reactions. After 4 min, 180 µL of the second reaction mixture of the kit (containing ACS) was added and the acetate-mediated increase in absorption at 340 nm was measured after 20 min of incubation at room temperature. Acetate concentrations in media samples were calculated by using the calibration curve obtained for the absorbances determined for the acetate standards.

Extracellular β-hydroxybutyrate (bHB) was determined according to Kientsch-Engel and Siess [40] using a modification that was adapted to microtiter plate formate. bHB is oxidised by bHB dehydrogenase (bHBDH) to acetoacetate

and the NADH generated in this reaction is used to reduce the Fe^{3+}-BPS complex to the Fe^{2+}-BPS complex which strongly absorbs at 535 nm. For the assay, 180 µL of the bHB-containing incubation buffers or bHB standards (concentrations of up to 100 µM) were mixed in a well of a microtiter plate with 180 µL of a reaction mixture to obtain final concentrations of 350 mM potassium phosphate buffer pH 8.5, 8.8 mM NAD^+, 0.45 mM $FeCl_3$, 1.9 mM bathophenanthroline disulfonate (BPS), 3 µM phenazine methosulphate and 0.1 U bHBDH. The microtiter plate was then incubated for 90 min at room temperature in the dark before the absorbance of Fe^{2+}-BPS at 535 nm was determined. bHB concentrations in media samples were calculated by using the calibration curve generated from the absorbances determined for the bHB standards.

Quantification of Cellular ATP Content

Cellular ATP contents were determined for neutralized perchloric acid cell lysates of astrocyte cultures by using a commercial luciferase-based assay kit. After the indicated incubation, the media samples were collected and the cells were washed twice with 1 mL ice-cold PBS. Afterwards, the cells were lysed in 200 µL of ice-cold 0.5 M $HClO_4$ on ice for 1 min. The cell lysates were collected and diluted by a factor of 20 in 0.5 M $HClO_4$ before the pH was neutralised by the addition of an appropriate amount of 2 M KOH. Thereafter, the samples were vortexed and subsequently centrifuged for 5 min at 12,100×*g* to precipitate the $KClO_4$ before the supernatant was transferred into a new cup. To adjust the pH, 10 µL of 1.4 M Tris-acetate buffer (pH 7.75) was added. ATP-standards in concentrations of up to 1000 nM in $HClO_4$ were prepared and treated identically. Finally, 50 µL of each neutralised cell lysate or ATP standard was transferred into the wells of a black 96-well plate and mixed with 50 µL of the ATP detection reagent (Cell Titer Glo® 2.0 ATP Assay Kit). After 20 min of incubation in the dark at RT the luminescence signal was recorded by a Fluoroskan Ascent FL chemiluminescence plate reader (Thermo Fisher Scientific, Schwerte, Germany). ATP concentrations were calculated by comparison of the detected luminometric signals from the diluted cell lysates with the linear calibration curve of the values obtained from the ATP standards. Specific ATP contents were calculated by normalizing the determined ATP values per well to the initial cellular protein content per well.

Staining for Mitochondrial Membrane Potential

After a given incubation period, cultured astrocytes were stained with tetramethylrhodamine ethyl ester (TMRE) to visualize the mitochondrial membrane potential [19]. The cells were incubated for 90 min in IB containing 0.5 mM pyruvate plus 40 nM TMRE in the absence or presence of 10 µM antimycin A or 1 µM BAM15. The incubation was performed at 37 °C in the humidified atmosphere of a cell incubator while the cell culture plates were wrapped in aluminum foil to prevent light exposure. After the incubation period, cellular fluorescence of TMRE was directly analyzed by fluorescence microscopy (Eclipse TE-2000-U with a DS-QiMc camera and imaging software NIS-Elements BR, Nikon, Düsseldorf, Germany) while the cells were kept in the incubation medium on a heating plate at 37 °C. The filter settings for detection of the fluorescence of TMRE were as follows: excitation at 510–565 nm, emission at 590 nm, dichromatic mirror at 575 nm. All images within one experiment were taken with the same light intensity and exposure time settings to allow for direct comparison of the different incubation conditions. TMRE fluorescence of the whole image section was quantified with the software ImageJ after subtraction of the background fluorescence using the rolling ball method within the software by applying the same radius for all images within one experiment.

Presentation of Data and Statistical Analysis

The quantitative data shown are means ± SD of values obtained from three individual experiments performed in triplicates on independently prepared astrocyte cultures. Analysis for statistical significance of groups of data was performed by ANOVA followed by the Bonferroni post-hoc test using the software GraphPad InStat. The level of significance compared to control conditions are indicated by $*p < 0.05$, $**p < 0.01$ and $***p < 0.001$. Analysis for statistical significance between pairs of data was calculated by the paired t-test. The level of significance between pairs is indicated by $\#p < 0.05$, $\#\#p < 0.01$ and $\#\#\#p < 0.001$. $p > 0.05$ was considered as not significant.

Results

Consumption of Mitochondrial Substrates by Cultured Astrocytes

To test for the ability of astrocytes to take up and metabolize extracellular substrates that can be oxidized by mitochondrial metabolism, primary astrocyte cultures were exposed to 0.5 mM of pyruvate, lactate, acetate, alanine or bHB in a glucose-free incubation buffer and the decline in concentrations of the substances applied was recorded during an incubation period of up to 5 h (Fig. 1). All applied extracellular substrates disappeared at least partially from the incubation buffer during incubation of the cells, but the consumption of extracellular pyruvate was the highest among the tested substrates (Fig. 1a, b). The specific consumption rate of

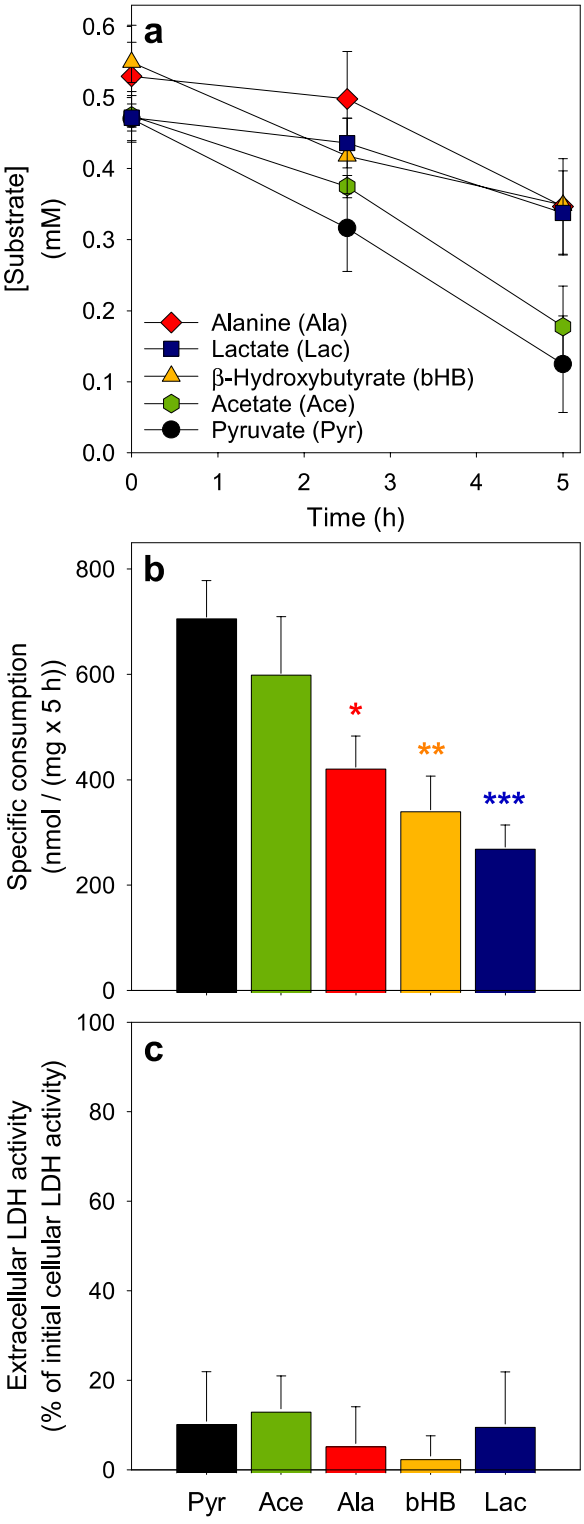

Fig. 1 Consumption of mitochondrial substrates by primary astrocytes cultures. The cells were incubated in a glucose-free incubation buffer with 0.5 mM of the indicated substrates and the extracellular concentrations of the substrates applied were monitored over an incubation period of up to 5 h (**a**). In addition, the specific consumption of the applied substrates during the 5 h incubation (**b**) as well as the percental extracellular LDH activity (**c**) as indicator of a potential loss in cell viability were calculated. The data shown are means ± SD of values obtained in three experiments performed on independently prepared cultures. The initial cellular LDH activity of the cultures was 119 ± 14 nmol/(min × well) and the initial protein content was 126 ± 17 µg/well. In panel b, the significance of differences (ANOVA) compared to the values obtained for a pyruvate treatment is indicated by *p<0.05, **p<0.01 and ***p<0.001

pyruvate was around 700 nmol/(mg × 5 h). A similar consumption rate was only observed for acetate, while the consumption rates calculated for incubations with alanine, bHB and lactate were significantly lower than those calculated for pyruvate (Fig. 1a, b). For comparison, cultured astrocytes that had been exposed to 0.5 mM glucose completely consumed the applied amount within the 5 h incubation period (data not shown). The viability of the cells was not affected by the treatments used, as indicated by the absence of any significant increase in extracellular LDH activity (Fig. 1c). In the absence of cells but otherwise under identical conditions, no decrease in the concentration of the applied substrates was observed (data not shown), demonstrating that viable cultured astrocytes can efficiently take up and metabolize the applied extracellular substrates.

Concentration-Dependency of Pyruvate Consumption by Astrocytes

To test for the concentration dependency of pyruvate consumption, cultured astrocytes were exposed to different concentrations of pyruvate and the loss in extracellular pyruvate was monitored (Fig. 2). For all concentrations applied, the extracellular pyruvate levels declined almost proportional with time (Fig. 2a) and the viability of the cells was not compromised as indicated by the absence of any significant increase in extracellular LDH activity (Fig. 2b). Calculation of the pyruvate consumption rates per minute for the initial 3 h of incubation revealed a hyperbolic relationship between the specific consumption rate and the concentration of pyruvate initially applied (Fig. 2c). Analysis of the data obtained by the Michaelis-Menten equation revealed half-maximal pyruvate consumption for an initial pyruvate concentration of 0.6 ± 0.1 mM and a maximal pyruvate consumption rate of 5.1 ± 0.8 nmol/(min × mg).

Inhibition of Astrocytic Pyruvate Consumption by an MCT1 Inhibitor or MCT1 Substrates

Pyruvate is considered to be transported into astrocytes via MCT1 [32, 33, 41]. To test whether MCT1-mediated uptake is involved in the observed pyruvate consumption by

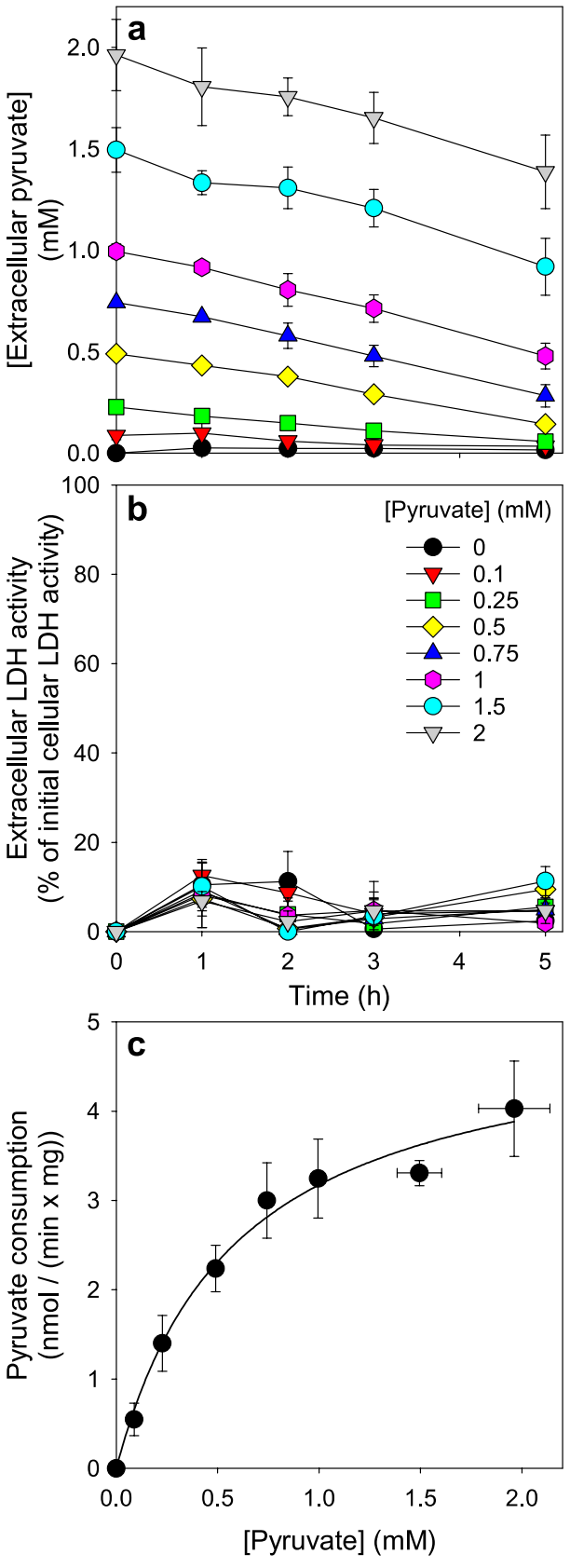

Fig. 2 Time- and concentration-dependent consumption of extracellular pyruvate by primary astrocyte cultures. The cells were incubated for up to 5 h in a glucose-free incubation buffer with pyruvate in the concentrations indicated. The extracellular concentration of pyruvate (**a**) and the extracellular LDH activity (**b**) were determined for the time periods given. The almost linear decline in the extracellular pyruvate concentrations during the first 3 h of incubation was used to calculate the specific pyruvate consumption rates. The initial cellular LDH activity of the cultures was 116 ± 9 nmol/(min × well) and the initial protein content was 122 ± 7 µg/well (**c**). Half-maximal pyruvate consumption (as calculated by using the Michaelis-Menten equation) was observed for an initial pyruvate concentration of 0.6 ± 0.1 mM and the maximal pyruvate consumption rate was calculated to be 5.1 ± 0.8 nmol/(min × mg). The data shown are means ± SD of values obtained in three experiments performed on independently prepared cultures

astrocytes, we studied the consequences of an application of the MCT1 inhibitor AR-C155858 [42–44] or of the known MCT1 substrates lactate and bHB [32, 35, 45] on the consumption of 0.5 mM pyruvate. Application of AR-C155858 caused a concentration-dependent impairment of the pyruvate consumption and 10 µM of the inhibitor lowered the pyruvate consumption by around 80% (Fig. 3a). In addition, a 10 times excess of lactate or bHB significantly lowered the pyruvate consumption, while the consumption was completely prevented in the presence of both lactate plus bHB (Fig. 3b). None of the conditions applied caused any obvious cell toxicity as indicated by the absence of any increase in extracellular LDH activity (Fig. 3c, d).

Pyruvate Consumption in the Presence of Lactate and Glucose

An excess of lactate (5 mM) lowered pyruvate consumption by astrocytes (Fig. 3b). To test whether the presence of lower concentrations of lactate as well as of lactate formed during incubation of astrocytes with glucose will affect pyruvate consumption, astrocytes were exposed to 0.5 mM pyruvate in the absence or the presence of 1 mM lactate and/or 1 mM glucose. After application of 1 mM glucose, almost all the glucose was consumed during incubation of the cells for 5 h (Fig. 4a) and around 1.7 mM of lactate were found released from the cells (Fig. 4b). Also for such conditions pyruvate was found to be consumed by the cells, although this consumption was significantly lowered by the presence of lactate and/or glucose (Fig. 4c). None of the conditions applied caused any obvious cell toxicity as indicated by the absence of any increase in extracellular LDH activity (Fig. 4d).

Pyruvate Consumption in the Presence of an Inhibitor of the Mitochondrial Pyruvate Carrier

Mitochondrial uptake is a prerequisite of a subsequent mitochondrial metabolism of pyruvate. To test whether

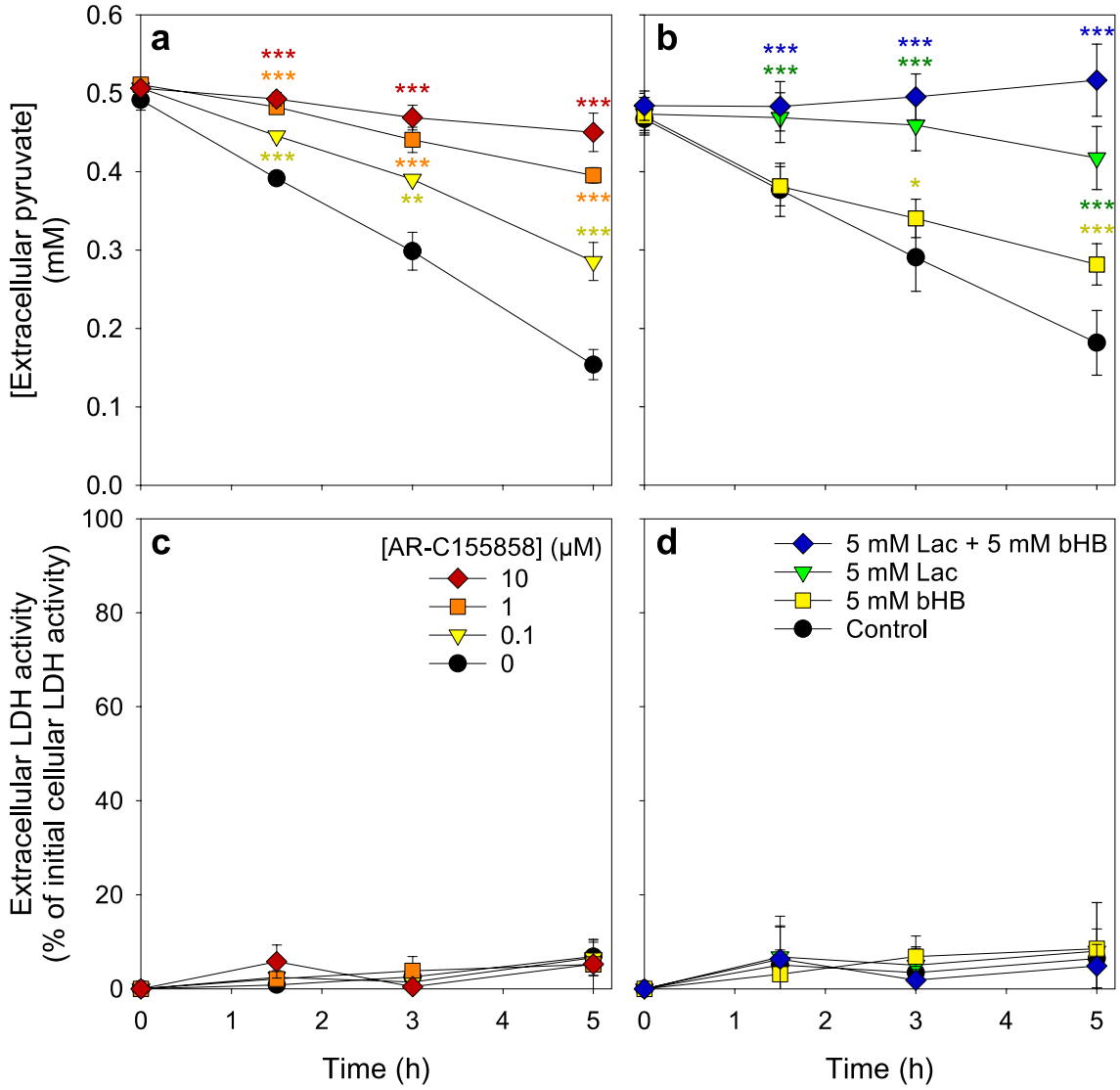

Fig. 3 Modulation of astrocytic pyruvate consumption by an MCT1 inhibitor or MCT1 substrates. Astrocyte cultures were incubated for up to 5 h in a glucose-free incubation buffer with 0.5 mM pyruvate in the absence or the presence of the MCT1 inhibitor AR-C155858 in the concentrations indicated (**a**, **c**) or in the absence or the presence of 5 mM of the MCT1 substrates lactate (Lac) and/or beta-hydroxybutyrate (bHB; **b**, **d**). The extracellular concentration of pyruvate (**a**, **b**) and the extracellular LDH activity (**c**, **d**) were determined for the incubation times indicated. The initial cellular LDH activities of the cultures were 150 ± 26 nmol/(min × well) (**a**, **c**) and 138 ± 18 nmol/(min × well) (**b**, **d**). The initial protein contents of the cultures were 113 ± 2 µg/well (**a**, **c**) and 129 ± 8 µg/well (**b**, **d**). The data shown are means ± SD of values obtained in three experiments performed on independently prepared cultures. The significance of differences (ANOVA) compared to the values obtained for the control incubation (no inhibitor or no other MCT1 substrate) is indicated by *p<0.05 and ***p<0.001

the mitochondrial pyruvate carrier (MPC) is involved in the observed astrocytic pyruvate consumption, we applied UK5099, an inhibitor of the mitochondrial pyruvate carrier [23, 46, 47]. The presence of UK5099 lowered the astrocytic pyruvate consumption in a concentration-dependent manner and completely prevented pyruvate consumption in a concentration of 100 µM (Fig. 5a). The viability of the cells was not affected by the presence of the inhibitor as indicated by the absence of any significant increase in extracellular LDH activity (Fig. 5b).

Neurochemical Research (2023) 48:1438–1454

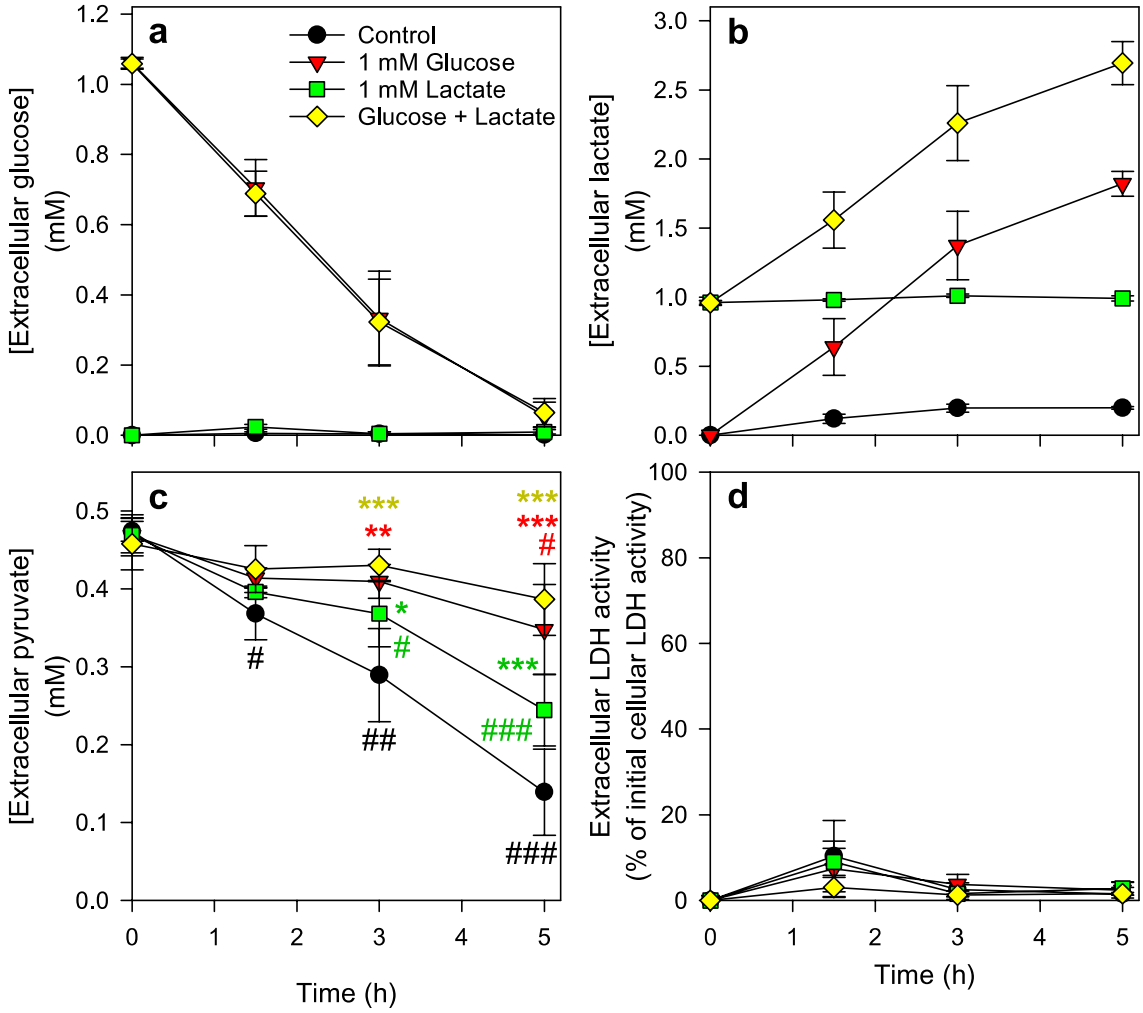

Fig. 4 Pyruvate consumption by cultured astrocytes in the presence of glucose and/or lactate. Cultured primary astrocytes were incubated for up to 5 h in a glucose-free incubation buffer with 0.5 mM pyruvate in the absence or the presence of 1 mM glucose and/or 1 mM lactate. The extracellular concentrations of glucose (**a**), lactate (**b**), pyruvate (**c**) and the extracellular LDH activity (**d**), as indicator of a potential loss in cell viability, were monitored over an incubation period of up to 5 h. The initial cellular LDH activity of the cultures was 150 ± 38 nmol/(min × well) and the initial protein content was 124 ± 21 µg/well. The data shown are means ± SD of values obtained in three experiments performed on independently prepared cultures. In panel c, the significance of differences (ANOVA) compared to the values obtained for the control incubation (only pyruvate) is indicated by *p<0.05, **p<0.01 and ***p<0.001 and the significance of differences (ANOVA) compared to the values obtained for the respective initial pyruvate concentrations is indicated by #p<0.05, ##p<0.01 and ###p<0.001

Consequences of a Modulation of Mitochondrial Metabolism on Astrocytic Pyruvate Consumption

To investigate to which extend mitochondrial oxidation may be involved in the observed pyruvate consumption, we incubated cultured astrocytes with 0.5 mM pyruvate in the presence of substances that are known to interfere with mitochondrial metabolism, such as the complex III inhibitor antimycin A [48, 49] and the respiratory chain uncoupler BAM15 [50]. Exposure of cultured astrocytes for 90 min to those substances lowered the mitochondrial membrane potential significantly (Fig. 6), but did not cause acute toxicity as indicated by the absence of any rapid increase in extracellular LDH activity (Fig. 7e). Pyruvate-treated cells consumed the applied pyruvate almost proportional to the time (Fig. 7a), maintained the high initial ATP content throughout an incubation for up to 5 h (Fig. 7d) and remained viable during this incubation (Fig. 7e). In contrast, pyruvate consumption in antimycin A-treated astrocytes was abolished following the initial incubation period of 90 min. Those cells contained already after 90 min hardly any ATP (Fig. 7d) and the viability of the cells was compromised as demonstrated by the significant increase in extracellular LDH activity found after 5 h of incubation (Fig. 7e). For

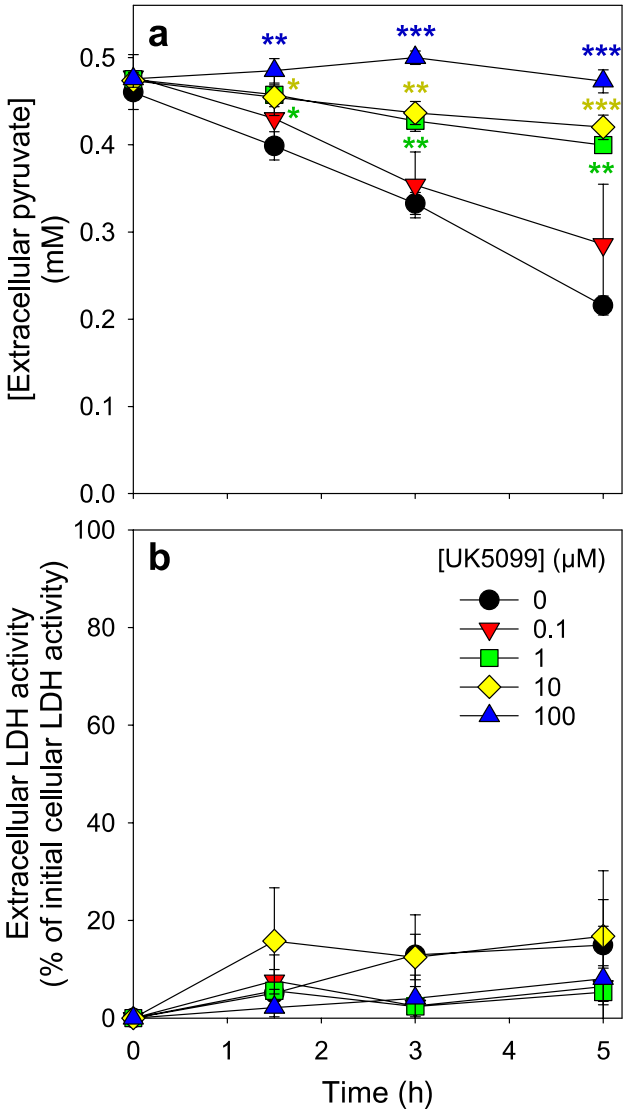

Fig. 5 Modulation of astrocytic pyruvate consumption by inhibition of the mitochondrial pyruvate carrier. Cultured astrocytes were incubated for up to 5 h in a glucose-free incubation buffer with 0.5 mM pyruvate in the absence or the presence of UK5099, an inhibitor of the mitochondrial pyruvate carrier, in the concentrations indicated. The extracellular concentration of pyruvate (**a**) and the extracellular LDH activity (**b**), as indicator of a potential loss in cell viability, were determined for the indicated time points of incubation. The initial cellular LDH activity of the cultures was 93 ± 6 nmol/(min × well) and the initial protein content of the cultures was 104 ± 10 µg/well. The data shown are means ± SD of values obtained in three experiments performed on independently prepared cultures. The significance of differences (ANOVA) compared to the values obtained for the control incubation (no inhibitor) is indicated by *p<0.05, **p<0.01 and ***p<0.001

BAM15-treated astrocyte cultures an accelerated pyruvate consumption was observed (Fig. 7a) that was accompanied by a gradual decline of cellular ATP contents throughout the 5 h incubation (Fig. 7d), while the cell viability was not compromised under those conditions (Fig. 7e). The strong acceleration of pyruvate consumption in BAM15-treated astrocytes (Figs. 7a and 8a-c) was prevented, in addition to the basal pyruvate consumption, in the presence of the MPC inhibitor UK5099 in concentrations as low as 1 µM (Fig. 8a–c). Such coincubations of astrocyte cultures with BAM15 and UK5099 caused some cell toxicity as demonstrated by the significant increase in extracellular LDH activity after 5 h of incubation (Fig. 8d).

Test for Release of Lactate and Alanine as Potential Products of Pyruvate Metabolism

As pyruvate has been reported to be metabolized by astrocytes to lactate and alanine [31], the extracellular concentrations of lactate and alanine were determined for cultures that had been exposed in the absence or the presence of 0.5 mM pyruvate (Fig. 7b, c). After a 3 h incubation in the absence of pyruvate, 34 ± 9 µM lactate and 32 ± 3 µM alanine were determined extracellularly, while higher levels of 159 ± 16 µM lactate and 55 ± 20 µM alanine were quantified for cells that had been exposed for 3 h to 0.5 mM pyruvate (Table 1). In contrast to those metabolites, no pyruvate-derived extracellular acetate and bHB were detected in astrocytes cultures that had been incubated with or without pyruvate (data not shown). The concentrations of extracellular lactate and alanine that were found for astrocytes incubated without pyruvate were subtracted from the respective concentrations of lactate or alanine that had been released from pyruvate-treated cells to quantify the pyruvate-derived lactate and alanine (Table 1). Within 3 h of incubation the cells consumed 481 ± 34 nmol/mg pyruvate and released 289 ± 17 nmol/mg pyruvate-derived lactate and 52 ± 36 nmol/mg pyruvate-derived alanine. Thus, extracellular lactate and alanine accounted for around 60% and 10%, respectively, of the pyruvate that had been consumed by the pyruvate-exposed cells (Table 1). Antimycin A-treated astrocytes consumed less pyruvate than control cells but similar concentrations of extracellular lactate and alanine were found, while extracellular lactate and alanine concentrations were significantly lower in BAM15-treated astrocytes (Fig. 7b, c), despite of the accelerated pyruvate consumption (Fig. 7a).

Discussion

Pyruvate is an important metabolite that links cytosolic glycolysis with mitochondrial metabolism [6, 7]. As pyruvate can also be released and taken up by astrocytes [29, 31, 51], we have investigated the astrocytic metabolism of extracellular pyruvate by using astrocyte primary cultures as a model system. Here we report that astrocytes efficiently consume and metabolize pyruvate and that its consumption strongly

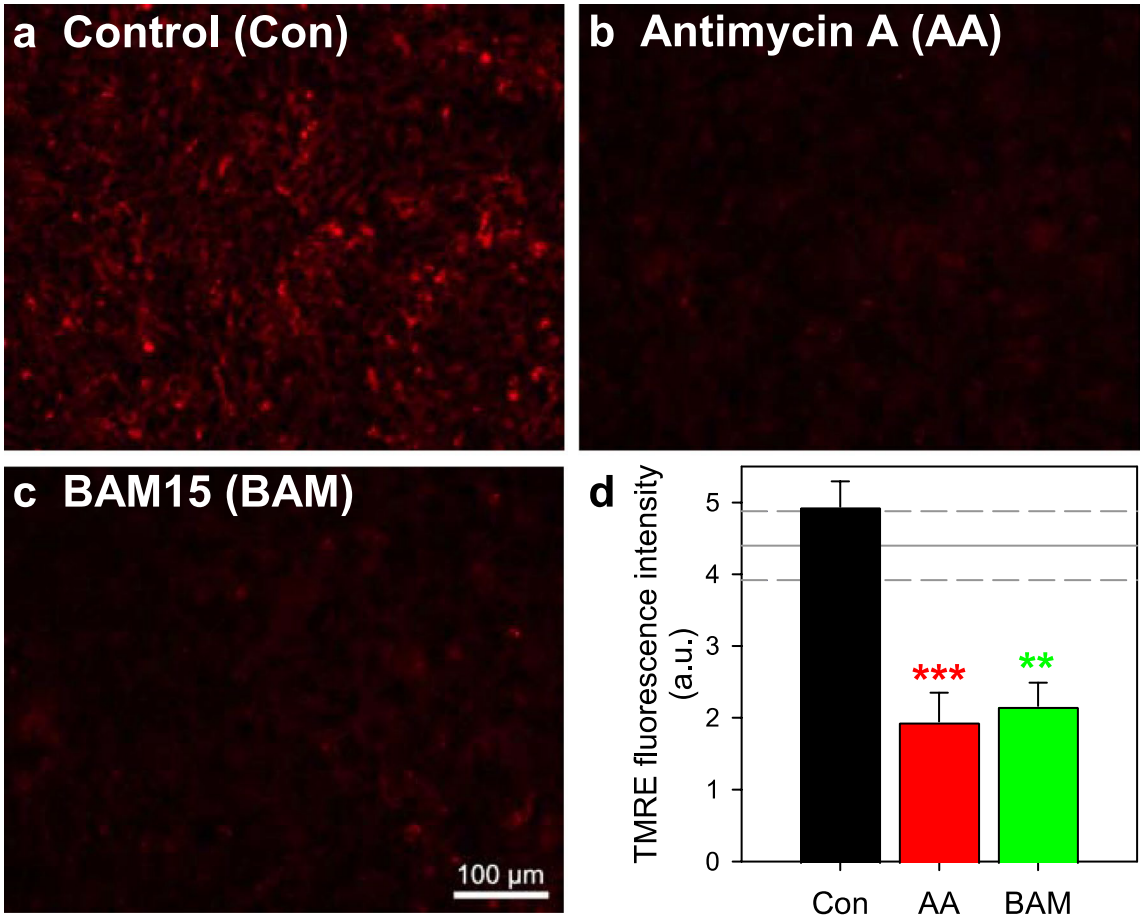

Fig. 6 Consequences of an application of modulators of mitochondrial metabolism on the mitochondrial membrane potential of cultured astrocytes. The cultures were incubated for 90 min without (**a**, **d**) or with 10 µM of the complex III inhibitor antimycin A (**b**, **d**) or 1 µM of the uncoupler BAM15 (**c**, **d**) before the cells were stained with TMRE to indicate the intensity of the mitochondrial membrane potential. Panels a to c show pictures of stained cultures from a representative experiment. The scale bar in panel c represents 100 µm and applies to panels a-c. Panel d shows the quantification of the mitochondrial TMRE staining for the conditions applied and the data presented are means ± SD obtained from three experiments performed on independently prepared cultures. The cellular TMRE fluorescence of glucose-fed cultures was 4.4 ± 0.5 a.u. and is indicated in panel d as horizontal lines. In panels d, the significance of differences (ANOVA) compared to the data for control incubations is indicated by **$p<0.01$ and ***$p<0.001$

depends on defined transport processes and mitochondrial activity.

Astrocytes are able to take up glucose efficiently and are considered to convert the internalized glucose via glycolysis mainly to lactate with quantitatively less mitochondrial pyruvate oxidation [2]. However, in addition to glucose, a variety of other extracellular substrates, including lactate, pyruvate, alanine, bHB and acetate, have been reported to be metabolized by astrocytes, at least in culture, and can be used as source for energy production and/or synthesis of other metabolites [4, 13, 14, 52]. In our study, these literature data on the consumption of the listed monocarboxylates were confirmed for cultured primary rat astrocytes.

The transporter primarily responsible for the uptake of the monocarboxylates pyruvate, lactate, bHB and acetate into astrocytes is MCT1 [32, 41, 53], while alanine is taken up into astrocytes mainly via the system L isoform LAT2 and partially via ASCT2 [54]. When comparing the different MCT1 substrates, pyruvate and acetate were found to be consumed more efficiently by astrocytes than bHB and lactate. Reasons for the observed difference in consumption rates are the low concentration of substrates applied (0.5 mM) and the different kinetic parameters of MCT1 for the substrates investigated. Reported K_m values for MCT1-mediated uptake are low for pyruvate (1 mM; [35]) and acetate (1.6 mM; [55]), but much higher for lactate (3.5–10 mM; [32, 35, 56]) and bHB (12.5 mM; [57]). Using these K_m values to calculate initial transport velocities by the Michaelis-Menten equation for a substrate concentration of 0.5 mM revealed that compared to the uptake velocity for pyruvate (100%) the initial uptake velocities of the other MCT1 substrates were lower with 71% for acetate, 14–38% for lactate

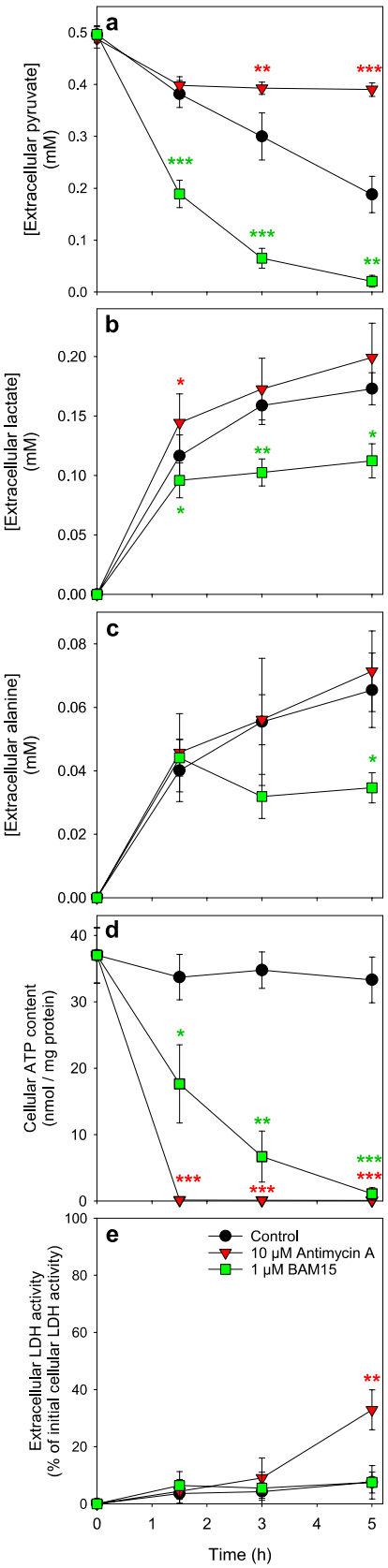

Fig. 7 Pyruvate consumption by astrocytes in the presence of antimycin A or BAM15. Primary astrocyte cultures were incubated for up to 5 h with 0.5 mM pyruvate in the absence or the presence of either 10 µM of the mitochondrial complex III inhibitor antimycin A or 1 µM of the uncoupler BAM15 before the extracellular concentrations of pyruvate (**a**), lactate (**b**), alanine (**c**), the specific cellular ATP content (**d**) and the extracellular LDH activity (**e**) were determined. The initial cellular protein content was 108 ± 12 µg/well and the initial cellular LDH activity 120 ± 16 nmol/(min × well). The data shown are means ± SD obtained from three experiments performed on independently prepared cultures. The significance of differences (ANOVA) compared to the data for controls without antimycin A and BAM15 are indicated by *p<0.05, **p<0.01 and ***p<0.001

and 11% for bHB. This explains why uptake and consumption of pyruvate and acetate by astrocytes are favored at a concentration of 0.5 mM in comparison to lactate and bHB.

The consumption of pyruvate by cultured astrocytes depends strongly on the initial pyruvate concentration applied. A half-maximal consumption rate was calculated for an initial pyruvate concentration of 0.6 ± 0.1 mM and the maximal specific consumption rate was found to be 5.1 ± 0.8 nmol/(min × mg). These kinetic data for pyruvate consumption for an incubation period of 3 h fit well with data reported for the initial (5 min) uptake of ^{14}C-labelled pyruvate revealing a K_m value of 1.0 ± 0.3 mM and a V_{max} value of 7.5 ± 0.4 nmol/(min × mg) for cellular pyruvate accumulation in primary astrocytes [31]. The half-maximal consumption rate determined for pyruvate (0.6 mM) is also similar to the reported K_m value for pyruvate uptake (1.01 ± 0.06 mM) in MCT1-expressing *Xenopus laevis* oocytes [35]. The contribution of MCT1 as the plasma membrane transporter responsible for the observed astrocytic pyruvate consumption is strongly supported by the impairment of pyruvate consumption in the presence of the MCT1 inhibitor AR-C155858 [42–44] or of an excess of the competing MCT1 substrates lactate and bHB [32, 41–44]. All these data are consistent with the view that MCT1 is mainly responsible for pyruvate uptake in astrocytes [33, 41, 56] and demonstrate that MCT1-mediated pyruvate uptake is a prerequisite for pyruvate consumption by astrocytes. Although MCT1 seems to play the main role in the uptake of pyruvate, a small part of pyruvate consumption could not be blocked by application of the MCT1 and 2 inhibitor AR-C155858. This could be due to the presence of the monocarboxylate transporter MCT4 which has been reported to be expressed in primary rat astrocyte cultures [58]. This transporter was originally thought to have a rather high K_M-value for pyruvate of around 36 mM [58], but a more recent study suggests a lower value of around 4 mM for pyruvate transport by MCT4 [59]. Thus, MCT4 could at least partially contribute to the astrocytic pyruvate consumption that is insensitive to MCT1-inhibition.

Pyruvate oxidation to CO_2 is a mitochondrial process that requires uptake of pyruvate through the inner mitochondrial

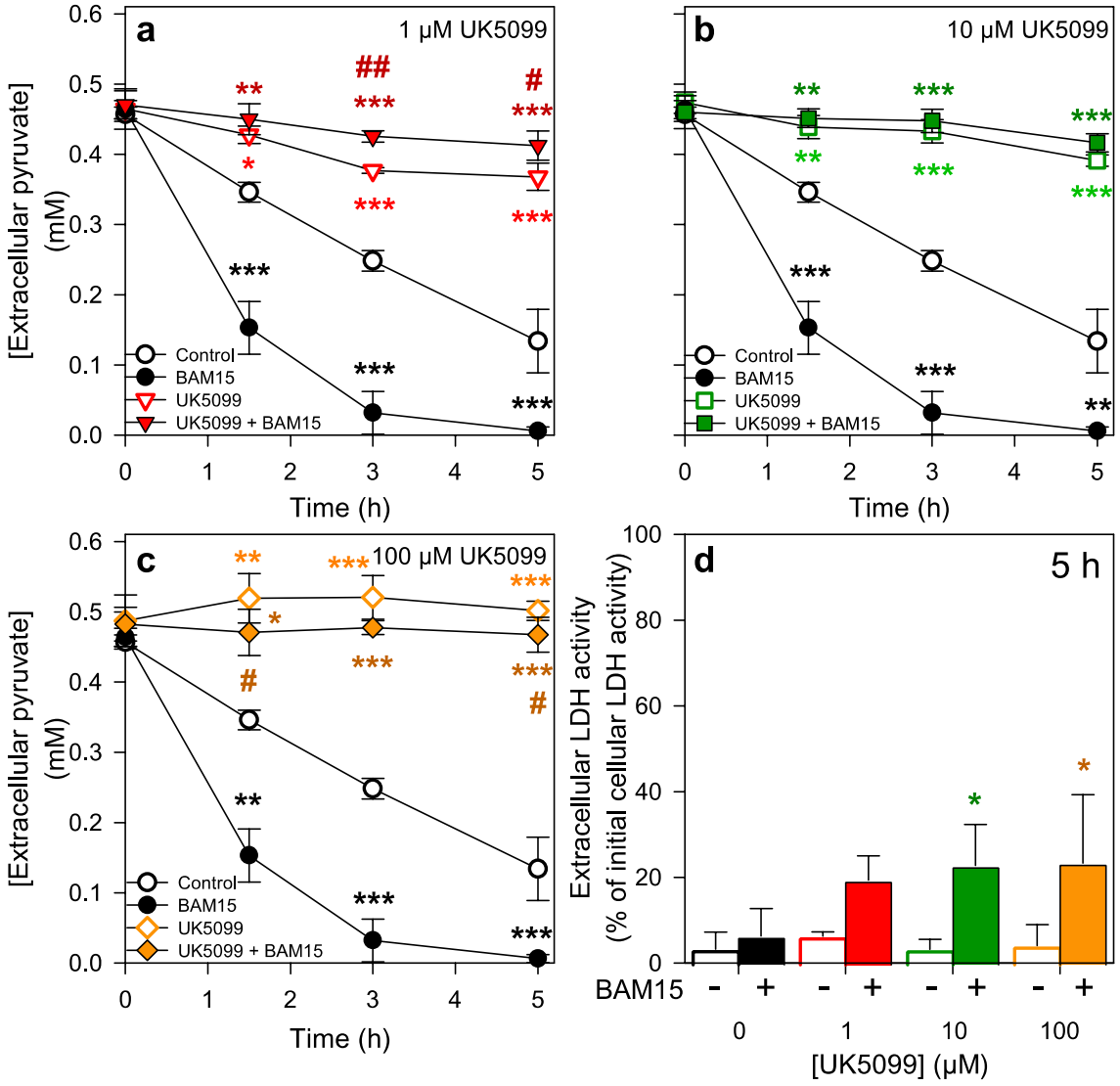

Fig. 8 Pyruvate consumption in astrocytes in the presence of an inhibitor of the mitochondrial pyruvate carrier and/or the uncoupler BAM15. Cultured primary astrocytes were incubated for up to 5 h in a glucose-free incubation buffer with 0.5 mM pyruvate in the absence or the presence of 1 µM (**a**), 10 µM (**b**) or 100 µM (**c**) UK5099, an inhibitor of the mitochondrial pyruvate carrier and/or 1 µM of the uncoupler BAM15. The extracellular concentrations of pyruvate (**a**, **b**, **c**) and the extracellular LDH activity (**d**), as indicator of a potential loss in cell viability, were determined for the indicated incubation periods. The initial cellular LDH activity of the cultures was 167 ± 26 nmol/(min × well) and the initial protein content of the cultures was 134 ± 21 µg/well. The data shown are means ± SD of values obtained in three experiments performed on independently prepared cultures. The significance of differences (ANOVA) compared to the values obtained for the control incubation (no inhibitor) is indicated by *p<0.05, **p<0.01 and ***p<0.001. The significance of differences (t-test) between incubations containing UK5099 and UK5099 plus BAM15 is indicated by #p<0.05 and ##p<0.01

membrane. This transport process is mediated by the mitochondrial pyruvate carrier (MPC) [22]. Mitochondrial uptake and metabolism of pyruvate appear to be key components of the observed pyruvate consumption by astrocytes as the presence of UK5099, an inhibitor of MPC [23, 46], almost completely abolished pyruvate consumption. Similarly, inhibition of mitochondrial respiration by antimycin A impaired the consumption of extracellular pyruvate by astrocytes as the NAD^+ consumed by pyruvate dehydrogenase and by the citric acid cycle during the complete oxidation of pyruvate to CO_2 cannot be regenerated by an inhibited respiratory chain [48, 60]. In contrast, BAM15-mediated uncoupling of the respiratory chain from mitochondrial ATP synthesis [50], increased pyruvate consumption, most likely by the accelerated mitochondrial NADH oxidation and NAD^+ regeneration for further mitochondrial pyruvate oxidation to CO_2. This is consistent with accelerated oxygen consumption in BAM15-treated C2C12 mouse

Table 1 Formation of lactate and alanine from the pyruvate consumed by astrocytes

	(μM)	(nmol/mg)	(%)
Pyruvate consumed			
0.5 mM Pyruvate	208 ± 28	481 ± 34	100.0 ± 7.1
Lactate released			
0.5 mM Pyruvate	159 ± 16	367 ± 7	
0 mM Pyruvate	34 ± 9	77 ± 12	
Δ (0.5–0 mM)	125 ± 8	289 ± 17	60.3 ± 4.1
Alanine released			
0.5 mM Pyruvate	55 ± 20	126 ± 34	
0 mM Pyruvate	32 ± 3	73 ± 3	
Δ (0.5–0 mM)	24 ± 17	52 ± 36	10.9 ± 7.9

Primary astrocyte cultures were incubated for 3 h without (0 mM) or with 0.5 mM pyruvate before the extracellular concentrations of pyruvate, lactate and alanine were determined. Pyruvate consumption as well as lactate or alanine release are given for the conditions investigated as μM and nmol/mg protein. In addition, for lactate and alanine release the difference between treatments with and without pyruvate (Δ 0.5-0 mM) were calculated and are given as μM, nmol/mg and as percent of the pyruvate consumed. The data shown are means ± SD obtained from three experiments performed on independently prepared cultures. The initial cellular protein content was 108 ± 12 μg/well

myotubes [61] and BAM15-treated mouse liver mitochondria [50]. Finally, the accelerated (and the normal) pyruvate consumption in BAM15-treated astrocytes was abolished by inhibition of the MPC and some toxicity was observed for this condition, demonstrating that mitochondrial pyruvate uptake is required for the BAM15-induced accelerated pyruvate consumption and for maintaining cell viability under such conditions. Already at the low concentration of 1 μM UK5099 was sufficient to prevent the BAM15-induced mitochondrial pyruvate consumption in cultured astrocytes, showing that indeed inhibition of MPC is the reason for the observed impairment of astrocytic pyruvate consumption by UK5099. For applications of high concentration of UK5099 such as 100 μM a potential partial contribution of an inhibition of MCTs by UK5099 cannot be excluded as UK5099 has been reported to also have some inhibitory potential on MCTs [62], although the Ki value of UK5099 for MCT-mediated transport is two to three orders of magnitude higher than that for MPC [57, 63, 64]. All these data strongly underline the importance of astrocytic MPC and functional oxidative phosphorylation for the mitochondrial metabolism of pyruvate in astrocytes.

Astrocytes that had been incubated with pyruvate in the absence of glucose maintained their viability, their mitochondrial membrane potential and a high cellular ATP content. In contrast, both antimycin A and BAM15 lowered the mitochondrial membrane potential to a similar extend and depleted the cells of ATP in the presence of pyruvate. However, application of antimycin A depleted the cells almost completely of ATP already within 1.5 h, while a gradual loss in cellular ATP content was observed for BAM15-treated cells. Consistently, cell toxicity was found for antimycin A-treated and pyruvate exposed astrocytes, but not for the respective BAM15-treated cells. These data demonstrate that mitochondrial ATP production is essential to maintain a high ATP content in pyruvate-treated astrocytes. Furthermore, these findings suggest that in BAM15-treated cells a residual capacity of the respiratory chain is available to at least partially slow down ATP loss in the uncoupled situation, in contrast to the antimycin A treatment that completely inhibited the electron flow through the respiratory chain.

Substantial amounts of extracellular lactate and alanine were determined in glucose-deprived and pyruvate-treated astrocytes. Part of the extracellular lactate and alanine may be derived from residual free glucose, glycolysis intermediates and/or glycogen that is mobilized after glucose deprivation [19, 65, 66]. However, even after correction of the values obtained from pyruvate-treated astrocytes for the respective data from pyruvate-free control incubations, the amounts of lactate and alanine determined accounted to around 60% and 10%, respectively, of the total amount of pyruvate consumed by the cells. Thus, the pyruvate consumed by astrocytes within 3 h appears to have been metabolized mainly to lactate and to a lower extent to alanine, both of which had been exported from the cells. The excessive metabolism of pyruvate to lactate is consistent with the reported rapid and substantial metabolism within minutes of internalized ^{14}C-pyruvate to ^{14}C-lactate in cultured astrocytes [31] and with the loss of cellular lactate from astrocytes in vivo after injection of a pyruvate-containing solution [67].

The low amounts of pyruvate-derived alanine are most likely generated by glutamate-pyruvate transaminase [18, 21] via transamination of internalized pyruvate with amino groups that are derived from amino acids present at the onset of the incubation. In contrast, the electrons required for pyruvate reduction to lactate via LDH are unlikely to be only derived from initially present cytosolic NADH. The cellular NADH pool in cultured astrocytes accounts for only 0.70 ± 0.03 nmol/mg [68] and, even if the entire amount would be present as cytosolic NADH, it would have to be recycled more than 400 times by cytosolic processes to allow the formation of the pyruvate-derived lactate that was found extracellularly (around 300 nmol/mg). This appears highly unlikely for glucose-depleted astrocytes, as they are unable to sustain their NADH levels under glucose-depletion [19, 68]. It appears more likely that the large amounts of NADH needed for cytosolic pyruvate reduction under the conditions studied are derived from mitochondria, where NADH

is continuously produced by mitochondrial pyruvate oxidation via the PDH and the citric acid cycle dehydrogenases.

Lactate and alanine account for around 70% of the pyruvate consumed. Assuming that the residual 30% of consumed pyruvate (around 145 nmol/mg) would have been fully oxidized in mitochondria to CO_2 to yield 4 NADH per pyruvate oxidized [7], a total amount of 580 nmol/mg NADH would have been generated by mitochondrial PDH and citric acid cycle. This would account for almost twice the amount needed for the generation of the pyruvate-derived lactate that was found to be released into the medium. However, mitochondrial NADH cannot be used directly for cytosolic LDH-dependent reduction of pyruvate and the electrons need to be metabolically transported [18]. A shuttle that could contribute to the electron transfer from mitochondrial NADH via the inner mitochondrial membrane to generate cytosolic NADH is the bidirectional malate-aspartate shuttle [69, 70]. Such a transfer of reducing equivalents from mitochondria to cytosol has already been postulated for rat liver cells [71] and is also required for the transfer of oxaloacetate as malate from the mitochondrial matrix to the cytosol to provide substrate for astrocytic glyconeogenesis [72, 73]. Furthermore, the higher levels of lactate found for antimycin A-treated, pyruvate-exposed astrocytes would be consistent with a potential use of mitochondrial NADH for pyruvate reduction to lactate. As efficient NADH oxidation via the respiratory chain is impaired by the antimycin A treatment [48, 60], more mitochondrial NADH would be available to supply electrons for malate-aspartate shuttle-mediated transport into the cytosol. Conversely, the NADH produced in BAM15-treated astrocytes during rapid mitochondrial oxidation of pyruvate is likely to be instantly oxidized by the uncoupled respiratory chain, thereby lowering the potential of mitochondrial NADH to feed electrons into the malate-aspartate shuttle. Further studies are now required to experimentally elucidate to which extent electrons derived from pyruvate oxidation are shuttled from the mitochondrial matrix into the cytosol to support cytosolic pyruvate reduction to lactate.

Extracellular pyruvate has been reported to be present in brain in concentrations of around 160 µM [74, 75] and pyruvate concentrations in the cerebrospinal fluid range between 30 and 200 µM [76–78]. Thus, the observed consumption of micromolar concentrations of extracellular pyruvate by cultured astrocytes appears to take place at extracellular pyruvate concentrations that are physiologically present in brain. By their ability to release pyruvate [20, 29] and to consume extracellular pyruvate [31] (present report), astrocytes may regulate extracellular pyruvate levels to establish a suitable concentration that is sufficiently high to allow the reported neuroprotective function of astrocyte-derived extracellular pyruvate [30, 79, 80].

In conclusion, the results presented here demonstrate that in glucose-deprived astrocytes the pyruvate transporters MCT1 and MPC are mainly mediating the cellular uptake of pyruvate into astrocytes and the transport of pyruvate from cytosol into mitochondria, respectively. In addition, mitochondrial activity appears to be the main regulator for the consumption of extracellular pyruvate. The ultimate end-point of pyruvate oxidation will be CO_2, but we assume that the fate of extracellular pyruvate that is taken up by astrocytes will strongly differ depending on the metabolic situation of the cells and the respective need for potential products of pyruvate metabolism, such as alanine, acetyl-CoA, oxaloacetate or intermediates of the citric acid cycle. Further studies are now required to explore in more detail the generation of pyruvate-derived products in cells and media of cultured astrocytes for various metabolic conditions. For such studies the mass spectroscopic analysis of metabolic products derived from ^{13}C-labeled pyruvate should be considered as a suitable approach as previously demonstrated for other studies on astrocytic metabolism [81, 82].

Acknowledgements The authors would kindly like to thank Julius Berger for his initial contribution to the establishment of the ATP quantification assay.

Author Contributions ND did all pyruvate consumption experiments. ARH determined bHB concentrations and performed with ND the substrate consumption experiments. CA did the stainings for mitochondrial membrane potential. ND and RD wrote the manuscript. All authors reviewed and approved the manuscript.

Funding Open Access funding enabled and organized by Projekt DEAL. This project was funded by the basal finacial support provided to the Dringen group by the University Bremen.

Data Availability Enquiries about data availability should be directed to the authors.

Declarations

Conflict of interest The authors have no conflict of interest to declare.

References

1. Langen UH, Ayloo S, Gu C (2019) Development and cell biology of the blood-brain barrier. Annu Rev Cell Dev Biol 35:591–613. https://doi.org/10.1146/annurev-cellbio-100617-062608
2. Bonvento G, Bolanos JP (2021) Astrocyte-neuron metabolic cooperation shapes brain activity. Cell Metab 33:1546–1564. https://doi.org/10.1016/j.cmet.2021.07.006
3. Khakh BS, Deneen B (2019) The emerging nature of astrocyte diversity. Annu Rev Neurosci 42:187–207. https://doi.org/10.1146/annurev-neuro-070918-050443
4. Dienel GA, Hertz L (2001) Glucose and lactate metabolism during brain activation. J Neurosci Res 66:824–838. https://doi.org/10.1002/jnr.10079
5. Hirrlinger J, Dringen R (2010) The cytosolic redox state of astrocytes: maintenance, regulation and functional implications for metabolite trafficking. Brain Res Rev 63:177–188. https://doi.org/10.1016/j.brainresrev.2009.10.003
6. Schousboe A, Waagepetersen HS, Sonnewald U (2019) Astrocytic pyruvate carboxylation: Status after 35 years. J Neurosci Res 97:890–896. https://doi.org/10.1002/jnr.24402
7. Rose J, Brian C, Pappa A, Panayiotidis MI, Franco R (2020) Mitochondrial metabolism in astrocytes regulates brain bioenergetics, neurotransmission and redox balance. Front Neurosci 14:536682. https://doi.org/10.3389/fnins.2020.536682
8. Zwingmann C, Leibfritz D (2003) Regulation of glial metabolism studied by 13 C-NMR. NMR Biomed 16:370–399. https://doi.org/10.1002/nbm.850
9. Magistretti PJ, Allaman I (2018) Lactate in the brain: from metabolic end-product to signalling molecule. Nat Rev Neurosci 19:235–249. https://doi.org/10.1038/nrn.2018.19
10. Dringen R, Bergbauer K, Wiesinger H, Hamprecht B (1994) Utilization of mannose by astroglial cells. Neurochem Res 19:23–30. https://doi.org/10.1007/BF00966724
11. Bergbauer K, Dringen R, Verleysdonk S, Gebhardt R, Hamprecht B, Wiesinger H (1996) Studies on Fructose metabolism in cultured Astroglial cells and control hepatocytes: lack of Fructokinase activity and immunoreactivity in astrocytes. Dev Neurosci 18:371–379. https://doi.org/10.1159/000111430
12. Lopes-Cardozo M, Larsson OM, Schousboe A (1986) Acetoacetate and glucose as lipid precursors and energy substrates in primary cultures of astrocytes and neurons from mouse cerebral cortex. J Neurochem 46:773–778. https://doi.org/10.1111/j.1471-4159.1986.tb13039.x
13. Achanta LB, Rowlands BD, Thomas DS, Housley GD, Rae CD (2017) β-Hydroxybutyrate boosts mitochondrial and neuronal metabolism but is not preferred over glucose under activated conditions. Neurochem Res 42:1710–1723. https://doi.org/10.1007/s11064-017-2228-6
14. Rowlands BD, Klugmann M, Rae CD (2017) Acetate metabolism does not reflect astrocytic activity, contributes directly to GABA synthesis, and is increased by silent information regulator 1 activation. J Neurochem 140:903–918. https://doi.org/10.1111/jnc.13916
15. Erecińska M, Pleasure D, Nelson D, Nissim I, Yudkoff M (1993) Cerebral aspartate utilization: near-equilibrium relationships in aspartate aminotransferase reaction. J Neurochem 60:1696–1706. https://doi.org/10.1111/j.1471-4159.1993.tb13393.x
16. Shanker G, Allen JW, Mutkus LA, Aschner M (2001) The uptake of cysteine in cultured primary astrocytes and neurons. Brain Res 902:156–163. https://doi.org/10.1016/S0006-8993(01)02342-3
17. Jackson JG, O'Donnell JC, Takano H, Coulter DA, Robinson MB (2014) Neuronal activity and glutamate uptake decrease mitochondrial mobility in astrocytes and position mitochondria near glutamate transporters. J Neurosci 34:1613–1624. https://doi.org/10.1523/jneurosci.3510-13.2014
18. Zwingmann C, Richter-Landsberg C, Leibfritz D (2001) 13 C isotopomer analysis of glucose and alanine metabolism reveals cytosolic pyruvate compartmentation as part of energy metabolism in astrocytes. Glia 34:200–212. https://doi.org/10.1002/glia.1054
19. Arend C, Ehrke E, Dringen R (2019) Consequences of a metabolic glucose-depletion on the survival and the metabolism of cultured rat astrocytes. Neurochem Res 44:2288–2300. https://doi.org/10.1007/s11064-019-02752-1
20. McKenna MC (2012) Substrate competition studies demonstrate oxidative metabolism of glucose, glutamate, glutamine, lactate and 3-hydroxybutyrate in cortical astrocytes from rat brain. Neurochem Res 37:2613–2626. https://doi.org/10.1007/s11064-012-0901-3
21. Baytas O, Davidson SM, Deberardinis RJ, Morrow EM (2022) Mitochondrial enzyme GPT2 regulates metabolic mechanisms required for neuron growth and motor function in vivo. Hum Mol Genet 31:587–603. https://doi.org/10.1093/hmg/ddab269
22. McCommis KS, Finck BN (2015) Mitochondrial pyruvate transport: a historical perspective and future research directions. Biochem J 466:443–454. https://doi.org/10.1042/BJ20141171
23. Arce-Molina R, Cortés-Molina F, Sandoval PY, Galaz A, Alegría K, Schirmeier S, Barros LF, San Martín A (2020) A highly responsive pyruvate sensor reveals pathway-regulatory role of the mitochondrial pyruvate carrier MPC. eLife. https://doi.org/10.7554/elife.53917
24. Halim ND, McFate T, Mohyeldin A, Okagaki P, Korotchkina LG, Patel MS, Jeoung NH, Harris RA, Schell MJ, Verma A (2010) Phosphorylation status of pyruvate dehydrogenase distinguishes metabolic phenotypes of cultured rat brain astrocytes and neurons. Glia 58:1168–1176. https://doi.org/10.1002/glia.20996
25. Auestad N, Korsak RA, Morrow JW, Edmond J (1991) Fatty acid oxidation and ketogenesis by astrocytes in primary culture. J Neurochem 56:1376–1386. https://doi.org/10.1111/j.1471-4159.1991.tb11435.x
26. Thevenet J, De Marchi U, Domingo JS, Christinat N, Bultot L, Lefebvre G, Sakamoto K, Descombes P, Masoodi M, Wiederkehr A (2016) Medium-chain fatty acids inhibit mitochondrial metabolism in astrocytes promoting astrocyte-neuron lactate and ketone body shuttle systems. FASEB J 30:1913–1926. https://doi.org/10.1096/fj.201500182
27. Shank RP, Bennett GS, Freytag SO, Campbell GL (1985) Pyruvate carboxylase: an astrocyte-specific enzyme implicated in the replenishment of amino acid neurotransmitter pools. Brain Res 329:364–367. https://doi.org/10.1016/0006-8993(85)90552-9
28. Cesar M, Hamprecht B (1995) Immunocytochemical examination of neural rat and mouse primary cultures using monoclonal antibodies raised against pyruvate carboxylase. J Neurochem 64:2312–2318. https://doi.org/10.1046/j.1471-4159.1995.64052312.x
29. Selak I, Skaper S, Varon S (1985) Pyruvate participation in the low molecular weight trophic activity for central nervous system neurons in glia-conditioned media. J Neurosci 5:23–28. https://doi.org/10.1523/JNEUROSCI.05-01-00023.1985
30. Wang XF, Cynader MS (2001) Pyruvate released by astrocytes protects neurons from copper-catalyzed cysteine neurotoxicity. J Neurosci. https://doi.org/10.1523/JNEUROSCI.21-10-03322.2001
31. Hamprecht B, Dringen R (1994) On the role of glycogen and pyruvate uptake in astroglial-neuronal interaction. In: Krieglstein J, Oberpichler-Schwenk H (eds) Pharmacology of cerebral ischemia. WVG, Stuttgart, pp 191–202

32. Bröer S, Rahman B, Pellegri G, Pellerin L, Martin J-L, Verleysdonk S, Hamprecht B, Magistretti PJ (1997) Comparison of lactate transport in astroglial cells and monocarboxylate transporter 1 (MCT 1) expressing *Xenopus laevis* oocytes. J Biol Chem 272:30096–30102. https://doi.org/10.1074/jbc.272.48.30096
33. Leino R, Gerhart D, Drewes L (1999) Monocarboxylate transporter (MCT1) abundance in brain of suckling and adult rats: a quantitative electron microscopic immunogold study. Brain Res Dev Brain Res 113:47–54. https://doi.org/10.1016/S0165-3806(98)00188-6
34. Nguyen YTK, Ha HTT, Nguyen TH, Nguyen LN (2022) The role of SLC transporters for brain health and disease. Cell Mol Life Sci. https://doi.org/10.1007/s00018-021-04074-4
35. Bröer S, Schneider H-P, Bröer A, Rahman B, Hamprecht B, Deitmer JW (1998) Characterization of the monocarboxylate transporter 1 expressed in *Xenopus laevis* oocytes by changes in cytosolic pH. Biochem J. https://doi.org/10.1042/bj3330167
36. Tulpule K, Hohnholt MC, Hirrlinger J, Dringen R (2014) Primary cultures of astrocytes and neurons as model systems to study the metabolism and metabolite export from brain cells. In: Hirrlinger J, Waagepetersen H (eds) Neuromethods 90: brain energy metabolism. Springer, pp 45–72
37. Petters C, Dringen R (2014) Comparison of primary and secondary rat astrocyte cultures regarding glucose and glutathione metabolism and the accumulation of iron oxide nanoparticles. Neurochem Res 39:46–58. https://doi.org/10.1007/s11064-013-1189-7
38. Lowry OH, Rosebrough NJ, Farr AL, Randall RJ (1951) Protein measurement with the folin phenol reagent. J Biol Chem 193:265–275. https://doi.org/10.1016/S0021-9258(19)52451-6
39. Clarke PM, Payton MA (1983) An enzymatic assay for acetate in spent bacterial culture supernatants. Anal Biochem 130:402–405. https://doi.org/10.1016/0003-2697(83)90607-3
40. Kientsch-Engel RI, Siess EA (1985) D-(-)-3-hydroxybutyrate and acetoacetate. In: Bergmeyer HU, Bergmeyer J, Graßl M (eds) Methods of enzymatic analysis. VCH, Weinheim
41. Halestrap AP (2012) The monocarboxylate transporter family-structure and functional characterization. IUBMB Life 64:1–9. https://doi.org/10.1002/iub.573
42. Ovens MJ, Davies AJ, Wilson MC, Murray CM, Halestrap AP (2010) AR-C155858 is a potent inhibitor of monocarboxylate transporters MCT1 and MCT2 that binds to an intracellular site involving transmembrane helices 7–10. Biochem J 425:523–530. https://doi.org/10.1042/BJ20091515
43. Nancolas B, Richard A (2015) Identification of key binding site residues of MCT1 for AR-C155858 reveals the molecular basis of its isoform selectivity. Biochem J 466:177–188. https://doi.org/10.1042/bj20141223
44. Guan X, Rodriguez-Cruz V, Morris ME (2019) Cellular uptake of MCT1 inhibitors AR-C155858 and AZD3965 and their effects on MCT-mediated transport of L-lactate in murine 4T1 breast tumor cancer cells. AAPS J 21:13. https://doi.org/10.1208/s12248-018-0279-5
45. Tang F, Lane S, Korsak A, Paton JFR, Gourine AV, Kasparov S, Teschemacher AG (2014) Lactate-mediated glia-neuronal signalling in the mammalian brain. Nat Commun. https://doi.org/10.1038/ncomms4284
46. Halestrap AP (1976) The mechanism of the inhibition of the mitochondrial pyruvate transportater by α-cyanocinnamate derivatives. Biochem J 156:181–183. https://doi.org/10.1042/bj1560181
47. Xu L, Phelix CF, Chen LY (2021) Structural insights into the human mitochondrial pyruvate carrier complexes. J Chem Inf Model 61:5614–5625. https://doi.org/10.1021/acs.jcim.1c00879
48. Bryla J, Kaniuga Z, Slater EC (1969) Studies on the mechanism of inhibition of the mitochondrial electron transport by antimycin. 3. Binding of antimycin to sub-mitochondrial particles and to complex III. Biochim Biophys Acta 189:327–336. https://doi.org/10.1016/0005-2728(69)90163-7
49. Pauwels PJ, Opperdoes FR, Trouet A (1985) Effects of antimycin, glucose deprivation, and serum on cultures of neurons, astrocytes, and neuroblastoma cells. J Neurochem 44:143–148. https://doi.org/10.1111/j.1471-4159.1985.tb07123.x
50. Kenwood BM, Weaver JL, Bajwa A, Poon IK, Byrne FL, Murrow BA, Calderone JA, Huang L, Divakaruni AS, Tomsig JL, Okabe K, Lo RH, Cameron Coleman G, Columbus L, Yan Z, Saucerman JJ, Smith JS, Holmes JW, Lynch KR, Ravichandran KS, Uchiyama S, Santos WL, Rogers GW, Okusa MD, Bayliss DA, Hoehn KL (2014) Identification of a novel mitochondrial uncoupler that does not depolarize the plasma membrane. Mol Metab 3:114–123. https://doi.org/10.1016/j.molmet.2013.11.005
51. San Martín A, Ceballo S, Baeza-Lehnert F, Lerchundi R, Valdebenito R, Contreras-Baeza Y, Alegría K, Barros LF (2014) Imaging mitochondrial flux in single cells with a FRET sensor for pyruvate. PLoS ONE 9:e85780. https://doi.org/10.1371/journal.pone.0085780
52. Gonzalez SV, Nguyen NHT, Rise F, Hassel B (2005) Brain metabolism of exogenous pyruvate. J Neurochem 95:284–293. https://doi.org/10.1111/j.1471-4159.2005.03365.x
53. Rae C, Fekete AD, Kashem MA, Nasrallah FA, Broer S (2012) Metabolism, compartmentation, transport and production of acetate in the cortical brain tissue slice. Neurochem Res 37:2541–2553. https://doi.org/10.1007/s11064-012-0847-5
54. Bröer S, Bröer A, Hansen JT, Bubb WA, Balcar VJ, Nasrallah FA, Garner B, Rae C (2007) Alanine metabolism, transport, and cycling in the brain. J Neurochem 102:1758–1770. https://doi.org/10.1111/j.1471-4159.2007.04654.x
55. Galić S, Schneider H-P, Bröer A, Deitmer JW, Bröer S (2003) The loop between helix 4 and helix 5 in the monocarboxylate transporter MCT1 is important for substrate selection and protein stability. Biochem J 376:413–422. https://doi.org/10.1042/bj20030799
56. Perez-Escuredo J, Van Hee VF, Sboarina M, Falces J, Payen VL, Pellerin L, Sonveaux P (2016) Monocarboxylate transporters in the brain and in cancer. Biochim Biophys Acta 1863:2481–2497. https://doi.org/10.1016/j.bbamcr.2016.03.013
57. Carpenter L, Halestrap AP (1994) The kinetics, substrate and inhibitor specificity of the lactate transporter of Ehrlich-Lettre tumour cells studied with the intracellular pH indicator BCECF. Biochem J 304:751–760. https://doi.org/10.1042/bj3040751
58. Dimmer K-S, Friedrich B, Lang F, Deitmer JW, Bröer S (2000) The low-affinity monocarboxylate transporter MCT4 is adapted to the export of lactate in highly glycolytic cells. Biochem J 350:219–227. https://doi.org/10.1042/bj3500219
59. Contreras-Baeza Y, Sandoval PY, Alarcón R, Galaz A, Cortés-Molina F, Alegría K, Baeza-Lehnert F, Arce-Molina R, Guequén A, Flores CA, San Martín A, Barros LF (2019) Monocarboxylate transporter 4 (MCT4) is a high affinity transporter capable of exporting lactate in high-lactate microenvironments. J Biol Chem 294:20135–20147. https://doi.org/10.1074/jbc.ra119.009093
60. Zhang Y, Chevalier A, Khdour OM, Soto LM, Hecht SM (2017) Inhibition of human cancer cell growth by analogues of antimycin A. Planta Med 83:1377–1383. https://doi.org/10.1055/s-0043-112343
61. Axelrod CL, King WT, Davuluri G, Noland RC, Hall J, Hull M, Dantas WS, Zunica ER, Alexopoulos SJ, Hoehn KL, Langohr I, Stadler K, Doyle H, Schmidt E, Nieuwoudt S, Fitzgerald K, Pergola K, Fujioka H, Mey JT, Fealy C, Mulya A, Beyl R, Hoppel CL, Kirwan JP (2020) BAM15-mediated mitochondrial uncoupling protects against obesity and improves glycemic control. EMBO Mol Med. https://doi.org/10.15252/emmm.202012088
62. Yang J, Ruchti E, Petit J-M, Jourdain P, Grenningloh G, Allaman I, Magistretti PJ (2014) Lactate promotes plasticity gene

expression by potentiating NMDA signaling in neurons. Proc Natl Acad Sci USA 111:12228–12233. https://doi.org/10.1073/pnas.1322912111
63. Halestrap AP (1975) The mitochondrial pyruvate carrier. Kinetics and specificity for substrates and inhibitors. Biochem J 148:85–96. https://doi.org/10.1042/bj1480085
64. Hildyard JC, Ammala C, Dukes ID, Thomson SA, Halestrap AP (2005) Identification and characterisation of a new class of highly specific and potent inhibitors of the mitochondrial pyruvate carrier. Biochim Biophys Acta 1707:221–230. https://doi.org/10.1016/j.bbabio.2004.12.005
65. Dringen R, Gebhardt R, Hamprecht B (1993) Glycogen in astrocytes: possible function as lactate supply for neighboring cells. Brain Res 623:208–214. https://doi.org/10.1016/0006-8993(93)91429-V
66. Brown AM, Ransom BR (2007) Astrocyte glycogen and brain energy metabolism. Glia 55:1263–1271. https://doi.org/10.1002/glia.20557
67. Mächler P, Wyss MT, Elsayed M, Stobart J, Gutierrez R, Alexandra, Kaelin V, Zuend M, Alejandro, Romero-Gómez I, Baeza-Lehnert F, Lengacher S, Bernard, Aebischer P, Pierre L, Weber B (2016) In vivo evidence for a lactate gradient from astrocytes to neurons. Cell Metab 23:94–102. https://doi.org/10.1016/j.cmet.2015.10.010
68. Ehrke E, Steinmeier J, Stapelfeldt K, Dringen R (2020) The menadione-mediated WST1 reduction by cultured astrocytes depends on NQO1 activity and cytosolic glucose metabolism. Neurochem Res. https://doi.org/10.1007/s11064-019-02930-1
69. Abbrescia DI, La Piana G, Lofrumento NE (2012) Malate-aspartate shuttle and exogenous NADH/cytochrome c electron transport pathway as two independent cytosolic reducing equivalent transfer systems. Arch Biochem Biophys 518:157–163. https://doi.org/10.1016/j.abb.2011.12.021
70. Xiao W, Wang RS, Handy DE, Loscalzo J (2018) NAD(H) and NADP(H) redox couples and cellular energy metabolism. Antioxid Redox Signal 28:251–272. https://doi.org/10.1089/ars.2017.7216
71. Berry MN (1971) Energy-dependent reduction of pyruvate to lactate by intact isolated parenchymal cells from rat liver. Biochem Biophys Res Commun 44:1449–1456. https://doi.org/10.1016/S0006-291X(71)80248-6
72. Dringen R, Schmoll D, Cesar M, Hamprecht B (1993) Incorporation of radioactivity from [^{14} C]lactate into the glycogen of cultured mouse astroglial cells. Evidence for gluconeogenesis in brain cells. Biol Chem Hoppe Seyler 374:343–347. https://doi.org/10.1515/bchm3.1993.374.1-6.343
73. Schmoll D, Fuhrmann E, Gebhardt R, Hamprecht B (1995) Significant amounts of glycogen are synthesized from 3-carbon compounds in astroglial primary cultures from mice with participation of the mitochondrial phosphoenolpyruvate carboxykinase isoenzyme. Eur J Biochem 227:308–315. https://doi.org/10.1111/j.1432-1033.1995.tb20390.x
74. Reinstrup P, Ståhl N, Mellergård P, Uski T, Ungerstedt U, Nordstrom CH (2000) Intracerebral Microdialysis in Clinical Practise: baseline values for chemical markers during Wakefulness, Anesthesia, and Neurosurgery. Neurosurgery 47:701–710. https://doi.org/10.1097/00006123-200009000-00035
75. Schulz M, Wang L, Tange M, Bjerre P (2000) Cerecral microdialysis monitoring: determination of normal and ischemic cerecral metabolism in patients with aneurysmal subarachnoid hemorrhage. J Neurosurg 93:808–814. https://doi.org/10.3171/jns.2000.93.5.0808
76. Benoist J-FO, Alberti C, Leclercq S, Rigal O, Jean-Louis R, Ogier De Baulny HL, Porquet D, Biou D (2003) Cerebrospinal fluid lactate and pyruvate concentrations and their ratio in children: age-related reference intervals. Clin Chem 49:487–494. https://doi.org/10.1373/49.3.487
77. Zhang W-M, Natowicz MR (2013) Cerebrospinal fluid lactate and pyruvate concentrations and their ratio. Clin Biochem 46:694–697. https://doi.org/10.1016/j.clinbiochem.2012.11.008
78. Granholm L (1969) The effect of blood in the CSF on the CSF lactate, pyruvate and bicarbonate concentrations. Scand J Clin Lab Investig 23:361–366. https://doi.org/10.3109/00365516909081702
79. Desagher S, Glowinski J, Prémont J (1997) Pyruvate protects neurons against hydrogen peroxide-induced toxicity. J Neurosci 17:9060–9067. https://doi.org/10.1523/jneurosci.17-23-09060.1997
80. Miao Y, Qiu Y, Lin Y, Miao Z, Zhang J, Lu X (2011) Protection by pyruvate against glutamate neurotoxicity is mediated by astrocytes through a glutathione-dependent mechanism. Mol Biol Rep 38:3235–3242. https://doi.org/10.1007/s11033-010-9998-0
81. Andersen JV, Westi EW, Jakobsen E, Urruticoechea N, Borges K, Aldana BI (2021) Astrocyte metabolism of the medium-chain fatty acids octanoic acid and decanoic acid promotes GABA synthesis in neurons via elevated glutamine supply. Mol Brain. https://doi.org/10.1186/s13041-021-00842-2
82. Hohnholt MC, Blumrich EM, Waagepetersen HS, Dringen R (2017) The antidiabetic drug metformin decreases mitochondrial respiration and tricarboxylic acid cycle activity in cultured primary rat astrocytes. J Neurosci Res 95:2307–2320. https://doi.org/10.1002/jnr.24050

2.2 Publication 2

Modulation of Pyruvate Export and Extracellular Pyruvate Concentration in Primary Astrocyte Cultures

Denker N. and Dringen R. (2024)

Neurochemical Research 49: 1331 – 1346
DOI: 10.1007/s11064-024-04120-0

Contribution of Nadine Denker:

- 100 % of the experimental work
- Preparation of all figures and tables
- 20 % of preparation of the first draft of the manuscript

Neurochemical Research (2024) 49:1331–1346
https://doi.org/10.1007/s11064-024-04120-0

ORIGINAL PAPER

Modulation of Pyruvate Export and Extracellular Pyruvate Concentration in Primary Astrocyte Cultures

Nadine Denker[1] · Ralf Dringen[1]

Received: 10 November 2023 / Revised: 2 February 2024 / Accepted: 2 February 2024 / Published online: 20 February 2024

Abstract
Astrocyte-derived pyruvate is considered to have neuroprotective functions. In order to investigate the processes that are involved in astrocytic pyruvate release, we used primary rat astrocyte cultures as model system. Depending on the incubation conditions and medium composition, astrocyte cultures established extracellular steady state pyruvate concentrations in the range between 150 µM and 300 µM. During incubations for up to 2 weeks in DMEM culture medium, the extracellular pyruvate concentration remained almost constant for days, while the extracellular lactate concentration increased continuously during the incubation into the millimolar concentration range as long as glucose was present. In an amino acid-free incubation buffer, glucose-fed astrocytes released pyruvate with an initial rate of around 60 nmol/(h × mg) and after around 5 h an almost constant extracellular pyruvate concentration was established that was maintained for several hours. Extracellular pyruvate accumulation was also observed, if glucose had been replaced by mannose, fructose, lactate or alanine. Glucose-fed astrocyte cultures established similar extracellular steady state concentrations of pyruvate by releasing pyruvate into pyruvate-free media or by consuming excess of extracellular pyruvate. Inhibition of the monocarboxylate transporter MCT1 by AR-C155858 lowered extracellular pyruvate accumulation, while inhibition of mitochondrial pyruvate uptake by UK5099 increased the extracellular pyruvate concentration. Finally, the presence of the uncoupler BAM15 or of the respiratory chain inhibitor antimycin A almost completely abolished extracellular pyruvate accumulation. The data presented demonstrate that cultured astrocytes establish a transient extracellular steady state concentration of pyruvate which is strongly affected by modulation of the mitochondrial pyruvate metabolism.

Keywords Astrocytes · Metabolism · Mitochondria · MCT1 · Pyruvate · Transport

Introduction

Astrocytes play an important role in brain energy metabolism [1–4], but have also crucial functions in brain development [5], (ion) homeostasis [6–9], the regulation and modulation of neuronal signals [10, 11], memory formation [12] and the protection against toxins and oxidative stress [13–15]. Although astrocytes are considered as a rather glycolytic cell type [16], also the oxidative metabolism plays an important role for astrocytic energy regeneration [17–19]. In this context, the α-ketoacid pyruvate is of high interest as it links cytosolic glycolysis and mitochondrial metabolism [17, 20, 21]. Pyruvate, the end product of glycolysis, can be taken up into mitochondria via the proton-coupled mitochondrial pyruvate carrier (MPC) [22–24], and subsequently be decarboxylated to acetyl-CoA via the pyruvate dehydrogenase complex [17, 25], or carboxylated to oxaloacetate by pyruvate carboxylase [26–28]. As the rate of pyruvate decarboxylation in mitochondria is slow in astrocytes [29], the cytosolic reduction of pyruvate by lactate dehydrogenase (LDH) is a favoured reaction at least in cultured astrocytes in order to regenerate NAD^+ for further glycolytic glucose degradation [30, 31]. Extracellular pyruvate can be efficiently taken up and metabolized by cultured astrocytes [18, 32, 33]. However, such cultures have also been reported to release pyruvate [34–36]. Pyruvate transport over the astrocytic plasma membrane is mainly mediated by proton-coupled monocarboxylate transporters (MCTs) [37–40].

y/Chemistry) and Centre for Environmental Research and Sustainable Technologies, University of Bremen, P.O. Box 330440, 28334 Bremen, Germany

Extracellular pyruvate has been shown to be neuroprotective in models of glutamate-toxicity [41, 42], oxidative stress [36, 43] and ischemia [44] and several potential mechanisms have been discussed that may contribute to this neuroprotective function [45]. For brain, extracellular pyruvate concentrations of around 160 µM have been reported [46, 47]. Although astrocytic pyruvate export is likely to contribute to this extracellular pyruvate pool, little is known so far on the metabolic processes and pathways that modulate pyruvate release from astrocytes.

We have previously reported that cultured rat astrocytes efficiently consume extracellular pyruvate in the absence of glucose [32, 33] in a process that depends on MCT1 and MPC and is strongly modulated by mitochondrial activity [33]. For our current study, we have investigated the pyruvate release from glucose-fed cultured astrocytes and have tested for the involvement of potential transporters and/or metabolic pathways that modulate pyruvate export and the extracellular pyruvate concentration. Here we report that cultured astrocytes establish transient extracellular steady state concentrations of pyruvate in a concentration range between around 150–300 µM, which are independent from the initial extracellular pyruvate concentration applied. The extracellular pyruvate concentration was increased by inhibition of mitochondrial pyruvate uptake, but lowered after inhibition of MCT1 or by application of the mitochondrial uncoupler BAM15 or of the respiratory chain inhibitor antimycin A. These data demonstrate that pyruvate release and the extracellular concentration of pyruvate are strongly affected by a modulation of mitochondrial pyruvate metabolism.

Materials and Methods

Penicillin G / streptomycin sulfate solution and powder to prepare Dulbecco's modified Eagles medium (DMEM with 25 mM glucose; catalog number: 52100-021) were obtained from Thermo Fisher Scientific (Schwerte, Germany; RRID:SCR_008452). Glucose-free DMEM powder (catalog number: D5030), fetal calf serum (FCS), antimycin A, BAM15 and UK5099 were purchased from Sigma-Aldrich (Darmstadt, Germany; RRID:SCR_008988). AR-C155858 was purchased at Tocris Bioscience (Bristol, UK; RRID:SCR_003689). All enzymes used for the assays to determine pyruvate, lactate and glucose were purchased from Roche Diagnostics (Mannheim, Germany; RRID:SCR_001326). Other chemicals of the highest purity available were obtained from Merck (Darmstadt, Germany; RRID:SCR_001287), Sigma-Aldrich (Steinheim, Germany; RRID:SCR_008988), AppliChem (Darmstadt, Germany; RRID:SCR_005814) or Carl Roth (Karlsruhe, Germany; RRID:SCR_005711). Sterile cell culture materials and unsterile 96-well plates were from Sarstedt (Nümbrecht, Germany).

Astrocyte Cultures

Astrocyte-rich primary cultures were prepared as previously described in detail from the total brains of newborn Wistar rats [48]. From the harvested cell suspension, 300,000 cells were seeded per well of 24-well dishes in 1 mL culture medium (90% DMEM containing 25 mM glucose, 44.6 mM sodium bicarbonate, 1 mM pyruvate, 20 U/mL penicillin G, 20 µg/mL streptomycin sulfate, supplemented with 10% FCS). The cultures were maintained in a humidified atmosphere with 10% CO_2 in a Sanyo CO_2 incubator (Osaka, Japan). The culture medium was renewed every seventh day and one day prior to an experiment. If not stated otherwise, confluent astrocyte cultures of an age between 19 and 27 days were used for experiments. It should be noted here, that the specific pyruvate export from cultured astrocytes was found to be lowered to some extend with increasing culture age, while the glucose consumption and lactate release were not affected by the cultured age (Fig. S1). Astrocyte-rich primary cultures are strongly enriched in astrocytes and contain only low amounts of contaminating microglial cells and oligodendrocytes [48, 49].

Experimental Incubation of the Cells

For long-time incubations of up to 14 d (Fig. 1), the culture medium was aspirated from the cultures (age of 13 or 14 d), the cells were washed twice with 1 mL pre-warmed (37 °C) glucose-free DMEM (containing 44.6 mM sodium bicarbonate, 20 U/mL penicillin G and 20 µg/mL streptomycin sulfate) and were subsequently incubated with 1 mL of glucose-free DMEM that had been supplemented with glucose in the indicated concentrations. After the given incubation periods the incubation medium was harvested for determination of the cell viability and the extracellular concentrations of glucose, lactate and pyruvate.

For short-time incubations of up to 12 h, the cells in the cultures (age between 19 and 27 d) were washed twice with 1 mL incubation buffer (IB; 145 mM NaCl, 20 mM HEPES, 5.4 mM KCl, 1.8 mM $CaCl_2$, 1 mM $MgCl_2$, 0.8 mM Na_2HPO_4, pH adjusted with NaOH to 7.4 at 37 °C) and subsequently incubated for the time periods indicated at 37 °C in the humidified atmosphere of a CO_2-free incubator with 250 µL of IB that had been supplemented with glucose, other substrates, inhibitors of transporters and/or modulators of metabolic pathways, if not indicated otherwise. For all supplements that had been dissolved as concentrated stock solutions in DMSO, appropriate solvent controls were performed that confirmed that the final concentration of DMSO present during the incubation did not

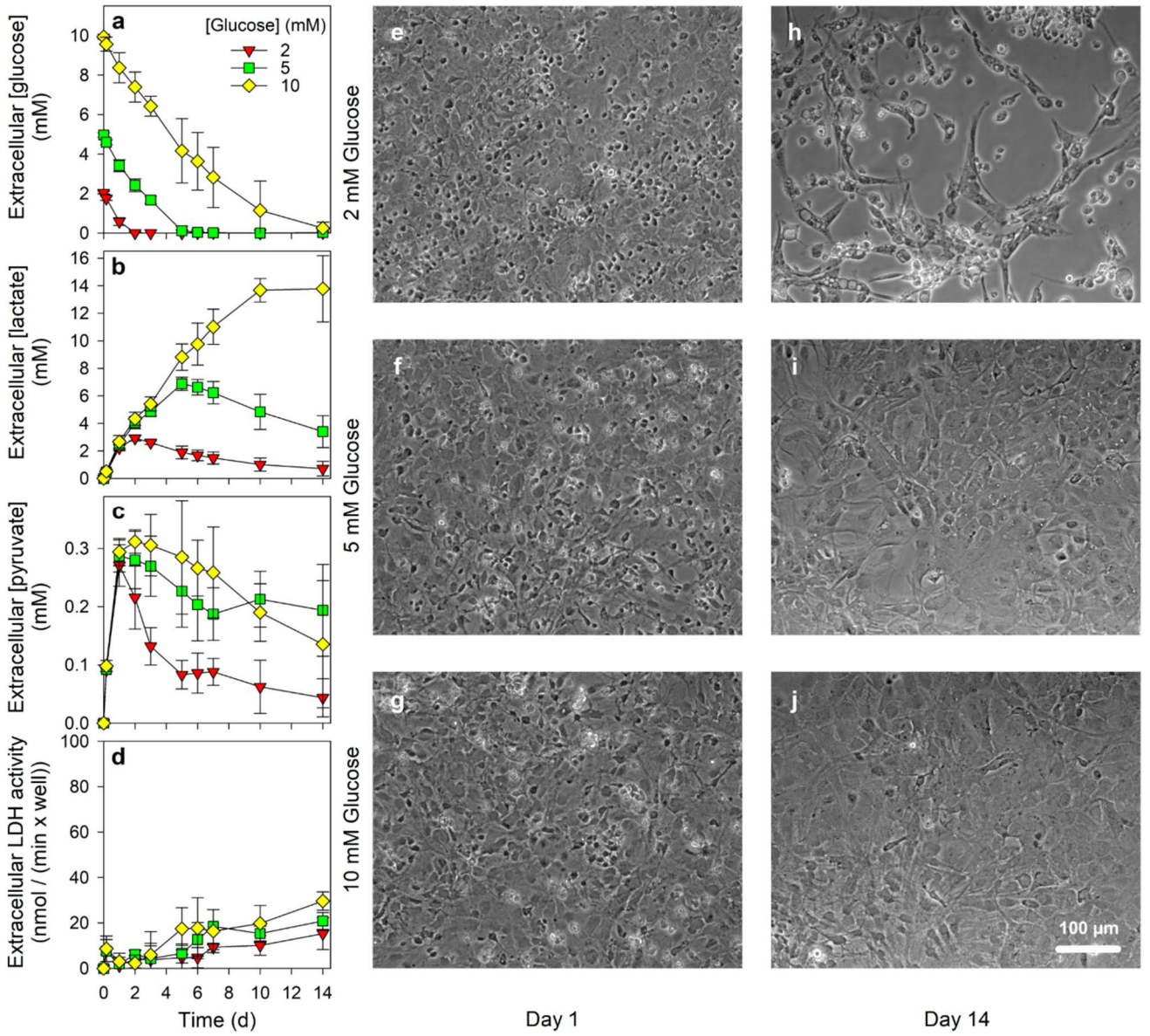

Fig. 1 Glucose consumption and extracellular accumulation of pyruvate and lactate in primary astrocyte cultures. Astrocyte cultures were incubated for up to 14 days in serum-free DMEM that contained the initial glucose concentrations indicated in panel a. The extracellular concentrations of glucose (**a**), lactate (**b**) and pyruvate (**c**) as well as the extracellular LDH activity (**d**) as an indicator of a potential loss in cell viability were measured for the indicated time points. The initial cellular LDH activity of the cultures at the onset of the incubation (100%) was 106 ± 19 nmol/(min × well) and the initial protein content was 121 ± 55 µg/well. The data presented are means ± SD of data obtained in three individually performed experiments on independently prepared cultures. Panels **e–g** show representative phase-contrast pictures of the cultures after incubation for 1 day, while panels h to j show pictures of the same cultures after 14 days of incubation

affect the parameters investigated (data not shown). After the given incubation periods the incubation medium was harvested for determination of potential LDH release (as indicator for cell toxicity) and of the extracellular concentrations of glucose, lactate and/or pyruvate.

Determination of Cellular Protein and Cell Viability

For determination of the cellular protein content per well the cultures were washed twice with 1 mL ice-cold (4 °C) phosphate-buffered saline (PBS; 10 mM potassium phosphate

buffer pH 7.4 containing 150 mM NaCl) and stored frozen until the protein determination was performed by the Lowry method [50] using bovine serum albumin as standard protein. To test for potential cell toxicity of a given treatment the extracellular activity of the cytosolic enzyme LDH was determined after the treatment for 10 µL media samples and compared with the initial cellular LDH activity of untreated cells, as previously described in detail [48].

Determination of Extracellular Pyruvate, Glucose and Lactate

Pyruvate was determined by a photometric microtiter plate assay using the LDH- and NADH-dependent reduction to lactate by a modification [33] of the method described previously by Clarke and Payton [51]. The concentration of extracellular glucose was determined by a coupled enzymatic assay using hexokinase and glucose-6-phosphat dehydrogenase as previously described in detail [48]. Glucose and pyruvate consumptions were calculated as difference between the concentrations applied and the concentrations determined after a given incubation period. Extracellular lactate was quantified by a coupled enzymatic assay using LDH and glutamate-pyruvate transaminase in an alkaline glutamate buffer as previously described in detail [48].

Determination of Cellular Lactate

Cellular lactate content was determined in neutralized perchlorate lysates of cultured astrocytes [33]. Briefly, the cells were washed twice with 1 mL ice-cold PBS on ice and lysed with 100 µL ice-cold 0.25 M $HClO_4$ per well. Subsequently, the cell lysates from two wells were collected and pooled. The cell lysates were neutralized by addition of an appropriate amount of 2 M KOH to a pH of 7 and centrifuged for 5 min at 12,100×*g* to precipitate the $KClO_4$ formed. Of the lysate supernatant, 190 µL were mixed with 10 µL of alkaline glutamate buffer (500 mM glutamate buffer pH 8.9, adjusted with NaOH) and 180 µL of the mixture was used to quantify lactate by a coupled enzymatic assay with LDH and glutamate-pyruvate transaminase [48].

Presentation of Data and Statistical Analysis

Quantitative data are shown as means ± SD of values that have been obtained from three individual experiments performed on independently prepared astrocyte cultures. For this low number of individual experiments, statistical analysis was done under the assumption of normal distribution. Analysis for statistical significance of groups of data was performed by ANOVA followed by the Bonferroni post-hoc test using the software GraphPad InStat (GraphPad, Boston, USA; RRID:SCR_000306). The paired *t*-test was used to calculate the statistical significance between pairs of data. The level of significance of differences compared to the data obtained for the respective control condition or between pairs of data is indicated by the symbols given in the legends of the individual figures. A p-value above 0.05 was considered as not significant.

Results

Extracellular Pyruvate and Lactate Accumulation in Cultured Primary Astrocytes During a Long-Time Incubation for 14 d

To investigate the extracellular accumulation of pyruvate and lactate during a long-time incubation of cultured astrocytes to media that contained limited concentrations of glucose, the cells were exposed to an initial glucose concentration of 2 mM, 5 mM or 10 mM in DMEM incubation medium and the extracellular concentrations of glucose, lactate and pyruvate as well as the cell viability were monitored for an incubation period of up to 14 d. After exposure of cultured astrocytes to a given concentration of glucose, the cells efficiently consumed the available glucose from the medium (Fig. 1a). For media containing glucose in initial concentrations of 2 mM, 5 mM and 10 mM, the detectable glucose had been almost completely metabolized within 2 d, 5 d and 14 d (Fig. 1a), respectively. This cell-dependent metabolic glucose depletion was accompanied by a rapid increase in the extracellular concentration of lactate, which reached for media that contained initially 2 mM, 5 mM and 10 mM glucose maximal lactate value of around 3 mM (after 2 d), around 7 mM (after 5 d) and of around 13 mM (after 10 d), respectively, representing around 150% of the concentration of glucose initially applied (Fig. 1b). In contrast, extracellular pyruvate accumulated for all glucose concentrations applied within 24 h to an extracellular concentration of around 0.3 mM (Fig. 1c). For cultures that had been fed with 10 mM glucose, extracellular pyruvate concentrations above 0.2 mM were maintained for several days, while extracellular pyruvate concentrations of cultures that had been exposed to initial glucose concentrations of 2 mM or 5 mM declined earlier (Fig. 1c). For all conditions, pyruvate levels were lowered during incubations (Fig. 1c) already before the extracellular lactate concentrations started to decline (Fig. 1b).

The viability of the cells, as demonstrated by the absence of a substantial increase in extracellular LDH activity (Fig. 1d) and by inspection of the cell morphology (Fig. 1e–g), was not compromised during the initial phase of the incubation for all the conditions applied. However, damage in the confluent cell layer was observed after a 14 d-incubation of cultures that had been exposed to only 2 mM

glucose (Fig. 1h), but not for cultures that had been incubated with media that contained initially 5 mM or 10 mM glucose (Fig. 1i, j). Nevertheless, for the latter treatments the majority of bright cells on top of the basal astrocyte cell layer, that had been visible in the cultures after 1 d of treatment (Fig. 1e–g), disappeared during the incubation for 14 d (Fig. 1i, j), suggesting that some cells in the culture may have not survived the respective treatments.

Application of pyruvate in an initial concentration of 0.5 mM to cultured astrocytes in DMEM containing initial glucose concentration of 2 mM, 5 mM or 10 mM resulted in almost identical results on glucose consumption, extracellular lactate accumulation and cell viability (Fig. S2a, c, d), compared to those recorded for the respective incubations without initial pyruvate application (Fig. 1a, b, d). In the glucose-containing media extracellular pyruvate concentrations between 0.3 and 0.4 mM were established within 2 d that were found further lowered during longer incubations (Fig. S2b). For longer incubations in glucose-containing media, almost identical extracellular pyruvate concentrations were found (Fig. S2b) as those determined for astrocyte cultures that had been exposed to the respective media that did not contain initial pyruvate (Fig. 1c).

Glucose-Dependent Extracellular Pyruvate Accumulation in Short-Time Experiments

To investigate a potential glucose dependency of pyruvate release from astrocytes in a short-time setting, the cultures were incubated in 250 µL of HEPES-buffered incubation buffer (IB) containing different initial concentrations of glucose and the extracellular concentrations of glucose, lactate and pyruvate were monitored during incubations for up to 12 h. During these incubations, glucose was consumed (Fig. 2a) while pyruvate (Fig. 2b) and lactate (Fig. 2c) accumulated extracellularly. For glucose concentrations above 3 mM, the decline in extracellular glucose (Fig. 2a) as well as the extracellular accumulation of lactate (Fig. 2c) were almost proportional to the incubation time as long as glucose was present. For initial glucose concentrations of 3 mM and below, the applied glucose was found completely metabolized before the end of the 12 h incubation (Fig. 2a) which limited the extracellular lactate accumulation (Fig. 2c). In contrast, for all the initial concentrations of glucose applied, extracellular pyruvate accumulated with a similar initial specific accumulation rate during the first hours of around 60 nmol/(h × mg), reaching after 5 h maximal extracellular pyruvate concentrations of 150 to 200 µM (Fig. 2b) that were maintained for several hours before they were lowered during longer incubations. None of the conditions applied had any obvious toxic potential as indicated by the absence of any LDH release from the cells during the 12 h incubation (Fig. 2d).

Similar Extracellular Concentrations of Pyruvate are Established by Pyruvate Export and/or Pyruvate Consumption

Astrocytes have been reported to efficiently consume extracellularly applied pyruvate [33]. To test how the initial application of an excess of pyruvate may affect pyruvate release and/or the extracellular pyruvate concentration in glucose-fed astrocytes, the cells were exposed to glucose in the absence or the presence of pyruvate in different initial concentrations of up to 1 mM (Fig. 3). None of the conditions applied had any obvious toxic potential as indicated by the absence of any LDH release from the cells during the incubation (Fig. 3c). Astrocytes that were incubated without or with 0.1 mM pyruvate, exported pyruvate during the incubation and the extracellular pyruvate concentrations were found to increase to values of around 150 µM within 5 h of incubation (Fig. 3a). In contrast, if pyruvate had been applied to the cells in initial concentrations above 0.2 mM, the extracellular pyruvate concentrations declined during the incubation and reached within 12 h of incubation extracellular concentrations between 100 µM and 200 µM (Fig. 3a). In contrast, for all pyruvate concentrations applied, glucose-fed astrocytes released lactate during the incubation at a rate that was almost proportional to the incubation time (Fig. 3b), causing an extracellular lactate accumulation to a concentration of around 6 mM within 12 h (Fig. 3b).

Test for a Potential Protection of Extracellular Pyruvate by Antioxidative Enzymes

Pyruvate has been reported to be efficiently oxidized to acetate by the presence of hydrogen peroxide [52]. For peripheral cell lines, the detectable extracellular pyruvate level has been reported to be lowered to some extent by such a reaction [53]. As the release of small amounts of hydrogen peroxide has been reported for an astroglial cell line [54] as well as for cultured primary and secondary astrocytes [55–57], we tested whether extracellular oxidation of pyruvate by cell-generated extracellular hydrogen peroxide may also lower the detectable extracellular pyruvate concentration in astrocyte cultures. The cells were incubated for 5 h with 5 mM glucose without or with 1 mM pyruvate in the absence or the presence of catalase and/or superoxide dismutase (SOD) to efficiently remove extracellular superoxide and hydrogen peroxide during the incubation, as previously shown for cultured astrocytes [58, 59]. However, the extracellular presence of the enzymes did not alter the extracellular pyruvate or lactate concentrations determined for cultures that had been incubated in the absence or the presence of 1 mM pyruvate (Table 1). None of the conditions applied had any obvious toxic potential as indicated by the absence of any LDH release from the cells during the incubation

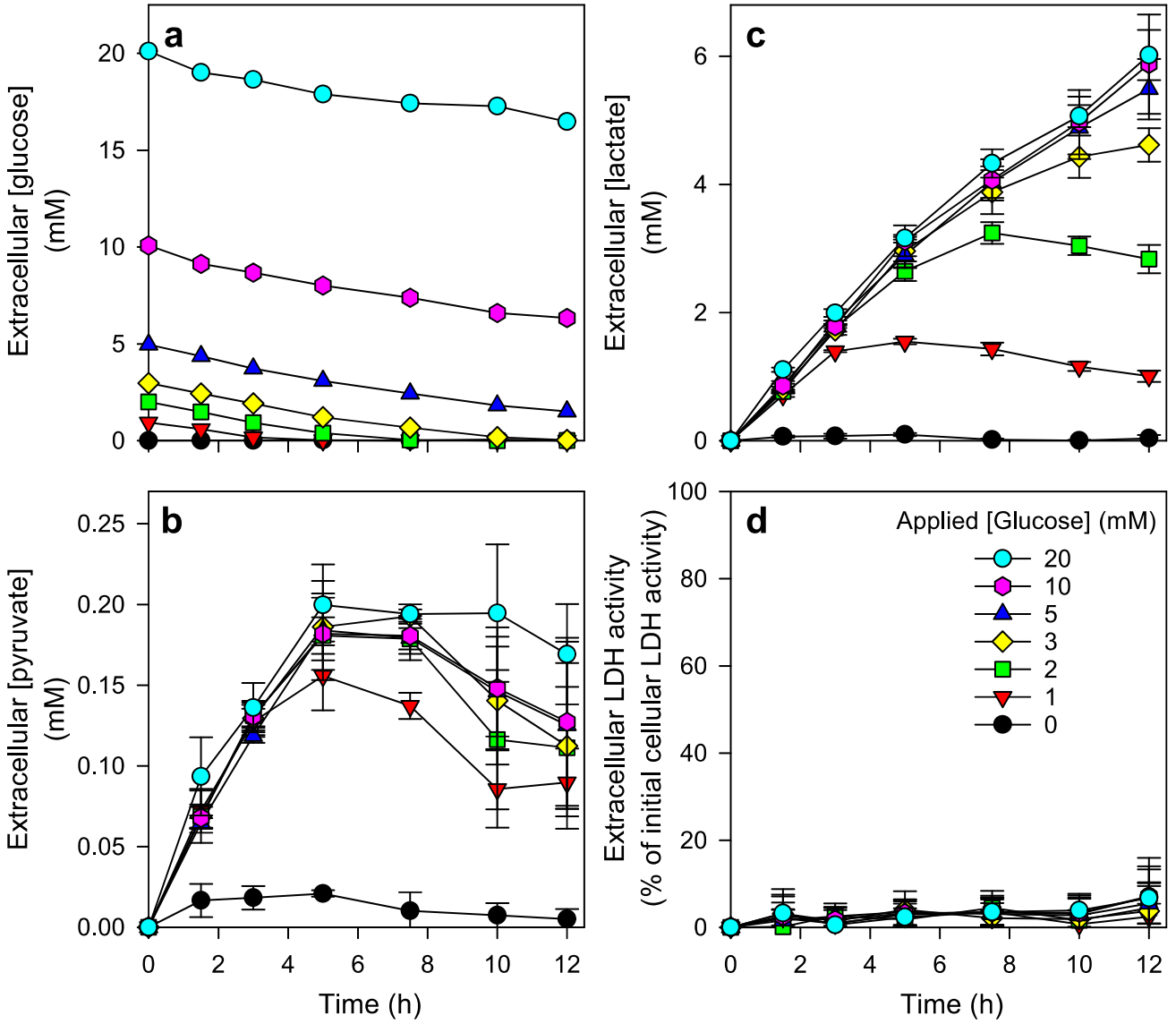

Fig. 2 Glucose-dependency of pyruvate and lactate release from cultured astrocytes. Cultured primary astrocytes were incubated for up to 12 h in incubation buffer containing the initial glucose concentrations indicated in panel d. For the given time points the concentrations of extracellular glucose (**a**), pyruvate (**b**) and lactate (**c**) were measured. In addition, extracellular LDH activity (**d**), as an indicator of a potential loss in cell viability, was determined. The initial cellular LDH activity of the cultures was 159 ± 17 nmol/(min × well) and the initial protein content was 137 ± 11 µg/well. The data shown represents means ± SD of values derived from experiments performed on three independently prepared cultures

(Table 1). Thus, for the conditions used a potential chemical oxidation of released pyruvate by cell-derived hydrogen peroxide appears not to affect the cell-derived extracellular pyruvate levels.

Substrate-Dependency of Extracellular Pyruvate and Lactate Accumulation in Astrocyte Cultures

Lactate and pyruvate are efficiently released from glucose-fed astrocytes (Figs. 1–3). To test for a potential release of pyruvate from astrocytes that had been exposed to other metabolic substrates than glucose, the cells were incubated for 5 h in 250 µL glucose-free buffer that had been supplemented with 5 mM of other hexoses or known mitochondrial substrates [18, 33, 60]. Compared to glucose-fed astrocytes, almost identical extracellular pyruvate concentrations were found for cells that had been exposed to mannose or lactate, but the cell established also in the presence of fructose, sorbitol or alanine extracellular pyruvate concentrations that were significantly higher than those determined for the substrate-free incubation (None) (Fig. 4a). Significantly increased extracellular lactate concentrations compared to

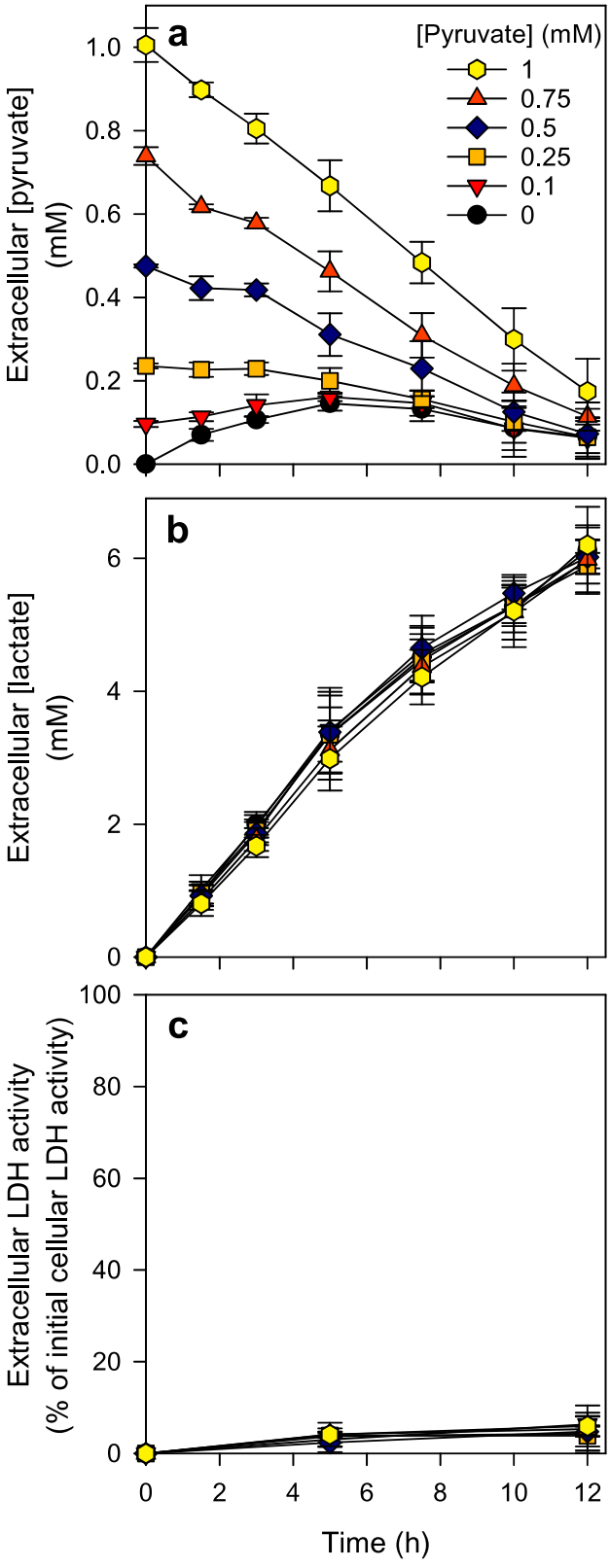

Fig. 3 Extracellular pyruvate concentrations in glucose-fed astrocyte cultures after application of different initial pyruvate concentrations. The cultures were incubated with 20 mM glucose in the absence (0 mM) or the presence of pyruvate in the concentrations indicated (panel a) for up to 12 h. For the time points indicated extracellular concentrations of pyruvate (**a**) and lactate (**b**) as well as the extracellular LDH activity (**c**) as an indicator for potential cell toxicity were measured. The initial cellular LDH activity of the cultures was 150 ± 5 nmol/(min × well) and the initial protein content was 150 ± 8 µg/well. The data shown are means ± SD from three individual experiments performed on independently prepared cultures

the substrate-free condition were found for incubations with glucose, mannose, fructose and lactate (Fig. 4b). None of the conditions applied had any obvious toxic potential as indicated by the absence of any LDH release from the cells during the 5 h incubation (Fig. 4c).

Astrocytes that had been incubated with either glucose or lactate release similar amounts of pyruvate (Fig. 5). To test whether pyruvate-formation and release by the presence of glucose and lactate may have a potential additive effect on the extracellular pyruvate accumulation, the cells were incubated without or with 5 mM of glucose and/or lactate. Although the extracellular lactate concentration determined after the incubation with lactate plus glucose were almost identical to the sum of lactate found for incubations with the individual substrates (Fig. 5b), similar concentrations of extracellular pyruvate of around 200 µM were found for the incubation with either glucose or lactate or with both substrates (Fig. 5a), demonstrating that extracellular pyruvate accumulation that is derived from the metabolism of glucose and lactate is not additive. None of the conditions applied had any obvious toxic potential as indicated by the absence of any LDH release from the cells during the 5 h incubation (Fig. 5c).

Modulation of Extracellular Pyruvate Concentrations by Inhibitors of Pyruvate Transporters

Pyruvate transport through the plasma membrane of astrocytes is mainly mediated by MCT1 [33, 37] while the mitochondrial MPC is involved in the uptake of cytosolic pyruvate into astrocytic mitochondria [18, 33, 61]. To test whether MCT1- and/or MPC-mediated transport may interfere with the extracellular pyruvate accumulation of glucose-fed astrocytes, the cells were incubated for 5 h in the absence or the presence of the MCT1 inhibitor AR-C155858 [62–64] and/or the MPC inhibitor UK5099 [24, 65, 66]. The presence of the MCT1 inhibitor lowered the cellular glucose consumption and lactate production by around 40%, while the MPC inhibitor did not affect these processes and was at best partially able to prevent the inhibitory potential of the AR-C155858 treatment (Fig. 6a, b). In contrast, the presence of the MCT1 inhibitor lowered significantly the extracellular pyruvate concentration by around 80%, while inhibition of MPC doubled the extracellular pyruvate concentration.

Table 1 Test for peroxide-mediated pyruvate degradation in cultured astrocytes

		None	SOD	Catalase	Catalase + SOD
0 mM Pyruvate	[Pyruvate] (µM)	122 ± 8	126 ± 14	136 ± 10	125 ± 9
	[Lactate] (mM)	3.87 ± 0.07	3.69 ± 0.16	3.53 ± 0.19	3.59 ± 0.14
	Extracellular LDH (% of initial cellular LDH)	7 ± 3	3 ± 2	5 ± 4	4 ± 4
1 mM Pyruvate	[Pyruvate] (µM)	573 ± 25	613 ± 55	591 ± 28	586 ± 51
	[Pyruvate] consumed (µM)	347 ± 90	358 ± 74	404 ± 56	399 ± 109
	[Lactate] (mM)	3.48 ± 0.05	3.26 ± 0.26	3.22 ± 0.05	3.22 ± 0.03
	Extracellular LDH (% of initial cellular LDH)	11 ± 6	7 ± 4	5 ± 5	4 ± 3

Primary astrocyte cultures were incubated for 5 h with 20 mM glucose without or with 1 mM pyruvate in the absence or the presence of 260 U catalase, 100 U SOD or 260 U catalase plus 100 U SOD before the extracellular concentrations of pyruvate and lactate as well as the extracellular LDH activity were determined. The data shown are means ± SD obtained from three experiments performed on independently prepared cultures

The initial cellular protein content was 157 ± 2 µg/well

No significant differences (ANOVA) compared to the values obtained for the control condition (None) were observed

The co-application of both inhibitors eliminated the strong effects observed for the individual inhibitors on the extracellular pyruvate concentration (Fig. 6c). None of the conditions applied had any obvious toxic potential as indicated by the absence of any LDH release from the cells during the incubation (Fig. 6d).

Consequences of a Modulation of Mitochondrial Metabolism on the Extracellular Pyruvate Concentration of Astrocyte Cultures

To investigate whether a modulation of mitochondrial metabolism may affect the extracellular pyruvate concentration in cultured astrocytes, the cells were incubated with 5 mM glucose in the presence of the complex III inhibitor antimycin A [67, 68] and/or the respiratory chain uncoupler BAM15 [69]. Exposure of cultured astrocytes for 5 h to those substances did not cause acute toxicity as indicated by the absence of any significant increase in extracellular LDH activity (Fig. 7d). Presence of antimycin A and BAM15 as well as the co-application of both compounds strongly increased glycolytic lactate production in cultured astrocytes as demonstrated by high values for glucose consumption (Fig. 7a) and lactate accumulation (Fig. 7c) that were more than doubled compared to the values for the control condition. In contrast, antimycin A and BAM15 almost completely diminished the extracellular pyruvate accumulation (Fig. 7b).

Discussion

Pyruvate is an important metabolite that can be taken up [32, 33, 70] and released [34–36] by astrocytes. To investigate the processes that may affect astrocytic pyruvate release we have used astrocyte-rich primary cultures as a model system. During long-time incubations in DMEM culture medium, glucose-fed astrocytes released within the first day of incubation pyruvate to establish an extracellular concentration of around 300 µM that remained almost constant for days, at least if the cells had been exposed to a high concentration of glucose. This observation confirms literature data that report similar extracellular steady state concentrations in astrocyte-conditioned media during incubation of astrocytes for periods of up to 1 d [35] or 2 d [36]. However, the formation of an extracellular steady state pyruvate concentration appears not to be an exclusive feature of astrocytes, as it has also been reported for cultured neurons [35, 36] and for several cell lines of peripheral origin [53].

In contrast to the transient extracellular pyruvate accumulation, cultured astrocytes produced large amounts of lactate that accumulated almost proportional to time till the extracellular glucose had been consumed. As soon as the applied glucose had been metabolized, the cells started to consume the extracellular lactate that had been generated by glycolytic glucose metabolism, as previously reported [31], but also the extracellular pyruvate was consumed by the cells. Some decline in the extracellular steady state pyruvate concentration was also observed during extended incubation in DMEM supplemented with 10 mM glucose before the extracellular glucose had been completely metabolized. This partial decline in extracellular pyruvate concentration is consistent with the age-dependent tendency of cultured astrocytes to accumulate less extracellular pyruvate with increasing culture age (Fig. S1). Whether an increased mitochondrial activity or other reasons contribute to this age-dependent decline of extracellular pyruvate accumulation remains to be elucidated.

Pyruvate that was produced and released during incubation of cultured primary astrocytes in glucose-containing Hepes-buffered IB accumulated rapidly in the medium for around 5 h and established a transient extracellular

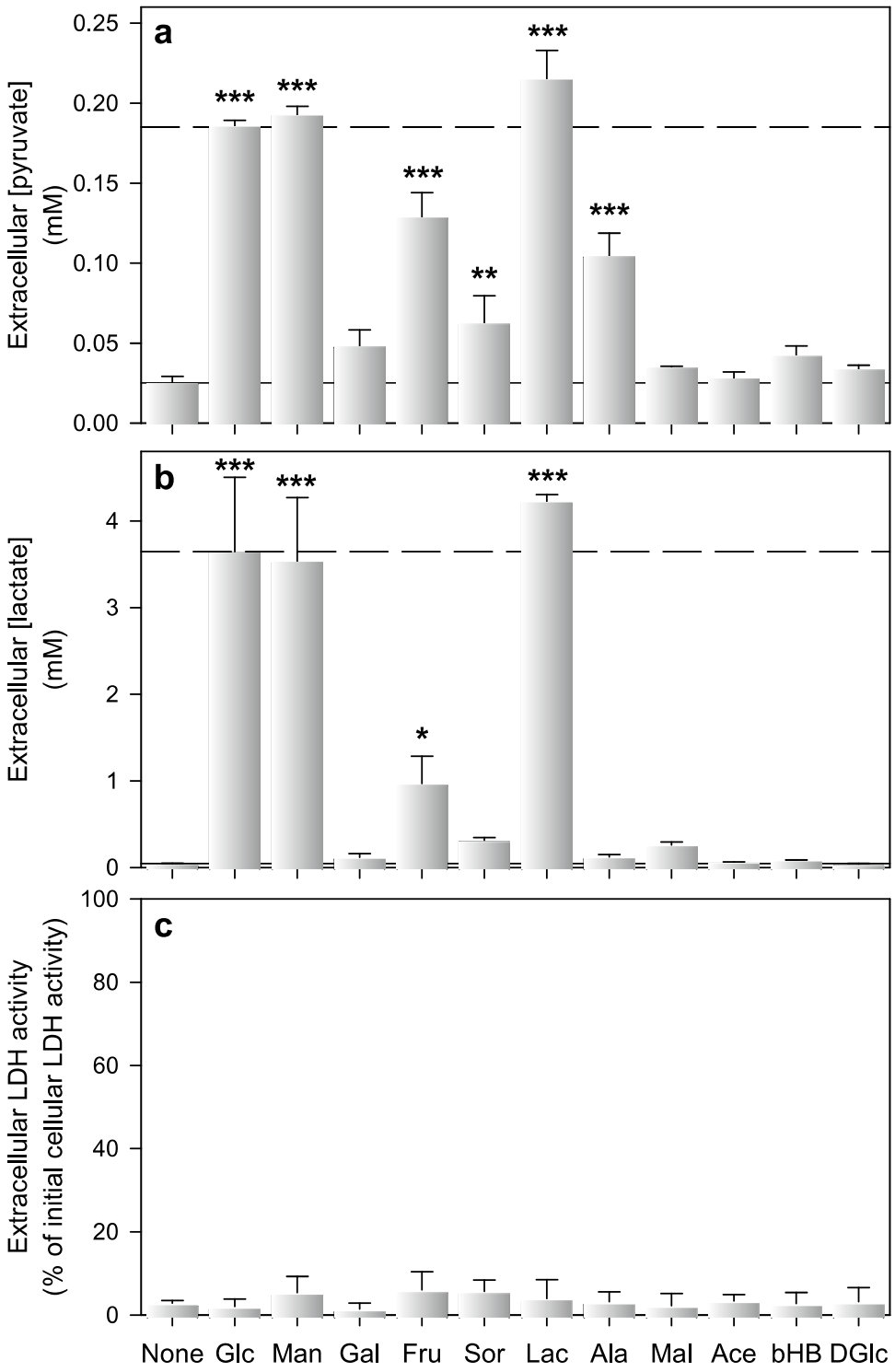

Fig. 4 Extracellular accumulation of pyruvate and lactate after exposure of cultured astrocytes to different substrates. The cells were incubated for 5 h in glucose-free incubation buffer containing 5 mM of the indicated substrates before the extracellular concentrations of pyruvate (**a**) and lactate (**b**) as well as the extracellular LDH activity (**c**) were determined. The initial intracellular LDH activity was 170 ± 33 nmol/(min × well) and the initial protein content was 155 ± 19 µg/well. The data shown are means ± SD of values obtained in three experiments performed on independently prepared astrocyte cultures. The significance of differences (ANOVA) compared to the values obtained without any substrate (None) is indicated by *p < 0.05, **p < 0.01 and ***p < 0.001. Glc, glucose; Man, mannose; Gal, galactose; Fru, Fructose; Sor, sorbitol; Lac, lactate; Ala; alanine; Mal, Malate; Ace, acetate; bHB, β-hydroxybutyrate; DGlc, 2-deoxyglucose

steady state concentration of around 150–200 µM that was maintained for around 5 h. Reason for the discrepancy in the levels and the maintenance of extracellular pyruvate steady state concentrations observed for complex incubation media (DMEM) and the more simple HEPES-buffered IB appears to be mainly the use of the different buffer systems, as the extracellular pyruvate accumulation was also found accelerated in bicarbonate-buffered IB (Fig. S3). However, the more complex composition of the DMEM compared to IB affected also to some extent the extracellular pyruvate level as demonstrated by the doubling in extracellular pyruvate concentration in HEPES-buffered DMEM compared to HEPES-buffered IB (Fig. S3).

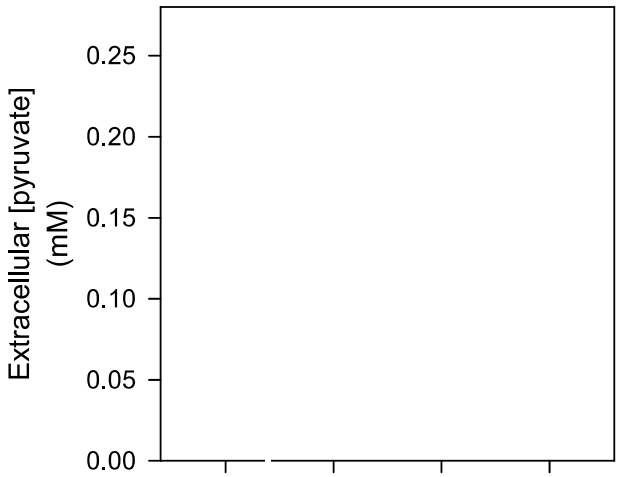

nificance of differences (ANOVA) compared to the values obtained for the glucose only condition is indicated by *p < 0.05 and ***p < 0.001

As excess of lactate has been shown to lower pyruvate consumption at least in glucose-deprived astrocytes [33], the accumulation of large extracellular concentrations of glucose-derived lactate should lower pyruvate uptake during extended incubation periods, thereby increasing extracellular pyruvate concentration. However, this appears not to be the case as the extracellular pyruvate concentration declined from a given transient steady state concentration in both DMEM- and IB-treated astrocytes after substantial amounts of the applied glucose had been metabolized. As lactate had accumulated under such conditions to millimolar extracellular concentrations, and as the cells are able to generate and export pyruvate from lactate as extracellular substrate, other factors than the available concentrations of the substrates lactate and glucose appear to be responsible for the observed decline in extracellular pyruvate concentration during extended incubation periods. For example, the absence of amino acids in IB, which could serve as anaplerotic substrates for citric acid cycle intermediates, may cause a delayed stimulated mitochondrial pyruvate consumption, thereby lowering cytosolic pyruvate concentration and subsequently stimulating consumption of extracellular pyruvate. At least for incubations in DMEM, a redistribution of mitochondria has been reported for the cells in astrocyte cultures after metabolic glucose-depletion that requires a metabolic shift from glycolytic glucose metabolism to oxidative lactate metabolism [31].

The delayed decline in detectable extracellular pyruvate levels over time could also be caused be the ability of extracellular pyruvate to chemically react with cell-derived hydrogen peroxide [52] which has been reported to protect neurons against toxicity induced by hydrogen peroxide [36, 43]. For peripheral cell lines, the detectable extracellular pyruvate level has been reported to be lowered to some extent by such a reaction [53]. However, although cultured astrocytes have frequently been reported to release hydrogen peroxide [55–57], the extracellular pyruvate accumulation and the detectable extracellular pyruvate concentration in cultured astrocytes were under the conditions used not affected by the presence of high activities of catalase and/or SOD. Thus, extracellular peroxide clearance by pyruvate can be excluded to contribute to the establishment of the transient steady state concentration of extracellular pyruvate in cultured astrocytes.

The initial constant velocity of pyruvate release from glucose-fed astrocytes suggests that pyruvate production by

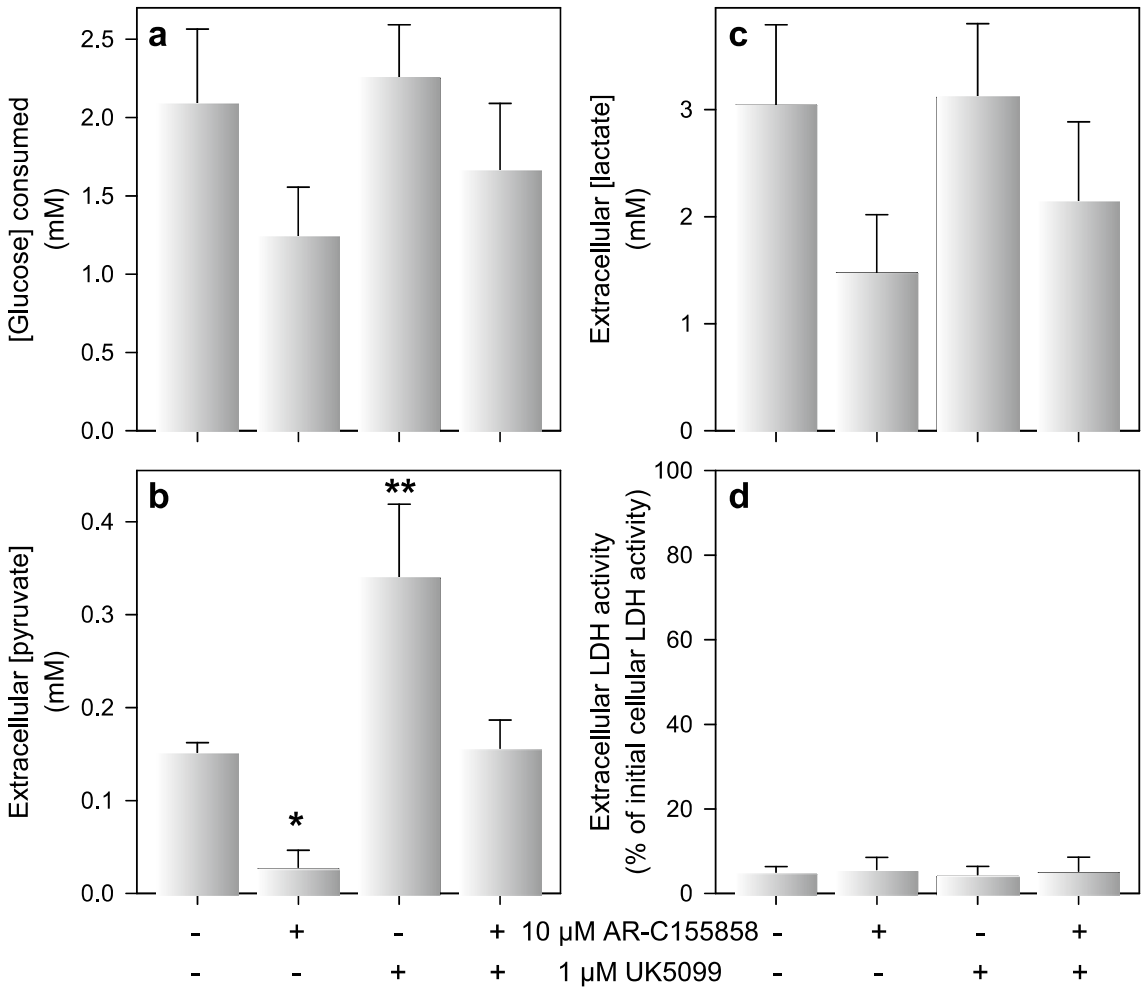

Fig. 6 Modulation of the extracellular pyruvate and lactate concentrations by inhibitors of monocarboxylate transporters. Astrocyte cultures were incubated with 5 mM of glucose in the absence or presence of 10 µM of the MCT1 inhibitor AR-C155858 and/or 1 µM of the mitochondrial pyruvate carrier inhibitor UK5099. After 5 h of incubation, glucose consumption (**a**) and the concentrations of extracellular pyruvate (**b**) and lactate (**c**) were determined. In addition, extracellular LDH activity (**d**), as an indicator of a potential loss in cell viability, was measured. The initial intracellular LDH activity was 149 ± 40 nmol/(min × well) and the culture had an initial protein value of 134 ± 26 µg/well. The data represent means ± SD of data obtained in three experiments performed on independently prepared cultures. The significance of differences (ANOVA) compared to the values obtained for the control condition (no inhibitor) is indicated by *p < 0.05 and **p < 0.01

glycolysis and pyruvate consuming reactions establish for both incubation media almost constant intracellular pyruvate concentrations that define the velocity of pyruvate export. As pyruvate is transported through the plasma membrane of astrocytes mainly by the proton co-transporter MCT1 [33, 37], the proton gradient between the cytosol and the extracellular environment could affect pyruvate export and import. However, as the intracellular pH of cultured astrocytes rapidly adapts within minutes to the applied extracellular pH [71], it can be assumed that the intracellular pH remains rather constant during incubations of glucose-fed astrocytes under the conditions used and that the concentration gradient of pyruvate is the main driving force for its net transport over the astrocytic cell membrane.

We were unable to directly quantify cellular pyruvate contents for cultured astrocytes as cytosolic pyruvate concentrations are rather low in the micromolar range as demonstrated by genetically encoded sensors for cultured mouse astrocytes [24] or pyruvate-exposed HEK293 cells [70]. However, we at least calculated cytosolic pyruvate concentrations from the initial pyruvate release rates for glucose-fed astrocytes in HEPES-buffered IB (68 nmol/(h × mg)) and bicarbonate-buffered DMEM (108 nmol/(h × mg) (Fig. S3; means ± SD of data obtained in three experiments performed on independently prepared cultures). By using the Michaelis–Menten equation with the kinetic parameters previously determined for pyruvate transport in cultured astrocytes (Vmax = 7.5 nmol/

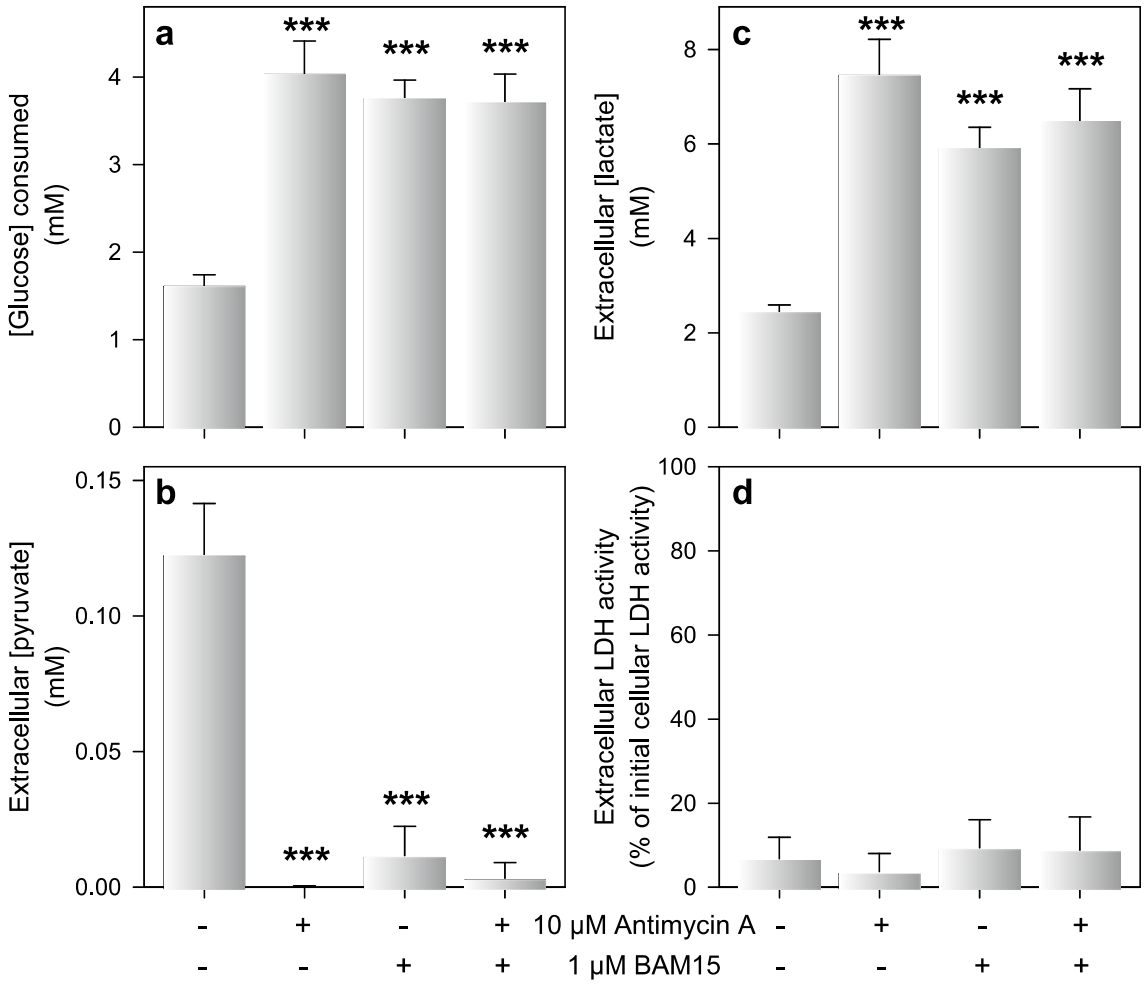

Fig. 7 Alteration of extracellular pyruvate and lactate concentrations by application of the mitochondrial modulators antimycin A and/or BAM15. Astrocyte primary cultures were incubated with 5 mM glucose in the absence or the presence of 10 µM of the complex III inhibitor antimycin A and/or 1 µM of the uncoupler BAM15. After 5 h of incubation, glucose consumption (**a**), extracellular concentrations of pyruvate (**b**) and lactate (**c**) as well as the extracellular LDH activity (**d**) were determined. The cultures had an initial cellular LDH activity of 159 ± 31 nmol/(min × well) and an initial protein content of 148 ± 12 µg/well. The data shown represent means ± SD of data obtained in three experiments performed on individually prepared cultures. The significance of differences (ANOVA) compared to the values obtained for the control condition (no inhibitor or uncoupler) is indicated by ***$p < 0.001$

(min × mg), $K_M = 1$ mM [32]), cytosolic pyruvate concentrations of 177 µM (IB) and 316 µM (DMEM) were calculated which fit quite well to the transient extracellular pyruvate steady state concentrations determined for glucose-fed cultured astrocytes in the respective media. The proposed adjustment of the extracellular steady state concentration of pyruvate to the intracellular pyruvate concentration would also explain why astrocytes consume excess of extracellular pyruvate to reach an appropriate extracellular pyruvate concentration. All these data support the view that the pyruvate concentration gradient is the main driving force for the extracellular accumulation of pyruvate and that net export of pyruvate is ceased after the extracellular concentration has reached the cytosolic pyruvate concentration.

Although both pyruvate and lactate are transported in astrocytes mainly by MCT1 [33, 37, 38, 72], the extracellular accumulation of pyruvate and lactate differ substantially. Extracellular pyruvate reached a transient stead state concentration in the micromolar range within hours while the extracellular lactate concentration continued to increase into the millimolar concentration range without reaching an extracellular steady state concentration. This observation, which confirms literature data [35], is likely to be the consequence of substantial differences in the cellular concentrations of both monocarboxylates as expected from the thermodynamic equilibrium of the LDH-catalyzed reaction [30]. Indeed, a specific cellular lactate content of 25.7 ± 2.1 nmol/mg (data from 4 experiments performed on independently prepared cultures) was determined for untreated cultured astrocytes

and this value was not significantly altered by a 5 h incubation in IB with 10 mM glucose (data not shown). By using the specific cytosolic volume of 4.1 µL/mg protein [73], the cytosolic lactate concentration of untreated astrocytes was calculated to be around 6 mM. Thus, considering this high concentration of cytosolic lactate it is not surprising that lactate continues to accumulate in the extracellular medium of cultured astrocytes to the millimolar concentration range.

Assuming that the cytosolic pyruvate concentration is the main regulator of the extracellular pyruvate concentration in astrocyte cultures, at least for the initial phases of the incubations till a maximal extracellular pyruvate concentration has been reached, all treatments which modulate cellular pyruvate transport or metabolism should also affect the extracellular pyruvate concentration. Accordingly, in glucose-deprived astrocytes substantial concentrations of extracellular pyruvate were only found for incubations with either lactate or with other exogenous substrates that have previously been reported to be converted by astrocytes to lactate via pyruvate, including mannose, fructose, sorbitol and alanine [74–78]. In contrast, neither extracellular pyruvate nor lactate were found in glucose-deprived astrocytes that had been exposed to substrates such as acetate or beta-hydroxybutyrate which are unable to serve as precursors for pyruvate net synthesis but can be consumed for mitochondrial ATP synthesis in astrocytes [17, 18].

Pharmacological modulation of transporters and metabolic pathways that are known to modulate astrocytic pyruvate consumption [33] strongly affected the extracellular pyruvate concentration in glucose-fed astrocyte cultures. An increased extracellular pyruvate concentration was found for cultures that had been treated with UK5099, an inhibitor of mitochondrial pyruvate uptake [24, 33, 66], consistent with the importance of this transporter for mitochondrial pyruvate consumption [18, 33]. In contrast, extracellular pyruvate concentrations were severely lowered in glucose-fed astrocytes that had been treated with the uncoupler BAM15 or the respiratory chain inhibitor antimycin A. This can be explained for BAM15-treated astrocytes by a lowered cytosolic pyruvate concentration due to the accelerated mitochondrial pyruvate consumption reported for BAM15-treated astrocytes [33, 69]. In addition, the observed doubling of glycolytic lactate production by antimycin A, which confirms literature data [31, 68], and by BAM15 demonstrates for these conditions an increased cytosolic pyruvate consumption by LDH to regenerate the NAD^+ needed to enable continuous glycolytic ATP regeneration. Extracellular pyruvate accumulation was also strongly inhibited by the MCT1 inhibitor AR-C155858, consistent with the function of MCT1 in pyruvate export and with the potential of this inhibitor to lower pyruvate consumption in astrocytes [33]. However, treatment with AR-C155858 lowered also glucose consumption and lactate release. Reason for this observation is most likely an acidification of the cellular pH by impairing proton-coupled export of glucose-derived lactate, consistent with the slower glycolytic glucose consumption in slightly acidified media (Fig. S4) [79, 80].

In conclusion, we have demonstrated that cultured astrocytes establish extracellular pyruvate concentrations that are likely to reflect their intracellular pyruvate concentrations which in turn depend on glycolytic pyruvate production, pyruvate reduction to lactate as well as on the mitochondrial pyruvate metabolism. A number of questions remains currently unanswered and should be addressed in future studies. A detailed analysis of the morphology and cellular composition of the astrocyte cultures after extended incubations in media with limited glucose concentrations should be done, for example by immunocytochemical characterization. Also, the molecular reasons underlying the observed decline in pyruvate export with age of the astrocyte cultures remain to be elucidated. Pyruvate release and extracellular pyruvate concentrations appear to be affected by multiple parameters, including the composition and pH of the incubation medium and the incubation time. It remains to be identified, which components in the incubation media applied are responsible for the different export rates for pyruvate and for the observed differences in the concentrations of pyruvate in astrocyte-conditioned media. Extracellular pyruvate concentrations are rapidly established, but they are transient and decline during longer incubations, although in many of the investigated conditions glucose is still available and large extracellular concentrations of glucose-derived lactate are present, which can also serve as exogenous substrate to generate pyruvate. The factors which are responsible for this decline in extracellular pyruvate are currently unknown and should be identified. Finally, the hypothesis that during the initial phase of incubation an equilibrium between cytosolic and extracellular pyruvate concentrations is established should be experimentally confirmed in a future study. For this, genetically encoded sensors [24] could be used and the detected cytosolic pyruvate concentrations could be directly correlated to the determined extracellular pyruvate concentrations for the various incubation conditions applied.

Cultured astrocytes establish a transient extracellular steady state concentration in the range of 150 to 300 µM which is quite similar to extracellular pyruvate concentrations (around 160 µM) that have been reported for brain tissue [46, 47] and the cerebrospinal fluid (CSF) (between 30 and 200 µM) [36, 81–83]. Due to their ability to release and consume pyruvate, it appears likely that astrocytes contribute to the reported extracellular pyruvate concentrations in brain and CSF. Pyruvate has been reported to by neuroprotective in neuropathological conditions such as glutamate-toxicity [41, 42], oxidative stress [36, 43] and ischemia [44] and several potential mechanisms for these neuroprotective functions have been discussed [45]. Pyruvate export has also been reported

for cultured neurons, although the established extracellular pyruvate concentrations are lower than those found for astrocytes [35, 36]. Further in vivo studies are required to elucidate to which extent astrocytes contribute to the reported extracellular concentration of pyruvate in brain and CSF and whether a modulation of astrocytic pyruvate metabolism and release will have consequences for extracellular pyruvate levels in brain and/or on the neuroprotective potential of astrocytes.

Supplementary Information The online version contains supplementary material available at https://doi.org/10.1007/s11064-024-04120-0.

Acknowledgements The authors would like to acknowledge the basal financial support of the University of Bremen for the project presented here.

Authors Contributions ND and RD designed the study concept. ND performed all experiments and prepared all figures. RD wrote most parts of the manuscript. All authors reviewed and approved the manuscript.

Funding Open Access funding enabled and organized by Projekt DEAL. The project was funded by the University of Bremen (basal financial support of the Dringen group).

Data Availability Enquiries about data availability should be directed to the authors.

Declarations

Competing Interests The authors declare no competing interests.

References

1. Brown AM, Ransom BR (2007) Astrocyte glycogen and brain energy metabolism. Glia 55:1263–1271. https://doi.org/10.1002/glia.20557
2. Weber B, Barros LF (2015) The astrocyte: powerhouse and recycling center. Cold Spring Harb Perspect Biol 7:a020396. https://doi.org/10.1101/cshperspect.a020396
3. Langen UH, Ayloo S, Gu C (2019) Development and cell biology of the blood-brain barrier. Annu Rev Cell Dev Biol 35:591–613. https://doi.org/10.1146/annurev-cellbio-100617-062608
4. Roumes H, Pellerin L, Bouzier-Sore AK (2023) Astrocytes as metabolic suppliers to support neuronal activity and brain functions. Essays Biochem 67:27–37. https://doi.org/10.1042/EBC20220080
5. Clarke LE, Barres BA (2013) Emerging roles of astrocytes in neural circuit development. Nat Rev Neurosci 14:311–321. https://doi.org/10.1038/nrn3484
6. Simard M, Nedergaard M (2004) The neurobiology of glia in the context of water and ion homeostasis. Neuroscience 129:877–896. https://doi.org/10.1016/j.neuroscience.2004.09.053
7. Olsen ML, Khakh BS, Skatchkov SN, Zhou M, Lee CJ, Rouach N (2015) New insights on astrocyte ion channels: critical for homeostasis and neuron-glia signaling. J Neurosci 35:13827–13835. https://doi.org/10.1523/jneurosci.2603-15.2015
8. Theparambil SM, Hosford PS, Ruminot I, Kopach O, Reynolds JR, Sandoval PY, Rusakov DA, Barros LF, Gourine AV (2020) Astrocytes regulate brain extracellular pH via a neuronal activity-dependent bicarbonate shuttle. Nat Commun 11:5073. https://doi.org/10.1038/s41467-020-18756-3
9. Wang S, Wang B, Shang D, Zhang K, Yan X, Zhang X (2022) Ion channel dysfunction in astrocytes in neurodegenerative diseases. Front Physiol 13:814285. https://doi.org/10.3389/fphys.2022.814285
10. Halassa MM, Florian C, Fellin T, Munoz JR, Lee SY, Abel T, Haydon PG, Frank MG (2009) Astrocytic modulation of sleep homeostasis and cognitive consequences of sleep loss. Neuron 61:213–219. https://doi.org/10.1016/j.neuron.2008.11.024
11. Oliveira JF, Araque A (2022) Astrocyte regulation of neural circuit activity and network states. Glia 70:1455–1466. https://doi.org/10.1002/glia.24178
12. Bohmbach K, Henneberger C, Hirrlinger J (2023) Astrocytes in memory formation and maintenance. Essays Biochem 67:107–117. https://doi.org/10.1042/ebc20220091
13. Dringen R, Brandmann M, Hohnholt MC, Blumrich EM (2015) Glutathione-dependent detoxification processes in astrocytes. Neurochem Res 40:2570–2582. https://doi.org/10.1007/s11064-014-1481-1
14. Robinson SR, Lee A, Bishop GM, Czerwinska H, Dringen R (2015) Inhibition of astrocytic glutamine synthetase by lead is associated with a slowed clearance of hydrogen peroxide by the glutathione system. Front Integr Neurosci 9:61. https://doi.org/10.3389/fnint.2015.00061
15. Zhang W, Hong J, Zhang H, Zheng W, Yang Y (2021) Astrocyte-derived exosomes protect hippocampal neurons after traumatic brain injury by suppressing mitochondrial oxidative stress and apoptosis. Aging 13:21642–21658
16. Barros LF, Ruminot I, San Martin A, Lerchundi R, Fernandez-Moncada I, Baeza-Lehnert F (2021) Aerobic glycolysis in the brain: warburg and crabtree contra pasteur. Neurochem Res 46:15–22. https://doi.org/10.1007/s11064-020-02964-w
17. Rose J, Brian C, Pappa A, Panayiotidis MI, Franco R (2020) Mitochondrial metabolism in astrocytes regulates brain bioenergetics, neurotransmission and redox balance. Front Neurosci 14:536682. https://doi.org/10.3389/fnins.2020.536682
18. Harders AR, Arend C, Denieffe SC, Berger J, Dringen R (2023) Endogenous energy stores maintain a high ATP concentration for hours in glucose-depleted cultured primary rat astrocytes. Neurochem Res 48:2241–2252. https://doi.org/10.1007/s11064-023-03903-1
19. Karger G, Berger J, Dringen R (2024) Modulation of cellular levels of adenosine phosphates and creatine phosphate in cultured primary astrocytes. Neurochem Res 49:402–414. https://doi.org/10.1007/s11064-023-04039-y
20. Waagepetersen HS, Qu H, Hertz L, Sonnewald U, Schousboe A (2002) Demonstration of pyruvate recycling in primary cultures of neocortical astrocytes but not in neurons. Neurochem Res 27:1431–1437. https://doi.org/10.1023/a:1021636102735
21. Gray LR, Tompkins SC, Taylor EB (2014) Regulation of pyruvate metabolism and human disease. Cell Mol Life Sci 71:2577–2604. https://doi.org/10.1007/s00018-013-1539-2

22. Papa S, Francavilla A, Paradies G, Meduri B (1971) The transport of pyruvate in rat liver mitochondria. FEBS Lett 12:285–288. https://doi.org/10.1016/0014-5793
23. Halestrap AP (1978) Pyruvate and ketone-body transport across the mitochondrial membrane. Exchange properties, pH-dependence and mechanism of the carrier. Biochem J 172:377–387. https://doi.org/10.1042/bj1720377
24. Arce-Molina R, Cortés-Molina F, Sandoval PY, Galaz A, Alegría K, Schirmeier S, Barros LF, San Martín A (2020) A highly responsive pyruvate sensor reveals pathway-regulatory role of the mitochondrial pyruvate carrier MPC. Elife 9:e53917. https://doi.org/10.7554/eLife.53917
25. McKenna MC (2012) Substrate competition studies demonstrate oxidative metabolism of glucose, glutamate, glutamine, lactate and 3-hydroxybutyrate in cortical astrocytes from rat brain. Neurochem Res 37:2613–2626. https://doi.org/10.1007/s11064-012-0901-3
26. Shank RP, Bennett GS, Freytag SO, Campbell GL (1985) Pyruvate carboxylase: an astrocyte-specific enzyme implicated in the replenishment of amino acid neurotransmitter pools. Brain Res 329:364–367. https://doi.org/10.1016/0006-8993(85)90552-9
27. Cesar M, Hamprecht B (1995) Immunocytochemical examination of neural rat and mouse primary cultures using monoclonal antibodies raised against pyruvate carboxylase. J Neurochem 64:2312–2318. https://doi.org/10.1046/j.1471-4159.1995.64052312.x
28. Amaral AI, Hadera MG, Tavares JM, Kotter MRN, Sonnewald U (2016) Characterization of glucose-related metabolic pathways in differentiated rat oligodendrocyte lineage cells. Glia 64:21–34. https://doi.org/10.1002/glia.22900
29. Halim ND, McFate T, Mohyeldin A, Okagaki P, Korotchkina LG, Patel MS, Jeoung NH, Harris RA, Schell MJ, Verma A (2010) Phosphorylation status of pyruvate dehydrogenase distinguishes metabolic phenotypes of cultured rat brain astrocytes and neurons. Glia 58:1168–1176. https://doi.org/10.1002/glia.20996
30. Bak LK, Schousboe A (2017) Misconceptions regarding basic thermodynamics and enzyme kinetics have led to erroneous conclusions regarding the metabolic importance of lactate dehydrogenase isoenzyme expression. J Neurosci Res 95:2098–2102. https://doi.org/10.1002/jnr.23994
31. Arend C, Ehrke E, Dringen R (2019) Consequences of a metabolic glucose-depletion on the survival and the metabolism of cultured rat astrocytes. Neurochem Res 44:2288–2300. https://doi.org/10.1007/s11064-019-02752-1
32. Hamprecht B, Dringen R (1994) On the role of glycogen and pyruvate uptake in astroglial-neuronal interaction. In: Krieglstein J, Oberpichler-Schwenk H (eds) Pharmacology of cerebral ischemia. Pharmacology of Cerebral Ischemia WVG, Stuttgart, pp 191–202
33. Denker N, Harders AR, Arend C, Dringen R (2023) Consumption and metabolism of extracellular pyruvate by cultured rat brain astrocytes. Neurochem Res 48:1438–1454. https://doi.org/10.1007/s11064-022-03831-6
34. Selak I, Skaper S, Varon S (1985) Pyruvate participation in the low molecular weight trophic activity for central nervous system neurons in glia-conditioned media. J Neurosci 5:23–28. https://doi.org/10.1523/JNEUROSCI.05-01-00023.1985
35. Kala G, Hertz L (2005) Ammonia effects on pyruvate/lactate production in astrocytes-interaction with glutamate. Neurochem Int 47:4–12. https://doi.org/10.1016/j.neuint.2005.04.001
36. Wang XF, Cynader MS (2001) Pyruvate released by astrocytes protects neurons from copper-catalyzed cysteine neurotoxicity. J Neurosci 21:3322–3331. https://doi.org/10.1523/JNEUROSCI.21-10-03322.2001
37. Bröer S, Schneider H-P, Bröer A, Rahman B, Hamprecht B, Deitmer JW (1998) Characterization of the monocarboxylate transporter 1 expressed in *Xenopus laevis* oocytes by changes in cytosolic pH. Biochem J 333:167–174. https://doi.org/10.1042/bj3330167
38. Dimmer K-S, Friedrich B, Lang F, Deitmer JW, Bröer S (2000) The low-affinity monocarboxylate transporter MCT4 is adapted to the export of lactate in highly glycolytic cells. Biochem J 350:219–227. https://doi.org/10.1042/bj3500219
39. Halestrap AP (2013) Monocarboxylic acid transport. Compr Physiol 3:1611–1643. https://doi.org/10.1002/cphy.c130008
40. Contreras-Baeza Y, Sandoval PY, Alarcón R, Galaz A, Cortés-Molina F, Alegría K, Baeza-Lehnert F, Arce-Molina R, Guequén A, Flores CA, San Martín A, Barros LF (2019) Monocarboxylate transporter 4 (MCT4) is a high affinity transporter capable of exporting lactate in high-lactate microenvironments. J Biol Chem 294:20135–20147. https://doi.org/10.1074/jbc.ra119.009093
41. Maus M, Marin P, Israël M, Glowinski J, Prémont J (1999) Pyruvate and lactate protect striatal neurons against N-methyl-D-aspartate-induced neurotoxicity. Eur J Neurosci 11:3215–3224. https://doi.org/10.1046/j.1460-9568.1999.00745.x
42. Miao Y, Qiu Y, Lin Y, Miao Z, Zhang J, Lu X (2011) Protection by pyruvate against glutamate neurotoxicity is mediated by astrocytes through a glutathione-dependent mechanism. Mol Biol Rep 38:3235–3242. https://doi.org/10.1007/s11033-010-9998-0
43. Desagher S, Glowinski J, Prémont J (1997) Pyruvate protects neurons against hydrogen peroxide-induced toxicity. J Neurosci 17:9060–9067. https://doi.org/10.1523/jneurosci.17-23-09060.1997
44. Lee JY, Kim YH, Koh JY (2001) Protection by pyruvate against transient forebrain ischemia in rats. J Neurosci. https://doi.org/10.1523/jneurosci.21-20-j0002.2001
45. Zilberter Y, Gubkina O, Ivanov AI (2015) A unique array of neuroprotective effects of pyruvate in neuropathology. Front Neurosci 9:17. https://doi.org/10.3389/fnins.2015.00017
46. Reinstrup P, Ståhl N, Mellergård P, Uski T, Ungerstedt U, Nordstrom CH (2000) Intracerebral microdialysis in clinical practise: baseline values for chemical markers during wakefulness, anesthesia, and neurosurgery. Neurosurgery 47:701–710. https://doi.org/10.1097/00006123-200009000-00035
47. Schulz M, Wang L, Tange M, Bjerre P (2000) Cerecral microdialysis monitoring: determination of normal and ischemic cerecral metabolism in patients with aneurysmal subarachnoid hemorrhage. J Neurosurg 93:808–814. https://doi.org/10.3171/jns.2000.93.5.0808
48. Tulpule K, Hohnholt MC, Hirrlinger J, Dringen R (2014) Primary cultures of astrocytes and neurons as model systems to study the metabolism and metabolite export from brain cells. In: Hirrlinger J, Waagepetersen H (eds) Brain energy metabolism. Springer, New York, pp 45–72
49. Petters C, Dringen R (2014) Comparison of primary and secondary rat astrocyte cultures regarding glucose and glutathione metabolism and the accumulation of iron oxide nanoparticles. Neurochem Res 39:46–58. https://doi.org/10.1007/s11064-013-1189-7
50. Lowry OH, Rosebrough NJ, Farr AL, Randall RJ (1951) Protein measurement with the folin phenol reagent. J Biol Chem 193:265–275. https://doi.org/10.1016/S0021-9258(19)52451-6
51. Clarke PM, Payton MA (1983) An enzymatic assay for acetate in spent bacterial culture supernatants. Anal Biochem 130:402–405. https://doi.org/10.1016/0003-2697(83)90607-3
52. Guarino VA, Oldham WM, Loscalzo J, Zhang YY (2019) Reaction rate of pyruvate and hydrogen peroxide: assessing antioxidant capacity of pyruvate under biological conditions. Sci Rep 9:19568. https://doi.org/10.1038/s41598-019-55951-9
53. O'Donnell-Tormey J, Nathan CF, Lanks K, Deboer CJ, De La Harpe J (1987) Secretion of pyruvate. An antioxidant defense of mammalian cells. J Exp Med 165:500–514. https://doi.org/10.1084/jem.165.2.500

54. Sameti M, Castello PR, Lanoue M, Karpova T, Martino CF (2021) Assessing bioenergetic function in response to reactive oxygen species in neural cells. React Oxyg Species 11:r14–r22
55. Choi JW, Shin CY, Yoo BK, Choi MS, Lee WJ, Han BH, Kim WK, Kim HC, Ko KH (2004) Glucose deprivation increases hydrogen peroxide level in immunostimulated rat primary astrocytes. J Neurosci Res 75:722–731. https://doi.org/10.1002/jnr.20009
56. McNaught KS, Jenner P (2000) Extracellular accumulation of nitric oxide, hydrogen peroxide, and glutamate in astrocytic cultures following glutathione depletion, complex I inhibition, and/or lipopolysaccharide-induced activation. Biochem Pharmacol 60:979–988. https://doi.org/10.1016/s0006-2952(00)00415-9
57. Vicente-Gutierrez C, Bonora N, Bobo-Jimenez V, Jimenez-Blasco D, Lopez-Fabuel I, Fernandez E, Josephine C, Bonvento G, Enriquez JA, Almeida A, Bolaños JP (2019) Astrocytic mitochondrial ROS modulate brain metabolism and mouse behaviour. Nat Metab 1:201–211. https://doi.org/10.1038/s42255-018-0031-6
58. Hirrlinger J, Hamprecht B, Dringen R (1999) Application and modulation of a permanent hydrogen peroxide-induced oxidative stress to cultured astroglial cells. Brain Res Protoc 4:223–229. https://doi.org/10.1016/s1385-299x(99)00023-9
59. Steinmeier J, Kube S, Karger G, Ehrke E, Dringen R (2020) b-Lapachone induces acute oxidative stress in rat primary astrocyte cultures that is terminated by the NQO1-inhibitor dicoumarol. Neurochem Res 45:2442–2455. https://doi.org/10.1007/s11064-020-03104-0
60. Watermann P, Dringen R (2023) β-lapachone-mediated WST1 reduction as indicator for the cytosolic redox metabolism of cultured primary astrocytes. Neurochem Res 48:2148–2160. https://doi.org/10.1007/s11064-023-03878-z
61. Barros LF, Ruminot I, Sotelo-Hitschfeld T, Lerchundi R, Fernández-Moncada I (2023) Metabolic recruitment in brain tissue. Ann Rev Physiol 85:115–135. https://doi.org/10.1146/annurev-physiol-021422-091035
62. Ovens MJ, Davies AJ, Wilson MC, Murray CM, Halestrap AP (2010) AR-C155858 is a potent inhibitor of monocarboxylate transporters MCT1 and MCT2 that binds to an intracellular site involving transmembrane helices 7–10. Biochem J 425:523–530. https://doi.org/10.1042/BJ20091515
63. Nancolas B, Richard A (2015) Identification of key binding site residues of MCT1 for AR-C155858 reveals the molecular basis of its isoform selectivity. Biochem J 466:177–188. https://doi.org/10.1042/bj20141223
64. Guan X, Rodriguez-Cruz V, Morris ME (2019) Cellular uptake of MCT1 inhibitors AR-C155858 and AZD3965 and their effects on MCT-mediated transport of L-lactate in murine 4T1 breast tumor cancer cells. AAPS J 21:13. https://doi.org/10.1208/s12248-018-0279-5
65. Halestrap AP (1976) The mechanism of the inhibition of the mitochondrial pyruvate transportater by α-cyanocinnamate derivatives. Biochem J 156:181–183. https://doi.org/10.1042/bj1560181
66. Xu L, Phelix CF, Chen LY (2021) Structural insights into the human mitochondrial pyruvate carrier complexes. J Chem Inf Model 61:5614–5625. https://doi.org/10.1021/acs.jcim.1c00879
67. Bryla J, Kaniuga Z, Slater EC (1969) Studies on the mechanism of inhibition of the mitochondrial electron transport by antimycin. III. Binding of antimycin to sub-mitochondrial particles and to complex III. Biochim Biophys Acta 189:327–336. https://doi.org/10.1016/0005-2728(69)90163-7
68. Pauwels PJ, Opperdoes FR, Trouet A (1985) Effects of antimycin, glucose deprivation, and serum on cultures of neurons, astrocytes, and neuroblastoma cells. J Neurochem 44:143–148. https://doi.org/10.1111/j.1471-4159.1985.tb07123.x
69. Kenwood BM, Weaver JL, Bajwa A, Poon IK, Byrne FL, Murrow BA, Calderone JA, Huang L, Divakaruni AS, Tomsig JL, Okabe K, Lo RH, Cameron Coleman G, Columbus L, Yan Z, Saucerman JJ, Smith JS, Holmes JW, Lynch KR, Ravichandran KS, Uchiyama S, Santos WL, Rogers GW, Okusa MD, Bayliss DA, Hoehn KL (2014) Identification of a novel mitochondrial uncoupler that does not depolarize the plasma membrane. Mol Metab 3:114–123. https://doi.org/10.1016/j.molmet.2013.11.005
70. San Martín A, Ceballo S, Baeza-Lehnert F, Lerchundi R, Valdebenito R, Contreras-Baeza Y, Alegría K, Barros LF (2014) Imaging mitochondrial flux in single cells with a FRET sensor for pyruvate. PLoS ONE 9:e85780. https://doi.org/10.1371/journal.pone.0085780
71. Mellergård P, Ouyang Y-B, Siesjö BK (1994) The regulation of intracellular pH is strongly dependent on extracellular pH in cultured rat astrocytes and neurons. In: Ito U, Baethmann A, Hossmann KA, Kuroiwa T, Marmarou A, Reulen HJ, Takakura K (eds) Brain edema IX. Springer, Vienna
72. Bröer S, Rahman B, Pellegri G, Pellerin L, Martin J-L, Verleysdonk S, Hamprecht B, Magistretti PJ (1997) Comparison of lactate transport in astroglial cells and monocarboxylate transporter 1 (MCT 1) expressing *Xenopus laevis* oocytes. J Biol Chem 272:30096–30102. https://doi.org/10.1074/jbc.272.48.30096
73. Dringen R, Hamprecht B (1998) Glutathione restoration as indicator for cellular metabolism of astroglial cells. Dev Neurosci 20:401–407. https://doi.org/10.1159/000017337
74. Wiesinger H, Thiess U, Hamprecht B (1990) Sorbitol pathway activity and utilization of polyols in astroglia-rich primary cultures. Glia 3:277–282. https://doi.org/10.1002/glia.440030407
75. Dringen R, Bergbauer K, Wiesinger H, Hamprecht B (1994) Utilization of mannose by astroglial cells. Neurochem Res 19:23–30. https://doi.org/10.1007/BF00966724
76. Bergbauer K, Dringen R, Verleysdonk S, Gebhardt R, Hamprecht B, Wiesinger H (1996) Studies on fructose metabolism in cultured astroglial cells and control hepatocytes: lack of fructokinase activity and Immunoreactivity in astrocytes. Dev Neurosci 18:371–379. https://doi.org/10.1159/000111430
77. Zwingmann C, Richter-Landsberg C, Leibfritz D (2001) ^{13}C isotopomer analysis of glucose and alanine metabolism reveals cytosolic pyruvate compartmentation as part of energy metabolism in astrocytes. Glia 34:200–212. https://doi.org/10.1002/glia.1054
78. Baytas O, Davidson SM, Deberardinis RJ, Morrow EM (2022) Mitochondrial enzyme GPT2 regulates metabolic mechanisms required for neuron growth and motor function in vivo. Hum Mol Genet 31:587–603. https://doi.org/10.1093/hmg/ddab269
79. Erecińska M, Deas J, Silver IA (1995) The effect of pH on glycolysis and phosphofructokinase activity in cultured cells and synaptosomes. J Neurochem 65:2765–2772. https://doi.org/10.1046/j.1471-4159.1995.65062765.x
80. Theparambil SM, Weber T, Schmälzle J, Ruminot I, Deitmer JW (2016) Proton fall or bicarbonate rise. Glycolytic rate in mouse astrocytes is paved by intracellular alkalinization. J Biol Chem 291:19108–19117. https://doi.org/10.1074/jbc.m116.730143
81. Granholm L (1969) The effect of blood in the CSF on the CSF lactate, pyruvate and bicarbonate concentrations. Scand J Clin Lab Invest 23:361–366. https://doi.org/10.3109/00365516909081702
82. Benoist J-FO, Alberti C, Leclercq S, Rigal O, Jean-Louis R, Ogier De Baulny HL, Porquet D, Biou D (2003) Cerebrospinal fluid lactate and pyruvate concentrations and their ratio in children: age-related reference intervals. Clin Chem 49:487–494. https://doi.org/10.1373/49.3.487
83. Zhang W-M, Natowicz MR (2013) Cerebrospinal fluid lactate and pyruvate concentrations and their ratio. Clin Biochem 46:694–697. https://doi.org/10.1016/j.clinbiochem.2012.11.008

Modulation of pyruvate export and extracellular pyruvate concentration in primary astrocyte cultures

Nadine Denker and Ralf Dringen

Supporting Information

Figure S1

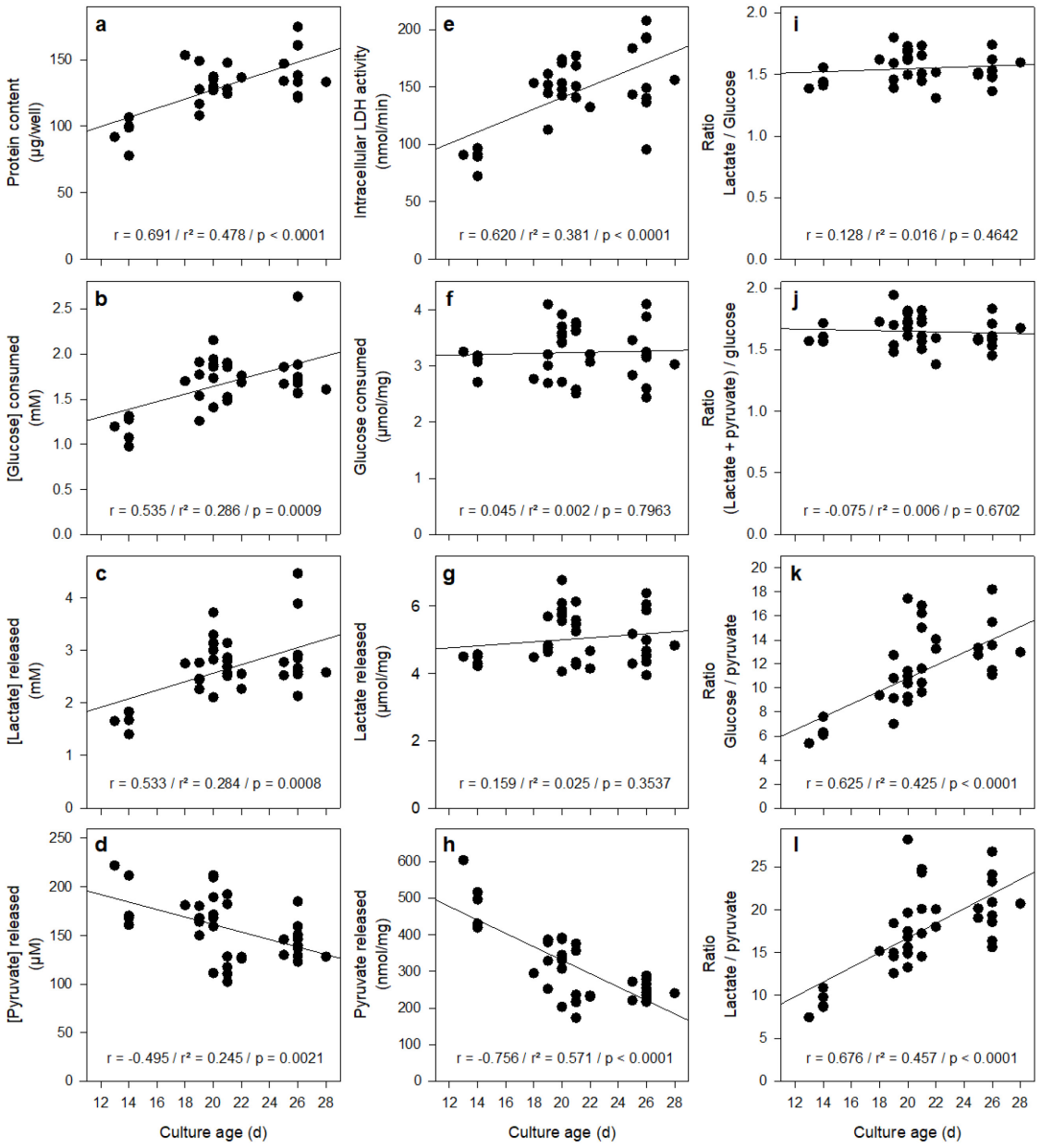

Figure S1: Effect of culture age on glucose consumption and the release of lactate and pyruvate from astrocytes. Primary astrocyte cultures were incubated in an incubation medium containing 5 mM of glucose for 5 h. Afterwards, the respective initial protein contents (a), the initial cellular LDH activities (e). the glucose consumption in mM (b) as well as the extracellular concentrations of lactate (c) and pyruvate (d) were determined. Panels f, g and h give the specific values for the glucose consumption (f) and the extracellular accumulations of

lactate (g) or pyruvate (h). The data obtained were used to calculate the ratios of lactate release to the glucose consumption (i), the ratio of the sum of pyruvate plus lactate release to glucose consumption (j), the ratio of glucose consumption to pyruvate release (k) and the ratio of lactate release to pyruvate release (l). The data are derived from a total of 36 experiments performed on 25 independently prepared cultures. Each data point represents the result of one individual experiment. Lines in the panels are derived from first order regression analyses of the data obtained and the respective correlation parameters are given in the individual panels.

Figure S2

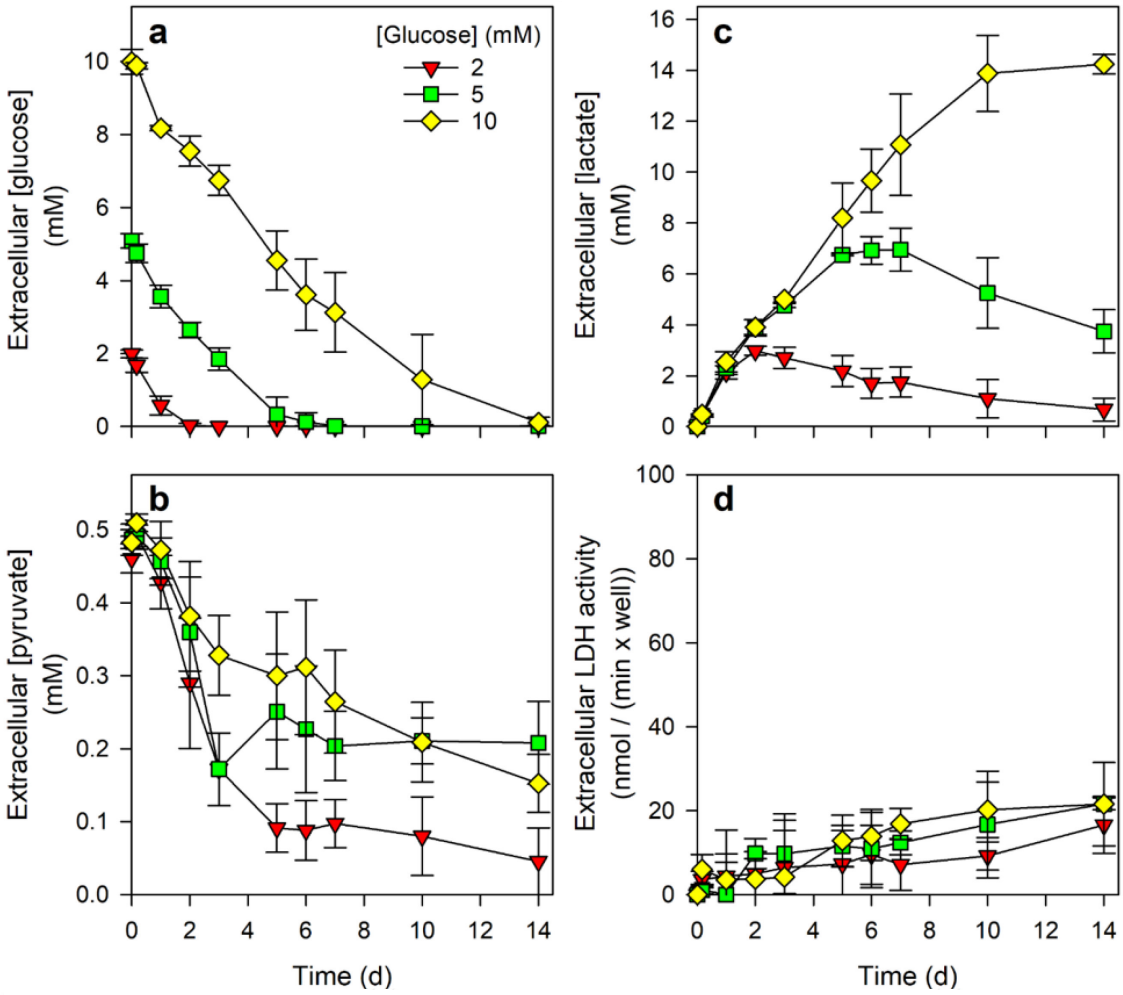

Figure S2: Glucose consumption and extracellular concentrations of pyruvate and lactate in pyruvate-treated primary astrocyte cultures. Astrocyte cultures were incubated with serum-free DMEM that contained pyruvate in an initial concentration of 0.5 mM and glucose in the initial concentrations indicated in panel a for up to 14 days. The extracellular concentrations of glucose (a), pyruvate (b) and lactate (c) as well as the extracellular LDH activity (d) were measured for the indicated time points. The initial cellular LDH activity of the cultures at the onset of the incubation (100%) was 106 ± 19 nmol/(min x well) and the initial protein content was 121 ± 55 µg/well. The data presented are means ± SD of data obtained in three individually performed experiments on independently prepared cultures.

Figure S3

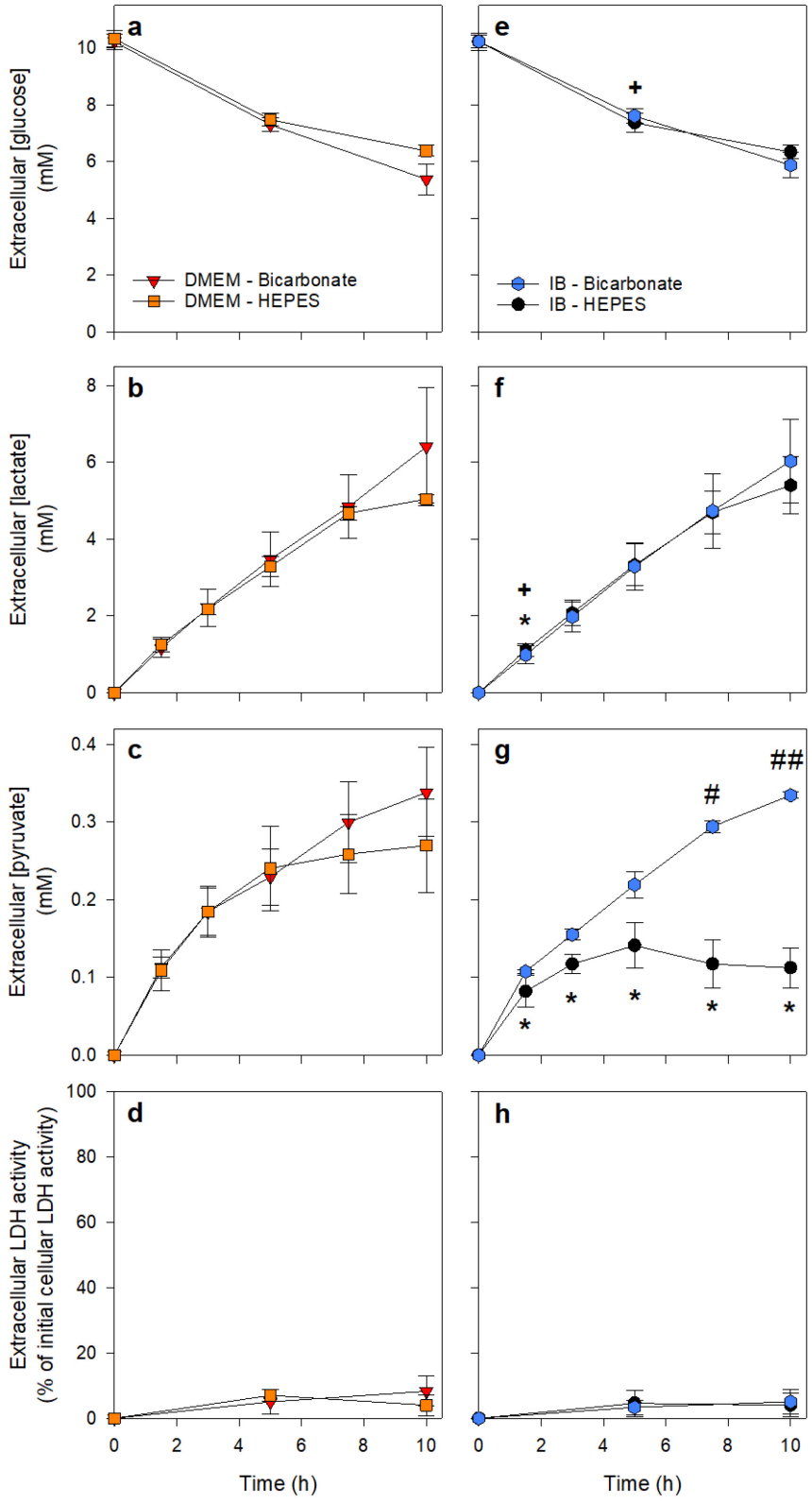
a
e
b
f
c
g
d
h
Extracellular [glucose] (mM)
Extracellular [lactate] (mM)
Extracellular [pyruvate] (mM)
Extracellular LDH activity (% of initial cellular LDH activity)
DMEM - Bicarbonate
DMEM - HEPES
IB - Bicarbonate
IB - HEPES
Time (h)
Time (h)

Figure S3: Glucose consumption and accumulation of pyruvate and lactate in different incubation buffers. Primary rat astrocyte cultures were incubated with 10 mM glucose for up to 10 h in incubation buffer (145 mM NaCl, 5.4 mM KCl, 1.8 mM $CaCl_2$, 1 mM $MgCl_2$, 0.8 mM Na_2HPO_4) that had been buffered at 37°C to pH 7.4 with 20 mM HEPES/NaOH (IB-HEPES) or with 44.6 mM sodium bicarbonate/10% CO_2 (containing 40 µM phenol red as pH indicator; IB-Bicarbonate). In addition, cultures were incubated in pyruvate-free DMEM that had been buffered either with 20 mM HEPES/NaOH (DMEM-HEPES) or with 44.6 mM sodium bicarbonate/10% CO_2 (DMEM-Bicarbonate). The incubations in bicarbonate-buffered solutions were performed at 37°C in an incubator providing 10% CO_2, while incubations in HEPES-buffered solutions were performed at 37°C in an incubator without CO_2 supply. For the indicated incubation periods, the extracellular concentrations of glucose (a, e), lactate (b, f) and pyruvate (c, g) as well as the extracellular activity of LDH (d, h) were determined. The initial protein content of the cultures was 136 ± 7 µg/well and the initial cellular LDH activity was 209 ± 22 nmol/(min x well). The significance of difference (paired t-test) between values obtained for incubations in HEPES- and bicarbonate-buffered IB (e-h) is indicated by $^{\#}p<0.05$ and $^{\#\#}p<0.01$, that between bicarbonate-buffered DMEM (a-d) and bicarbonate-buffered IB (e-f) by $^{+}p<0.05$ and that between HEPES-buffered DMEM (a-d) and HEPES-buffered IB (e-h) is indicated by $^{*}p<0.05$. No significant differences ($p<0.05$) were observed for the data obtained for incubations with HEPES- and bicarbonate-buffered DMEM (a-d).

Figure S4

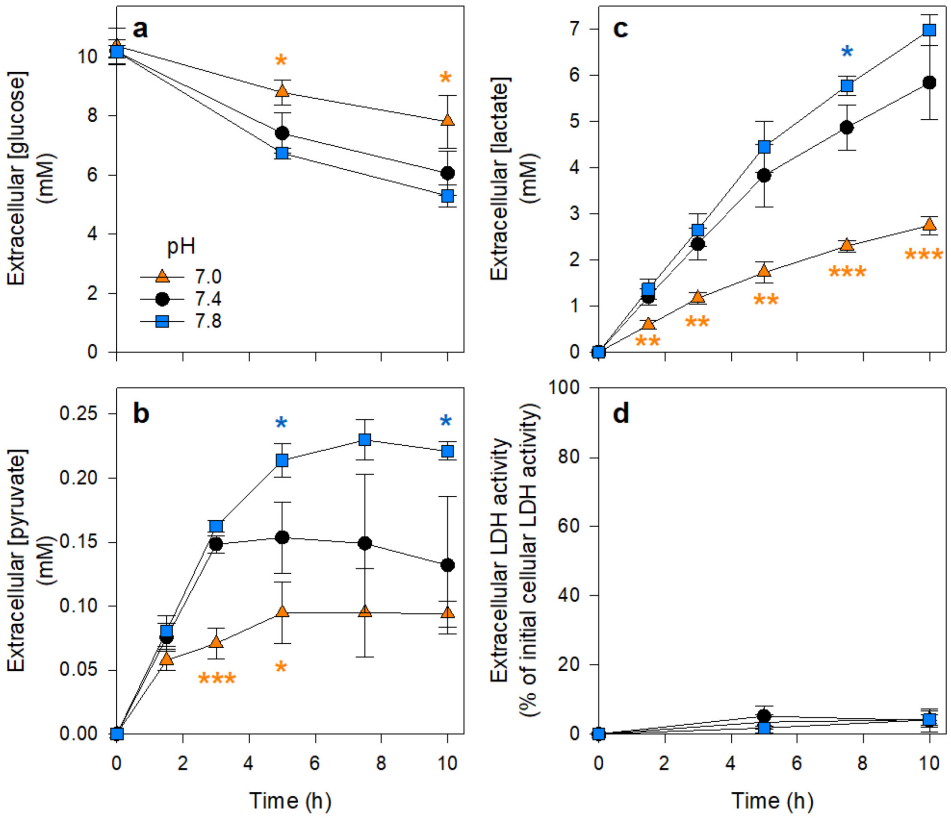

Figure S4: Glucose consumption and extracellular pyruvate and lactate accumulation in incubation buffers of different pH values. Astrocytes were incubated for up to 10 h in HEPES-buffered incubation buffers (containing 10 mM glucose) that had been adjusted to the pH values 7.0, 7.4 or 7.8. After the indicated time points, the extracellular concentrations of glucose (a), pyruvate (b) and lactate (c) as well as the extracellular LDH activity (d) were determined. The initial cellular LDH activity of the cultures was 224 ± 19 nmol/(min x well) and the initial protein content was 158 ± 19 µg/well. The significance of differences (ANOVA) compared to the values obtained for the control condition (pH 7.4) is indicated by $^{*}p<0.05$, $^{**}p<0.01$ and $^{***}p<0.001$.

3 Summarizing discussion

The data presented in this thesis demonstrate that astrocytes are able to consume and release pyruvate. Despite pyruvate being a potent substrate for astrocytic energy production (Harders *et al.* 2023, Harders *et al.* 2024), it appears that glucose-fed astrocyte cultures release pyruvate dependent on their intracellular pyruvate concentration and establish an equilibrium between the intracellular and extracellular pyruvate concentrations. Similarly, glucose-deprived astrocytes showed an accelerated or repressed consumption of extracellularly applied pyruvate depending on their capacity to utilize cellular pyruvate which was also dependent on the intracellular pyruvate concentration. The intracellular concentration is likely to be influenced by the availability of other metabolic substrates, either for pyruvate or for energy production, by the redox status of the cells (especially by the NAD^+/NADH ratio), as well as by intracellular compartmentation between cytosol and mitochondria (**Fig. 3-1**).

3.1 Astrocytes and pyruvate

Astrocytes that are provided with pyruvate as exclusive energy substrate consume all extracellular pyruvate. In contrast, astrocytes that are maintained in a glucose-containing environment establish a transient extracellular steady state concentration of around 150 - 300 µM pyruvate, depending on the incubation medium. This concentration is probably dependent on the intracellular pyruvate concentration and is established as the external pyruvate concentration adjusts to the cytosolic pyruvate concentration. In accordance with this observation, it was demonstrated that astrocytes incubated with varying extracellular volumes established similar extracellular steady-state concentrations in low and in high incubation volumes due to a prolonged release of a greater absolute quantity of pyruvate in larger volumes (**Figure S1**).

When comparing rates of pyruvate consumption and release, the maximal pyruvate consumption rate (300 nmol / h x mg protein) was found to be 5 times higher than the maximal pyruvate release rate (60 nmol / h x mg protein) for astrocyte cultures in HEPES-buffered incubation buffer. However, it is important to consider that the high consumption

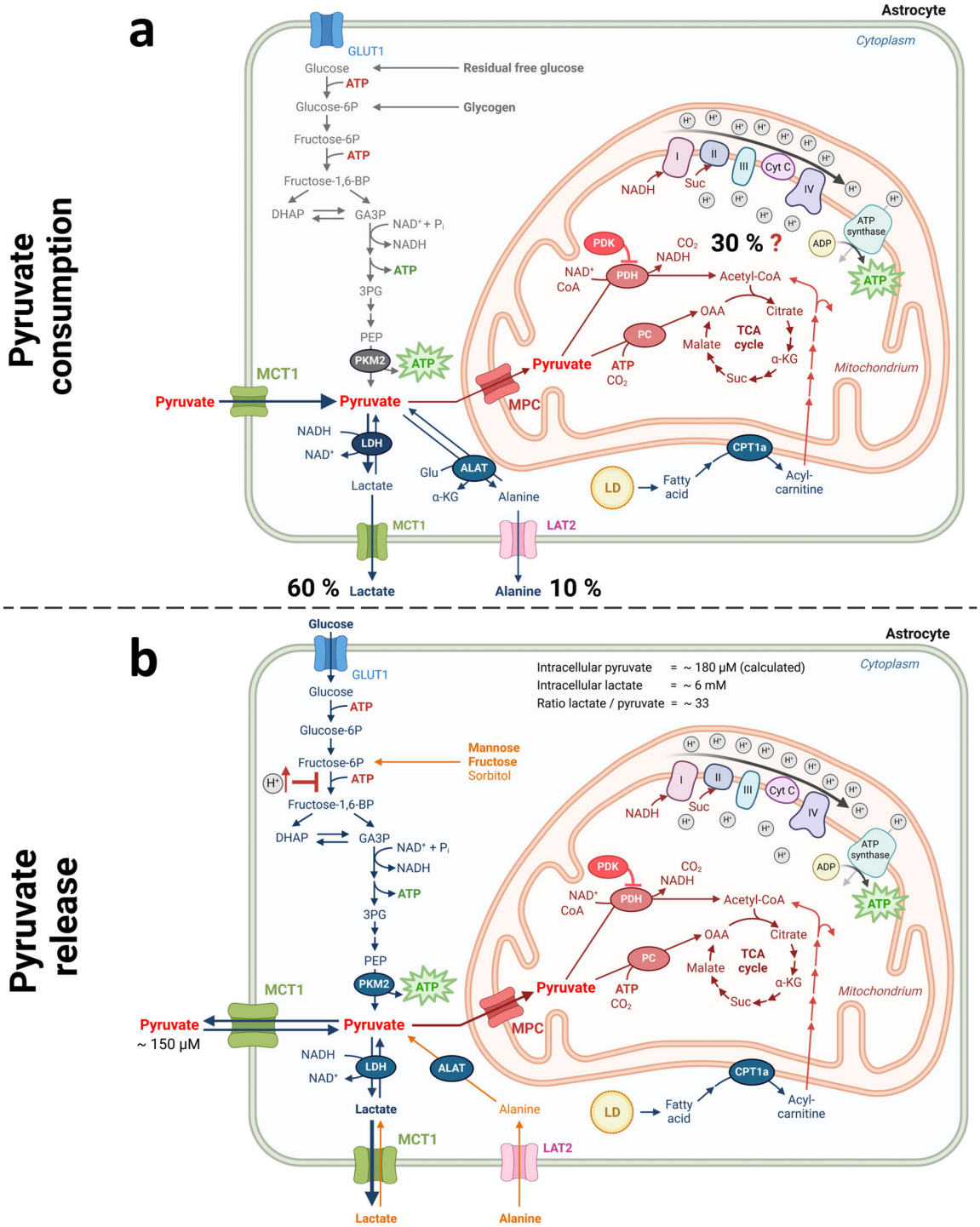

Figure 3-1: Pyruvate consumption and glucose-dependent pyruvate release of primary astrocytes cultures under control conditions (HEPES-buffered incubation buffer). This figure illustrates important pathways and processes involved in pyruvate consumption (**a**) and release (**b**). To emphasize the subordinate role of glycolysis in glucose-deprived astrocytes (a), the reactions involved are colored gray. In orange, additional substrates that resulted in extracellular pyruvate accumulation are indicated. Acetyl-CoA = acetyl coenzyme A; ALAT = alanine amino transaminase; CoA = coenzyme A; CPT1a = carnitine palmitoyltransferase 1A; DHAP = dihydroxyacetonephosphate; Glu = glutamate; GLUT1 = glucose transporter 1; α-KG = α-ketoglutarate; LAT2 = L-type amino acid transport 2; LD = lipid droplet LDH = lactate dehydrogenase; MCT1 = monocarboxylate transporter 1; MPC = mitochondrial pyruvate carrier; OAA = oxaloacetate; PC = pyruvate carboxylase; PDC = pyruvate dehydrogenase complex; 3PG = 3-phosphoglycerate; P_i = inorganic phosphate; PKM2 = pyruvate kinase M2; Suc = succinate; Created with Biorender.

rate was measured for glucose-deprived astrocytes and that pyruvate was the only extracellular energy substrate added for such incubations. Although astrocytes cultures have been demonstrated to maintain their cellular energy stores even in the absence of glucose over the investigated 5 h time period (Harders *et al.* 2023, Karger *et al.* 2024), such malnutrition quickly depletes intracellular pyruvate levels (San Martín *et al.* 2014) and alternative endogenous energy substrate reservoirs (Dringen *et al.* 1993, Cabodevilla *et al.* 2013). Consequently, astrocytes favor a rather rapid uptake of the substrate pyruvate in glucose-free conditions, eventually consuming all available pyruvate as nutrient source. The importance of externally applied pyruvate as a mitochondrial energy substrate was emphasized by the finding that both MPC inhibition by UK5099 as well as complex III inhibition by antimycin A strongly impaired pyruvate consumption.

The different velocities for consumption and release are likely also related to the varying pyruvate concentrations present for import and export. Maximal pyruvate consumption occurs at extracellular pyruvate concentrations exceeding 2 mM, whereas the intracellular pyruvate concentration in glucose-fed astrocytes is likely to be significantly lower, approximating that of the extracellular steady-state concentration. This may suggest the existence of residual velocity capacity for pyruvate export at higher intracellular pyruvate concentrations. Accordingly, inhibition of mitochondrial pyruvate consumption by UK5099, which increases the intracellular pyruvate concentration by blocking mitochondrial pyruvate utilization (Arce-Molina *et al.* 2020), did increase the initial rate of pyruvate release in glucose-fed astrocytes by around 60 %, which persisted for at least 10 h (**Table 3-1; Fig. S2**). This increased pyruvate release supports the view that export might not be at maximal capacity under control conditions in HEPES-buffered glucose-containing incubation buffer. Whether different import and export kinetics of pyruvate transport contribute to the different velocities, analog to how it was reported for lactate import and export based on intracellular and extracellular ^{13}C-lactate pools produced by prostate cancer cells from ^{13}C-pyruvate (Breukels *et al.* 2015), cannot be assessed as the intracellular pyruvate concentration remains to be elucidated. But, an inhibition of pyruvate export by the estimated 30 - 40-fold higher intracellular lactate concentration (6 mM) is likely to also affect the export rate of pyruvate by MCT1, analogous to the impairment by a two-fold and ten-fold extracellular lactate concentration shown for pyruvate import (**Table 3-1**).

Furthermore, a modification of the extracellular environment by altering the incubation buffer composition to the more complex pyruvate-free DMEM or/and by substituting HEPES

Table 3-1: Comparison of important results on pyruvate consumption and release by primary astrocyte cultures. This table highlights the effects of various pharmacological modulators or incubation conditions on pyruvate consumption and pyruvate release compared to the respective control condition (astrocytes incubated in incubation buffer containing 20 mM HEPES, 145 mM NaCl, 5.4 mM KCl, 1,8 mM $CaCl_2$, 1 mM $MgCl_2$, 0,8 mM Na_2HPO_4, pH 7.4; containing either 0.5 mM pyruvate or 5/10 mM glucose). The pyruvate consumption rate in control conditions (100 %) ranged between 110 - 180 nmol/h x mg protein (mean = 138 nmol/h x mg protein). The extracellular pyruvate concentration of glucose-fed astrocytes (100 %) ranged between 120 µM - 190 µM (mean = 142 µM) and the release rate of pyruvate (100 %) was around 70 nmol/ h x mg protein. $Pyruvate_{extra}$ = extracellular pyruvate; $lactate_{extra}$ = extracellular lactate.

		Pyruvate consumption	Pyruvate release	
	Chapter	2.1	2.2	
	Presence of glucose	no	yes	
Effect of treatment in comparison to control in HEPES-buffered incubation buffer (100%)		Consumption rate (during linear range)	$Pyruvate_{extra}$ (after 5 h)	Release rate (during first 3 h)
	AR-C155858 (MCT1 inhibitor)	**20 %** (Chapter 2.1 - Fig.3)	**20 %** (Chapter 2.2 - Fig. 6)	-
	UK5099 (MPC inhibitor)	**30 %** (Chapter 2.1 - Fig.5)	**220 %** (Chapter 2.2 - Fig. 6)	**160 %** (Chapter 4 - Fig. S2)
	Antimycin A (Complex III inhibitor)	**0 % (time-delayed)** (Chapter 2.1 - Fig. 7)	**0 %** (Chapter 2.2 - Fig. 7)	-
	BAM15 (mitochondrial uncoupler)	**280 %** (Chapter 2.1 - Fig. 7)	**10 %** (Chapter 2.2 - Fig. 7)	-
	Etomoxir (CPT1a inhibitor)	**accelerated** (preliminary, data not shown)	**50 %** (Chapter 4 - Fig. S6)	-
	5 mM $lactate_{extra}$	**20 %** (Chapter 2.1 - Fig.3)	**120 %** (Chapter 2.2 - Fig. 5)	-
	Bicarbonate-buffered incubation buffer	**no effect** (preliminary, data not shown)	**160 %** (Chapter 2.2 - Fig. S3)	**130 %** (Chapter 2.2 - Fig. S3)
	HEPES-buffered pyruvate-free DMEM	**no effect** (preliminary, data not shown)	**170 %** (Chapter 2.2 - Fig. S3)	**160 %** (Chapter 2.2 - Fig. S3)
	Bicarbonate-buffered pyruvate-free DMEM	**180 %** (Chapter 4 - Fig. S3)	**170 %** (Chapter 2.2 - Fig. S3)	**160 %** (Chapter 2.2 - Fig. S3)

by bicarbonate as an alternative buffer substance increased the astrocytic pyruvate release rate as well as the extracellular pyruvate accumulation after 5 h (**Table 3-1**). However, the equilibration process leading to the extracellular steady-state pyruvate concentration, that is each approximately 2.5- to 3-fold higher than in HEPES-buffered medium, appeared to take longer, with a minimum of 10 h required (see **Chapter 2. - Fig. S3**). The extracellular pyruvate level appears to be slightly more elevated when bicarbonate is present, relative to data from similar incubations in an amino acid and vitamin-containing but bicarbonate-free medium. Interestingly, also pyruvate consumption was accelerated when astrocytes were presented with pyruvate in bicarbonate-buffered DMEM (**Fig. S3**). However, unlike pyruvate release, pyruvate consumption did not appear to be altered by changing only the buffer substance (HEPES to bicarbonate) or the buffer complexity (physiological salt solution to DMEM) (**Table 3-1**). Possibly, employing a physiological bicarbonate buffering system may enhance the capacity of the intracellular buffering system, since bicarbonate can enter astrocytes, mainly facilitated by the electrogenic Na^+/HCO_3^- cotransporter (NBCe1) that enables the bidirectional symport of bicarbonate and Na^+ (Deitmer *et al.* 2019). Additionally, astrocytes were shown to express cytosolic carbonic anhydrase II that facilitates a fast conversion of bicarbonate to CO_2 (Deitmer *et al.* 2019), thereby trapping protons (**Fig. 3-2**).

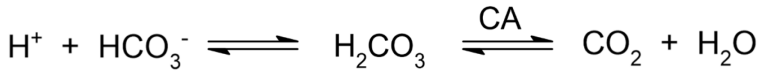

Figure 3-2: Reversible spontaneous and carbonic anhydrase (CA)-mediated conversion of bicarbonate (HCO_3^-) and CO_2. Created with ChemSketch.

An elevated cellular buffering capacity has the ability to more efficiently prevent cellular acidification that can occur from pyruvate and subsequent lactate production via glycolysis (Barros *et al.* 2021, Daverio *et al.* 2023). The activity of the glycolytic enzyme 6-phosphofructokinase-1 (PFK1) depends on the intracellular pH, and is inhibited by high proton concentration (**Fig. 3-1**) (Trivedi and Danforth 1966, Erecińska *et al.* 1995). Therefore, astrocytes incubated in a bicarbonate-containing buffer might utilize glucose more efficiently in glycolysis and consequently increase their pyruvate production and release. However, it is important to note that intracellular alkalization by bicarbonate might also slow pyruvate export by limiting proton availability for export via MCT1, a proton co-transporter (Bröer *et al.* 1998). In contrast, this increased intracellular buffer capacity by bicarbonate might contribute to an increased pyruvate consumption. Because of the proton-coupled import, an intracellular interception of protons by an improved buffer capacity may

improve the transport efficiency. Supporting this hypothesis, it has been demonstrated that astrocytes derived from human induced pluripotent stem cells cultured in bicarbonate-containing medium exhibit a higher intracellular pH compared to astrocytes in HEPES-containing medium (Yao *et al.* 2016). However, given that the exclusive alteration of the buffer system did not result in a change of pyruvate consumption, or alternatively, that the single change of the complexity of the buffer system exerted an influence on the pyruvate release, it can be postulated that the underlying mechanisms are likely to be more multifaceted. DMEM contains a variety of amino acids and vitamins, with glutamine being the most abundant. Astrocytes in culture have been shown to contain glutaminase (Cardona *et al.* 2015), which enables them to deaminate glutamine to glutamate. Astrocytes have been shown to produce lactate from glutamine and glutamate via pyruvate recycling (Sonnewald *et al.* 1996, Westergaard *et al.* 1996). Consequently, pyruvate derived from glutamine could also contribute to the increased extracellular pyruvate concentration for the experimental conditions applied, although this remains to be elucidated. Overall these findings highlight the fascinating complexity of cellular mechanisms, and the importance to thoroughly evaluate the experimental conditions used, as both pyruvate release and consumption seem to be influenced by the extracellular environment.

Since glucose is the preferred energy substrate of the brain (Dienel 2019), astrocyte cultures incubated in glucose-rich medium produced lactate from glycolytically-derived pyruvate and released, as expected, millimolar concentrations of lactate, whereas glucose- and pyruvate-deprived astrocytes released lactate only to low micromolar concentrations. This lactate likely originates from glycogen, which is known to be present in astrocytes and to quickly degrade under glucose deprivation (Dringen *et al.* 1993, Markussen *et al.* 2023). Potentially, there is an additional contribution of lactate derived from residual free intracellular glucose present at the onset of the incubation (Blumrich *et al.* 2016), since the cells come from a high glucose environment (DMEM, 25 mM glucose). It could be shown that astrocytes also produce a substantial amount of lactate from pyruvate consumed in the absence of glucose (**Chapter 2.1**). This is striking, as the glycolytic NADH production necessary for pyruvate reduction by LDH (Dienel 2019) is limited with only pyruvate as extracellularly applied substrate. Nonetheless, as expected, this lactate production was significantly lower compared to glucose-rich conditions. As discussed in Chapter 2.1, the reversible malate-aspartate shuttle (MAS) might facilitate the provision of cytosolic NADH from mitochondrially derived NADH. Unfortunately, attempts to elucidate the role of the MAS in LDH-mediated lactate production from pyruvate by applying the inhibitor aminooxy

acetate were unsuccessful. Aminooxy acetate, a non-specific inhibitor of aminotransferases (John and Charteris 1978), that is often used to elucidate a potential contribution of the malate-aspartate shuttle (Chen *et al.* 2015, Wang *et al.* 2016), severely lowered the pyruvate concentration present in the incubation medium cell-independently (data not shown). This observed disappearance of pyruvate is most likely caused by quick formation of methoxamate adducts of aminooxy acetate with pyruvate (Yang *et al.* 2008).

By application of the antioxidative enzymes SOD and catalase, it was demonstrated that the established extracellular pyruvate levels are not influenced by cell-derived H_2O_2, that chemically oxidizes pyruvate to acetate (Guarino *et al.* 2019). For astrocytes fed with pyruvate, no extracellular acetate release was measurable. Given the one to one stoichiometry of the reaction of pyruvate to acetate induced by H_2O_2 (**Fig. S4**), it is also unlikely for pyruvate oxidation by H_2O_2 to substantially contribute to the disappearance of pyruvate from the extracellular medium.

3.2 Plasma membrane pyruvate transport

Astrocytes have been shown to express the high affinity proton-coupled monocarboxylate transporter 1 (Bröer *et al.* 1997), as well as the low affinity proton-coupled monocarboxylate transporter 4 (Dimmer *et al.* 2000). Pyruvate transport by MCT1 expressed in *Xenopus laevis* oocytes was found to exhibit a K_M value of 1 mM (Bröer *et al.* 1998), and this value fits well with kinetic data obtained for initial transport of ^{14}C-labelled pyruvate by astrocyte cultures (Hamprecht and Dringen 1994). By inhibiting MCT1 with the specific inhibitor AR-C155858 (Ovens *et al.* 2010), it was shown that MCT1 is indeed the main transporter involved in pyruvate transport over the plasma membrane (**Fig. 3-1**). For both consumption and release of pyruvate, inhibition of MCT1 by AR-C155858 resulted in a strong inhibition by around 80 %, highlighting that MCT1 is the main transporter involved in both processes. In contrast, AZD0095-mediated inhibition of MCT4, for which a K_M value of around 4 mM for pyruvate has recently been described (Contreras-Baeza *et al.* 2019), had, as expected, no effect on the pyruvate release (**Fig. S5**), since the estimated intracellular pyruvate concentration (around 150 µM) is far below this K_M value of MCT4 (Contreras-Baeza *et al.* 2019).

Despite a reduction in glucose consumption resulting from MCT1 inhibition, likely due to a cytosolic acidification and subsequent inhibition of glycolysis (Trivedi and Danforth 1966,

Erecińska *et al.* 1995), a considerable amount of lactate was still released. Intracellular lactate accumulation has been demonstrated for MCT1-inhibited glucose-fed astrocytes (Lerchundi *et al.* 2015). Astrocytic MCT4 is considered a transporter with reserve capacity for lactate export upon intracellular lactate accumulation (Halestrap 2013, Contreras-Baeza *et al.* 2019). Accordingly, while inhibition of MCT1 and MCT4 did not have an additive inhibitory effect on pyruvate export, simultaneous inhibition further decreased but yet did not abolish lactate export (**Fig. S6**), indicating a compensatory effect of MCT4 for inhibited lactate, but not pyruvate export by astrocyte cultures. This fits well to the proposed better kinetic parameters for lactate transport by MCT4 (Contreras-Baeza *et al.* 2019, Felmlee *et al.* 2020), as well as to the estimated substantially higher intracellular lactate concentration. In contrast, exclusive MCT4 inhibition also did not alter the lactate release, further indicating that both pyruvate and lactate compete for export via MCT1 under normal conditions. Residual import and export of lactate and of those small amounts of pyruvate released under MCT1 and MCT4 inhibition might be facilitated by connexin hemichannels. These have been described to contribute to astrocytic lactate and gliotransmitter release (Karagiannis *et al.* 2016, Linsambarth *et al.* 2022), and to physiologically form gap junctions for substrate distribution throughout the brain (Orthmann-Murphy *et al.* 2008). Furthermore, anion channels, that have been described to release lactate upon K^+-mediated cell depolarization (Sotelo-Hitschfeld *et al.* 2015), might contribute to residual lactate export. However, given that the astrocytes were incubated in a buffer containing a physiological salt composition, it can be concluded that these play at best a minor role in the MCT independent lactate release under the conditions used in the current study.

A two-fold excess of extracellular lactate lowered pyruvate consumption of glucose-deprived cells by 30 %, while a ten-fold excess had a strong impact and lowered the pyruvate consumption by 80 % (**Table 3-1**). In contrast, application of 5 mM lactate in the presence or in the absence of glucose only increased the extracellular pyruvate accumulation by 20 %. In the case of pyruvate uptake, it is likely that the inhibition occurs via classic competition for import by MCT1, as it has also been demonstrated for a 500-fold excess of pyruvate over lactate (Bröer *et al.* 1997). With regard to export, the transporters involved might have been cross-stimulated (Dimmer *et al.* 2000, Mächler *et al.* 2016), resulting in the acceleration of pyruvate export by a directly preceding import of extracellularly presented lactate. However, this effect could not be demonstrated for astrocytes in a glucose-rich but initially lactate-free environment, where extracellular lactate concentration reached 5 mM after approximately 7.5 h. Nonetheless, lactate export possibly still dominated at this time (**Fig.**

3-1). Therefore, a genuine comparison with a situation in which lactate is predominantly taken up is challenging. Furthermore, the increased pyruvate accumulation under lactate administration is more likely to be explained by an altered intracellular pyruvate concentration, as pyruvate and lactate are in a direct equilibrium with each other via LDH. While this equilibrium is clearly on the side of reduction (Dienel 2017), i.e., lactate production, intracellular lactate concentrations were shown for various cell types to increase after lactate administration (Contreras-Baeza *et al.* 2019). Assuming a constant NAD^+/NADH ratio and intracellular pH (Christensen *et al.* 2014), a higher intracellular lactate concentration should also result in a higher intracellular pyruvate concentration. Given the establishment of an equilibrium between the intracellular and extracellular pyruvate concentration, this higher intracellular pyruvate concentration in turn results in a higher extracellular pyruvate level.

3.3 Mitochondrial pyruvate transport and metabolism

Impairment of the plasma membrane transport of pyruvate by inhibition of MCT1 almost completely abolished both pyruvate consumption and release. In contrast, inhibition of mitochondrial pyruvate uptake by the MPC-inhibitor UK5099 strongly decreased pyruvate consumption, while it strongly accelerated pyruvate release of glucose-fed astrocytes (**Table 3-1, Fig 3-3**). Since UK5099 presumably increases the cytosolic pyruvate concentration by blocking mitochondrial pyruvate uptake (Arce-Molina *et al.* 2020), both phenomena can be explained by this mechanism. On the one hand, it is reasonable to conclude that the cytosolic pyruvate accumulation resulting from the inability of astrocytes to metabolize extracellularly applied pyruvate in mitochondria decreased additional pyruvate uptake. On the other hand, due to the increased intracellular concentration and constant further production of pyruvate from glucose, it is probable that this caused the significantly increased linear export of pyruvate (**Fig. S2**), as discussed above. The sustained high extracellular pyruvate concentration as well as the markedly elevated pyruvate release both demonstrate the pivotal role of mitochondrial pyruvate utilization in pyruvate metabolism of astrocytes.

Glucose consumption and lactate release, in contrast, were not influenced by low UK5099 concentrations that specifically inhibit MPC (**Fig. 3-3b**) (Halestrap 1975, Carpenter and Halestrap 1994, Hildyard *et al.* 2005), indicating that the cellular energy charge is not

impaired by an inhibited mitochondrial pyruvate uptake, as seen by the absence of accelerated glycolytic flux (Almeida *et al.* 2004, Voss *et al.* 2020). Accordingly, the

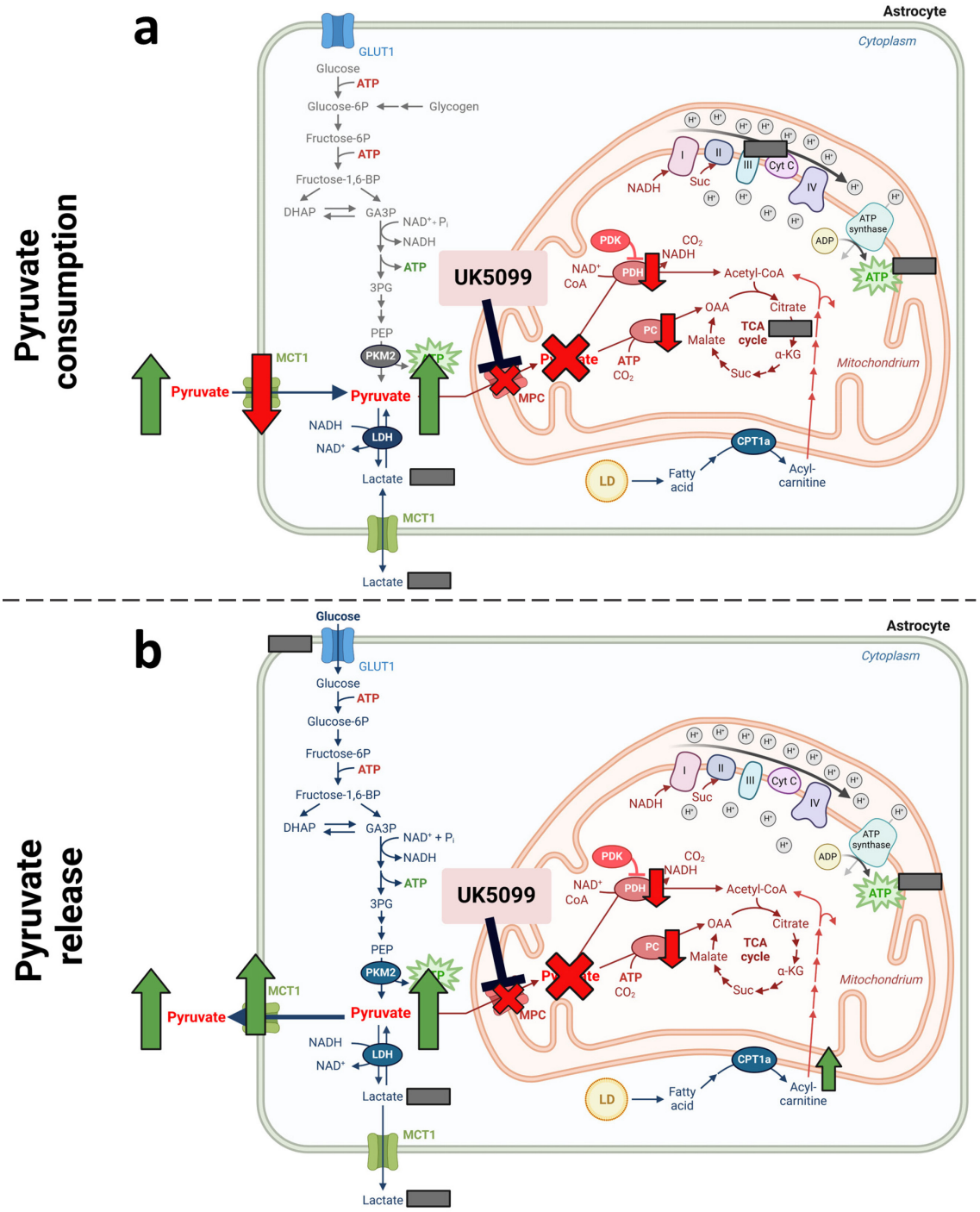

Figure 3-3: The postulated effect of the MPC inhibitor UK5099 on astrocytic pyruvate and energy metabolism. This figure illustrates the effect of UK5099, an MPC inhibitor, on different pathways and metabolites involved in pyruvate and energy metabolism. Pyruvate consumption (**a**) and pyruvate release (**b**) are shown separately. For glucose-deprived astrocytes(**a**), the reactions involved in glycolysis are colored in grey to highlight their subordinate role under these circumstances. The green arrows indicate an increase of concentrations of metabolites and transport compared to control conditions (without inhibitor), while the red arrows indicate a decrease of transport and enzyme activities. The red crosses symbolize a block of transport and the depletion of mitochondrial pyruvate. The grey squares indicate unchanged conditions. Created with Biorender.

application of UK5099 was confirmed to have no influence on the ATP level of glucose-fed astrocytes (**Fig. S6**). Even in the absence of glucose and in the presence of UK5099, astrocytes have been demonstrated to maintain their high cellular ATP concentration for a remarkably long time (Harders *et al.* 2023). Astrocytes were shown to be able to utilize other internally stored substrates such as fatty acids (Cabodevilla *et al.* 2013, Harders *et al.* 2023, Morant-Ferrando *et al.* 2023), that likely contribute to maintenance of ATP content under UK5099-mediated MPC inhibition. Conversely, astrocytes incubated with glucose in the presence of etomoxir, a CPT1a inhibitor and thus an inhibitor of fatty acid utilization in mitochondria, released around 50 % less pyruvate within 5 h (**Fig. S7**), confirming the use of both pyruvate and fatty acids for mitochondrial ATP production. Nonetheless, astrocytes incubated with pyruvate and UK5099 released slightly less lactate (**Fig. S8**), indicating a decreased availability of cytosolic NADH for LDH-mediated pyruvate reduction. Whether this results from a reduced mitochondrial NADH production, that does not affect cellular ATP concentration, or/and a reduced MAS activity remains to be elucidated.

The inhibition of mitochondrial pyruvate utilization by UK5099 was shown to have a strong impact on pyruvate consumption and release. Accordingly, an indirect modulation of mitochondrial pyruvate utilization by manipulation of the respiratory chain by the complex III inhibitor antimycin A or the uncoupler BAM15 also significantly influenced both processes.

By inhibiting the re-oxidation of cytochrome b_H of complex III (Gabellini *et al.* 1989), antimycin A is supposed to interrupt the electron flow and block the respiratory chain completely (**Fig. 3-4**). This is supported by the observed complete inhibition of oxygen consumption by antimycin A (Kenwood *et al.* 2013). As a result, mitochondria are unable to re-oxidize NADH formed in the TCA cycle (Ragan and Heron 1978), which is likely to bring the TCA cycle to a halt. Consequently, acetyl-CoA and oxaloacetate derived from pyruvate in astrocytes via PDH and PC, respectively (Rose *et al.* 2020), cannot be metabolized in the TCA cycle, which likely reduces overall mitochondrial pyruvate metabolism. Furthermore, an increased PDH phosphorylation and thus inactivation induced by the decrease of NAD^+/NADH ratio in mitochondria, which was shown for PDH in HeLa cells (Titov *et al.* 2016), is believed to contribute to a decreased mitochondrial pyruvate utilization. Consequently, astrocytes likely lose the capacity to metabolize pyruvate in mitochondria. In astrocyte cultures incubated with antimycin A and extracellular pyruvate, this resulted in a time-delayed but complete inhibition of pyruvate uptake (**Fig. 3-4a, Table 3-1**), whereas no

pyruvate release was observed in cells that were treated with antimycin A and glucose (**Fig. 3-4b, Table 3-1**). Yet, the absence of extracellular pyruvate accumulation does not imply

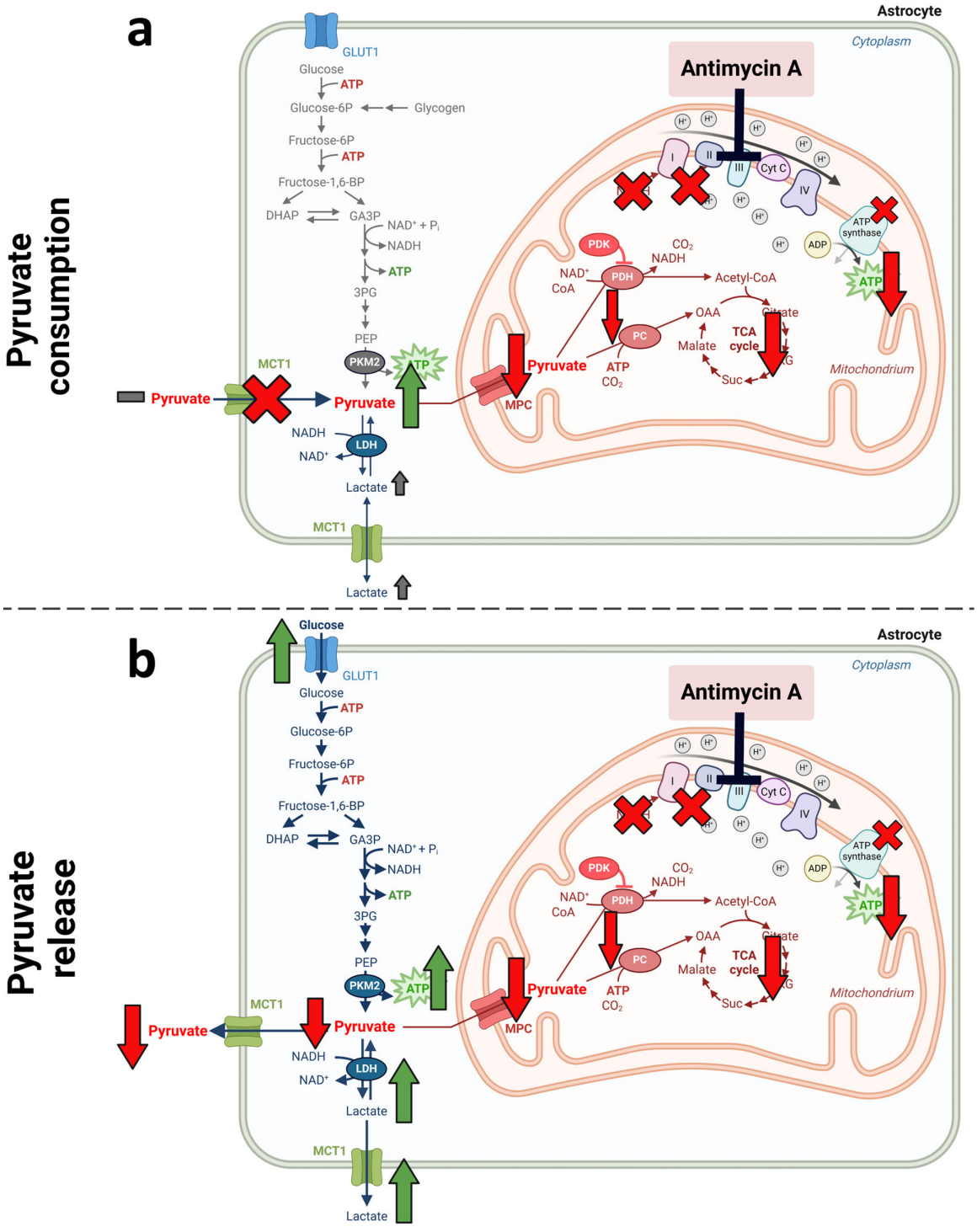

Figure 3-4: The postulated effect of the complex III inhibitor antimycin A on astrocytic pyruvate and energy metabolism. In this figure, the effects of the complex III inhibitor antimycin A on different pathways and metabolites involved in pyruvate and energy metabolism are illustrated. Pyruvate consumption (**a**) and pyruvate release (**b**) are demonstrated separately. To emphasize the subordinate role of glycolysis in glucose-deprived astrocytes (**a**), the reactions involved are colored in grey. The green arrows indicate an increase compared to control conditions (no inhibitor), while the red arrows and red crosses indicate a decrease or block of transport processes, enzyme activities or substance concentration. Created with Biorender.

that pyruvate was consumed in mitochondria under this condition. Instead, a markedly elevated glycolytic flux was observed, characterized by a pronounced increase in glucose consumption and lactate release. Likely, the loss of energy charge by mitochondrial impairment through antimycin A leads to an activation of the cellular energy sensor AMP-dependent protein kinase (AMPK), which was shown to be activated in astrocytes by inhibition of respiration (Almeida *et al.* 2004). Activated AMPK in turn could phosphorylate and thereby activate astrocytic 6-phosphofructo-2-kinase/fructo-2,6-bisphosphatase 3 (PFKFB3) (Almeida *et al.* 2004). PFKFB3 is known to enhance glycolysis in astrocytes by favorably facilitating the production of the strong allosteric activator of PFK1, fructose-2,6-bisphosphate (Bonvento and Bolanos 2021), thus this likely contributes to the accelerated glycolytic flux induced by antimycin A. In this line, antimycin A was shown to induce the phosphorylation and thereby activation of AMPK in hamster lung cells (Ohkubo *et al.* 2024). Furthermore, the ratio of glucose consumption to lactate release was found to be altered in general by application of antimycin A (see **Chapter 2.2 - Fig. 7**), from approximately 1.3 under control conditions to a ratio of nearly 2. This reflects that under antimycin A treatment, nearly all glycolytically derived pyruvate is quickly reduced to lactate, which is then released to prevent intracellular acidification. Thereby, also NADH is rapidly re-oxidized to NAD^+ (Luengo *et al.* 2021), likely to facilitate ongoing enhanced glycolysis. Eventually, while astrocytes incubated with pyruvate and antimycin A were fully depleted of ATP, those incubated with glucose demonstrated the capacity to maintain cellular ATP levels of about 50 % (Harders *et al.* 2023) through enhanced glycolysis, which abolished pyruvate release due to an almost complete conversion of glycolytically derived pyruvate to lactate.

While antimycin A directly inhibits the respiratory chain (Gabellini *et al.* 1989), the uncoupler BAM15 indirectly impairs oxidative phosphorylation by depleting the proton gradient over the inner mitochondrial membrane (Kenwood *et al.* 2013). Under this condition, the electron transport chain and mitochondrial respiration are not impaired and likely strongly accelerated to counteract the decrease of cellular ATP levels that occurs even in the presence of glucose (Harders *et al.* 2023). In line with this, it was demonstrated that the application of BAM15 significantly increases oxygen consumption in various cell types (Kenwood *et al.* 2013, Axelrod *et al.* 2020, Taylor *et al.* 2024). To facilitate the increased need of electrons by the electron transport chain, more succinate and NADH have to be oxidized (Dienel 2019). As a result, it can be postulated that the velocity of the TCA cycle will also

increase (**Fig. 3-5**). Indeed, such an acceleration of the oxidative TCA cycle by BAM15 has been demonstrated for neuroblastoma cell lines (Jiang *et al.* 2023). Ultimately, in order to

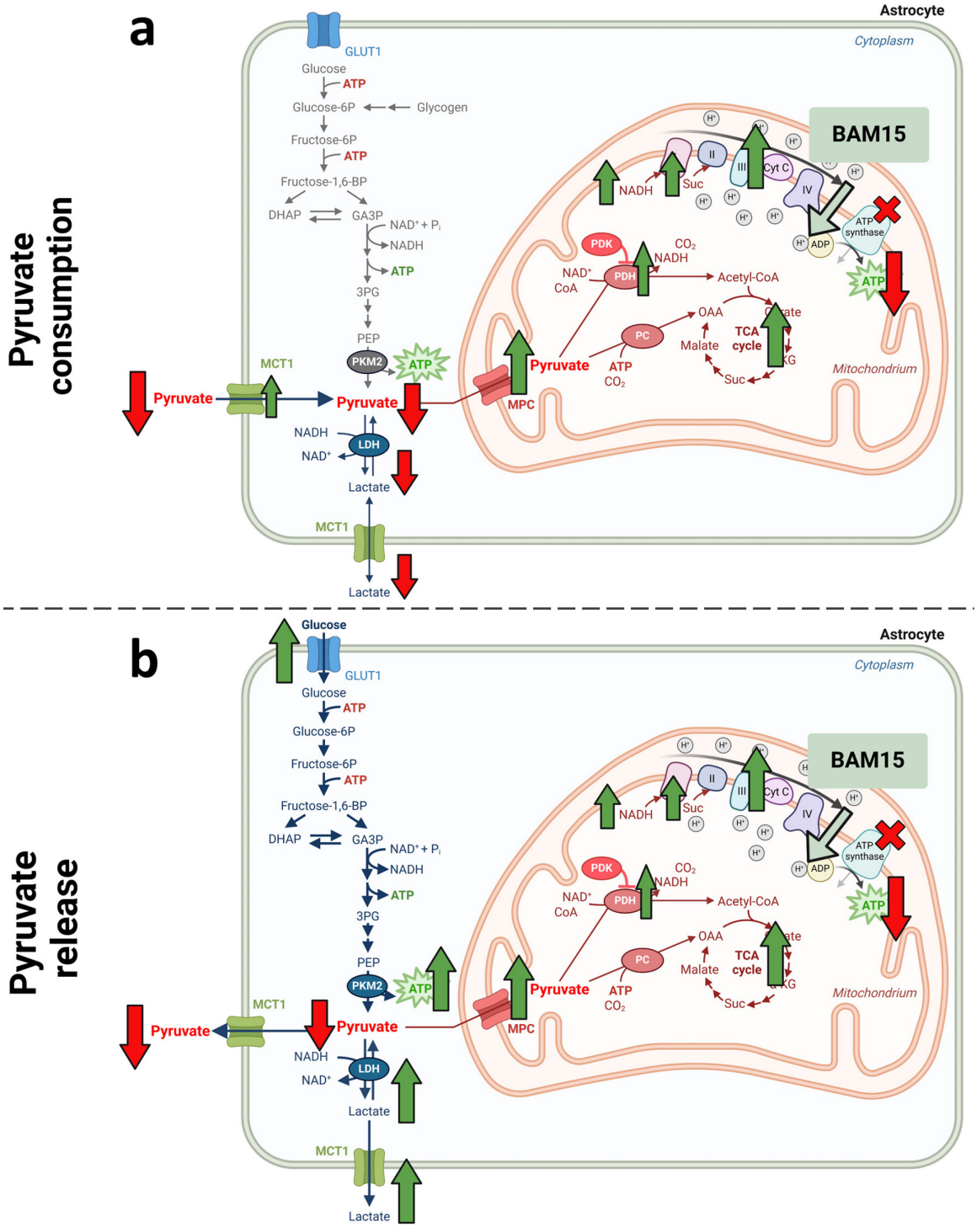

Figure 3-5: The postulated effect of the mitochondrial uncoupler BAM15 on astrocytic pyruvate and energy metabolism. The illustration pictures the effects of the uncoupler BAM15 on different pathways and metabolites involved in pyruvate and energy metabolism. Pyruvate consumption (**a**) and pyruvate release (**b**) are illustrated separately. The reactions involved in glycolysis are colored in grey in the absence of glucose (**a**) to emphasize the subordinate role in this context. The green arrows indicate an increase, while the red arrows and red crosses indicate a decrease or block of transport processes, enzyme activities or substance concentration compared to control conditions (no uncoupler). Created with Biorender.

ensure that sufficient quantities of acetyl-moieties are available for oxidation in the TCA cycle, more pyruvate has to be oxidized by PDH (Jiang *et al.* 2019). Indeed, the mitochondrial pyruvate utilization was significantly accelerated by BAM15, as evidenced by a strong 3-fold acceleration of pyruvate consumption (**Table 3-1**) that could be stopped by inhibition of mitochondrial pyruvate uptake, as well as by a decrease in lactate and alanine production. In accordance with this observations, application of an alternative uncoupler, FCCP, was shown to increase mitochondrial pyruvate utilization in astrocytes also by 300 % (Arce-Molina *et al.* 2020), further demonstrating that the mitochondrial pyruvate oxidation is the main pathway involved in accelerated pyruvate consumption. For glucose-fed astrocytes, the extracellular pyruvate accumulation was also almost abolished in the presence of BAM15 (**Table 3-1; Fig. 3-5**). But, in contrast to pyruvate-fed astrocytes, where the majority of pyruvate is likely to be oxidized in mitochondria, a substantial fraction of the glycolytically derived pyruvate is reduced to lactate. In addition, the glycolytic flux, hence the glucose consumption and lactate release, is generally higher for glucose-fed BAM15-treated astrocytes than for cultures incubated under control condition. Similarly to the inhibition of respiration by antimycin A, the depletion of the mitochondrial membrane potential also induced a decrease in cellular ATP levels even in the presence of glucose (Harders *et al.* 2023), which is probably the cause of the accelerated glycolysis. An activation of glycolysis by AMPK might play a role, as also BAM15 was shown to activate AMPK in various cell types (Tai *et al.* 2018, Axelrod *et al.* 2020). However, the ratio of lactate release to glucose consumption is lower for BAM15-treated astrocytes (1.6) compared to antimycin A-treated cells (1.9). Consequently, also in glucose-fed astrocytes a large quantity of pyruvate appears to be metabolized within the mitochondria, as nearly as much glucose was consumed as under antimycin A treatment, yet less lactate was released.

3.4 Future Perspectives

The extracellular pyruvate concentration could be successfully established as an indicator for alterations of the cellular pyruvate metabolism, but unfortunately, it was not possible to measure the corresponding intracellular pyruvate concentrations with the available resources. To thoroughly understand the astrocytic pyruvate metabolism, it would be very beneficial to close this gap, which could potentially be accomplished by culturing in the presence of ^{13}C-enriched substrates. Such a method for a measurement of intracellular metabolite concentrations has been established using human fibroblasts, but is described to

be suitable for other mammalian cell cultures if the intracellular volume is known (Bennett *et al.* 2008). This is the case for cultured astrocytes (4.1 µL/mg protein) (Dringen and Hamprecht 1998). Briefly, in order to ensure an abundant labeling of metabolites at the time of sample extraction, dividing cells are incubated in DMEM containing U-^{13}C-glucose and U-^{13}C-glutamine for a period of at least two cell doublings (Bennett *et al.* 2008). Therefore, treatment of astrocytes would have to be initiated early after seeding before they become confluent. After harvesting cell samples in solutions containing known concentrations of unlabeled metabolites as internal standards, intracellular concentrations can be calculated from ratios of labeled to unlabeled metabolites determined by liquid chromatography (LC)-mass spectrometry (MS) (Bennett *et al.* 2008). Therefore, by solubilizing astrocytes in solutions containing unlabeled pyruvate, intracellular pyruvate concentrations could be measured. Unlabeled metabolites, which may occur if the incubation medium still requires adjustment such as an addition of further labeled substrates, can be detected by collecting and analyzing the lysed sample without addition of unlabeled internal standards (Bennett *et al.* 2008).

An alternative method to elucidate the intracellular fate of pyruvate is the use of intracellularly expressed fluorescence-based pyruvate sensors, which have previously been employed in astrocytes (San Martín *et al.* 2014, Arce-Molina *et al.* 2020). For intracellular expression, these genetically encoded sensors, or more precisely their DNA sequences, are incorporated into vectors suitable for transfection of eukaryotic cells. Transfection of these vectors into astrocytes was reported to be carried out at 60 % confluence (San Martín *et al.* 2014, Arce-Molina *et al.* 2020). During transfections of a vector encoding a lactate sensor into astrocytes, an efficiency of 20 % was observed using the transfection reagent Lipofectamine 2000. Additionally, a transfection rate exceeding 90 % was achieved using a customized recombinant adenovirus (San Martín *et al.* 2013). Given that these sensors have already been successfully expressed in astrocytes, it is reasonable to believe that the method could be adapted for the astrocyte cultures used in this study. Moreover, as the process primarily involves microscopic observation of individual cells, it should not be problematic if not all cells are successfully transfected.

Expression of pyruvate sensors allows real-time imaging and can therefore be valuable to study the effects of pharmacological modulators on the intracellular pyruvate concentration. For instance, a FRET sensor for pyruvate was used in combination with the MCT1-inhibitor AR-C155858 to characterize mitochondrial pyruvate utilization of

stimulated neurons and astrocytes (San Martín *et al.* 2014). Dependent on the type of fluorophore, sensor use may be time-limited by photobleaching (Verma *et al.* 2023). However, existing pyruvate sensors are based on fluorescent proteins (San Martín *et al.* 2014, Arce-Molina *et al.* 2020), whose signals are relatively stable (Verma *et al.* 2023). Thus, pyruvate sensors could be a great way to study acute as well as long term effects of modulation of the astrocytic cellular pyruvate metabolism. Furthermore, quantitative measurements of cellular steady-state pyruvate concentrations have already been performed using fluorescence-based sensors (Arce-Molina *et al.* 2020). Therefore, expression of sensors provides another opportunity to resolve the for our primary astrocyte cultures unknown intracellular pyruvate concentration without and with pharmacological modulation. Interestingly, also variances in pyruvate consumption among mitochondria located in different regions within the same astrocyte were observed (Arce-Molina *et al.* 2020), which offers the possibility to investigate even intra-individual differences in mitochondrial metabolism. Especially for astrocytes, that can in brain be particularly large and extensively branched with long processes (Zhang and Barres 2010), such investigations could be of great interest. Precisely manipulating a small extracellular area could provide a valuable insight into the mitochondrial pyruvate metabolism following neurotransmission of, e.g., different astrocytic regions of an astrocyte that is part of a tripartite synapse. Moreover, dysfunctional astrocytic mitochondria appear to gain interest in the context of pathologies such as the neurodegenerative Parkinson's disease, whose phenotypic characteristics like locomotor deficits could be induced by impairment of the astrocytic mitochondrial membrane potential within the *substancia nigra pars compacta* of mice (Li *et al.* 2024). Investigating mitochondrial pyruvate utilization in cell culture disease models may enhance our understanding of metabolic abnormalities associated with various (neurodegenerative) disease (Mulica *et al.* 2021, Anderson 2022, Yu and Martins 2024, Zhang *et al.* 2024).

Beyond the measurement of intracellular concentrations, application of ^{13}C-enriched pyruvate in general might be a great way to further investigate the intracellular fate of extracellularly applied pyruvate. The application of ^{13}C-enriched substrates has been successfully applied on numerous occasions to elucidate other aspects of the astrocytic metabolism in the physiological and pathophysiological context (Zwingmann and Leibfritz 2003, Nissen *et al.* 2015, Cerdan 2017, Andersen *et al.* 2020, Salcedo *et al.* 2024). To elucidate the fate of cellular pyruvate, astrocytes could be incubated with stable ^{13}C isotope-enriched pyruvate alone, or in the presence of unlabeled glucose or other additional substrates, and

isotope enrichment of cellular metabolites could be determined by gas chromatography (GC)-MS (Walls *et al.* 2014). Through analysis with nuclear magnetic resonance (NMR) spectroscopy, in addition to isotope enrichment, labelling patterns could be obtained, but more sample is needed as NMR is less sensitive than MS (Westi *et al.* 2023). Incubations with stable ^{13}C isotope-enriched metabolites have, e.g., recently been used to elucidate the metabolism of the neurotransmitter GABA (Andersen *et al.* 2020), or the metabolism of medium chain fatty acids (Andersen *et al.* 2021) in brain slices. After a correction for naturally occurring ^{13}C nuclei (Walls *et al.* 2014) following an incubation with ^{13}C enriched pyruvate, the measured labelled metabolites should only be derived from this pyruvate. Therefore, isotope tracing would bring the great opportunity to determine the cellular fate of pyruvate by directly measuring products of pyruvate in cultured astrocytes. Through the addition of a combination of labeled pyruvate and unlabeled substrates such as glucose, the intracellular labeled pyruvate pool might be diluted by the production of unlabeled pyruvate from the other substrate applied (Westi *et al.* 2023). But, since the labeled metabolites in cells incubated with an additional unlabeled energy substrate will still be derived from the applied labeled pyruvate, this would be an adequate approach to analyze differences of pyruvate metabolism of astrocytes in different environments such as less or more complex incubation media. For example, application of labelled pyruvate and labelled pyruvate precursors to cortical neurons revealed different labelling patterns of metabolites dependent on the applied mixture of substrates (Cruz *et al.* 2001).

An advancement of the rather insensitive ^{13}C NMR spectroscopy (Walls *et al.* 2014), ^{13}C hyperpolarized magnetic resonance imaging (MRI), offers the fascinating possibility of conducting live *in vivo* measurements (Miller *et al.* 2018). This technique provides a powerful tool to elucidate the fate of pyruvate in brain *in vivo* (Miller *et al.* 2018). For this procedure, ^{13}C-enriched substrates are hyperpolarized prior to their application to living subjects, mainly by a method called dissolution Dynamic Nuclear Polarization (dDNP) (Miller *et al.* 2018, Wodtke *et al.* 2023). Briefly, the substrate, mixed with free radicals, undergoes polarization in a strong magnetic field (3.35 - 7 T) at cryogenic temperatures (~ 1 K). Under these circumstances, the electron spins of the added free radicals align with the magnetic field, and this polarization is then transferred to the ^{13}C nuclei through application of a specific microwave frequency, inducing a transient increase in nuclear polarization (Wodtke *et al.* 2023). After rapid dissolution of the polarized substance in a heated liquid and subsequent cooling to physiological temperature, it must be injected immediately into a subject for MRI due to the transient nature of the polarization (Wodtke

et al. 2023). This pretreatment drastically enhances the signal in MRI, enabling direct and non-invasive *in vivo* measurements of a hyperpolarized substance and its products (Miller *et al.* 2018, Wodtke *et al.* 2023). [1-^{13}C]-pyruvate is thereby the most commonly used substrate (Wodtke *et al.* 2023), and is already being tested in clinical studies for clinical application (Grist *et al.* 2019, Hackett *et al.* 2020, Rider *et al.* 2020).

Given the extensive experience especially with [1-^{13}C]-pyruvate, ^{13}C-hyperpolarized MRI presents an excellent opportunity to get an insight into the brains' pyruvate metabolism in physiological or pathophysiological conditions. E.g., studies on healthy humans injected with hyperpolarized [1-^{13}C]-pyruvate revealed in brain a faster incorporation of label into lactate than into the bicarbonate pool, indicating that pyruvate in the brain is faster reduced than oxidized (Grist *et al.* 2019). Furthermore, intravenous applied hyperpolarized pyruvate was shown to be an indicator of an increased BBB permeability in a rat brain metastasis model and a porcine mannitol osmotic shock model by measurements of the appearance of [1-^{13}C]-pyruvate and [1-^{13}C]-lactate in the brain parenchyma (Miller *et al.* 2018). In a LPS-induced neuroinflammation model, the [1-^{13}C]-lactate to pyruvate ratio was shown to be increased in the area of LPS injection (Le Page *et al.* 2019). However, this commonly used approach of pyruvate, lactate and bicarbonate measurements is to date not able to distinguish between cell types directly. Moreover, the results obtained are presented as metabolic ratios and conversion rates (Wodtke *et al.* 2023). Nonetheless, correlating results with cell type specific pathways could suggest the activity of specific cells. For instance, pyruvate carboxylase is in brain predominantly expressed in astrocytes (Cesar and Hamprecht 1995, Sonnewald and Rae 2010). Therefore, carboxylation of hyperpolarized [1-^{13}C]-pyruvate by PC should result in the production of [1-^{13}C]-, and subsequently [4-^{13}C]-oxaloacetate almost specifically by astrocytes. Measurements of this oxaloacetate could increase our knowledge of basic brain metabolism by assessing the activity of PC in the brain *in vivo*. Hyperpolarized oxaloacetate, which is a rather unstable β-ketoacid (Pollack 1978), could nonetheless be measured in mouse liver (Lee *et al.* 2013). In general, the highly interesting approach to measure hyperpolarized metabolites and their conversion rates non-invasive *in vivo* will possibly bring an important insight into brains' metabolism, and the application of hyperpolarized [1-^{13}C]pyruvate will likely advance the diagnostic methods for diverse disease (Miller *et al.* 2018, Choi *et al.* 2019, Hackett *et al.* 2020, Anderson *et al.* 2021, Andelius *et al.* 2024).

Externally supplied pyruvate was shown to have neuroprotective functions *in vitro* (Selak *et al.* 1985, Desagher *et al.* 1997, Lee *et al.* 2001, Wang and Cynader 2001, Ryou *et al.* 2012) and *in vivo* (Lee *et al.* 2001, Ryou *et al.* 2012). Besides serving as an additional energy substrate (Lee *et al.* 2001), pyruvate was discussed to exert neuroprotective effects through its antioxidative capacity (Desagher *et al.* 1997, Wang and Cynader 2001, Ryou *et al.* 2012). To elucidate the contribution of pyruvate derived from astrocytes *in vivo*, one could try to manipulate metabolism in astrocytes specifically, e.g., by MCT1 inhibition. One approach used antisense oligonucleotides to study the impact of MCT1 and MCT4 knockdown in astrocytes within the rat dorsal campus, focusing on memory impairment. Administration of pyruvate thereby restored the memory formation impaired by MCT1 and MCT4 knockdown (Descalzi *et al.* 2019). The local administration of antisense oligonucleotides results in effective distribution in the brain parenchyma, targeting RNA transcripts to reduce protein production (Schoch and Miller 2017). But, since MCT1 is in brain not exclusively expressed in astrocytes, but also in oligodendrocytes, microglia and even some neurons (Felmlee *et al.* 2020), more specific methods are needed to accurately assess astrocytic pyruvate release *in vivo*. In a mouse mutant model, mitochondrial respiration in astrocytes could be selectively disabled by tamoxifen administration. These mice remained viable without apparent cell death (Supplie *et al.* 2017). Using such mouse models, one could investigate whether pyruvate concentrations within the interstitial fluid diver between conditions with and without functional mitochondrial respiration. This approach may help clarify the influence of astrocytic mitochondrial and pyruvate metabolism on overall brain pyruvate dynamics. However, fully abolishing pyruvate metabolism is likely not feasible due to the critical importance of these metabolic pathways.

Overall, the findings presented provide insights into the multifaceted nature of astrocytic pyruvate metabolism and contributes to laying the groundwork for future research in the field of brain pyruvate metabolism. By shedding light on the metabolic fate of pyruvate in astrocytes, these findings offer valuable insights into the intricate mechanisms underlying brain pyruvate metabolism, ultimately helping to advance our understanding of brain pyruvate functions. Furthermore, this knowledge could pave the way for future studies aimed to elucidate the role of mismatched pyruvate metabolism in neurological disease, which is particularly important as defective metabolism is increasingly recognized as a contributing factor in pathophysiology (Mocking *et al.* 2018, Aldana 2019, Westi *et al.* 2023, Hanin *et al.* 2024).

3.5 References

Aldana BI (2019). Microglia-specific metabolic changes in neurodegeneration. *J Mol Biol*, **431**: 1830-1842

Almeida A, Moncada S and Bolaños JP (2004). Nitric oxide switches on glycolysis through the AMP protein kinase and 6-phosphofructo-2-kinase pathway. *Nat Cell Biol*, **6**: 45-51

Andelius TCK, Hansen ESS, Bøgh N, Pedersen MV, Kyng KJ, Henriksen TB and Laustsen C (2024). Hyperpolarized ^{13}C magnetic resonance imaging in neonatal hypoxic–ischemic encephalopathy: First investigations in a large animal model. *NMR Biomed*, **37**

Andersen JV, Jakobsen E, Westi EW, Lie MEK, Voss CM, Aldana BI, Schousboe A, Wellendorph P, Bak LK, Pinborg LH and Waagepetersen HS (2020). Extensive astrocyte metabolism of γ-aminobutyric acid (GABA) sustains glutamine synthesis in the mammalian cerebral cortex. *Glia*, **68**: 2601-2612

Andersen JV, Westi EW, Jakobsen E, Urruticoechea N, Borges K and Aldana BI (2021). Astrocyte metabolism of the medium-chain fatty acids octanoic acid and decanoic acid promotes GABA synthesis in neurons via elevated glutamine supply. *Mol Brain*, **14**

Anderson G (2022). Depression pathophysiology: astrocyte mitochondrial melatonergic pathway as crucial hub. *Int J Mol Sci*, **24**: 350

Anderson S, Grist JT, Lewis A and Tyler DJ (2021). Hyperpolarized ^{13}C magnetic resonance imaging for noninvasive assessment of tissue inflammation. *NMR Biomed*, **34**

Arce-Molina R, Cortés-Molina F, Sandoval PY, Galaz A, Alegría K, Schirmeier S, Barros LF and San Martín A (2020). A highly responsive pyruvate sensor reveals pathway-regulatory role of the mitochondrial pyruvate carrier MPC. *eLife*, **9**: e53917

Axelrod CL, King WT, Davuluri G, Noland RC, Hall J, Hull M, Dantas WS, Zunica ER, Alexopoulos SJ, Hoehn KL, Langohr I, Stadler K, Doyle H, Schmidt E, Nieuwoudt S, Fitzgerald K, Pergola K, Fujioka H, Mey JT, Fealy C, Mulya A, Beyl R, Hoppel CL and Kirwan JP (2020). BAM15-mediated mitochondrial uncoupling protects against obesity and improves glycemic control. *EMBO Mol Med*, **12**: e12088

Barros LF, Ruminot I, San Martin A, Lerchundi R, Fernandez-Moncada I and Baeza-Lehnert F (2021). Aerobic glycolysis in the brain: warburg and crabtree contra pasteur. *Neurochem Res*, **46**: 15-22

Bennett BD, Yuan J, Kimball EH and Rabinowitz JD (2008). Absolute quantitation of intracellular metabolite concentrations by an isotope ratio-based approach. *Nat Protoc*, **3**: 1299-1311

Blumrich E-M, Kadam R and Dringen R (2016). The protein tyrosine kinase inhibitor tyrphostin 23 strongly accelerates glycolytic lactate production in cultured primary astrocytes. *Neurochem Res*, **41**: 2607-2618

Bonvento G and Bolanos JP (2021). Astrocyte-neuron metabolic cooperation shapes brain activity. *Cell Metab*, **33**: 1546-1564

Breukels V, Jansen KFJ, Van Heijster FHA, Capozzi A, Van Bentum PJM, Schalken JA, Comment A and Scheenen TWJ (2015). Direct dynamic measurement of intracellular and extracellular lactate in small-volume cell suspensions with ^{13}C hyperpolarised NMR. *NMR Biomed*, **28**: 1040-1048

Bröer S, Rahman B, Pellegri G, Pellerin L, Martin J-L, Verleysdonk S, Hamprecht B and Magistretti PJ (1997). Comparison of lactate transport in astroglial cells and monocarboxylate transporter 1 (MCT 1) expressing *Xenopus laevis* oocytes. *J Biol Chem*, **272**: 30096 - 30102

Bröer S, Schneider H-P, Bröer A, Rahman B, Hamprecht B and Deitmer JW (1998). Characterization of the monocarboxylate transporter 1 expressed in *Xenopus laevis* oocytes by changes in cytosolic pH. *Biochem J*, **333**: 167 - 174

Cabodevilla AG, Sánchez-Caballero L, Nintou E, Boiadjieva VG, Picatoste F, Gubern A and Claro E (2013). Cell survival during complete nutrient deprivation depends on lipid droplet-fueled β-oxidation of fatty acids. *J Biol Chem*, **288**: 27777-27788

Cardona C, Sánchez-Mejías E, Dávila JC, Martín-Rufián M, Campos-Sandoval JA, Vitorica J, Alonso FJ, Matés JM, Segura JA, Norenberg MD, Rama Rao KV, Jayakumar AR, Gutiérrez A and Márquez J (2015). Expression of Gls and Gls2 glutaminase isoforms in astrocytes. *Glia*, **63**: 365-382

Carpenter L and Halestrap AP (1994). The kinetics, substrate and inhibitor specificity of the lactate transporter of Ehrlich-Lettre tumour cells studied with the intracellular pH indicator BCECF. *Biochem J*, **304**: 751-760

Cerdan S (2017). Twenty-seven years of cerebral pyruvate recycling. *Neurochem Res*, **42**: 1621-1628

Cesar M and Hamprecht B (1995). Immunocytochemical examination of neural rat and mouse primary cultures using monoclonal antibodies raised against pyruvate carboxylase. *J Neurochem*, **64**: 2312-2318

Chen H, Wang C, Wei X, Ding X and Ying W (2015). Malate-aspartate shuttle inhibitor aminooxyacetate acid induces apoptosis and impairs energy metabolism of both resting microglia and LPS-activated microglia. *Neurochem Res*, **40**: 1311-1318

Choi Y-S, Song JE, Lee JE, Kim E, Kim CH, Kim D-H and Song H-T (2019). Hyperpolarized [1-^{13}C]lactate flux increased in the hippocampal region in diabetic mice. *Mol Brain*, **12**

Christensen CE, Karlsson M, Winther JR, Jensen PR and Lerche MH (2014). Non-invasive in-cell determination of free cytosolic [NAD^+]/[NADH] ratios using hyperpolarized glucose show large variations in metabolic phenotypes. *J Biol Chem*, **289**: 2344-2352

Contreras-Baeza Y, Sandoval PY, Alarcón R, Galaz A, Cortés-Molina F, Alegría K, Baeza-Lehnert F, Arce-Molina R, Guequén A, Flores CA, San Martín A and Barros LF (2019). Monocarboxylate transporter 4 (MCT4) is a high affinity transporter capable of exporting lactate in high-lactate microenvironments. *J Biol Chem*, **294**: 20135-20147

Cruz F, Villalba M, García-Espinosa MA, Ballesteros P, Bogónez E, Satrústegui J and Cerdán S (2001). Intracellular compartmentation of pyruvate in primary cultures of cortical neurons as detected by ^{13}C NMR spectroscopy with multiple ^{13}C labels. *J Neurosci Res*, **66**: 771-781

Daverio Z, Kolkman M, Perrier J, Brunet L, Bendridi N, Sanglar C, Berger M-A, Panthu B and Rautureau GJP (2023). Warburg-associated acidification represses lactic fermentation independently of lactate, contribution from real-time NMR on cell-free systems. *Sci Rep*, **13**

Deitmer JW, Theparambil SM, Ruminot I, Noor SI and Becker HM (2019). Energy dynamics in the brain: Contributions of astrocytes to metabolism and pH homeostasis. *Front Neurosci*, **13**: 1301

Desagher S, Glowinski J and Prémont J (1997). Pyruvate protects neurons against hydrogen peroxide-induced toxicity. *J Neurosci*, **17**: 9060-9067

Descalzi G, Gao V, Steinman MQ, Suzuki A and Alberini CM (2019). Lactate from astrocytes fuels learning-induced mRNA translation in excitatory and inhibitory neurons. *Commun Biol*, **2**: 247

Dienel GA (2017). Lack of appropriate stoichiometry: Strong evidence against an energetically important astrocyte-neuron lactate shuttle in brain. *J Neurosci Res*, **95**: 2103-2125

Dienel GA (2019). Brain glucose metabolism: Integration of energetics with function. *Physiol Rev*, **99**: 949-1045

Dimmer K-S, Friedrich B, Lang F, Deitmer JW and Bröer S (2000). The low-affinity monocarboxylate transporter MCT4 is adapted to the export of lactate in highly glycolytic cells. *Biochem J*, **350**: 219-227

Dringen R, Gebhardt R and Hamprecht B (1993). Glycogen in astrocytes: possible function as lactate supply for neighboring cells. *Brain Res*, **623**: 208 - 214

Dringen R and Hamprecht B (1998). Glutathione restoration as indicator for cellular metabolism of astroglial cells. *Dev Neurosci*, **20**: 401-407

Erecińska M, Deas J and Silver IA (1995). The effect of pH on glycolysis and phosphofructokinase activity in cultured cells and synaptosomes. *J Neurochem*, **65**: 2765-2772

Felmlee MA, Jones RS, Rodriguez-Cruz V, Follman KE and Morris ME (2020). Monocarboxylate transporters (SLC16): Function, regulation, and role in health and disease. *Pharmacol Rev*, **72**: 466-485

Gabellini N, Gao Z, Oesterhelt D, Venturoli G and Melandri B (1989). Reconstruction of cyclic transport and photophosphorylation by incorporation of reaction center, cytochrom *bc*$_1$ complex and ATP synthase from *Rhodobacter capsulatus* into ubiquinone-10 / phospholipid vesicles. *Biochim Biophys Acta*, **974**: 202-210

Grist JT, McLean MA, Riemer F, Schulte RF, Deen SS, Zaccagna F, Woitek R, Daniels CJ, Kaggie JD, Matys T, Patterson I, Slough R, Gill AB, Chhabra A, Eichenberger R, Laurent MC, Comment A, Gillard JH, Coles AJ, Tyler DJ, Wilkinson I, Basu B, Lomas DJ, Graves MJ, Brindle KM and Gallagher FA (2019). Quantifying normal human brain metabolism using hyperpolarized [1-^{13}C]pyruvate and magnetic resonance imaging. *Neuroimage*, **189**: 171-179

Guarino VA, Oldham WM, Loscalzo J and Zhang Y-Y (2019). Reaction rate of pyruvate and hydrogen peroxide: Assessing antioxidant capacity of pyruvate under biological conditions. *Sci Rep*, **9**: 19568

Hackett EP, Pinho MC, Harrison CE, Reed GD, Liticker J, Raza J, Hall RG, Malloy CR, Barshikar S, Madden CJ and Park JM (2020). Imaging acute metabolic changes in patients with mild traumatic brain injury using hyperpolarized [1-^{13}C]pyruvate. *iScience*, **23**: 101885

Halestrap AP (1975). The mitochondrial pyruvate carrier. Kinetics and specificity for substrates and inhibitors. *Biochem J*, **148**: 85-96

Halestrap AP (2013). Monocarboxylic acid transport. *Compr Physiol*, **3**: 1611-1643

Hamprecht B and Dringen R (1994). On the role of glycogen and pyruvate uptake in astroglial-neuronal interaction. In: Pharmacology of Cerebral Ischemia: 191 - 202. Krieglstein J, Oberpichler-Schwenk H (eds), Pharmacology of Cerebral Ischemia, WVG, Stuttgart, Germany.

Hanin A, Chollet C, Demeret S, Lucas, Castelli F and Navarro V (2024). Metabolomic changes in adults with status epilepticus: A human case–control study. *Epilepsia*, **65**: 929-943

Harders AR, Arend C, Denieffe SC, Berger J and Dringen R (2023). Endogenous energy stores maintain a high ATP concentration for hours in glucose-depleted cultured primary rat astrocytes. *Neurochem Res*, **48**: 2241-2252

Harders AR, Spellerberg P and Dringen R (2024). Exogenous substrates prevent the decline in the cellular ATP content of primary rat astrocytes during glucose deprivation. *Neurochem Res*: 1188-1199

Hildyard JC, Ammala C, Dukes ID, Thomson SA and Halestrap AP (2005). Identification and characterisation of a new class of highly specific and potent inhibitors of the mitochondrial pyruvate carrier. *Biochim Biophys Acta*, **1707**: 221-230

Jiang H, Jin J, Duan Y, Xie Z, Li Y, Gao A, Gu M, Zhang X, Peng C, Xia C, Dong T, Li H, Yu L, Tang J, Yang F, Li J and Li J (2019). Mitochondrial uncoupling coordinated with PDH activation safely ameliorates hyperglycemia via promoting glucose oxidation. *Diabetes*, **68**: 2197-2209

Jiang H, He CJ, Li AM, He B, Li Y, Zhou MN and Ye J (2023). Mitochondrial uncoupling inhibits reductive carboxylation in cancer cells. *Mol Cancer Res*, **21**: 1010-1016

John RA and Charteris A (1978). The reaction of amino-oxyacetate with pyridoxal phosphate-dependent enzymes. *Biochem J*, **171**: 771-779

Karagiannis A, Sylantyev S, Hadjihambi A, Hosford PS, Kasparov S and Gourine AV (2016). Hemichannel-mediated release of lactate. *J Cereb Blood Flow Metab*, **36**: 1202-1211

Karger G, Berger J and Dringen R (2024). Modulation of cellular levels of adenosine phosphates and creatine phosphate in cultured primary astrocytes. *Neurochem Res*, **49**: 402-414

Kenwood BM, Weaver JL, Bajwa A, Poon IK, Byrne FL, Murrow BA, Calderone JA, Huang L, Divakaruni AS, Tomsig JL, Okabe K, Lo RH, Cameron Coleman G, Columbus L, Yan Z, Saucerman JJ, Smith JS, Holmes JW, Lynch KR, Ravichandran KS, Uchiyama S, Santos WL, Rogers GW, Okusa MD, Bayliss DA and Hoehn KL (2013). Identification of a novel mitochondrial uncoupler that does not depolarize the plasma membrane. *Mol Metab*, **3**: 114-123

Le Page LM, Guglielmetti C, Najac CF, Tiret B and Chaumeil MM (2019). Hyperpolarized ^{13}C magnetic resonance spectroscopy detects toxin-induced neuroinflammation in mice. *NMR Biomed*, **32**

Lee J-Y, Kim Y-H and Koh J-Y (2001). Protection by pyruvate against transient forebrain ischemia in rats. *J Neurosci*, **21**: RC171-RC171

Lee P, Leong W, Tan T, Lim M, Han W and Radda GK (2013). *In vivo* hyperpolarized carbon-13 magnetic resonance spectroscopy reveals increased pyruvate carboxylase flux in an insulin-resistant mouse model. *Hepatology*, **57**: 515-524

Lerchundi R, Fernández-Moncada I, Contreras-Baeza Y, Sotelo-Hitschfeld T, Mächler P, Wyss MT, Stobart J, Baeza-Lehnert F, Alegría K, Weber B and Barros LF (2015). NH_4^+ triggers the release of astrocytic lactate via mitochondrial pyruvate shunting. *Proc Natl Acad Sci USA*, **112**: 11090-11095

Li SM, Wang DD, Liu DH, Meng XY, Wang Z, Guo X, Liu Q, Liu PP, Li SA, Wang S, Yang RZ, Xu Y, Wang L and Kang JS (2024). Neurotransmitter accumulation and Parkinson's disease-like phenotype caused by anion channelrhodopsin opto-controlled astrocytic mitochondrial depolarization in substantia nigra pars compacta. *MedComm*, **5**: e568

Linsambarth S, Carvajal FJ, Moraga-Amaro R, Mendez L, Tamburini G, Jimenez I, Verdugo DA, Gomez GI, Jury N, Martinez P, van Zundert B, Varela-Nallar L, Retamal MA, Martin C, Altenberg GA, Fiori MC, Cerpa W, Orellana JA and Stehberg J (2022). Astroglial gliotransmitters released via Cx43 hemichannels regulate NMDAR-dependent transmission and short-term fear memory in the basolateral amygdala. *FASEB J*, **36**: e22134

Luengo A, Li Z, Gui DY, Sullivan LB, Zagorulya M, Do BT, Ferreira R, Naamati A, Ali A, Lewis CA, Thomas CJ, Spranger S, Matheson NJ and Vander Heiden MG (2021). Increased demand for NAD^+ relative to ATP drives aerobic glycolysis. *Mol Cell*, **81**: 691-707 e696

Mächler P, Wyss MT, Elsayed M, Stobart J, Gutierrez R, Alexandra, Kaelin V, Zuend M, Alejandro, Romero-Gómez I, Baeza-Lehnert F, Lengacher S, Bernard, Aebischer P, Pierre, L and Weber B (2016). In vivo evidence for a lactate gradient from astrocytes to neurons. *Cell Metab*, **23**: 94-102

Markussen KH, Corti M, Byrne BJ, Craig W, Sun RC and Gentry MS (2023). The multifaceted roles of the brain glycogen. *J Neurochem*, **168**: 728-743

Miller JJ, Grist JT, Serres S, Larkin JR, Lau AZ, Ray K, Fisher KR, Hansen E, Tougaard RS, Nielsen PM, Lindhardt J, Laustsen C, Gallagher FA, Tyler DJ and Sibson N (2018). ^{13}C pyruvate transport across the blood-brain barrier in preclinical hyperpolarised MRI. *Sci Rep*, **8**: 15082

Mocking RJT, Assies J, Ruhé HG and Schene AH (2018). Focus on fatty acids in the neurometabolic pathophysiology of psychiatric disorders. *J Inherit Metab Dis*, **41**: 597-611

Morant-Ferrando B, Jimenez-Blasco D, Alonso-Batan P, Agulla J, Lapresa R, Garcia-Rodriguez D, Yunta-Sanchez S, Lopez-Fabuel I, Fernandez E, Carmeliet P, Almeida A, Garcia-Macia M and Bolaños JP (2023). Fatty acid oxidation organizes mitochondrial supercomplexes to sustain astrocytic ROS and cognition. *Nat Metab*, **5**: 1290–1302

Mulica P, Grünewald A and Pereira SL (2021). Astrocyte-neuron metabolic crosstalk in neurodegeneration: A mitochondrial perspective. *Front Endocrinol*, **12**: 668517

Nissen JD, Pajęcka K, Stridh MH, Skytt DM and Waagepetersen HS (2015). Dysfunctional TCA-cycle metabolism in glutamate dehydrogenase deficient astrocytes. *Glia*, **63**: 2313-2326

Ohkubo K, Shibutani S and Iwata H (2024). AMP-activated protein kinase (AMPK) suppresses Ibaraki virus propagation. *Virology*, **590**: 109943

Orthmann-Murphy JL, Abrams CK and Scherer SS (2008). Gap junctions couple astrocytes and oligodendrocytes. *J Mol Neurosci*, **35**: 101-116

Ovens MJ, Davies AJ, Wilson MC, Murray CM and Halestrap AP (2010). AR-C155858 is a potent inhibitor of monocarboxylate transporters MCT1 and MCT2 that binds to an intracellular site involving transmembrane helices 7-10. *Biochem J*, **425**: 523-530

Pollack RM (1978). Decarboxylations of β-keto acids and related compounds. In: Gandour RD and Schowen RL (eds) Transition States of Biochemical Processes: 467-492. Springer US, Boston, MA.

Ragan CI and Heron C (1978). The interaction between mitochondrial NADH-ubiquinone oxidoreductase and ubiquinol-cytochrome *c* oxidoreductase. Evidence for stoicheiometric association. *Biochem J*, **174**: 783-790

Rider OJ, Apps A, Miller JJJJ, Lau JYC, Lewis AJM, Peterzan MA, Dodd MS, Lau AZ, Trumper C, Gallagher FA, Grist JT, Brindle KM, Neubauer S and Tyler DJ (2020). Noninvasive in vivo assessment of cardiac metabolism in the healthy and diabetic human heart using hyperpolarized ^{13}C MRI. *Circ Res*, **126**: 725-736

Rose J, Brian C, Pappa A, Panayiotidis MI and Franco R (2020). Mitochondrial metabolism in astrocytes regulates brain bioenergetics, neurotransmission and redox balance. *Front Neurosci*, **14**: 536682

Ryou M-G, Liu R, Ren M, Sun J, Mallet RT and Yang S-H (2012). Pyruvate protects the brain against ischemia–reperfusion injury by activating the erythropoietin signaling pathway. *Stroke*, **43**: 1101-1107

Salcedo C, Victoria, García-Adán B, Ameen AO, Gegelashvili G, Waagepetersen HS, Freude KK and Aldana BI (2024). Increased glucose metabolism and impaired glutamate transport in human astrocytes are potential early triggers of abnormal extracellular glutamate accumulation in hiPSC-derived models of Alzheimer's disease. *J Neurochem*, **168**: 822-840

San Martín A, Ceballo S, Ruminot I, Lerchundi R, Frommer WB and Barros LF (2013). A genetically encoded FRET lactate sensor and its use to detect the Warburg effect in single cancer cells. *PLoS ONE*, **8**: e57712

San Martín A, Ceballo S, Baeza-Lehnert F, Lerchundi R, Valdebenito R, Contreras-Baeza Y, Alegría K and Barros LF (2014). Imaging mitochondrial flux in single cells with a FRET sensor for pyruvate. *PLoS ONE*, **9**: e85780

Schoch KM and Miller TM (2017). Antisense oligonucleotides: Translation from mouse models to human neurodegenerative diseases. *Neuron*, **94**: 1056-1070

Selak I, Skaper S and Varon S (1985). Pyruvate participation in the low molecular weight trophic activity for central nervous system neurons in glia-conditioned media. *J Neurosci*, **5**: 23-28

Sonnewald U, Westergaard N, Jones P, Taylor A, Bachelard HS and Schousboe A (1996). Metabolism of [U-$^{13}C_5$]glutamine in cultured astrocytes studied by NMR spectroscopy: First evidence of astrocytic pyruvate recycling. *J Neurochem*, **67**: 2566-2572

Sonnewald U and Rae C (2010). Pyruvate carboxylation in different model systems studied by ^{13}C MRS. *Neurochem Res*, **35**: 1916-1921

Sotelo-Hitschfeld T, Niemeyer MI, Mächler P, Ruminot I, Lerchundi R, Wyss MT, Stobart J, Fernández-Moncada I, Valdebenito R, Garrido-Gerter P, Contreras-Baeza Y, Schneider BL, Aebischer P, Lengacher S, San Martín A, Le Douce J, Bonvento G, Magistretti PJ, Sepúlveda FV, Weber B and Barros LF (2015). Channel-mediated lactate release by K^+-stimulated astrocytes. *J Neurosci*, **35**: 4168-4178

Supplie LM, Düking T, Campbell G, Diaz F, Moraes CT, Götz M, Hamprecht B, Boretius S, Mahad D and Nave K-A (2017). Respiration-deficient astrocytes survive as glycolytic cells *in vivo*. *J Neurosci*, **37**: 4231-4242

Tai Y, Li L, Peng X, Zhu J, Mao X, Qin N, Ma M, Huo R, Bai Y and Dong D (2018). Mitochondrial uncoupler BAM15 inhibits artery constriction and potently activates AMPK in vascular smooth muscle cells. *Acta Pharm Sin B*, **8**: 909-918

Taylor AL, Dubuisson O, Pandey P, Zunica ERM, Vandanmagsar B, Dantas WS, Johnson A, Axelrod CL and Kirwan JP (2024). Restricting bioenergetic efficiency enhances longevity and mitochondrial redox capacity in *Drosophila melanogaster*. *Aging Cell*, **23**

Titov D, Cracan V, Goodmann R, Peng J, Grabarek Z and Mootha V (2016). Complementation of mitochondrial electron transport chain by manipulation of the NAD^+/NADH ratio. *Science*, **352**: 231-235

Trivedi B and Danforth WH (1966). Effect of pH on the kinetics of frog muscle phosphofructokinase. *J Biol Chem*, **241**: 4110-4114

Verma AK, Noumani A, Yadav AK and Solanki PR (2023). FRET Based Biosensor: Principle Applications Recent Advances and Challenges. *Diagnostics*, **13**: 1375

Voss CM, Andersen JV, Jakobsen E, Siamka O, Karaca M, Maechler P and Waagepetersen HS (2020). AMP-activated protein kinase (AMPK) regulates astrocyte oxidative metabolism by balancing TCA cycle dynamics. *Glia*, **68**: 1824-1839

Walls AB, Bak LK, Sonnewald U, Schousboe A and Waagepetersen HS (2014). Metabolic mapping of astrocytes and neurons in culture using stable isotopes and gas chromatography-mass spectrometry (GC-MS). In: Hirrlinger J and Waagepetersen HS (eds) Neuromethods: Brain Energy Metabolism, **90**: 73-105. Humana Press, New York.

Wang C, Chen H, Zhang M, Zhang J, Wei X and Ying W (2016). Malate-aspartate shuttle inhibitor aminooxyacetic acid leads to decreased intracellular ATP levels and altered cell cycle of C6 glioma cells by inhibiting glycolysis. *Cancer Lett*, **378**: 1-7

Wang XF and Cynader MS (2001). Pyruvate released by astrocytes protects neurons from copper-catalyzed cysteine neurotoxicity. *J Neurosci*, **21**: 3322 - 3331

Westergaard N, Drejer J, Schousboe A and Sonnewald U (1996). Evaluation of the importance of transamination versus deamination in astrocytic metabolism of [U-^{13}C] glutamate. *Glia*, **17**: 160-168

Westi EW, Andersen JV and Aldana BI (2023). Using stable isotope tracing to unravel the metabolic components of neurodegeneration: Focus on neuron-glia metabolic interactions. *Neurobiol Dis*, **182**: 106145

Wodtke P, Grashei M and Schilling F (2023). Quo vadis hyperpolarized ^{13}C MRI? *Z Med Phys*, **29**: S0939-3889(0923)00120-00124

Yang L, Kombu RS, Kasumov T, Zhu S-H, Cendrowski AV, David F, Anderson VE, Kelleher JK and Brunengraber H (2008). Metabolomic and mass isotopomer analysis of liver gluconeogenesis and citric acid cycle I. Interrelation between gluconeogenesis and cataplerosis; formation of methoxamates from aminooxyacetate and ketoacids. *J Biol Chem*, **283**: 21978-21987

Yao H, Azad P, Zhao HW, Wang J, Poulsen O, Freitas BC, Muotri AR and Haddad GG (2016). The Na^+/HCO_3^- co-transporter is protective during ischemia in astrocytes. *Neurosci*, **339**: 329-337

Yu Y and Martins LM (2024). Mitochondrial one-carbon metabolism and Alzheimer's Disease. *Int J Mol Sci*, **25**: 6302

Zhang L-Y, Hu Y-Y, Liu X-Y, Wang X-Y, Li S-C, Zhang J-G, Xian X-H, Li W-B and Zhang M (2024). The role of astrocytic mitochondria in the pathogenesis of brain ischemia. *Mol Neurobiol*, **61**: 2270-2282

Zhang Y and Barres BA (2010). Astrocyte heterogeneity: An underappreciated topic in neurobiology. *Curr Opin Neurobiol*, **20**: 588-594

Zwingmann C and Leibfritz D (2003). Regulation of glial metabolism studied by ^{13}C-NMR. *NMR Biomed*, **16**: 370-399

4 Appendix

Supporting information

List of figures

Figure S1

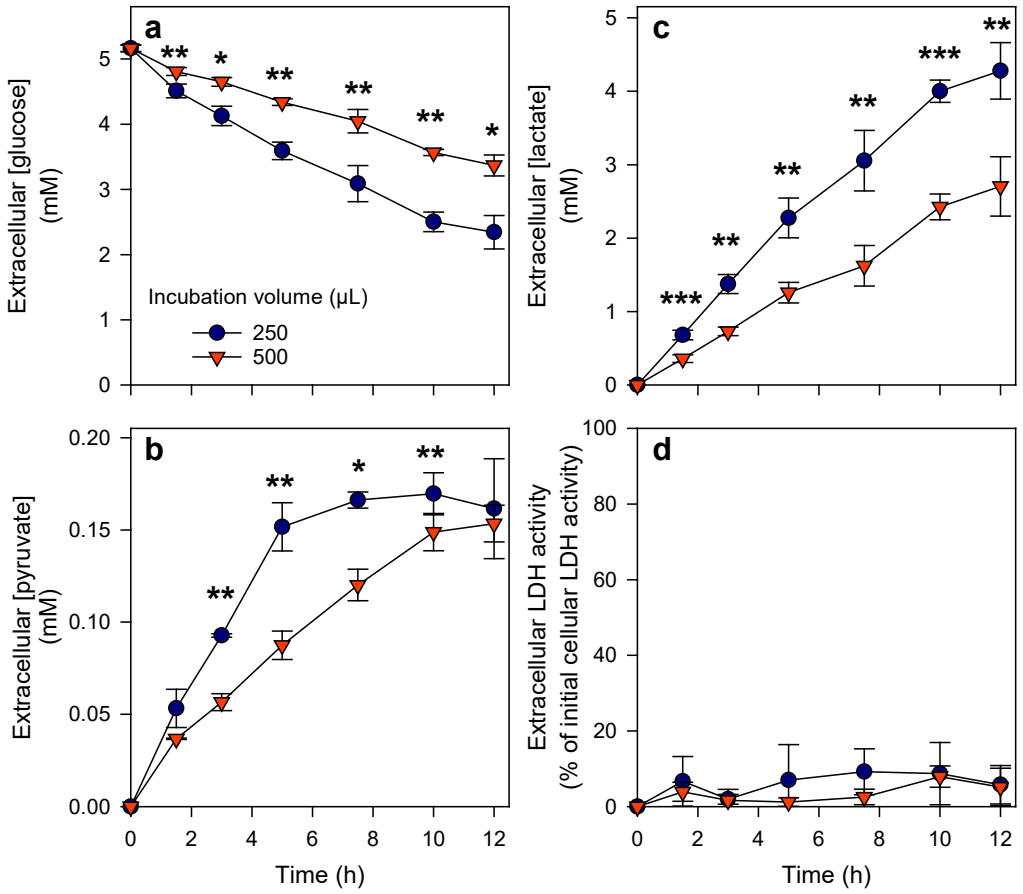

Figure S1: The transient extracellular steady-state concentration of pyruvate establishes independently of the extracellular volume. Astrocyte cultures were incubated in 250 µL or 500 µL incubation buffer (IB-HEPES) containing 5 mM glucose. For the given time points, the extracellular concentrations of glucose (a), pyruvate (b) and lactate (c) as well as the extracellular LDH activity (d) were determined. The initial LDH activity (100%) of the cultures was 144 ± 5 nmol/(min x well) and the initial protein content was 130 ± 8 µg/well. The data shown represents means ± SD of three experiments that had been performed on independently prepared cultures. The significance of differences (paired t-test) of data obtained for experiments with the two incubation volumes is indicated by $^{*}p<0.05$, $^{**}p<0.01$ and $^{***}p<0.001$.

Figure S2

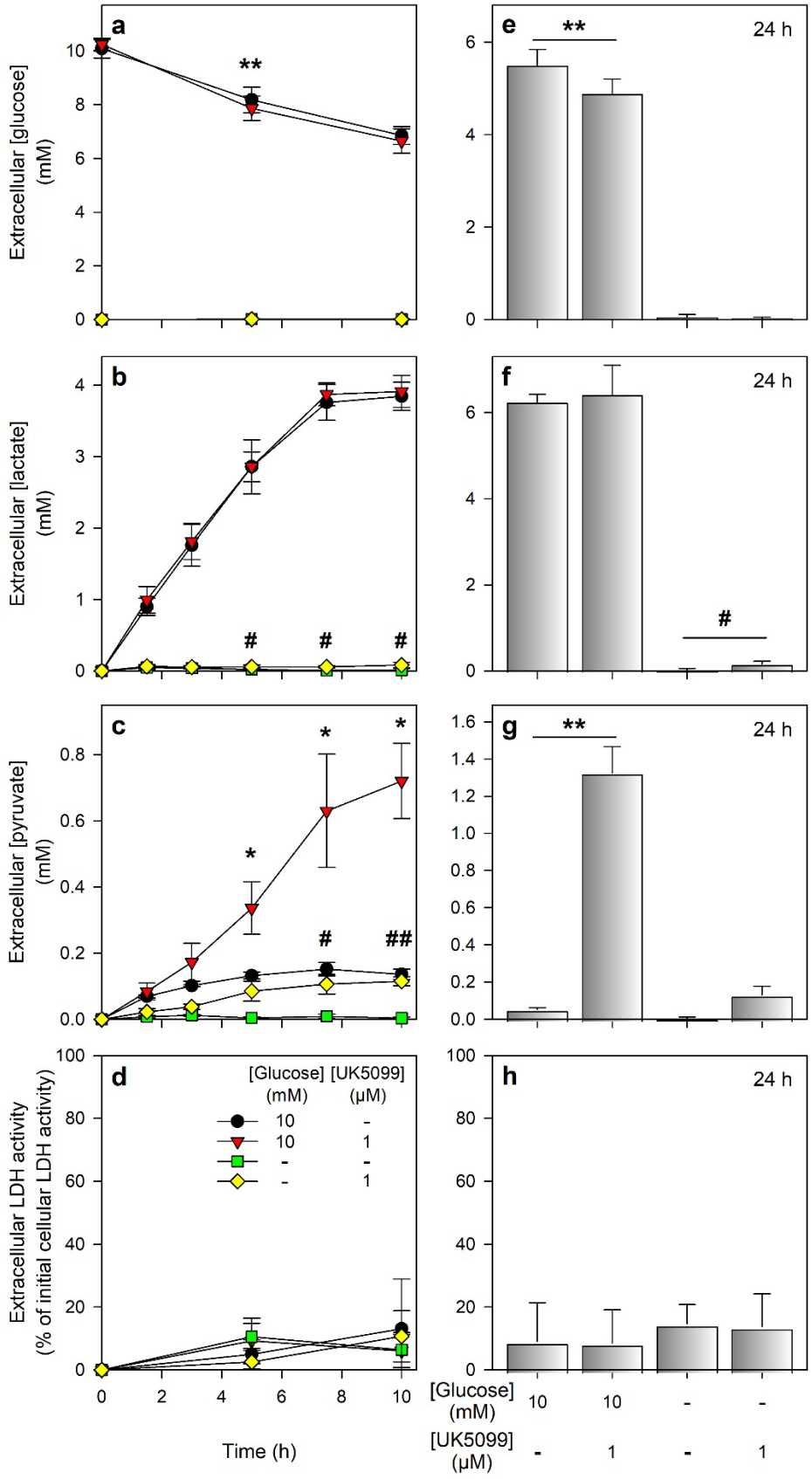
a
b
c
d
e
f
g
h
24 h
Extracellular [glucose] (mM)
Extracellular [lactate] (mM)
Extracellular [pyruvate] (mM)
Extracellular LDH activity (% of initial cellular LDH activity)
[Glucose] (mM)
[UK5099] (µM)
Time (h)

Figure S2: Time-dependent effect of the MPC inhibitor UK5099 on glucose consumption and release of lactate and pyruvate. Primary rat astrocyte cultures were incubated in glucose-free incubation buffer or incubation buffer containing 10 mM glucose without or with 1 µM UK5099, an inhibitor of the mitochondrial pyruvate carrier, for up to 24 h. After the indicated timepoints, the extracellular concentrations of glucose (a, e), lactate (b, f), and pyruvate (c, g) were determined. Extracellular LDH activity (d, h) was measured as a marker for decreased cell viability. The initial cellular LDH activity (100 %) was 141 ± 33 nmol/(mg x protein), and the initial protein content of the cultures was 115 ± 18 µg/well. The data represents means ± SD of values obtained from three experiments performed using independently prepared cultures. The significance of difference (paired t-test) between values obtained for glucose-containing incubation buffer without and with UK5099 is indicated by $^{*}p<0.05$ and $^{**}p<0.01$, and that between glucose-free incubation buffer without and with UK5099 by $^{\#}p<0.05$ and $^{\#\#}p<0.01$.

Figure S3

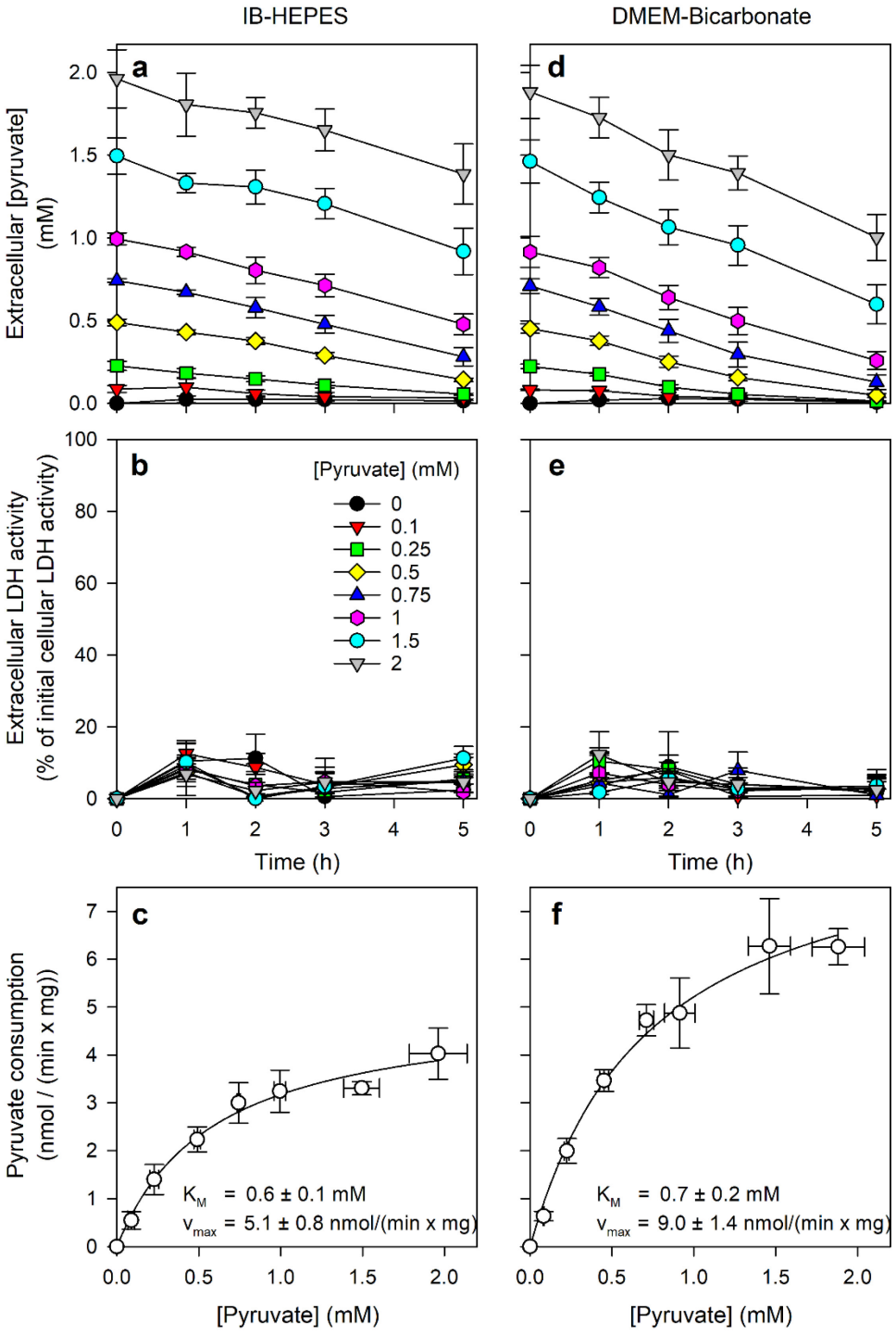
IB-HEPES
DMEM-Bicarbonate
a
d
Extracellular [pyruvate] (mM)
b
e
[Pyruvate] (mM)
0
0.1
0.25
0.5
0.75
1
1.5
2
Extracellular LDH activity (% of initial cellular LDH activity)
Time (h)
c
f
Pyruvate consumption (nmol / (min x mg))
K_M = 0.6 ± 0.1 mM
v_max = 5.1 ± 0.8 nmol/(min x mg)
K_M = 0.7 ± 0.2 mM
v_max = 9.0 ± 1.4 nmol/(min x mg)
[Pyruvate] (mM)

Figure S3: Pyruvate consumption by primary astrocyte cultures is altered in different incubation media. For up to 5 h, the cultures were incubated in glucose-free IB-HEPES (**a**, **b**, **c**; this data is already shown in Chapter 2.1, Figure 2 and is illustrated here again for direct comparison) or glucose-free DMEM-Bicarbonate (**d**, **e**, **f**) supplemented with the indicated pyruvate concentrations. The extracellular pyruvate concentrations (**a**, **d**), as well as the extracellular LDH activity (**b**, **e**) as an indicator of loss in cell viability were measured for the time periods given. The initial LDH activity (100 %) of the cultures was 116 ± 9 nmol/(min x well) and the initial protein content was 122 ± 7 µg/well. The specific pyruvate consumption rates were calculated using the almost linear decline of extracellular pyruvate during the first 3 h of incubation (**c**, **f**). By using the Michaelis-Menten equation, the concentration of half-maximal pyruvate consumption (K_M) and the maximal pyruvate consumption rate (v_{max}) were calculated for both incubation media. The data shown are means ± SD of values obtained from three experiments performed on independently prepared cultures.

Figure S4

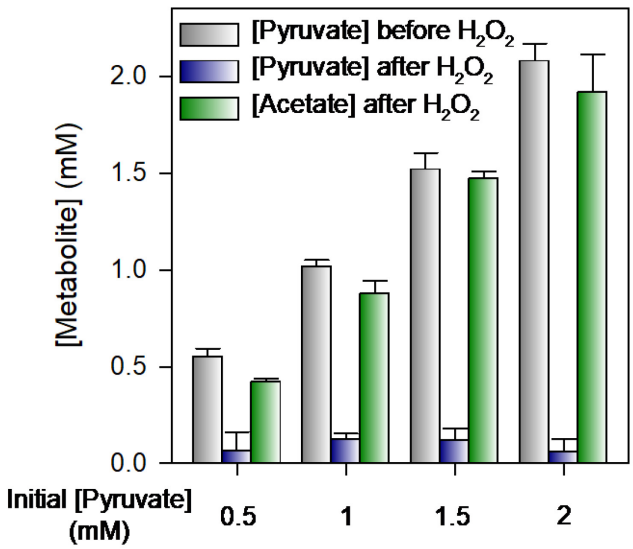

Figure S4: Quantitative chemical decarboxylation of pyruvate to acetate by H_2O_2. Samples of glucose-free incubation buffer containing the indicated concentrations of pyruvate were incubated for 30 min at room temperature with 10 mM H_2O_2 to decarboxylate pyruvate to acetate. Afterwards, 1040 U/mL catalase was added to deplete residual H_2O_2. The pyruvate concentrations before (grey bars) and after (blue bars) H_2O_2 treatment as well as the acetate formed (green bars) were determined. The data shown are means ± difference to the individual values of values obtained from two experiments.

Figure S5

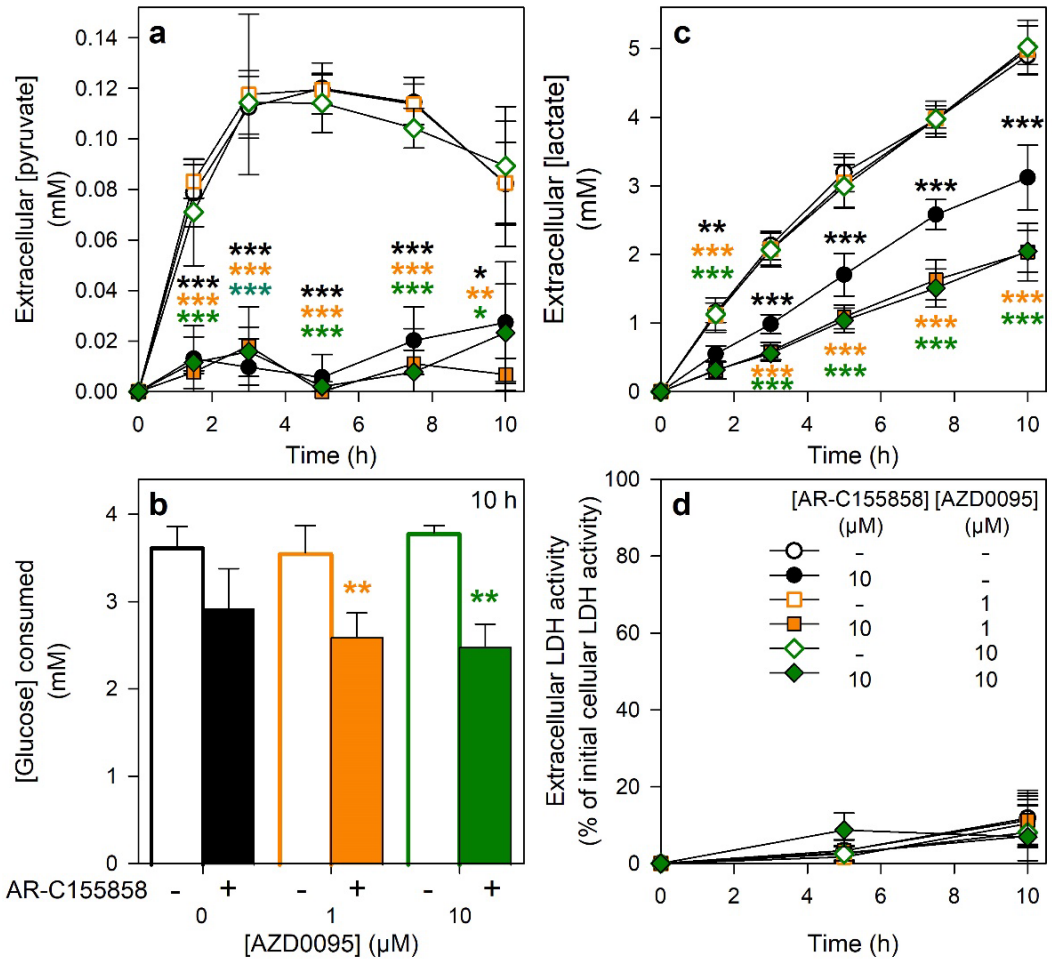

Figure S5: The influence of inhibition of different monocarboxylate transporters on astrocytic pyruvate and lactate release. Primary astrocyte cultures were incubated in incubation buffer (IB-HEPES) containing 10 mM glucose without or with 10 µM of the MCT1 inhibitor AR-C155858 or/and with the MCT4 inhibitor AZD0095 (purchased from MedChemExpress (Monmouth Junction, USA) in the indicated µmolar concentrations. After the indicated timepoints, extracellular pyruvate (a), lactate (c), and LDH (d) as an indicator of loss in cell viability were determined. Glucose consumption (b) after 10 h of incubation was calculated as the difference between the initial and the remaining extracellular glucose concentration after 10 h. The initial cellular LDH activity (100 %) was 206 ± 43 nmol/(min x well), and the initial protein content was 137 ± 16 µg/well. The data presented are means ± SD of results from three individual experiments performed on three individually prepared cultures. The significance of difference (ANOVA) compared to the control condition without inhibitors is indicated by $^{*}p<0.05$, $^{**}p<0.01$, and $^{***}p<0.001$.

Figure S6

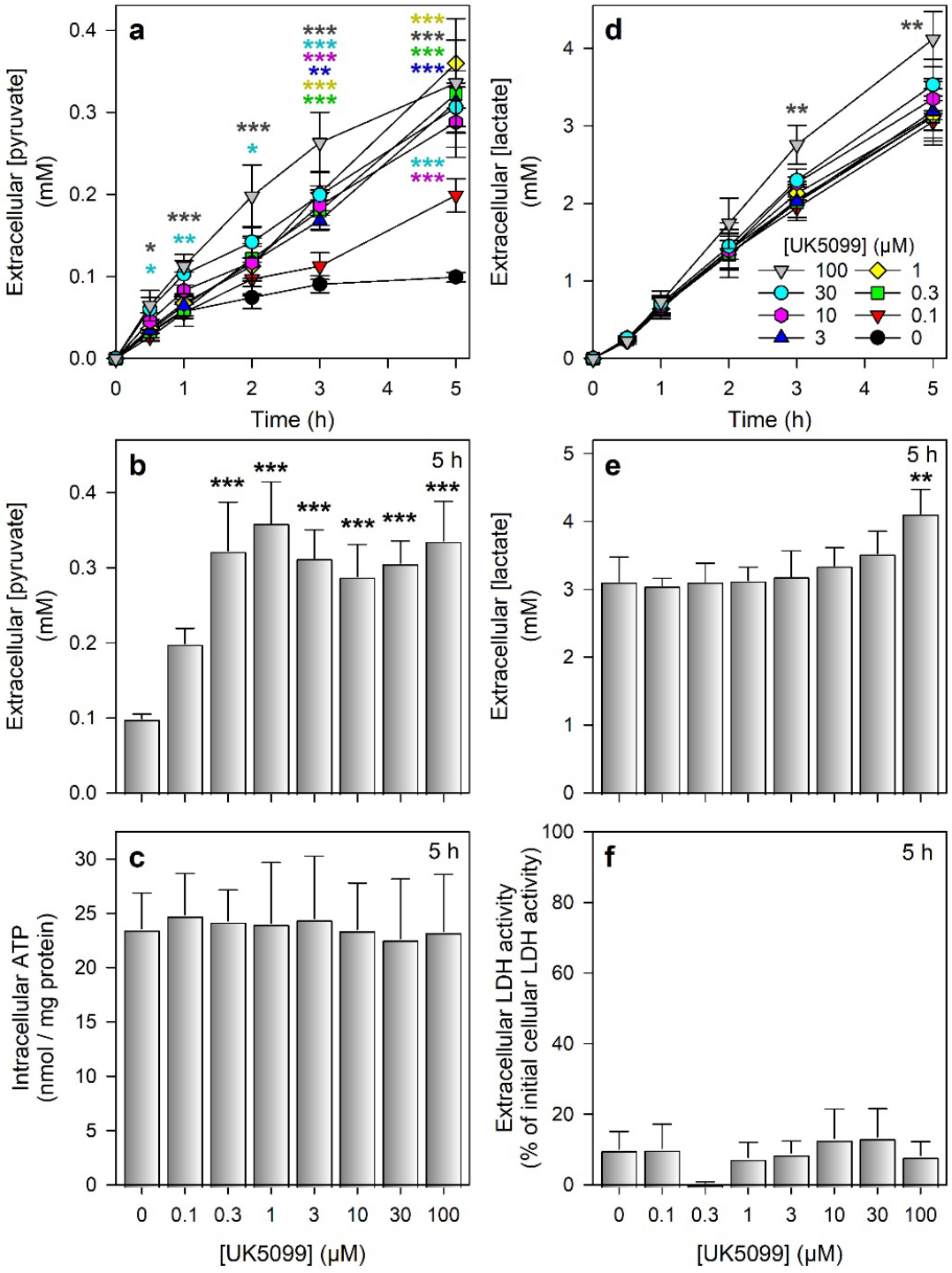
a
Extracellular [pyruvate] (mM)
Time (h)
d
Extracellular [lactate] (mM)
Time (h)
[UK5099] (µM)
100
30
10
3
1
0.3
0.1
0
b
5 h
Extracellular [pyruvate] (mM)
e
5 h
Extracellular [lactate] (mM)
c
5 h
Intracellular ATP (nmol / mg protein)
[UK5099] (µM)
f
5 h
Extracellular LDH activity (% of initial cellular LDH activity)
[UK5099] (µM)

Figure S6: Concentration-dependent effects of the mitochondrial pyruvate carrier inhibitor UK5099. Astrocyte cultures were incubated in incubation buffer (IB-HEPES) containing 10 mM glucose and the MPC inhibitor UK5099 in the indicated concentrations. Extracellular pyruvate (a, b) and lactate (d, e) concentration, as well as the specific intracellular ATP content (c) were determined at the specified time points. Extracellular LDH activity (f), serving as an indicator of a potential loss in cell viability, was measured, with an initial cellular LDH activity (100 %) of 173 ± 31 nmol/(mg x protein). The initial protein content was 145 ± 18 µg/well and the initial ATP content was 28 ± 5 nmol/(mg x protein). The data shown are means ± SD of values obtained in three experiments performed on independently prepared cultures. The significance of difference (ANOVA) compared to the values determined for the control condition (no inhibitor) is indicated by $^{*}p<0.05$, $^{**}p<0.01$, and $^{***}p<0.001$. P-values above 0.05 were considered as not significant.

Figure S7

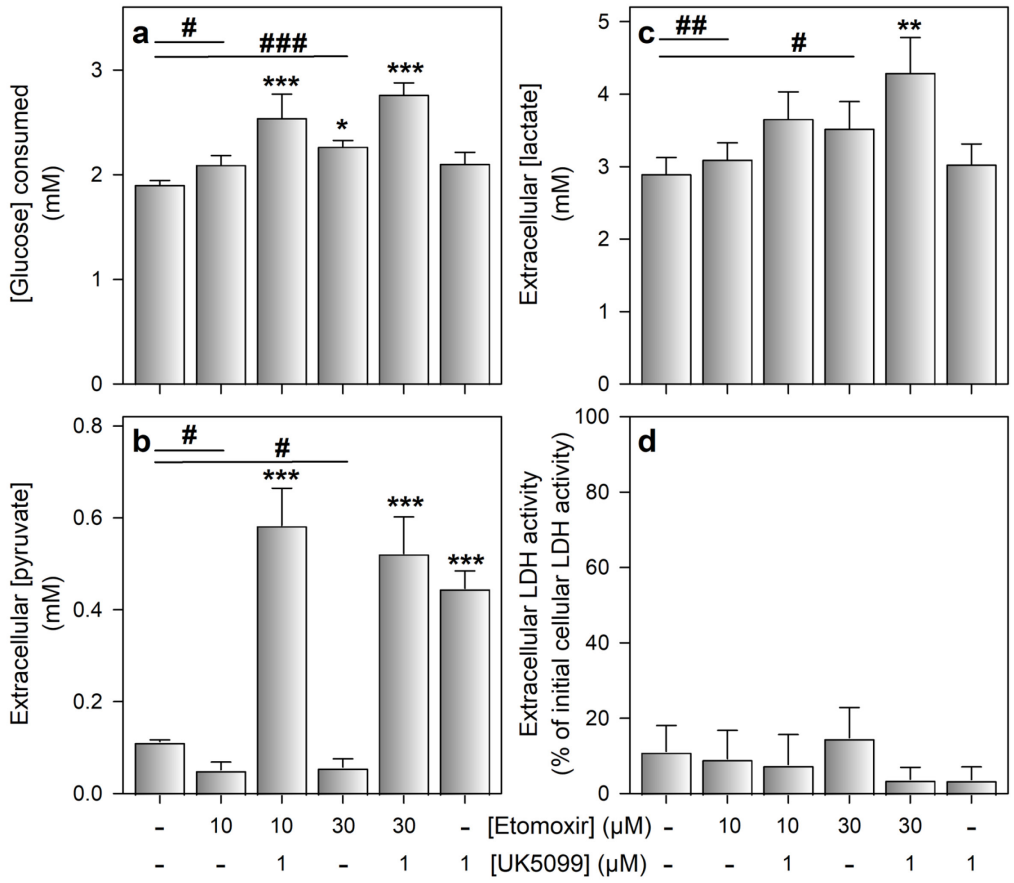

Figure S7: Modulation of extracellular pyruvate and lactate concentrations by inhibition of mitochondrial utilization of pyruvate or/and fatty acids. Astrocyte cultures were incubated with IB-HEPES containing 5 mM glucose in the absence or the presence of 1 µM of the MPC inhibitor UK5099 or/and the carnitine palmitoyltransferase 1 (CPT1) inhibitor etomoxir (purchased from Merck (Darmstadt, Germany) in the indicated µmolar concentrations. After an incubation period of 5 h, glucose consumption (a), the extracellular concentrations of pyruvate (b) and lactate (c), as well as the extracellular LDH activity (d) were determined. The initial protein content was 130 ± 7 µg/well and the initial cellular LDH activity (100 %) was 172 ± 5 nmol/(min x well). The data shown are means ± SD of three experiments performed on three individually prepared cultures. The significance of difference (ANOVA) compared to the control condition (no inhibitors) is indicated by $^{*}p<0.05$, $^{**}p<0.01$, and $^{***}p<0.001$. The significance of difference (paired t-test) between the control condition and incubation buffer containing etomoxir is indicated by $^{\#}p<0.05$ and $^{\#\#}p<0.01$.

Figure S8

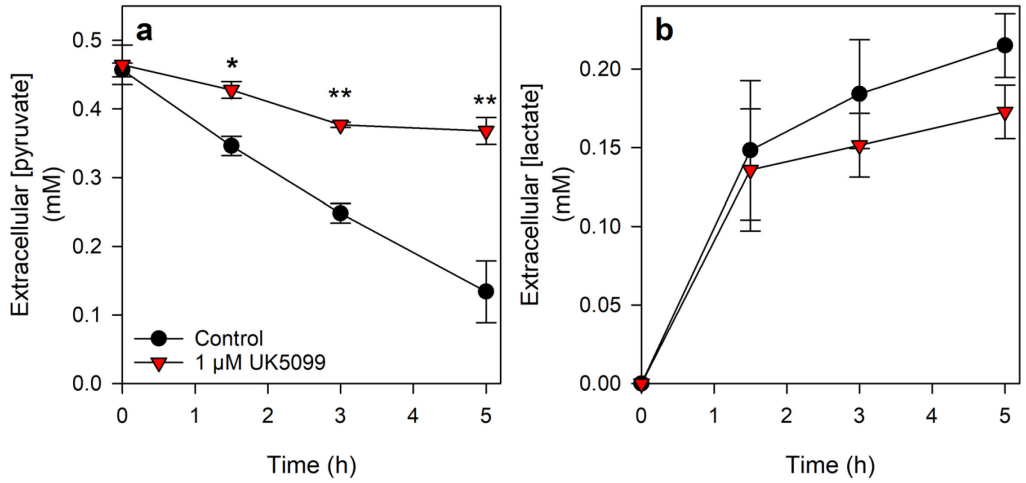

Figure S8: While pyruvate release is strongly inhibited by the MPC inhibitor UK5099, lactate release is only minimally impacted. Cultured astrocytes were incubated with IB-HEPES containing 0.5 mM pyruvate in the absence or presence of the MPC inhibitor UK5099. After the indicated timepoints, extracellular pyruvate (a; this data has already been shown in Chapter 2.1, Figure 8) and lactate (b) were measured. The initial cellular LDH activity of the cultures was 167 ± 26 nmol/(min x well) and the initial protein content was 134 ± 21 µg/well. The data shown are means ± SD of three experiments performed on three individually prepared cultures. The significance of difference (paired t-test) between the control condition and incubation buffer containing 1 µM UK5099 is indicated by $^{*}p<0.05$ and $^{**}p<0.01$.